DISSERTATION

IMPROVED DETECTION OF RADIOACTIVE MATERIAL USING A SERIES OF MEASUREMENTS

Submitted by

Jenelle Mann

Department of Environmental and Radiological Health Sciences

In partial fulfillment of the requirements

For the Degree of Doctor of Philosophy

Colorado State University

Fort Collins, Colorado

Summer 2016

Doctoral Committee:

Advisor: Alexander Brandl

Thomas Johnson
Piotr Kokoszka
Del Leary

ABSTRACT

IMPROVED DETECTION OF RADIOACTIVE MATERIAL USING A SERIES OF MEASUREMENTS

The goal of this project is to develop improved algorithms for detection of radioactive sources that have low signal compared to background. The detection of low signal sources is of interest in national security applications where the source may have weak ionizing radiation emissions, is heavily shielded, or the counting time is short (such as portal monitoring). Traditionally to distinguish signal from background the decision threshold (y^*) is calculated by taking a long background count and limiting the false negative error (α error) to 5%. Some problems with this method include: background is constantly changing due to natural environmental fluctuations and large amounts of data are being taken as the detector continuously scans that are not utilized.

Rather than looking at a single measurement, this work investigates looking at a series of N measurements and develops an appropriate decision threshold for exceeding the decision threshold n times in a series of N. This methodology is investigated for a rectangular, triangular, sinusoidal, Poisson, and Gaussian distribution.

ACKNOWLEDGEMENTS

This material is based upon work supported by the U.S. Department of Homeland Security under Grant Award Number, 2014-DN-077-ARI091-01

Disclaimer: The views and conclusions contained in this document are those of the authors and should not be interpreted as necessarily representing the official policies, either expressed or implied, of the U.S. Department of Homeland Security

DEDICATION

For my father, whose memory will always inspire me to reach farther than I thought I could.

TABLE OF CONTENTS

LIST OF TABLES

LIST OF FIGURES

INTRODUCTION

Radioactive material contains atoms whose nuclei are unstable and undergo radioactive decay. During radioactive decay, a particle and/or electromagnetic radiation is emitted from the unstable nucleus; in many instances, multiple decays will occur until the resulting nucleus is a more stable nucleus. Types of radioactive descay include the emission of a beta particle (neutron rich nucleus), alpha particle (heavy nucleus), positron particle (proton rich nucleus), electron capture (proton rich nucleus), and gamma emission (isomeric transition) [1] [2]. Other more exotic types of radioactive decay include neutron emission, proton emission, spontaneous fission (heavy nucleus), and cluster decay.

Radioactive decay is an inherently random process and the exact time of decay for an atom cannot be predicted. Instead, the behavior of a population of radioactive atoms is described through the half-life and mean life. The half-life and mean life are properties of the atom and are independent of the chemical and physical state of the atom [1]. The half-life for a particular radionuclide is the time period needed for the population to reduce to half of the original value. The decrease in population, N, over time is described through Equation 1, where N_0 is the original population and λ is the transformation constant or the fractional population decrease per unit time (Equation 2).

$$N = N_0 e^{-\lambda t} \quad (1)$$

$$\lambda = \frac{\ln(2)}{T_{\frac{1}{2}}} \quad (2)$$

The mean life (τ) is the average of the lifetimes of all the individual atoms and is described through Equation 3.

$$\tau = \frac{1}{\lambda} = \frac{T_{\frac{1}{2}}}{\ln(2)} \quad (3)$$

For radioactive decay, in addition to the change in population, the activity (A) or number of disintegrations per unit time is an important parameter. The activity is simply the population multiplied by the transformation constant.

$$A = \lambda N \quad (4)$$

Equation 1 can be rewritten in terms of the activity by multiplying both sides of the equation by the decay constant, where A_0 is the original activity:

$$A = A_0 e^{-\lambda t} \quad (5)$$

Radioactive material is naturally present in the environment. Sources of natural background radiation include radionuclides from the creation of the universe (primordial) and those created from cosmic ray interactions (cosmogenic) [2]. Radioactive material has also been created by man and contributes to background radiation. One of the goals of health physics is to accurately quantify radiation levels for applications such as regulatory compliance and risk assessments. Techniques for measurement of radioactive material depend on the energy and type of emitted particles, as well as desired measurement quantity. The measurement quantity of interest for this work is raw counts in a detection system.

Counting statistics are used to describe measurements of radioactive decay; because radioactive decay is a random process, there will be a degree of uncertainty in all measurements. Statistics can be used to check the performance of a detector by comparing detector fluctuations with those predicted from statistical models (Poisson); or to estimate the uncertainty on a single measurement [3].

Sources of background, detection of radiation, statistics basics, statistical analysis for radiation measurement, and the statistical analysis of background are discussed in more depth in the following sections.

Sources of Background

Sources of background for the measurement of radioactive material include background radiation and background from the detector, such as electronic noise. Radiation sources can be divided into natural background sources and man-made radiation sources. Sources of public exposure to ionizing radiation were investigated by the National Council on Radiation Protection (NCRP) in Report 160 in 2009. The findings of the report were that half of public exposures are due to manmade sources and the remaining exposure comes from natural background sources. The relative contribution of each source is shown in Figure 1, where natural sources are shown in blue and man-made sources are shown in purple [4].

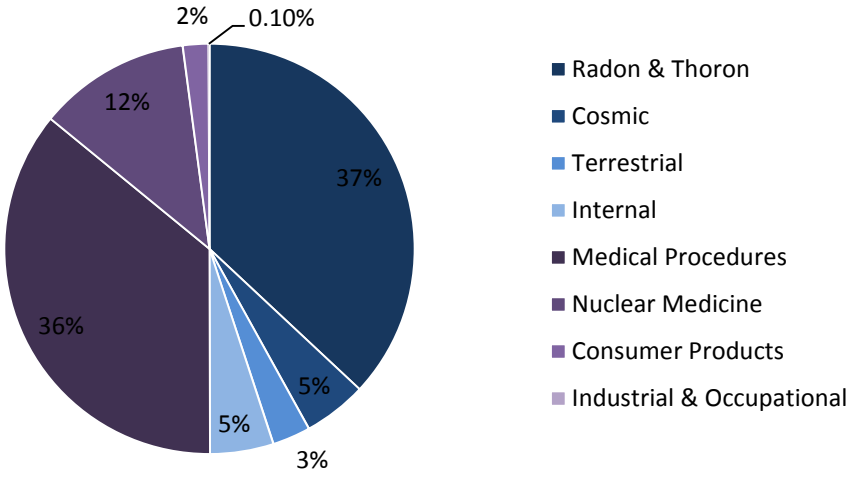

Figure 1 Sources of Radiation Exposure (U.S.) [4]

Sources of background radiation of interest for this study include radon and thorium, cosmic radiation, consumer products (such as building materials), and isotopes from industrial and occupational uses.

Detection of Radiation

The detection of radiation is accomplished by converting the radiation of interest into a signal that can be processed and analyzed by a detection system. The response of the detector needs to be proportional to the radiation effect or property being measured. The detector is one component of a system whose desired output is an electrical pulse that can be analyzed. The result is a chain of components, also known as a signal processing chain. A typical signal processing chain for radiation detection is displayed in Figure 2.

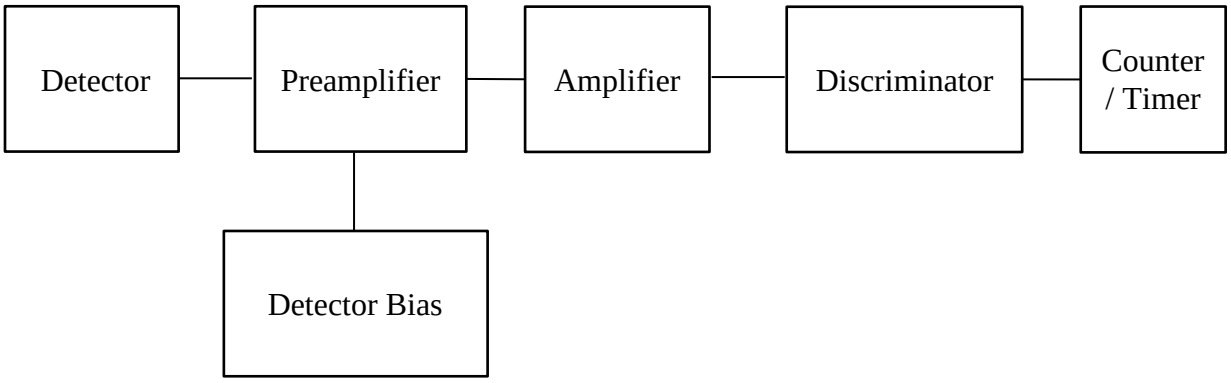

Figure 2 Typical Signal Processing Chain for Radiation Detector

The radiation interacts in the material of the detector; the desired response is proportional to the measured radiation property, such as energy deposited or raw counts. In many cases, the detector response signal is small compared to noise and does not have a desired shape. The signal from the detector is passed through a preamplifier which powers the detector and extracts the detector signal while maximizing the signal to noise ratio. The preamplifier also shapes the signal to make it optimal for processing by the amplifier, which further shapes and amplifies the

signal. The signal is passed through a discriminator, which uses lower and upper bounds to eliminate any information that is not signal (such as noise). The discriminator outputs a logic pulse, which is counted by the counter/timer.

Some newer detection systems incorporate detector bias, amplifier, discriminator, and counter time into one component, a digital signal processor; such that the digital signal processor provides power to the preamplifier and shapes the preamplifier signal into a useable form that is used internally to obtain counting data. The signal processing chain for a detection system that uses a digital signal processor is shown in Figure 3.

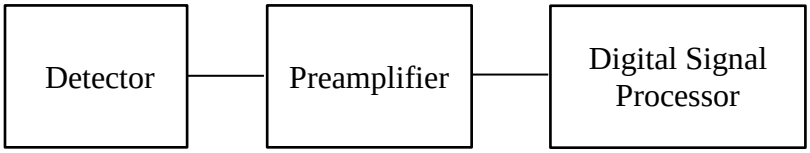

Figure 3 Signal Processor Chain for a Radiation Detector using a Digital Signal Processor

Three main types of detectors are used for radiation detection: gas-filled detectors, scintillation detectors, and semiconductor detectors. The three detector types mostly differ in the material used to convert the radiation into a signal. The methodology for this project can be incorporated into any detection system, but the main detector that will be used is a scintillation detector, specifically a Sodium Iodide detector.

In a scintillation detector, the radiation interacts in the scintillation medium to produce scintillation light. The scintillation in a Sodium Iodide detector occurs within a sodium iodide crystal due to the crystalline structure. The scintillation light is converted into an electrical signal using a photomultiplier tube (photocathode) and to amplify the signal (dynodes). The resulting electrical signal is proportional to the energy deposited within the scintillation crystal by the interacting radiation, such that energy discrimination can be accomplished. Sodium Iodide detectors are designed to detect photons (gammas and x-rays). Sodium iodide crystals readily

absorb water and must be housed in an airtight container. The use of the airtight container also prevents the penetration of the crystal by betas and alphas.

Statistics Basics

Random variables are used to describe processes that are random. Each value for the random variable corresponds to an outcome of an experiment or random event. Although the individual outcomes of the event or experiment cannot be accurately predicted, the frequency of each outcome over a long series is stable. The frequency of each outcome is otherwise known as the probability of an event occurring. The random variable takes on a set of the possible outcomes of the experiment or random event, each with an associated probability of occurrence. For example, in the case of radioactive decay, the random event would be whether or not the atom decays within the next time period, t. The random variable would consist of two possibilities: decay occurred or decay did not occur; the probability associated with the random event, radioactive decay, occurring is related to the half-life and the decay constant.

Two types of random variables can be distinguished: discrete and continuous. For each type of variable there exist several probability distributions that describe the occurrence of the random variable. Terminology is presented in Table 1, for reference.

Table 1 Terminology for Probability Distributions

Variable	Discrete		Continuous	
X	Discrete Random Variable	X	Continuous Random Variable	X
x	Outcomes of X	x	Outcomes of X	x
$P(X = x)$	Probability Mass Function	$p(x)$	Probability Density Function	$f(x)$
$P(X \leq x)$	Cumulative Distribution Function	$F(x)$	Cumulative Distribution Function	$F(x)$

Discrete random variables contain a finite or countable number of distinct outcomes. For a discrete random variable X, the random variable can be described through a set of n possible values or outcomes (Equation 6).

$$X = x_1, x_2, \dots, x_n \quad (6)$$

For each value x, an associated probability of occurrence can be identified: $P(X = x)$, otherwise known as the probability mass function $p(x)$. The total probability for all occurrences of x is 100%, or 1, giving rise to the following properties of the probability mass function:

- $p(x)$ must be between 0 and 1 for all x (7)
- $\sum_x p(x) = 1$ for n values of $p(x)$ (8)

The cumulative distribution function describes the probability of a random selection of the random variable X that yields a value less equal than x, or $F(x) = P(X \leq x)$. The cumulative distribution function can be related to the probability mass function by the following equation

$$F(x) = P(X \leq x) = \sum_{i=1}^{x} p(x_i) \quad (9)$$

Since, the probability mass function $p(x) = P(X = x)$ must be greater than or equal to 0, the cumulative distribution function has the following characteristics:

- $F(x)$ is a non-decreasing function of x (10)
- $F(-\infty) \equiv lim_{y \to -\infty} F(y) = 0$ (11)
- $F(\infty) \equiv lim_{y \to \infty} F(y) = 1$ (12)

The expectation value, $E(X)$, for a random variable is the stochastic mean value and is the first moment for X [5] [6]. For a discrete random variable, the expectation value is calculated by summing the product of each individual value x by the probability of occurrence for all x:

$$E(X) = \sum_x xp(x) = \mu \quad (13)$$

Similarly, the expectation for a function of X, $g(X)$, is calculated using Equation 14.

$$E(g(X)) = \sum_x g(x)p(x) \quad (14)$$

The variance, $V(X)$, for a distribution is a measure of the dispersion of the random variable X and is the second central moment of X and is calculated through Equation 15. The square root of the variance is known as the standard deviation [5].

$$V(X) = E\big(X - E(X)\big)^2 = E(X^2) - E(X)^2 \quad (15)$$

Discrete distributions such as the binomial distribution, geometric distribution, negative binomial distribution, hypergeometric distribution, and Poisson distribution are derived using discrete random variables. Binomial and Poisson distributions are used frequently for radiation detection and will be discussed more in depth.

Continuous random variables are random variables that are defined for any value in an interval. For continuous random variables, a probability density function, $f(x)$, is defined, similar to the probability mass function for discrete random variables. However, unlike for discrete random variables, the probability density distribution is defined for any value in an interval. The probability density distribution has the following characteristics:

- $f(x)$ must be between 0 and 1 for all x, $-\infty < x < \infty$ (16)
- $\int_{-\infty}^{\infty} f(x)dx = 1$ for all values of $f(x)$ (17)

The cumulative distribution function of X, $F(x)$, is the probability that a random selection of X yields a value less than or equal to x, or $P(X \leq x)$. The cumulative distribution function is related to the probability density distribution by Equations 18 and 19.

$$F(x) = P(X \leq x) = \int_{-\infty}^{x} f(t)dt \quad (18)$$

$$f(x) = \frac{dF(x)}{dx} = F'(x) \tag{19}$$

The cumulative distribution function has the following properties:

- $F(x)$ is a non-decreasing function of x (20)
- $F(-\infty) \equiv \lim_{x \to -\infty} F(x) = 0$ (21)
- $F(\infty) \equiv \lim_{x \to \infty} F(x) = 1$ (22)

The probability that X falls within a certain interval between $x = a$ and $x = b$ is calculated by integrating the probability density distribution from a to b, as described in Equation 23.

$$P(a \leq X \leq b) = \int_a^b f(x)dx \tag{23}$$

The expectation value, or stochastic mean, for a continuous random variable X is calculated by integrating the probability density multiplied by x for all x (Equation 24).

$$E(X) = \int_{-\infty}^{\infty} xf(x)dx \tag{24}$$

Similarly, the expectation value for a function of X is calculated using Equation 25.

$$E(g(X)) = \int_{-\infty}^{\infty} g(x)f(x)dx \tag{25}$$

Continuous distributions such as the uniform distribution, gamma distribution, beta distribution, and Gaussian distribution are derived using continuous random variables. The uniform distribution and Gaussian distribution have important uses in counting statistics and will be discussed more in depth. A triangular and sinusoidal distribution will also be discussed.

The probability mass function for the binomial and Poisson distributions, and the probability density function for the Gaussian distribution will be discussed in the following sections; while the parameters for the uniform, triangular, and sinusoidal distributions will be discussed here, the methodology for deriving the probability distributions will be discussed in Materials and Methods, and the derivation of equations used will be derived in Preliminary Results.

Binomial Distribution

The binomial distribution is used to describe a sequence of Bernoulli trials, in which each trial is independent and has one of two outcomes: success or failure. The probability of success, p, and the probability of failure, q, sum to unity, such that:

$$q = 1 - p \tag{26}$$

For n trials, the probability of x successes (probability distribution) is calculated through Equation 27 for $x \in (0, n)$ and $p \in (0,1)$.

$$p(x) = \binom{n}{x} p^x q^{n-x} = \binom{n}{x} p^x (1-p)^{n-x} \tag{27}$$

The parameter $\binom{n}{x}$ is the binomial coefficient and takes into account the number of outcomes (x) in an unordered set of n objects. The binomial coefficient also acts as a normalization coefficient to ensure that characteristics in Equations 7 and 8 for the probability mass function are satisfied. The binomial coefficient is calculated through Equation 28.

$$\binom{n}{x} = \frac{n!}{x!\,(x-n)!} \tag{28}$$

The expectation value, or mean, of the binomial distribution is calculated using Equation 13:

$$E(X) = \mu = np \quad (29)$$

Similarly, the variance of the distribution is calculated using Equation 15:

$$V(X) = npq = np(1-p) \quad (30)$$

The binomial distribution describes radioactive decay well. In radioactive decay, there are two outcomes: a decay occurs or a decay does not occur. If the number of successes (decays) is small compared to the population (total number of radioactive particles) the population will be approximately constant and the trials can be considered independent.

The probability of success and the probability of failure can be calculated by looking at Equation 1. This equation describes the number of radioactive atoms remaining after a time, t. The probability of an atom surviving, or not decaying, can be calculated through Equation 31.

$$q = e^{-\lambda t} \quad (31)$$

Using the relationship between the probability of success and failure, as described in Equation 26, the probability of success is calculated as follows:

$$p = 1 - q = 1 - e^{-\lambda t} \quad (32)$$

The probability of x decays for a population n equal to N over a time period t therefore is calculated through the following equation.

$$p(x) = \binom{N}{x} \left(1 - e^{-\lambda t}\right)^{x} (e^{-\lambda t})^{N-x} \quad (33)$$

The mean number of decays is calculated using Equations 29 and 32.

$$E(X) = N(1 - e^{-\lambda t}) \quad (34)$$

If instead, the parameter of interest is the total number of atoms that have not decayed (the remaining population of radioactive atoms), the expected value is given by Equation 35. If

the variables are reassigned such that $N = N_0$ and $N - X = N$, Equation 35 reduces to Equation 1, as expected.

$$E(N - X) = Nq = Ne^{-\lambda t} \tag{35}$$

While the binomial distribution is useful and accurate for describing radioactive decay, the presence of factorials in the binomial coefficient (Equation 28) renders it computationally extensive; instead, approximations of the binomial distribution, such as the Poisson distribution and Gaussian distribution are often used.

Poisson Distribution

The Poisson distribution is an approximation of the binomial distribution where the probability of success, p, is small (less than ~0.05) and the population, n, is large (greater than ~20). Additionally, the distribution is described in terms of the mean of the distribution, μ, which is the same as the binomial mean defined in Equation 34. When these approximations are applied to Equation 27, the probability mass function for the Poisson distribution is described through Equation 36 for μ greater than zero.

$$p(x) = \frac{\mu^x}{x!} e^{-\mu} \tag{36}$$

The expected value for the Poisson distribution is the mean, μ. The variance of the Poisson distribution can be calculated and is equal to the mean.

$$V(X) = \mu \tag{37}$$

The Poisson distribution works well for situations where the probability of success is small, the population is large, and the mean value is already known.

For radioactive decay, the likelihood of radioactive decay in a very small period of time can be described such that the probability of success, p, is small.

Gaussian Distribution

The Gaussian distribution, or normal distribution, is an approximation to the binomial distribution for a large number of trials (np or $n(1-p)$ is greater than 10). It is also assumed that the probability density function is narrow around the mean, such that $|n-\mu| \ll \mu$ [2]. The resulting Gaussian distribution is continuous and symmetric across the mean. It is defined in terms of the mean, μ, and the standard deviation, σ. The equation for the Gaussian probability density function is displayed in Equation 38 for $\sigma > 0$ and μ and $x \in (-\infty, \infty)$.

$$f(x) = \frac{1}{\sigma\sqrt{2\pi}} e^{-\frac{(x-\mu)^2}{2\sigma^2}} \tag{38}$$

A closed form of the integral of the Gaussian probability density function does not exist. The evaluation of this integral is accomplished through numerical integration. However, tables exist for quantile information for the standard normal distribution. The standard normal distribution has a mean of zero, and standard deviation of one, such that the standard normal probability density function for a random variable Z is:

$$f(z) = \frac{1}{\sqrt{2\pi}} e^{-\frac{z^2}{2}} \tag{39}$$

The cumulative distribution function for the standard normal distribution is shown in Equation 40. Although the integral cannot be evaluated in closed form, it can be analyzed through numerical integration, which is presented in normal tables for the standard normal distribution.

$$F(z) = \int_{-\infty}^{z} \frac{1}{\sqrt{2\pi}} e^{-\frac{z^2}{2}} dz \qquad 40$$

Using normal tables important information can be calculated for the standard normal distribution, which can be related back to the Gaussian density by relating the random variables Z and X using Equation 41.

$$Z = \frac{X - \mu}{\sigma} \qquad 41$$

Uniform Distribution

The uniform distribution is defined at a constant value, d, between $x = a$ and $x = b$. A plot of the probability density function for the uniform distribution is shown in Figure 4.

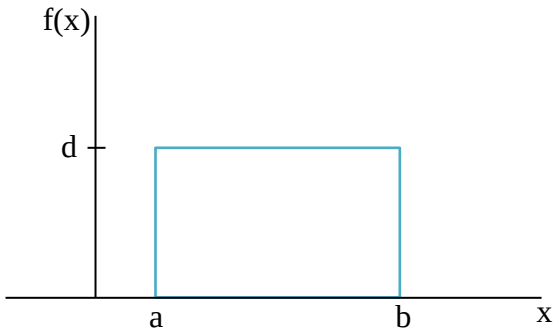

Figure 4 Probability Density Function for the Uniform Distribution

Triangular Distribution

The triangular distribution extends from $x = a$ to $x = b$, with the peak of the triangle at c. The peak height is $f(b)$ equal to d. For each leg of the triangle, the slopes m_1 between $x = a$ and $x = c$ and m_2 between $x = c$ and $x = b$ describe the functional dependence of the probability density function. An example plot of the probability density function for a triangular distribution is shown in Figure 5.

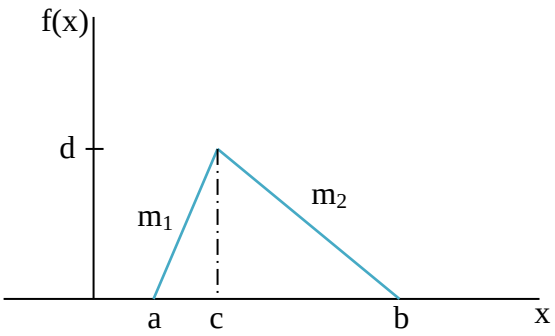

Figure 5 Probability Density Function for the Triangular Distribution

Sinusoidal Distribution

The sinusoidal distribution extends between $x = a$ and $x = b$, where $b \leq \frac{T}{2} + a$. An example plot of the probability density function for a sinusoidal distribution is displayed in Figure 6.

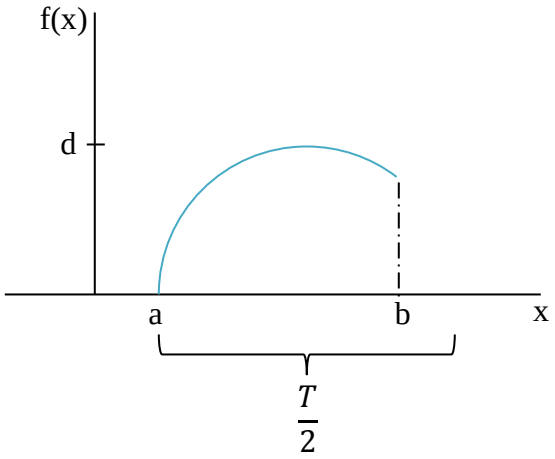

Figure 6 Probability Density Function for the Sinusoidal Distribution

Statistical Analysis for Radiation Measurement

Since there is background radiation present at any given time and for any given measurement, it is necessary to separate signal from background or noise. A level or limit therefore needs to be chosen, such that if a sample contains a higher count rate or activity than

that limit it is considered radioactive, while if the sample has a lower count rate or activity than that limit it is considered background.

Two possible errors are associated with assigning a limit to separating signal from background: the α, false positive error and the β, false negative error. The α error, or error of the first kind, occurs when background radiation is falsely categorized as radioactivity. The β error, or error of the second kind, occurs when a signal is falsely categorized as background. The false positive and negative errors are shown in Figure 7 for a background and signal distribution with an arbitrarily chosen limit.

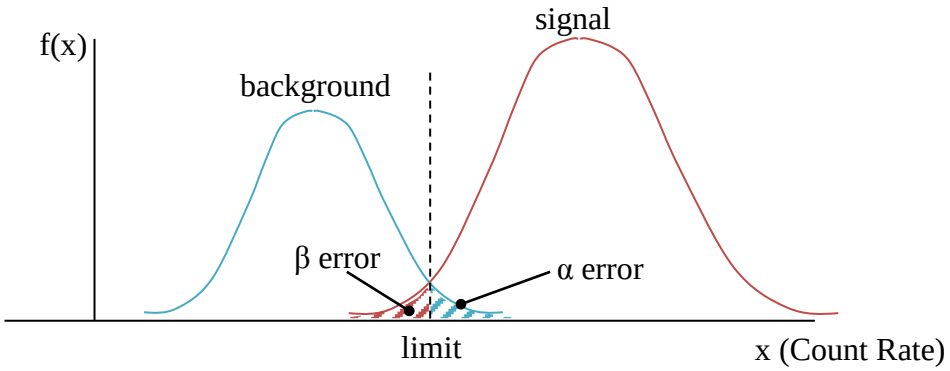

Figure 7 False Positive and False Negative Errors for a Background and Signal Distribution

The three characteristic limits for radiation detection are defined by ISO 11929: decision threshold, detection limit, and limits of the confidence interval. The decision threshold, previously also called the critical level, is the level below which a measurement result is considered background and above which that measurement result is considered radioactive. This limit is considered an investigatory level, but does not give any information about detection capabilities. The limit is derived by limiting the false positive error on the background count rate spectrum. The detection limit is used to specify detection capabilities of a detector. It is derived by limiting the false positive error for background and the false negative error for signal. The

limits of the confidence interval specifies an interval in which the true value exists with a certain confidence.

For this work, the characteristic limit of concern is the decision threshold. Since the decision threshold is based on the background distribution only the probability function for background needs to be known.

Statistical Analysis of Background

Five distributions will be investigated: Poisson distribution, Gaussian distribution, uniform distribution, triangular distribution, and sinusoidal distribution. These distributions correspond to commonly seen distributions in three domains: count space, energy space, and time space.

Statistical fluctuations within count space could be due to the natural decay process or variations in detector response. Radioactive decay is best modeled by the Binomial, Poisson, and Gaussian distributions, depending on the population of radioactive atoms and the decay rate.

Statistical fluctuations in energy space include fluctuations from Compton background and variations in the total energy deposited by radiation. Compton background would be most accurately described by a uniform distribution, while variations in total energy deposited would be best modeled by a Binomial, Poisson, or Gaussian distribution.

Fluctuations in time space could take any of the five distributions discussed, depending on the nature of the time fluctuations. For instance, radon undergoes cyclical patterns, depending on the time of day, and would be accurately modeled by the sinusoidal distribution. The withdrawal or removal of a source could be modeled by a triangular distribution that approximates a line.

PURPOSE AND HYPOTHESIS

The goals of this project are to improve the detection and identification capabilities of currently deployed and future instruments to detect radioactive material. Improvements would include reliable detection at lower signal levels than previous (higher positive identification rate), quicker detection than conventional techniques (lower time at first detection), and reduction of nuisance alarms (lower false positive rate).

Conventionally, determination if activity is present is accomplished by looking at whether a single measurement exceeds a decision threshold. This thesis assesses the effectiveness of looking at a series of measurements, rather than looking at an individual measurement to define a suitable decision threshold.

LITERATURE REVIEW

The development of an updating decision threshold has been explored for Bayesian and classical statistics for a Gaussian distribution of counts. Bayesian and classical statistics differ in their treatment of unknown parameters that represent population characteristics. In classical statistics, parameters are treated as fixed quantities, while in Bayesian statistics parameters are thought of as random variables with a probability distribution (prior distribution). Sampled data (likelihood function) is used with the prior distribution to develop a posterior distribution. By informing the posterior distribution with the likelihood function, the resulting distribution will then more accurately represent the population. In contrast, classical statistics relies on very large number sampling that converges to the true value.

Due to the variable nature of Bayesian statistics, it is useful for the analysis of background radiation. Bayesian statistics was used by Klumpp et al to characterize background during a counting measurement when the instantaneous background count rate was not fixed [7]. A moving target method was developed, which allowed for the background count rate to vary with time. A benefit of this method is variations in radiation background can be taken into account, such as time, location, and detector statistics. The mean was modeled as a Poisson mean, while the variation and the uncertainty on the average count rate were modeled by a gamma distribution. By using a moving target method, the mean was calculated to be 50% higher than with a fixed target method [7].

In addition, Klumpp and Brandl used a Bayesian approach that took into account energy information by dividing the energy range of the detector into different energy bins [8]. A two energy bin detector, eleven energy bin detector, and gross count rate detector were investigated.

The authors found that the average run lengths for the two energy and eleven energy detectors were less than for the gross count rate detector for all modeled count rates. Additionally, the detection probability for the two energy and eleven energy detectors was much higher; the result was a lower level of detection that was approximately half of the gross count rate detector [8].

An analysis of background radiation using classical statistics for a moving system was performed by Brandl and Jimenez [9]. Improvements in the decision threshold were about 11%. A more rigorous analysis was developed by Brandl for a Gaussian distribution of counts [10]. The decision threshold was updated by keeping the probability of exceeding the decision threshold constant, such that the cumulative probability for the next measurement exceeding the decision threshold was α. An equation for an updating false positive error, α_{new}, was developed as follows:

$$(\alpha_{new})^{n+1}(1-\alpha_{new})^{N-n} = 0.05\frac{(n+1)!\,(N-n)!}{(N+1)!} \quad 42$$

The decision threshold was updated using the equation for α_{new}. Depending on the number of successes and total number of trials, the decision threshold was lowered to as much as 20%-50% of its original value [10].

MATERIALS AND METHODS

The three main components to this project include the mathematical derivation of equations used, simulation of data, and implementation into a detection system.

Mathematical Derivation

Five different probability distributions were used for this work: the Poisson distribution, Gaussian distribution, uniform distribution, triangular distribution, and sinusoidal distribution. Of these five, the Poisson distribution is the only discrete distribution. To calculate the decision threshold for a series of measurements, a new false positive error needs to be calculated for each scenario, p. The new false positive error is used to keep the false positive rate for background measurements constant.

To test whether or not the decision threshold for a series of measurements improves detection of radiation, equations for the classical decision threshold and for a series of measurements have been developed. The following steps are performed for the mathematical derivation:

1. Development of the probability density distributions
2. Creating an equation for p
3. Deriving y^*

The development of the probability density function is accomplished by creating equations for different regions of the probability density function and ensuring that conditions in Equations 16 and 17 are met. This is accomplished by solving for a constant such that the integral of the probability density function is 1.

$$1 = \int_{-\infty}^{\infty} p(x)dx \quad (43)$$

The decision threshold for a time series is accomplished by creating a new false positive error, p, that keeps the false positive rate for background measurements constant. The probability of exceeding the decision threshold can be calculated by setting the random variable X in Equation 27 to be the probability that the decision threshold is exceeded. A success would be when the decision threshold is exceeded. The probability of exceeding the decision threshold would be α, the false positive error; while the probability of failure is $1 - \alpha$. A series of N measurements is investigated, and compared to the decision threshold for a single measurement. Two situations are assessed: when exactly n successes are desired (decision threshold is exceeded n out of N times) and when at least n successes are desired in a series of N measurements.

The classical decision threshold is developed by setting the integration from -∞ to the decision threshold, y^*, equal to $1 - \alpha$. The equation is then solved for y^*.

$$1 - \alpha = \int_{-\infty}^{y^*} f(x)dx \quad (44)$$

Similarly, for the time series measurements, the decision threshold is calculated through the following equation:

$$1 - p = \int_{-\infty}^{y^*} f(x)dx \quad (45)$$

An illustration of the calculation of the decision threshold is provided in Figure 8.

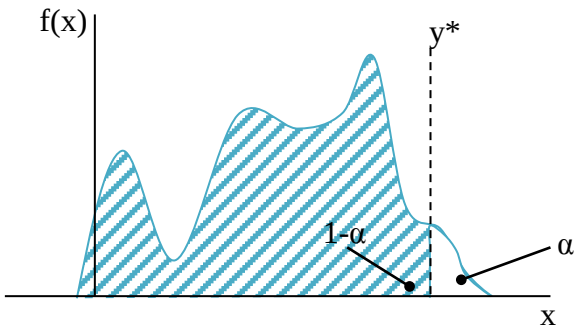

Figure 8 Decision Threshold for a Probability Density Function, f(x)

The probability density function was sampled using Monte Carlo sampling with the inversion technique. For the functions analyzed, the probability distribution or cumulative probability function were derived using Equation 9 and Equation 18, respectively. Inversion sampling transforms a uniform distribution using the probability distribution or cumulative distribution function, such that a non-uniform probability density function can be sampled.

A random number, u, is generated from a standard uniform distribution between 0 and 1. A value for x is computed such that:

$$F(x) = u \tag{46}$$

The value x is then the number drawn to describe F. The continuous uniform random variable U is related to the random variable X by the inversion:

$$X = F^{-1}(U) \tag{47}$$

Simulation of Data

Theoretical values were calculated using deterministic and stochastic techniques. Calculations were performed with Excel, and random numbers were generated using R, a data analysis software. For both techniques, the source probability density function was created two different ways: as the sum of a probability density function for the source and a probability density function for background; and as a probability density function of the sum of source and

background. For both deterministic and stochastic techniques, the predicted positive identification rate was calculated. Additionally, using stochastic techniques the time at first detection was calculated. Data were simulated for all five discussed distributions.

Using deterministic techniques, the predicted positive rate was calculated by determining the number of positives using the following equation, and dividing the result by the total number of trials.

$$Positives = \int_{-\infty}^{y^*} f(x)dx \tag{48}$$

Implementation into a Detection System

A Model 802-2x2 Scintillation detector by Canberra Industries Inc. (Meridan, CT) was used. The scintillation detector assembly includes a scintillation crystal, photomultiplier tube, and light shield, contained in aluminum housing. The scintillation crystal is a 2" by 2" sodium iodide (NaI) crystal. The detector has a resolution of 8.5% for the 662 keV peak of ^{137}Cs. The detector is attached at the base to a Model 2007P tube base and preamplifier. The signal from the preamplifier is further processed using a digital signal processor; for this application, a Lynx Digital Signal Processor by Canberra Industries Inc. (Meridan, CT) was used.

The Lynx Digital Signal Processor provides high voltage to the detector, as well as amplification and processing of the signal. The detector operates in several analysis modes; for this study, the multispectral scaling (MSS) mode is used. The MSS mode allows for continuous pulse height analysis (PHA) spectral acquisition; time between acquisitions is limited. The following figure, Figure 9, presents the signal processing chain for the detector.

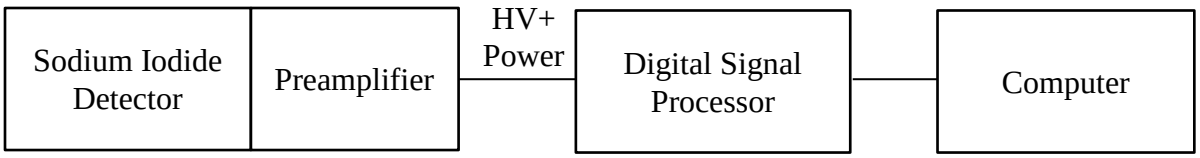

Figure 9 Signal Processing Chain for a NaI(Tl) Detector

Criteria Evaluated

The two main criteria evaluated were the positive identification rate and the time at first detection. These two criteria were used to compare different situations including:

- Exact and at least conditions
- Series length
- Number of successes in a series
- Different background strengths
- Different source strengths

RESULTS AND DISCUSSION

The results are reported in the same order as the distributions are presented in Materials and Methods – mathematical derivation, simulation of data, and implementation into a detection system. Additionally, a comparison between the simulation data and the implementation into a detection system is presented.

Mathematical Derivation

Each distribution is discussed individually and includes the derivation of the probability density function, classical decision threshold, time series decision threshold, and cumulative distribution function. After the discussion of each distribution, the development of the false positive error for a time series is described.

Uniform

The uniform distribution is uniform when $x \in (a, b)$. A depiction of the probability density function for the uniform distribution is provided in Figure 4 and Figure 10. The probability density function for the uniform distribution is calculated by recognizing that when $x \in (a, b)$ the function is equal to a constant value, d (Equation 49).

$$f(x) = \begin{Bmatrix} a \leq x \leq b & d \\ elsewhere & 0 \end{Bmatrix} \tag{49}$$

Using the characteristics of the probability density function outlined in Equations 16 and 17, the constant d is determined by setting the integral of the probability density function to 1, such that the probability density function is described by Equation 50.

$$f(x) = \begin{cases} a \leq x \leq b & \frac{1}{b-a} \\ elsewhere & 0 \end{cases} \quad 50$$

In the case where $a = 0$, Equation 50 reduces to:

$$f(x) = \begin{cases} 0 \leq x \leq b & \frac{1}{b} \\ elsewhere & 0 \end{cases} \quad 51$$

Once the probability density function is known, the decision threshold, y^*, is determined using Equation 44. A symbolic depiction of the calculation of y^* is provided in Figure 10, and the equation for y^* is provided in Equation 52.

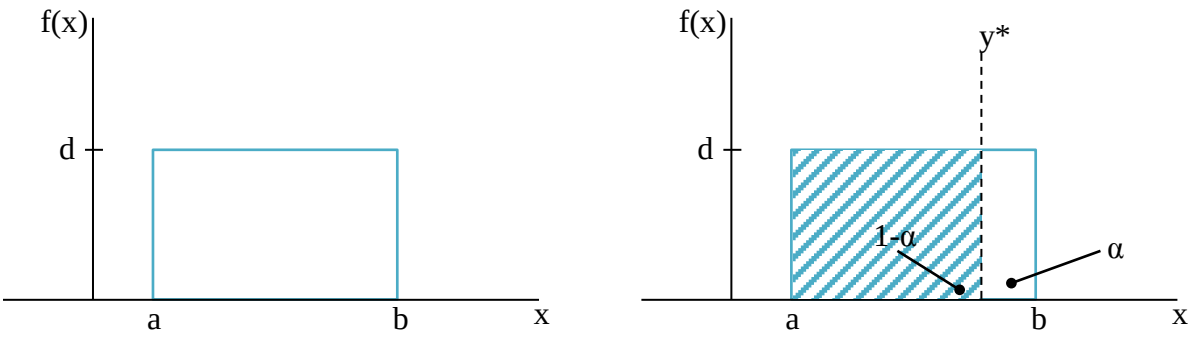

Figure 10 Calculation of y* for the Uniform Distribution

$$y^* = (1-\alpha)(b-a) + a \quad 52$$

If $a = 0$, the equation for the decision threshold simplifies to:

$$y^* = b(1-\alpha) \quad 53$$

To sample from the distribution, the cumulative distribution function needs to be calculated. The cumulative distribution function for a value x represents the likelihood that $X < x$ and is calculated using Equation 18. A schematic depiction of the calculation of the cumulative distribution function is provided in Figure 11, and the equation for the cumulative distribution function is provided in Equation 54.

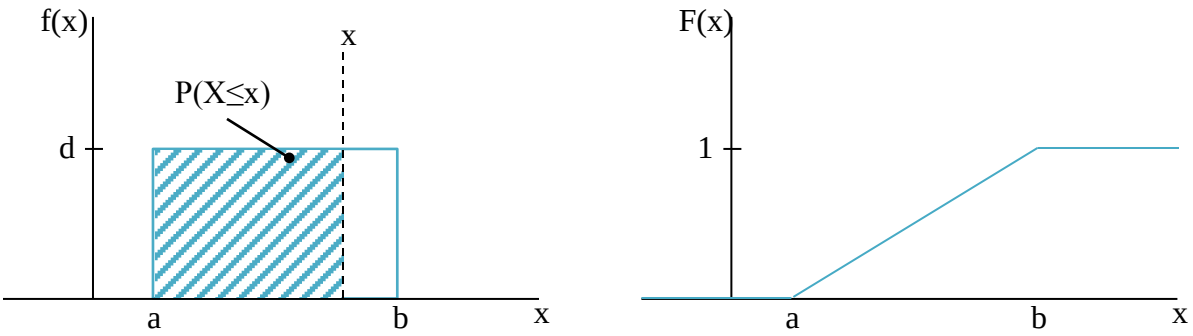

Figure 11 Calculation of the Cumulative Distribution Function for the Uniform Distribution

$$F(x) = \begin{Bmatrix} -\infty < x < a & 0 \\ a \leq x < b & \frac{x-a}{b-a} \\ b \leq x < \infty & 1 \end{Bmatrix} \quad 54$$

If a=0, the cumulative distribution function reduces to Equation 55.

$$F(x) = \begin{Bmatrix} -\infty < x < 0 & 0 \\ 0 \leq x < b & \frac{x}{b} \\ b \leq x < \infty & 1 \end{Bmatrix} \quad 55$$

To perform an inversion, the continuous uniform value u of the standard uniform random variable U is related to the cumulative distribution function as shown in Equation 46. When U is sampled, it can be related to the random variable X through Equation 47, such that

$$x(u) = \begin{Bmatrix} 0 \leq u \leq 1 & u(b-a)+a \\ elsewhere & 0 \end{Bmatrix} \quad 56$$

For $a = 0$, Equation 56 reduces to Equation 57.

$$x(u) = \begin{Bmatrix} 0 \leq u \leq 1 & ub \\ elsewhere & 0 \end{Bmatrix} \quad 57$$

Triangular

The triangular distribution consists of two components: a line with a positive slope (m_1) when $x \in (a, b)$; and a line with a negative slope (m_2) when $x \in (b, c)$. The resulting probability density function is a piecewise function with a maximum probability of d when $x = b$. The probability density function is depicted in Figure 4 and Figure 12. To create the probability density function, the two line equations necessary. The slopes can be calculated in terms of the maximum probability, d:

$$m = \begin{Bmatrix} m_1 = \dfrac{d}{c-a} \\ m_2 = -\dfrac{d}{b-c} \end{Bmatrix} \tag{58}$$

The equations for the lines are then determined; they assume the following functional forms:

$$f(x) = \begin{Bmatrix} a \le x < b & \dfrac{d(x-a)}{c-a} \\ b \le x < c & \dfrac{d(b-x)}{b-c} \\ elsewhere & 0 \end{Bmatrix} \tag{59}$$

The constant d is determined by setting the integral of the probability density function equal to 1 (Equation 17). The resulting probability density function is provided in Equation 60.

$$f(x) = \begin{Bmatrix} a \le x < b & \dfrac{2(x-a)}{(b-a)(c-a)} \\ b \le x < c & \dfrac{2(b-x)}{(b-a)(b-c)}x \\ elsewhere & 0 \end{Bmatrix} \tag{60}$$

In the case where $a = 0$, Equation 60 reduces to:

$$f(x) = \begin{Bmatrix} 0 \le x < c & \frac{2(x-a)}{cb} \\ c \le x \le b & \frac{2(b-x)}{b(b-c)}x \\ elsewhere & 0 \end{Bmatrix} \quad 61$$

The decision threshold is calculated by integrating the probability density function between -∞ and y^*, setting the integral to 1-α, and solving for y^*; as described in Figure 12. Due to the piecewise nature of the triangular distribution, two distinct cases need to be considered: when $y^* \in (a, c)$ or when $y^* \in (c, b)$. The equation for the decision threshold is provided in Equation 62. To calculate the decision threshold, an initial check needs to determine whether y^* is greater than or less than b.

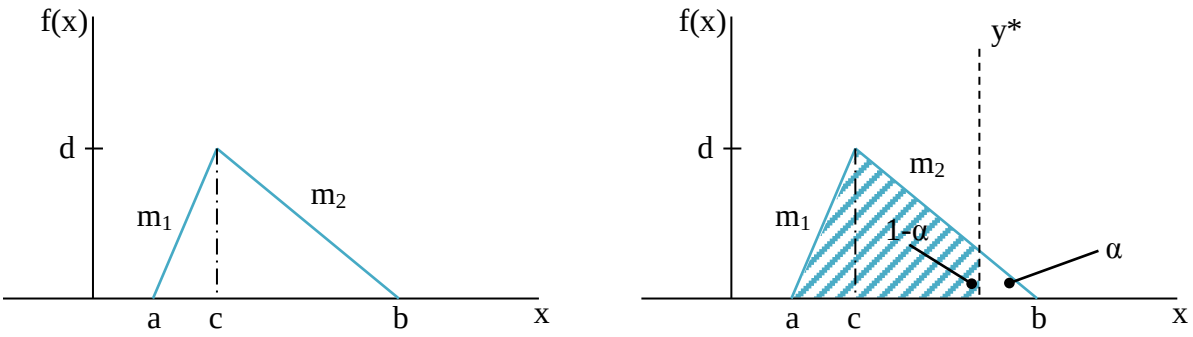

Figure 12 Calculation of y* for the Triangular Distribution

$$y^* = \begin{Bmatrix} a \le y^* < c & a + \sqrt{(1-\alpha)(b-a)(c-a)} \\ c \le y^* \le b & c - \sqrt{\alpha(b-c)(b-a)} \end{Bmatrix} \quad 62$$

For the case where $a = 0$, the equation for the decision threshold reduces to Equation 63.

$$y^* = \begin{Bmatrix} 0 \le y^* < c & \sqrt{cb(1-\alpha)} \\ c \le y^* \le b & b - \sqrt{\alpha b(b-c)} \end{Bmatrix} \quad 63$$

For the inversion for Monte Carlo sampling, the cumulative density function needs to be calculated. A depiction of the cumulative density function for the triangular distribution is shown in Figure 13, and the cumulative density function is provided in Equation 64.

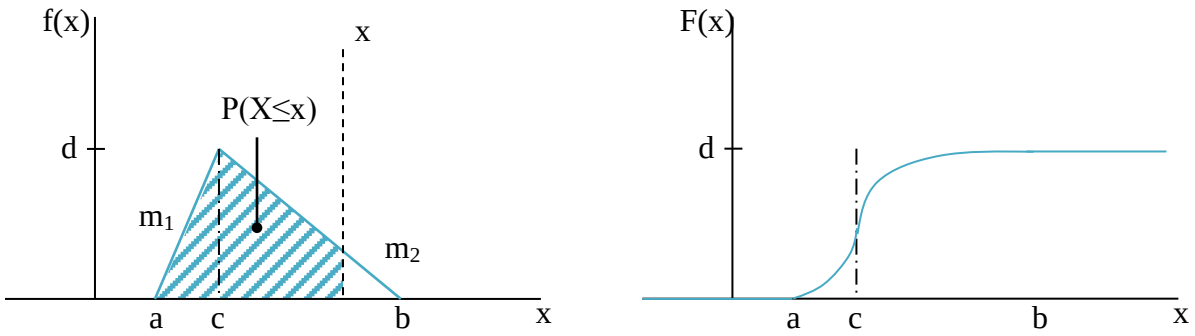

Figure 13 Calculation of the Cumulative Density Function for the Triangular Distribution

$$F(x) = \begin{Bmatrix} -\infty < x < a & 0 \\ a \le x < c & \dfrac{(x-a)^2}{(b-a)(c-a)} \\ c \le x < b & 1 - \dfrac{(x-b)^2}{(b-a)(b-c)} \\ b \le x < \infty & 1 \end{Bmatrix} \quad 64$$

For $a = 0$, Equation 64 reduces to Equation 65.

$$F(x) = \begin{Bmatrix} -\infty < x < 0 & 0 \\ 0 \le x < c & \dfrac{x^2}{bc} \\ c \le x < b & 1 - \dfrac{(x-b)^2}{b(b-c)} \\ b \le x < \infty & 1 \end{Bmatrix} \quad 65$$

Using the inversion technique in Equations 46 and 47, the random variable X can be related to the standard normal random variable U through Equation 66.

$$x(u) = \begin{Bmatrix} 0 \le u \le \dfrac{c-a}{b-a} & a + \sqrt{(c-a)(b-a)u} \\ \dfrac{c-a}{b-a} \le u \le 1 & b - \sqrt{(1-u)(b-a)(b-c)} \\ elsewhere & 0 \end{Bmatrix} \quad 66$$

If $a = 0$, Equation 66 reduces to Equation 67.

$$x(u) = \begin{cases} 0 \le u \le \frac{c}{b} & \sqrt{bcu} \\ \frac{c}{ba} \le u \le 1 & b - \sqrt{b(1-u)(b-c)} \\ elsewhere & 0 \end{cases} \quad 67$$

Sinusoidal

The sinusoidal distribution is zero at $x = a$ and exists between $x = a$ and $x = b$, where $b \le \frac{T}{2} + a$. The peak value of the probability density function at $x = a + \frac{T}{4}$ is equal to a value, d. A plot of the probability density function for the sinusoidal distribution is shown in Figure 6 and Figure 14. The probability density function for the sinusoidal distribution is a sine wave with an amplitude c, an angular frequency of $\omega = \frac{2\pi}{T}$, and a phase of $\varphi = a$; as described by Equation 68.

$$f(x) = \begin{cases} a \le x \le b & d \sin\left(\frac{2\pi}{T}(x-a)\right) \\ elsewhere & 0 \end{cases} \quad 68$$

Utilizing the characteristics of the probability density function in Equations 16 and 17, the constant d can be determined by setting the integral of the probability density function equal to 1. The probability density function can thus be described by Equation 69.

$$f(x) = \begin{cases} a \le x \le b & \frac{2\pi \sin\left(\frac{2\pi}{T}(x-a)\right)}{T\left[1 - \cos\left(\frac{2\pi}{T}(b-a)\right)\right]} \\ elsewhere & 0 \end{cases} \quad 69$$

In the case where $b = \frac{T}{2} + a$, Equation 69 becomes:

$$f(x) = \begin{Bmatrix} a \le x \le b & \dfrac{\pi \sin\left(\dfrac{\pi(x-a)}{b-a}\right)}{2(b-a)} \\ elsewhere & 0 \end{Bmatrix} \quad 70$$

If the phase $a = 0$, Equation 69 reduces to:

$$f(x) = \begin{Bmatrix} 0 \le x \le b & \dfrac{2\pi \sin\left(\dfrac{2\pi}{T}x\right)}{T\left[1 - \cos\left(\dfrac{2\pi}{T}b\right)\right]} \\ elsewhere & 0 \end{Bmatrix} \quad 71$$

In the case where the phase $a = 0$ and $b = T/2$:

$$f(x) = \begin{Bmatrix} 0 \le x \le b & \dfrac{\pi \sin\left(\dfrac{2\pi}{b}x\right)}{2b} \\ elsewhere & 0 \end{Bmatrix} \quad 72$$

After the probability density function is known, an equation for the decision threshold (y^*) can be derived by integrating the probability density function from -∞ to y^* and setting the integral to 1-α, as described by Equation 44. Figure 14 displays a depiction of the calculation of y^* and the equation for y^* is provided in Equation 73.

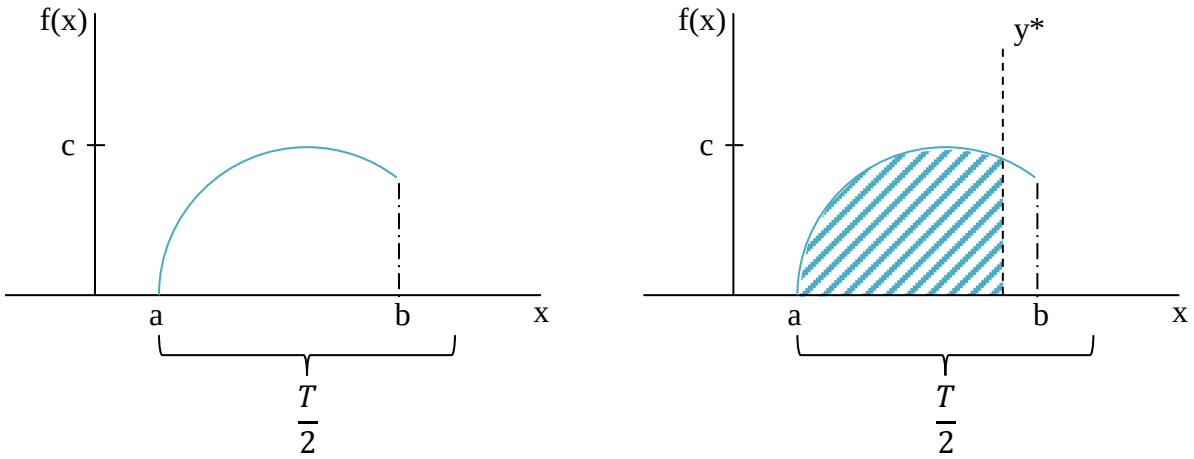

Figure 14 Calculation of y* for the Sinusoidal Distribution

$$y^* = \frac{T}{2\pi}\cos^{-1}\left[1-(1-\alpha)(1-\cos\left(\frac{2\pi(b-a)}{T}\right)\right] + a \quad 73$$

When $b = \frac{T}{2} + a$, Equation 73 can be rewritten as:

$$y^* = \frac{b-a}{\pi}\cos^{-1}[2\alpha - 1] + a \quad 74$$

If the phase $a = 0$, Equation 73 can be rewritten as Equation 75.

$$y^* = \frac{T}{2\pi}\cos^{-1}\left[1-(1-\alpha)(1-\cos\left(\frac{2\pi b}{T}\right)\right] \quad 75$$

In the case where $b = \frac{T}{2} + a$ and the phase $a = 0$, the equation reduces to the following:

$$y^* = \frac{b}{\pi}\cos^{-1}[2\alpha - 1] \quad 76$$

To sample from the sinusoidal distribution, an equation for the cumulative distribution function needs to be calculated. The cumulative distribution function can be calculated by using Equation 18. A descriptive image for the calculation of the cumulative distribution function for the sinusoidal function is shown in Figure 15, and the equation for the cumulative distribution function is provided in Equation 77.

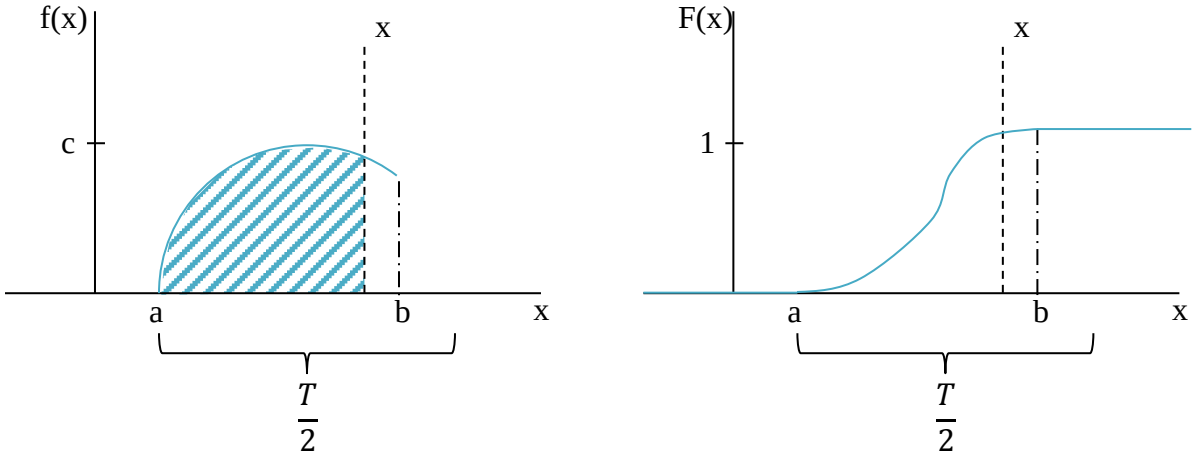

Figure 15 Calculation of the Cumulative Density Function for the Sinusoidal Distribution

$$F(x) = \begin{cases} -\infty < x < a & 0 \\ a \leq x < b & \dfrac{1 - \cos\left(\frac{2\pi}{T}(x-a)\right)}{1 - \cos\left(\frac{2\pi}{T}(b-a)\right)} \\ b \leq x < \infty & 1 \end{cases} \quad 77$$

Simplifications for the cumulative density function can be found in Equations 78, 79, and 80; for the cases where $a > 0$ and $b = \frac{T}{2} + a$, $a = 0$ and $b \leq \frac{T}{2} + a$, and $a = 0$ and $b = \frac{T}{2} + a$, respectively.

$$F(x) = \begin{cases} -\infty < x < a & 0 \\ a \leq x < b & \dfrac{1 - \cos\left(\frac{\pi(x-a)}{b-a}\right)}{2} \\ b \leq x < \infty & 1 \end{cases} \quad 78$$

$$F(x) = \begin{cases} -\infty < x < 0 & 0 \\ 0 \leq x < b & \dfrac{1 - \cos\left(\frac{2\pi}{T}x\right)}{1 - \cos\left(\frac{2\pi b}{T}\right)} \\ b \leq x < \infty & 1 \end{cases} \quad 79$$

$$F(x) = \begin{cases} -\infty < x < 0 & 0 \\ 0 \leq x < b & \dfrac{1 - \cos\left(\frac{\pi}{b}x\right)}{2} \\ b \leq x < \infty & 1 \end{cases} \quad 80$$

To perform an inversion, the sinusoidal random variable X needs to be related to a standard uniform random variable U. This can be accomplished using Equation 47, such that for a given value of u, x can be calculated using Equation 81.

$$x(u) = \begin{cases} 0 \le u < 1 & \frac{T}{2\pi}\cos^{-1}\left[1 - u\left(1 - \cos\left(\frac{2\pi(b-a)}{T}\right)\right)\right] + a \\ elsewhere & 0 \end{cases} \quad 81$$

The calculation of x from u can be simplified for the case where $a > 0$ and $b = \frac{T}{2} + a$, $a = 0$ and $b \le \frac{T}{2} + a$, and $a = 0$ and $b = \frac{T}{2} + a$. The equations corresponding to the listed simplifications are provided in Equations 82, 83, and 84, respectively.

$$x(u) = \begin{cases} 0 \le u < 1 & \frac{b-a}{\pi}\cos^{-1}(1-2u) + a \\ elsewhere & 0 \end{cases} \quad 82$$

$$x(u) = \begin{cases} 0 \le u < 1 & \frac{T}{2\pi}\cos^{-1}\left[1 - u\left(1 - \cos\left(\frac{2\pi b}{T}\right)\right)\right] \\ elsewhere & 0 \end{cases} \quad 83$$

$$x(u) = \begin{cases} 0 \le u < 1 & \frac{b}{\pi}\cos^{-1}[1-2u] \\ elsewhere & 0 \end{cases} \quad 84$$

Poisson

The probability mass function for the Poisson distribution is given by Equation 36. The Poisson distribution is unique to the other distribution functions discussed, because it is a discrete function. Rather than using an integral to find a point where the cumulative density function is equal to 1-α, a summation will be performed between 0 and y^* (Equation 9). The summation is given as

$$1 - \alpha = \sum_{i=0}^{y^*} \frac{\mu^i}{i!} e^{-\mu} \quad 85$$

When simplified, Equation 85 can be rewritten as Equation 86. It should be noted that the decision threshold cannot be solved for explicitly and finding y^* is an iterative process.

$$(1-\alpha)e^{\mu} = 1 + \mu + \frac{\mu^2}{2!} + \frac{\mu^3}{3!} + \cdots + \frac{\mu^{y^*}}{(y^*)!} \quad 86$$

The cumulative distribution function for the Poisson distribution can be calculated using Equation 9. Due to the discrete nature of the Poisson distribution, the cumulative distribution function is a stepwise function that increases at each x value with the $p(x)$.

$$F(x) = \sum_{i=0}^{x} \frac{\mu^i}{i!} e^{-\mu} \quad 87$$

To relate a discrete random variable X and the standard uniform distribution U, the sample space is divided into x segments with the length of each segment corresponding to the probability of the outcome occurring. When the uniform distribution is sampled, a logical statement can then be used to determine which segment the value u falls in. The segment can then be related to the value of x.

Gaussian

The probability density function for the Gaussian distribution is given by Equation 38. The decision threshold can be calculated by adding the number of standard deviations away (the quantile or z_α) the false positive error (α) is to the mean, μ, as shown in Equation 88.

$$y^* = \mu + z_\alpha \sigma \quad 88$$

The cumulative distribution function for the Gaussian distribution cannot be expressed analytically. To complete the inversion technique, numerical techniques must be used. A built-in function within R uses a numerical technique to sample off the Gaussian distribution: rnorm.

Numbers can be sampled using the function rnorm by supplying the value of the mean and the standard deviation. The built in function, rnorm, is used for sampling.

False Positive Error for a Series of Measurements

The probability that the decision threshold is exceeded n times in a series of N measurements can be described by a binomial process (Equation 27), where the probability of exceeding the decision threshold is p and the probability of not exceeding the decision threshold is 1-p. When looking at a series of measurements, it is desired to keep the same false positive error α as for a single measurement.

If it is desired that exactly n measurements exceed the threshold in a series, the decision threshold for the series can be calculated by setting $p(n)$ equal to α, as follows:

$$p(n) = \alpha = \binom{N}{n} p^n (1-p)^{N-n} \quad 89$$

However, if it is desired that at least n measurements exceed the decision threshold, the individual probabilities need to be summed between n and N, and set to α (Equation 90).

$$p(n+) = \alpha = \sum_{n}^{N} \binom{N}{n} p^n (1-p)^{N-n} \quad 90$$

Equations 89 and 90 cannot be directly solved for p. Thus it is only possible to solve for p under select conditions of α, n, and N. In the following section, p will be calculated for select conditions.

Simulation of Data

Data is simulated for five different series lengths between 1 and 5 measurements. The number of measurements exceeding the decision threshold (successes), n, in the measurement

length, N, was allowed to vary between 1 and N. The value for $p(n)$ was calculated for each scenario using a fixed false positive error, α of 0.05. Data is simulated deterministically by using the probability mass function and predicting the positive rate, and stochastically by randomly generating off of the probability mass function.

The measurement data was simulated in two ways. First, the measurement data was simulated by generating off of a source distribution and background distribution and adding the values. The second method involved generating off of a distribution characterized by the sum of the source and background mean. Both methods are investigated. Two different analyses of the data were performed: when exactly n measurements are above the decision threshold and when there are at least n measurements above the decision threshold.

First the calculation of p for different series lengths will be outlined. Following is the data calculated using the deterministic method for the five spectra discussed previously using several background levels, source strengths, and series lengths. Afterwards, similar scenarios are evaluated using a stochastic method. Finally, the results from the deterministic and stochastic method are compared.

Calculation of p for Different Series Length

Values of p were calculated for five different lengths of series: 1, 2, 3, 4, and 5 measurements. The false positive error (α) was fixed at 0.05, such that 5% of the measurements at background will be positive identifications. When exactly n successes in a series of N measurements are desired, values as displayed in Table 2 are obtained. When at least n successes in a series of N measurements are desired, values as displayed in Table 3 are obtained. Interestingly, once the series length increases to 5 and the number of successes is 5, the p values increases to greater than 0.5, indicating that the corresponding threshold will be less than the

mean. The p values when n equals N are the same for exact and at least. Otherwise, the p values for the *exact* condition are smaller than the ones for the *at least* condition; this will yield higher decision threshold values for the *exact* condition.

Table 2 Calculated Values of p for Combinations of n and N between 1 and 5 (Exact)

N	n				
	1	2	3	4	5
1	0.95				
2	0.0253206	0.223607			
3	0.0169524	0.13535	0.368403		
4	0.0127415	0.0976115	0.248605	0.472871	
5	0.014282	0.0764404	0.189255	0.342592	0.5492803

Table 3 Calculated Values of p for Combinations of n and N between 1 and 5 (At Least)

N	n				
	1	2	3	4	5
1	0.95				
2	0.0256584	0.223607			
3	0.0172571	0.139142	0.368403		
4	0.013005	0.101612	0.256137	0.472871	
5	0.0102062	0.0801513	0.198114	0.352529	0.5492803

Deterministic

The deterministic method looked at the five distributions discussed previously: uniform, triangular, sinusoidal, Poisson, and Gaussian. Only the positive rate was looked at for the deterministic method. The following scenarios were looked at scenarios:

Table 4 Scenarios Looked at for the Deterministic Method

Criteria	Values
Background Levels	50, 100, 250, 500, 750, 1000, 2500, 5000, 7500, 10000
Source Strength	0, 1, 3, 5, 8, 10, 15, 30, 50 (for $f(x)$ and $F(x)$) 0, 1, 3, 5, 8, 10, 15, 20, 25, 30, 35, 40, 45, 50, 75, 100, 125, 150, 175, 200, 225, 250, 275, 300, 325, 350 (positive rate)
Series Length	1, 2, 3, 4, 5

The *at least* and *exact* conditions were compared using a Gaussian distribution. For each background condition the decision threshold was calculated. At a background level of 50, 500,

and 5000, the source level was calculated for 50% and 100% positive rate. Representative plots for each of the five distributions were displayed for series of three measurements and include plots of the probability density function and cumulative distribution function, positive rate as a function of source strength for background equal to 500 ($b = 500$), positive rates for source equal to 10 ($s = 10$) and $b = 500$ for different combinations of n, and positive rate as a function of source strength/background for $n = 2$ for different backgrounds.

At Least vs. *Exact*

The two conditions of exactly n successes in a series of N measurements and at least n successes in a series of N measurements were compared for the Gaussian distribution at $b = 500$. Figure 16 contains a comparison of the positive rate with source strength for the exact and at least conditions using a series of two measurements. Figures for other values of N for the exact and at least conditions are in Appendix A in Figure 110 (Gaussian, $b = 500$, $N = 2$, $N = 3$) and Figure 111 (Gaussian, $b = 500$, $N = 4$, $N = 5$).

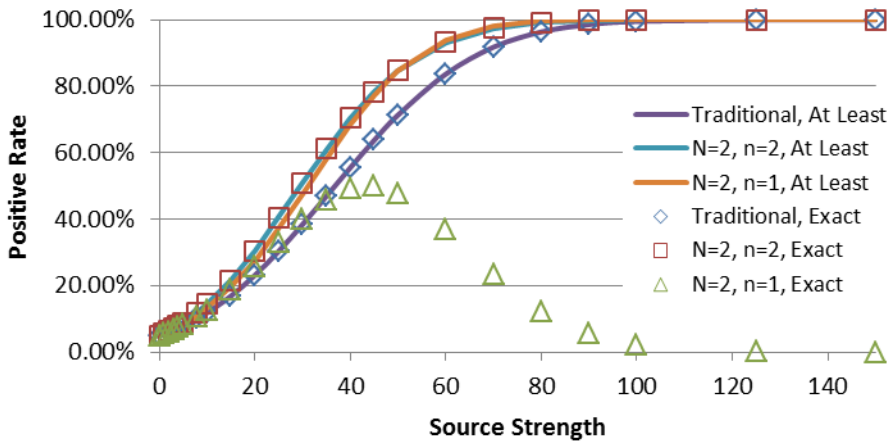

Figure 16 Positive Rate Comparison with Source Strength for the At Least and Exact Conditions (Gaussian, N=2, Deterministic)

As seen in Figure 16, there is no difference between techniques where the desired number of successes is equal to the number of measurements. When n is equal to N, Equations 89 and 90

converge resulting in the same values. For exact conditions when n does not equal N, the positive rate initially increases until reaching a maximum around 50% and then decreases. As source strength increases the likelihood of exceeding the decision threshold will increase, making the condition less likely. Due to this future discussed analysis will use the at least condition.

Rectangular

The width of the rectangular distribution was chosen such that the variance was equal to the variance for the Poisson distribution (μ). The probability density functions for each background level is in Figure 17. As the background level increases, the probability density function becomes wider and the probability of occurrence decreases.

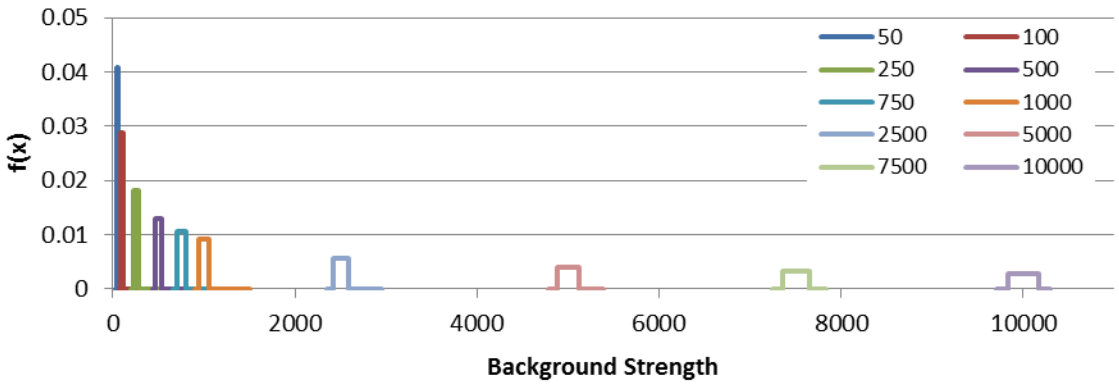

Figure 17 Probability Density Function for Different Background Levels (Rectangular, Deterministic)

Three background distributions will be discussed in depth: at 50, 500, and 5000. The generated source and background distribution for the rectangular distribution at $b = 50$, $b = 500$, and $b = 5000$ is in Figure 18. The plotted distributions are for source strengths between 0 and 50. As seen by Figure 18, the source and background distribution for the rectangular distribution changes the most significantly for lower background levels. As the source strength increases, the distribution widens.

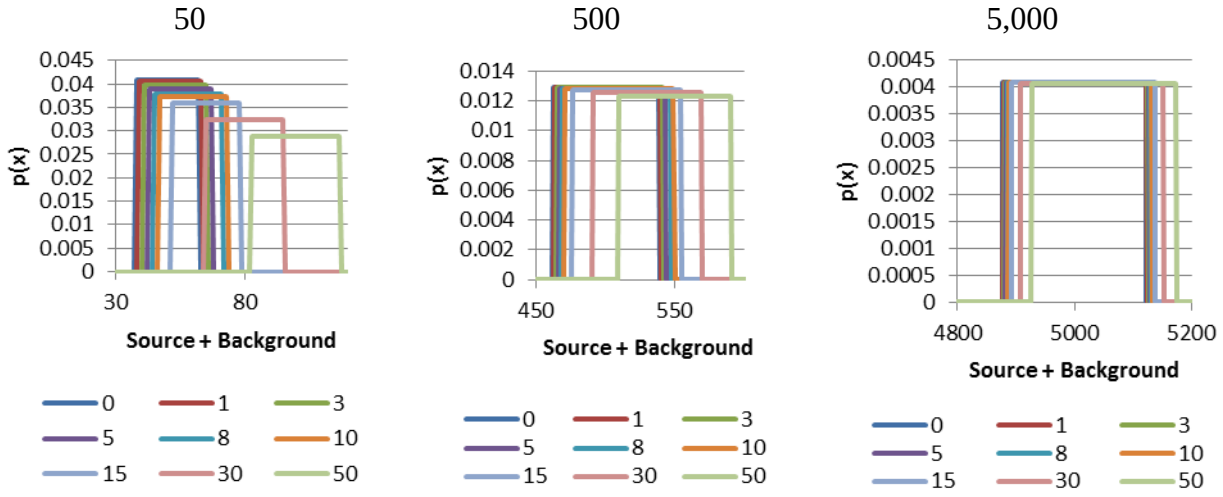

Figure 18 Probability Density Function at Different Source Strengths (Rectangular, b=50, 500, and 5000, Deterministic)

The calculated values for the decision threshold (y^*) for the rectangular distribution at a background of 50, 500, and 5000 are located in Table 5. Calculated decision thresholds for the rectangular distribution at all background strengths are contained in Table 12.

Table 5 Calculated Values of y^* and Source Strength at 50% and 100% Detection (Rectangular, Deterministic)

		y^*			50% Detection			100% Detection		
		Background Strength			Background Strength			Background Strength		
N	n	50	500	5000	50	500	5000	50	500	5000
1	1	61	535	5110	12	35	111	25	75	234
2	2	57	521	5068	13	39	120	20	61	191
	1	62	537	5116	7	21	66	25	77	240
3	3	53	510	5032	12	34	105	20	50	156
	2	59	528	5089	9	29	90	23	71	213
	1	62	537	5118	5	15	47	26	78	240
4	4	51	502	5007	10	30	91	14	42	130
	3	56	519	5062	10	29	90	20	59	185
	2	60	531	5099	7	23	71	24	71	222
	1	62	538	5119	4	12	36	26	76	233
5	5	49	496	4988	9	26	80	12	36	111
	4	54	512	5039	9	27	85	17	52	162
	3	58	524	5076	8	25	77	21	64	200
	2	60	533	5104	6	19	58	24	72	221
	1	62	538	5120	3	9	29	25	73	224

As the series length increases, the calculated y^* for the rectangular distribution increases for the same condition (larger N, but constant n). Additionally as the number of successes (times

exceeding the decision threshold) approaches the series length, the calculated y^* decreases for the rectangular distribution. Also listed in Table 5 is the source strength at which 50% and 100% detection is achieved. The ratio of the source strength to background strength for the rectangular distribution at the same conditions and level of detection decreases as background strength increases.

Trends in the positive rate for the rectangular distribution are illustrated through several representative figures for a series length of three. Additional figures are located in Appendix A and will be noted when available. Figure 19 contains a visual representative of the thresholds for a series of three measurements at $b = 500$. The probability density function and cumulative distribution for the rectangular distribution are displayed for a variety of source strengths. Additional graphs of the probability density function for different N is available in Figure 117 ($N = 2$), Figure 118 ($N = 3$), Figure 119 ($N = 4$), and Figure 120 ($N = 5$).

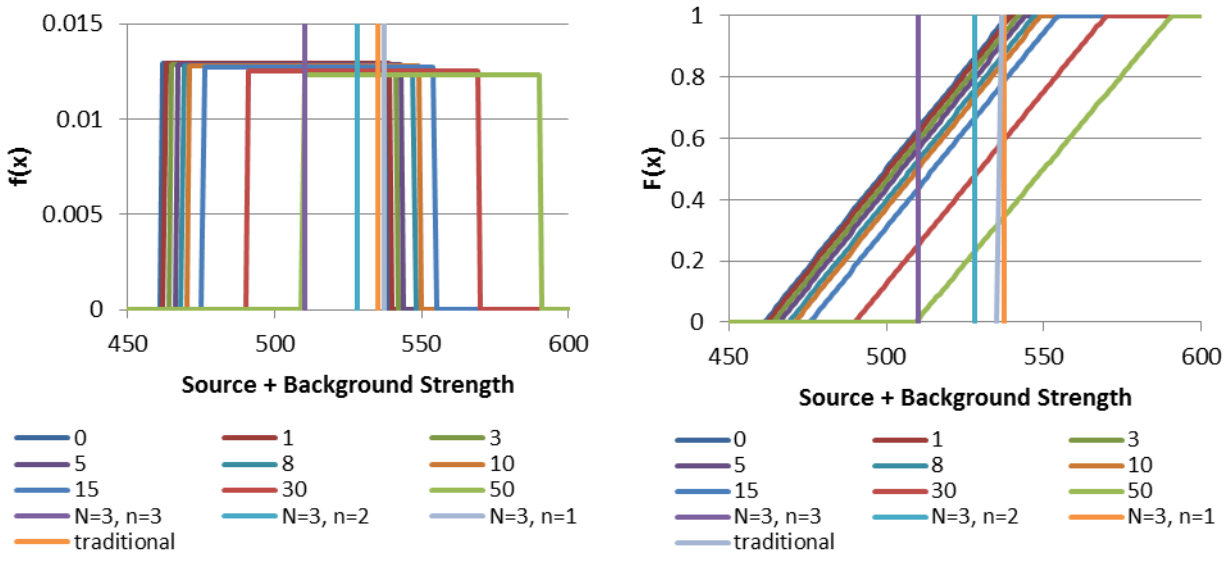

Figure 19 Probability Density Function and Cumulative Distribution for Different Source Strengths with Decision Thresholds for Different n Values (Rectangular, b=500, N=3, Deterministic)

Figure 20 contains a graph of the positive rate for the rectangular distribution with source strength for a series of three measurements. Additional graphs of the positive rate with

source strength for different N is available in Figure 117 ($N = 2$), Figure 118 ($N = 3$), Figure 119 ($N = 4$), and Figure 120 ($N = 5$).

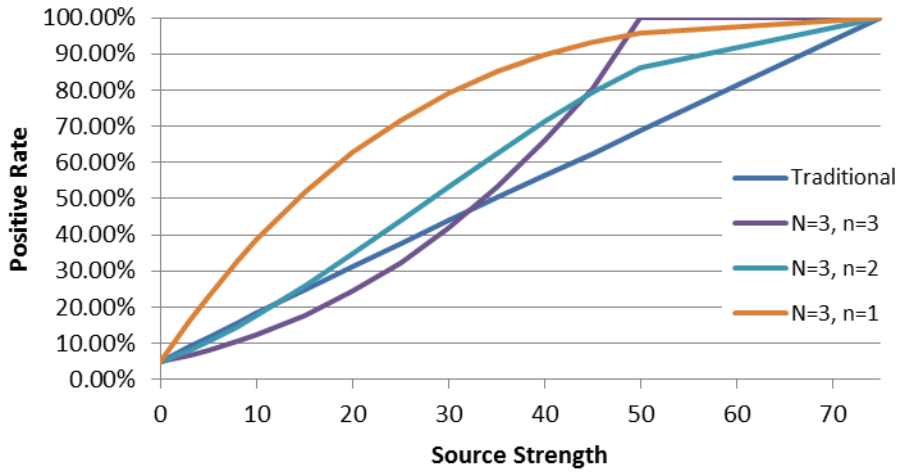

Figure 20 Positive Rate with Source Strength for Different n Values (Rectangular, b=500, N=3, Deterministic)

For the rectangular distribution, the positive rate using the traditional method ($N = 1, n = 1$) increases approximately linearly with source strength. When $n = 1$, the positive rate for the rectangular distribution increases rapidly at low source strength and then approaches 100% more slowly with increased source strength. At the other extreme, when $n = N$, the rectangular distribution positive rate increases slowly at low source strength and then more rapidly at higher source strengths, reaching 100% positives more quickly. For conditions between the two extremes, the relationship between positives and source strength is closer to a straight line.

The differences between the positive rate for the rectangular distribution for different conditions is highlighted in a bar graph in Figure 21 for a background of 500 and source strength of 10. For the rectangular distribution the positive rate is largest for the lower number of successes required ($n = 1$). The traditional method outperforms the conditions $n = 2$ and $n = 3$ for $N = 3$.

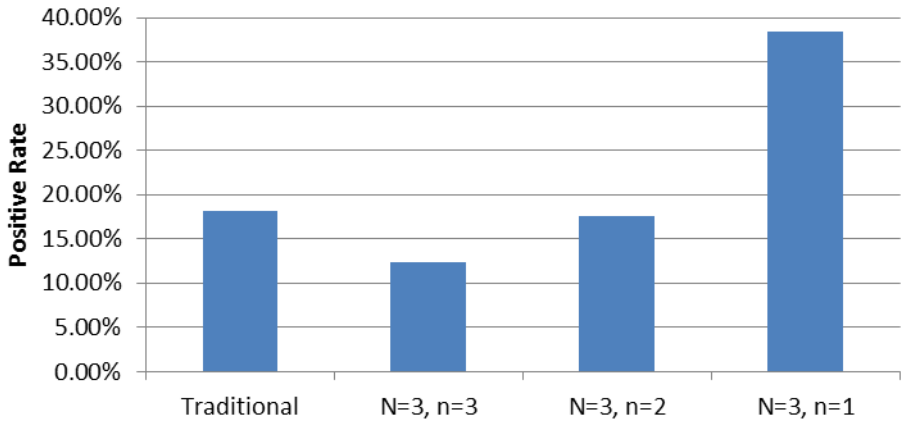

Figure 21 Positive Rate for Different n Values (Rectangular, b=500, s=10, N=3, Deterministic)

Figure 22 contains a graph for N=3, n=2 for different source to background strength ratios for the rectangular distribution. For larger backgrounds, 100% positive rate is achieved at lower source strength to background ratios (as seen in Table 5). Additional figures for the rectangular distribution for other series lengths are in Figure 112 (Traditional), Figure 113 ($N = 2$), Figure 114 ($N = 3$), Figure 115 ($N = 4$), and Figure 116 ($N = 5$).

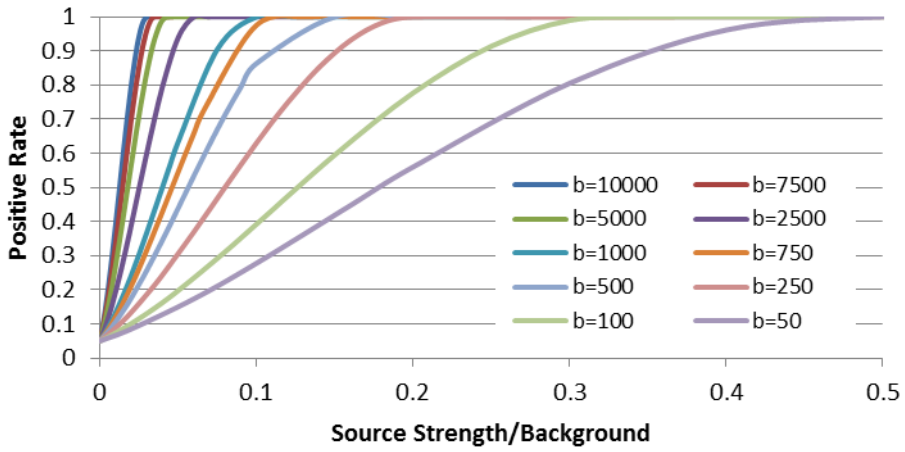

Figure 22 Positive Rate with Source/Background Strength at Different Background (Rectangular, N=3, Deterministic)

Triangular

The triangular distribution modeled is a symmetric triangle where $a = \mu - 3\sqrt{\mu}$ and $b = \mu + 3\sqrt{\mu}$ to approximate the width of the Gaussian distribution. A graph of the probability

function for each background level is located in Figure 23. Similar to the rectangular distribution, as the mean background increases, the probability density function widens and the probability of the peak occurrence lessens.

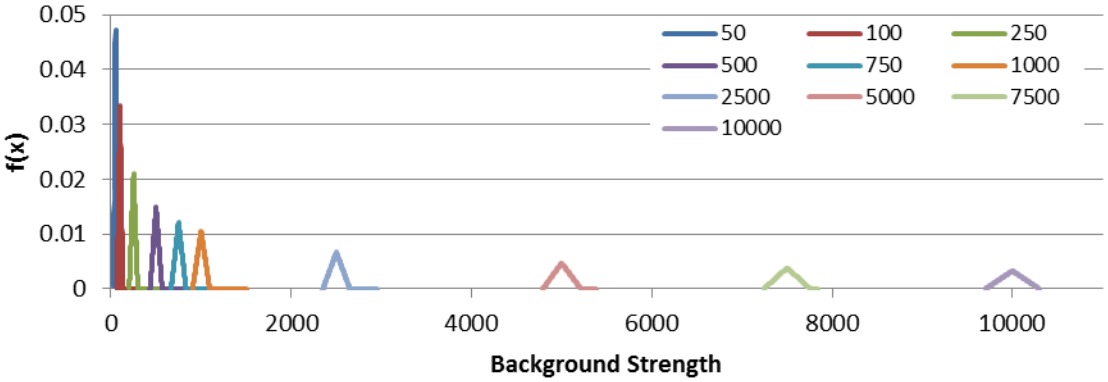

Figure 23 Probability Density Function for Different Background Levels (Triangular, Deterministic)

The background distributions at 50, 500, and 5000 will be discussed in depth. The generated source and background probability density function for the triangular distribution at $b = 50$, $b = 500$, and $b = 5000$ is in Figure 24. The plotted distributions are for source strengths between 0 and 50. As seen by Figure 24, the probability density function for the triangular distribution changes the most significantly for lower background levels. As the source strength increases, the distribution widens.

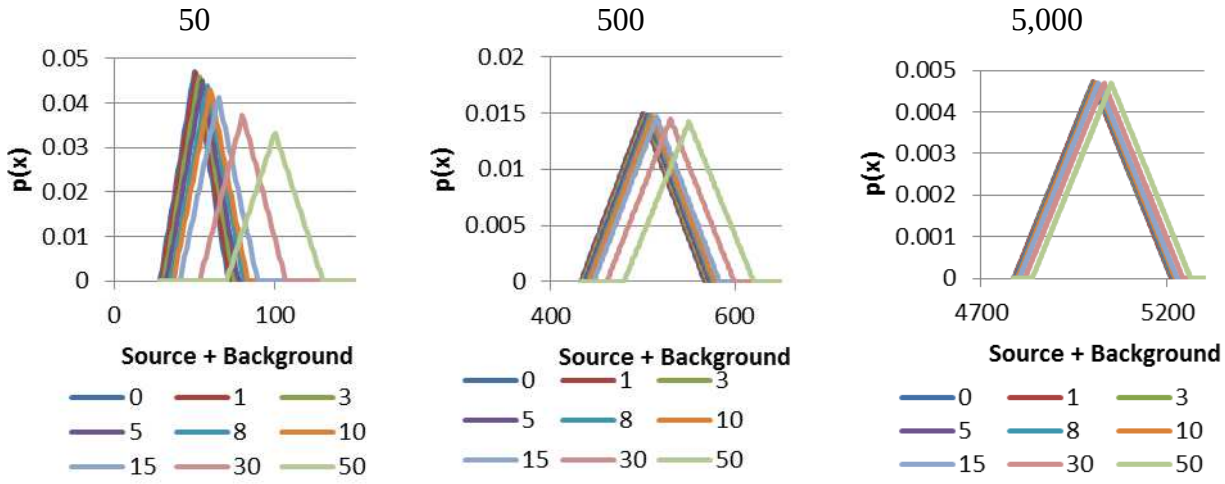

Figure 24 Probabity Density Function at Different Source Strengths (Triangular, b=50, 500, and 5000, Deterministic)

The calculated values for the decision threshold (y^*) for the triangular distribution at a background of 50, 500, and 5000 are located in Table 6. Calculated decision thresholds for all background strengths are contained in Table 13 within Appendix A.

Table 6 Calculated Values of y^* and Source Strength at 50% and 100% Detection (Triangular, Deterministic)

		y^*			50% Detection			100% Detection		
		Background Strength			Background Strength			Background Strength		
N	n	50	500	5000	50	500	5000	50	500	5000
1	1	64	586	5145	15	46	145	44	120	363
2	2	57	522	5070	13	39	121	35	95	287
	1	66	552	5164	11	36	114	42	118	358
3	3	53	509	5030	12	35	107	30	82	247
	2	60	532	5102	11	33	102	36	99	301
	1	67	555	5173	9	30	97	38	109	333
4	4	51	502	5006	11	33	100	27	74	222
	3	56	520	5063	9	29	89	32	87	264
	2	62	537	5118	9	29	93	34	95	290
	1	68	556	5178	8	27	85	34	100	308
5	5	49	497	4989	11	31	95	25	68	205
	4	54	512	5037	9	26	81	29	79	240
	3	58	526	5082	9	26	82	30	85	259
	2	63	541	5129	9	27	85	31	90	274
	1	68	557	5182	7	24	77	31	93	286

As with the rectangular distribution as the series length (N) increases, the calculated y^* increases for the same condition (constant n). As the number of times exceeding the decision threshold (number of successes) approaches the series length the calculated value of y^* decreases. Table 6 also contains information on the source strength required to achieve 50% and 100% detection. The ratio of the source strength to background strength for the same conditions and level of detection decreases as background strength increases.

Trends in the positive rate for the triangular distribution are illustrated through several representative figures for a series length of three (additional figures are located in Appendix A and are noted when applicable). Figure 25 contains a visual representative of the thresholds for the triangular distribution for a series of three measurements at $b = 500$. The probability density

function and cumulative distribution for the triangular distribution are displayed for a variety of source strengths. Additional graphs of the probability density function for different N are available in Figure 126 ($N = 2$), Figure 127 ($N = 3$), Figure 128 ($N = 4$), and Figure 129 ($N = 5$).

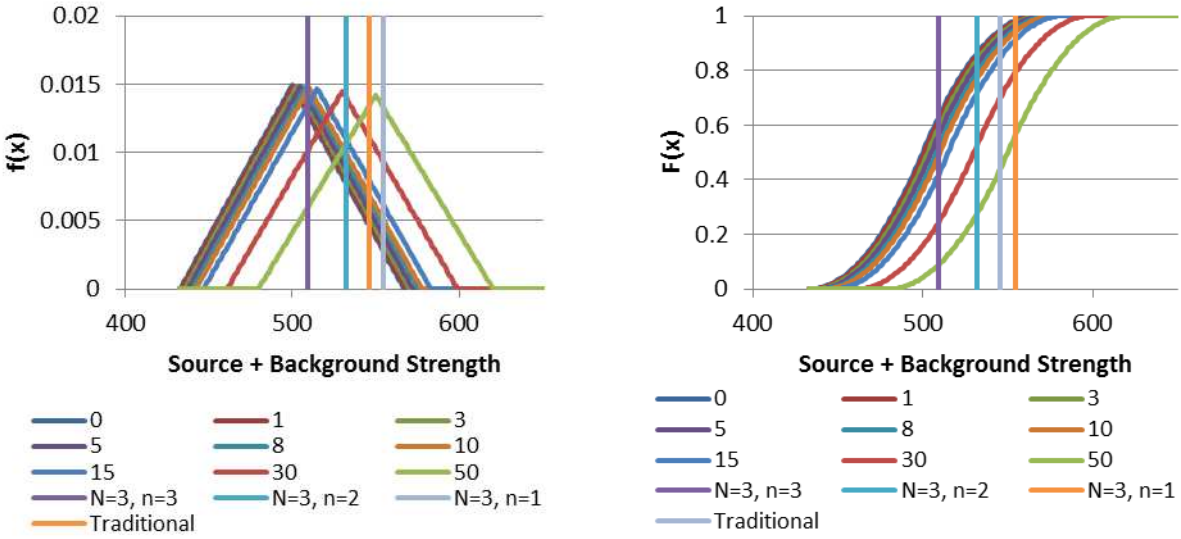

Figure 25 Probability Density Function and Cumulative Distribution for Different Source Strengths with Decision Thresholds for Different n Values (Triangular, b=500, N=3, Deterministic)

Figure 20 contains a graph of the positive rate for the triangular distribution with source strength for a series of three measurements.

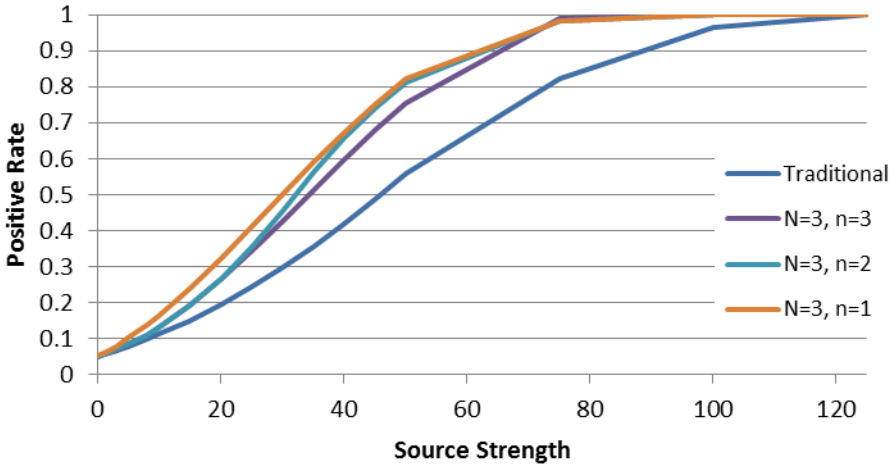

Figure 26 Positive Rate with Source Strength for Different n Values (Triangular, b=500, N=3, Deterministic)

For the triangular distribution, the positive rate for all conditions has a similar shape to the cumulative distribution function, increasing slowly at first, increasing more rapidly, and then more slowly. The values for all conditions of the measurement series are approximately the same for the triangular distribution as seen also in Table 6. All three conditions outperform the traditional method in terms of positive rate. Additional figures for other series lengths are in Figure 126 ($N = 2$), Figure 127 ($N = 3$), Figure 128 ($N = 4$), and Figure 129 ($N = 5$).

The differences between the positive rate for the triangular distribution using different conditions is highlighted in a bar graph in Figure 27 for $b = 500$ and $s = 10$. For the triangular distribution the positive rate is largest for the lower number of successes required ($n = 1$). Unlike the rectangular distribution, all conditions for the triangular distribution at $N = 3$ outperform the traditional method.

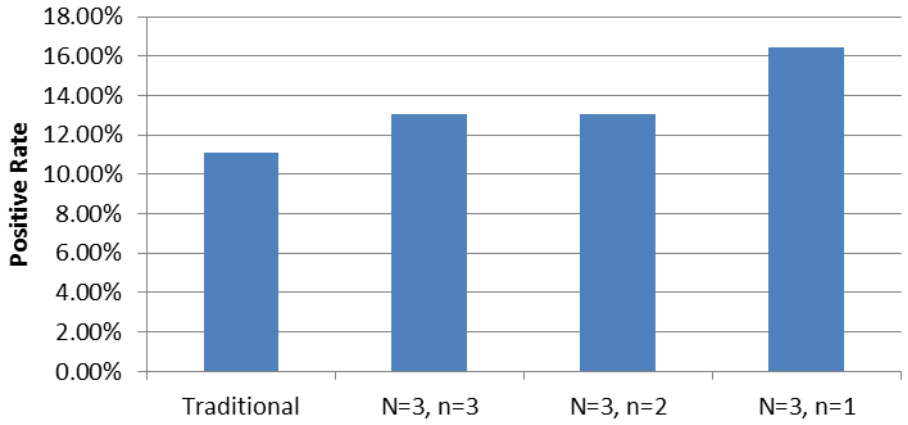

Figure 27 Positive Rate for Different n Values (Triangular, b=500, s=10, N=3, Deterministic)

Figure 28 contains a graph of the positive rate for the triangular distribution with source to background strength ratio for the condition $N = 3, n = 2$. Each background yields a similar shaped graph. For larger backgrounds, 100% positive rate is achieved at lower source strength to background ratios (as seen in Table 6). Additional figures of other series lengths for the

triangular distribution are located in Figure 121 (Traditional), Figure 122 ($N = 2$), Figure 123 ($N = 3$), Figure 124 ($N = 4$), Figure 125 ($N = 5$).

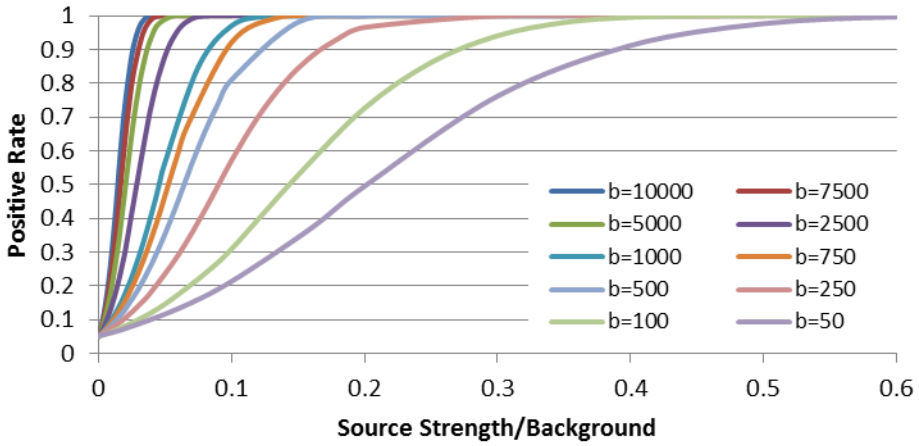

Figure 28 Positive Rate with Source/Background Strength at Different Background (Triangular, N=3, n=2, Deterministic)

Sinusoidal

The sinusoidal distribution was modeled as half of a sine wave, where $T = 2(b - a)$, $a = \mu - 3\sqrt{\mu}$, and $b = \mu + 3\sqrt{\mu}$ to approximate the width of the Gaussian distribution. A graph of the probability density function for the sinusoidal distribution at each background level for the sinusoidal distribution is located in Figure 29. Similar to the distributions previously discussed, as the mean background increases, the probability density function widens and the probability of the peak occurrence lessens.

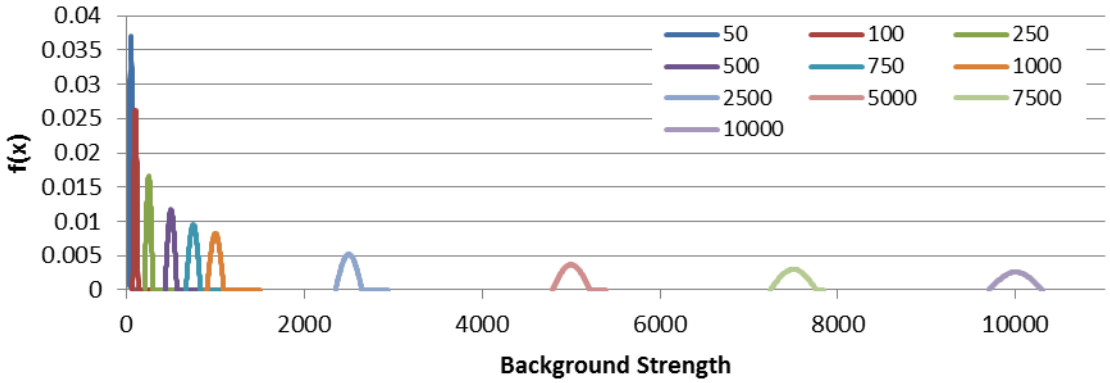

Figure 29 Probability Density Function for Different Background Levels (Sinusoidal, Deterministic)

Trends in positive rate for the sinusoidal distribution are discussed for $b = 50$, $b = 500$, and $b = 5000$. Figure 30 contains the generated source and background probability density function for the sinusoidal distribution for source strengths between 0 and 50.

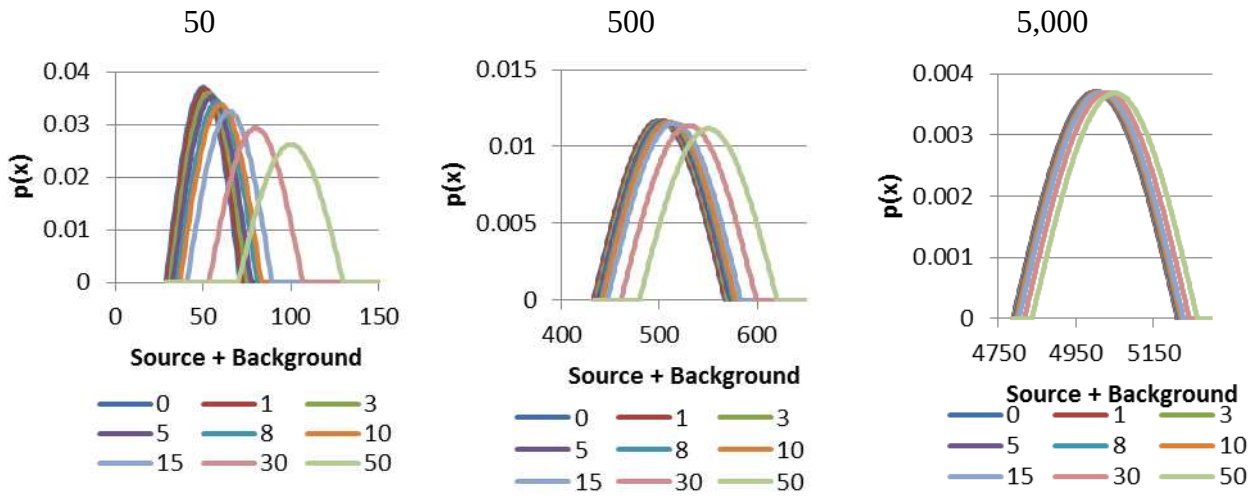

Figure 30 Probability Density Function at Different Source Strengths (Sinusoidal, b=50, b=500, b=500, Deterministic)

As seen in Figure 30, the source and background distribution for the sinusoidal distribution changes the most significantly for lower background levels. As the source strength increases, the distribution widens.

The decision threshold (y^*) is calculated at a background of 50, 500, and 5000 for the sinusoidal distribution; calculated values are located in Table 7. Calculated decision thresholds for all background strengths are contained in Table 14 within Appendix A. As seen by the previous distributions discussed, as the series length increases y^* decreases for the same conditions and as the number of successes (times exceeding the decision threshold) approaches the series length y^* decreases. Table 7 also contains the source strength at which 50% and 100% detection is achieved for the sinusoidal distribution. The ratio of the source strength to background strength for the same conditions and level of detection decreases as background strength increases.

Table 7 Calculated Values of y^* and Source Strength at 50% and 100% Detection (Sinusoidal, Deterministic)

		y^*			50% Detection			100% Detection		
		Background Strength			Background Strength			Background Strength		
N	n	50	500	5000	50	500	5000	50	500	5000
1	1	64	546	5145	15	46	145	44	121	363
2	2	57	522	5070	13	39	121	35	96	387
	1	66	552	5164	11	36	114	44	122	358
3	3	53	509	5030	12	35	107	30	82	247
	2	60	532	5102	11	33	102	37	103	301
	1	67	555	5173	9	30	97	41	116	333
4	4	51	502	5006	11	33	100	27	74	222
	3	56	520	5063	9	29	89	33	90	264
	2	62	537	5118	9	30	93	36	101	290
	1	68	556	5178	8	27	85	38	108	308
5	5	49	497	4989	11	31	95	25	69	205
	4	54	512	5037	9	26	81	30	82	240
	3	58	526	5082	9	26	82	32	90	259
	2	63	541	5129	9	27	85	34	96	274
	1	68	557	5182	7	24	77	35	101	286

Trends in the positive rate for the sinusoidal distribution are illustrated using a series of three measurements. Additional figures for other series lengths are located in Appendix A and will be noted when available. A visual representative of the thresholds for a series of three measurements at a background of 500 for the sinusoidal distribution is in Figure 31.

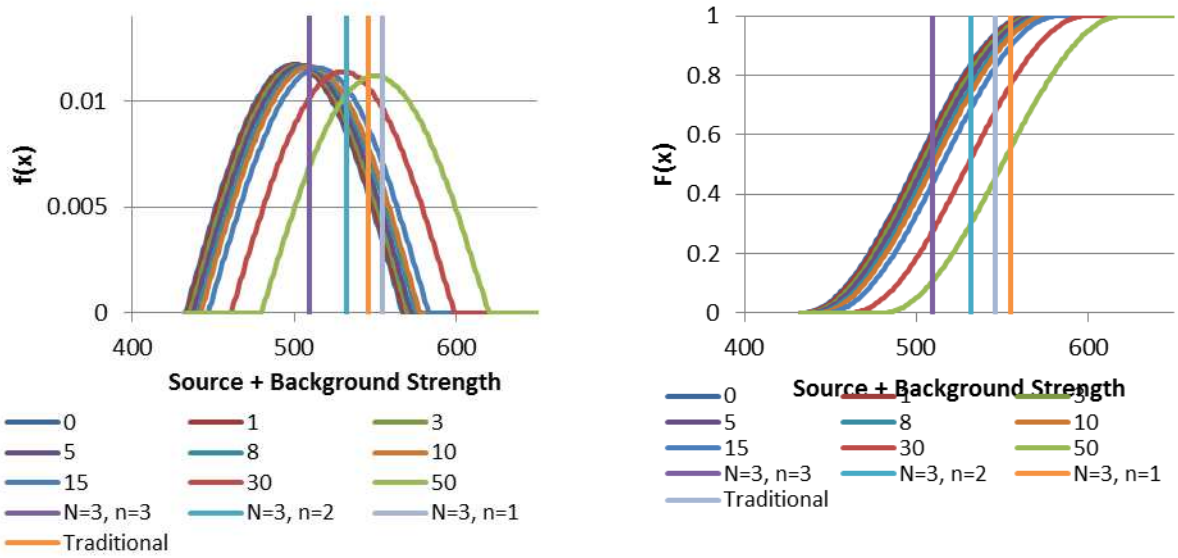

Figure 31 Probability Density Function and Cumulative Distribution for Different Source Strengths with Decision Threshold for Different n Values (Sinusoidal, b=500, N=3, Deterministic)

Figure 31 contains the probability density function and cumulative distribution for the sinusoidal distribution, which are displayed for a variety of source strengths. Additional graphs of the sinusoidal probability density function for different N is available in Figure 135 ($N = 2$), Figure 136 ($N = 3$), Figure 137 ($N = 4$), and Figure 138 ($N = 5$).

A graph of the positive rate for the sinusoidal distribution with source strength for a series of three measurements is in Figure 32. The positive rate for the sinusoidal distribution for all conditions has a similar shape to the positive rate for the triangular distribution as well as the cumulative distribution function: increasing slowly, more rapidly until it passes through an inflection, and then more slowly. The values for the decision threshold for all conditions of the measurement series are approximately the same, as seen also in Table 7. As seen in Figure 32, all three conditions outperform the traditional method in terms of positive rate. Additional figures for other series lengths are in Figure 135 ($N = 2$), Figure 136 ($N = 3$), Figure 137 ($N = 4$), and Figure 138 ($N = 5$).

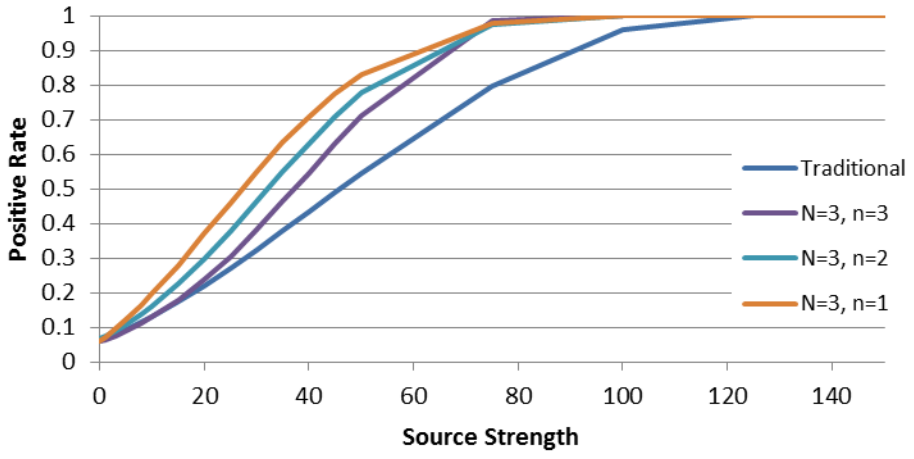

Figure 32 Positive Rate with Source Strength for Different n Values (Sinusoidal, b=500, N=3, Deterministic)

The differences between the positive rate at various n values for the sinusoidal distribution is highlighted in a bar graph in Figure 33 using different conditions for a background

of 500 and source strength of 10. Similar to previous discussed distributions, the positive rate for the sinusoidal distribution is largest for the lower number of successes required ($n = 1$). However, unlike the rectangular distribution, all conditions for $N = 3$ outperform the traditional method.

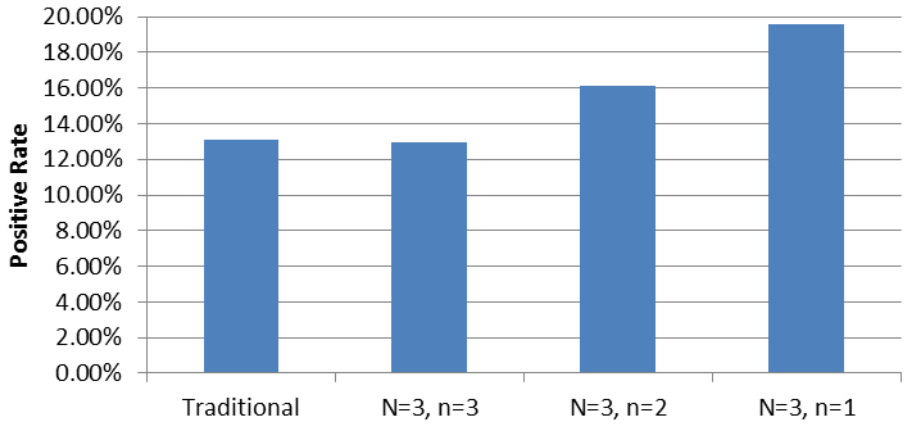

Figure 33 Positive Rate for Different n Values (Sinusoidal, b=500, s=10, N=3, Deterministic)

A graph of the sinusoidal positive rate with the source to background strength ratio is in Figure 34 for the condition $N = 3, n = 2$. The shape of the graph is similar for all backgrounds for the sinusoidal distribution. For larger backgrounds, 100% positive rate is achieved at lower source strength to background ratios (as seen in Table 7).

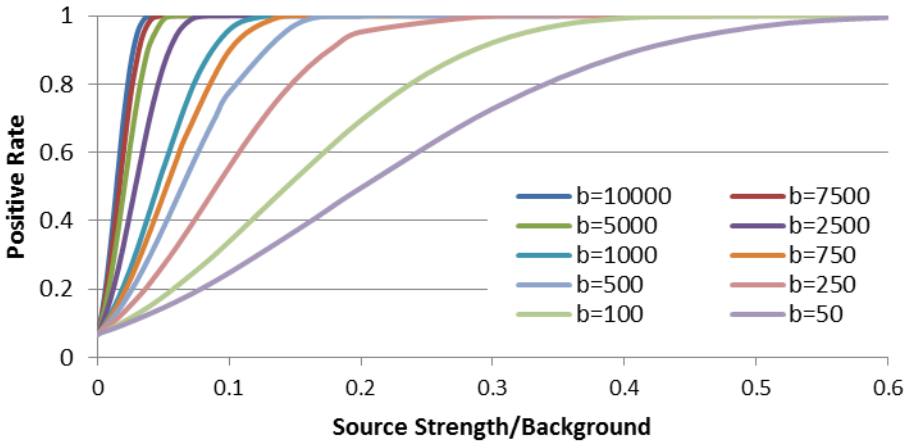

Figure 34 Positive Rate with Source/Background Strength at Different Background (Sinusoidal, N=3, n=2, Deterministic)

Additional figures of other series lengths for the sinusoidal distribution are located in Figure 130 (Traditional), Figure 131 ($N = 2$), Figure 132 ($N = 3$), Figure 133 ($N = 4$), and Figure 134 ($N = 5$).

Poisson

The modeled Poisson distribution is characterized by a mean value. Figure 35 contains the probability density functions for the Poisson distribution at each background level.

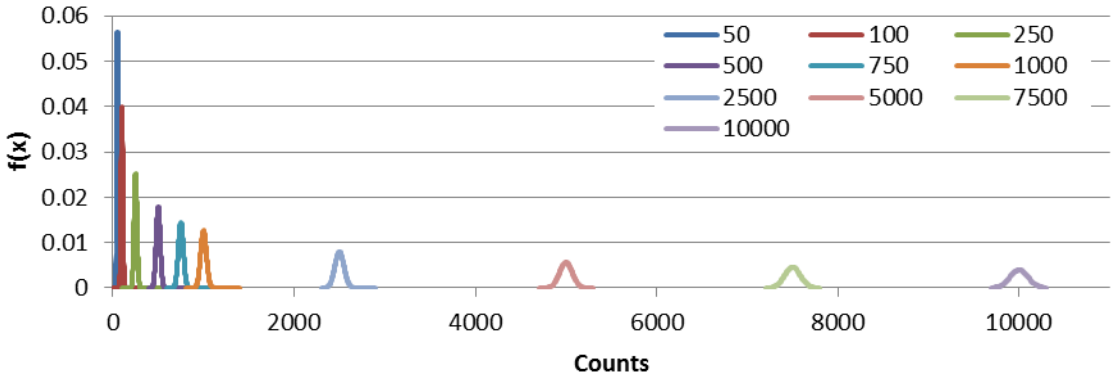

Figure 35 Probability Density Function for Different Background Levels (Poisson, Deterministic)

Data for three background strengths (50, 500, and 5000) are discussed here. The Poisson probability density function for the three background distributions with different source strengths between 0 and 50 is in Figure 36.

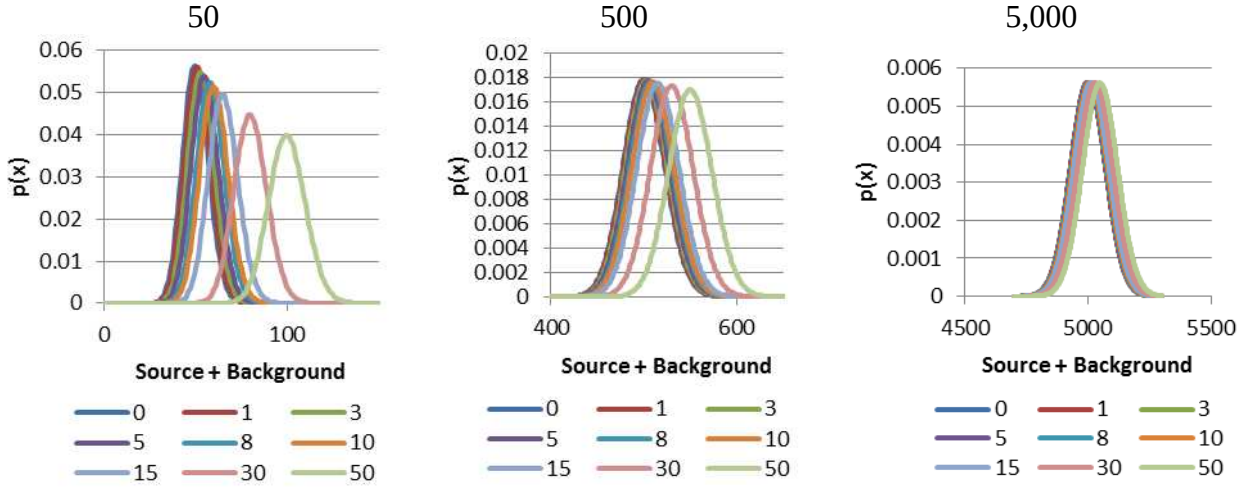

Figure 36 Probability Density Function at Different Source Strengths (Poisson, b=50, b=500, b=5000, Deterministic)

The source and background changes the most with an added source for lower background levels. As the source strength increases, the distribution widens.

The calculated values for the decision threshold (y^*) for the Poisson distribution at a background of 50, 500, and 5000 are located in Table 8. Calculated decision thresholds for other background strengths for the Poisson distribution are contained in Table 15 within Appendix A. As the series length increases, the calculated y^* for the Poisson distribution increases for the same condition (larger N, but constant n). Additionally as n approaches N, the calculated y^* decreases. Table 8 also lists the source strength at which 50% and 100% detection is achieved. The ratio of the source strength to background strength for the same conditions and level of detection decreases as background strength increases.

Table 8 Calculated Values of y^* and Source Strength at 50% and 100% Detection (Poisson, Deterministic)

		y^*			50% Detection			100% Detection		
		Background Strength			Background Strength			Background Strength		
N	n	50	500	5000	50	500	5000	50	500	5000
1	1	62	537	5117	13	38	118	49	133	402
2	2	55	517	5054	10	31	94	42	116	349
	1	64	544	5139	11	33	101	37	104	318
3	3	52	507	5024	9	27	83	39	107	325
	2	58	525	5078	9	26	79	32	89	270
	1	66	548	5151	11	30	94	33	92	282
4	4	50	501	5005	9	25	77	37	103	310
	3	55	515	5048	8	23	70	29	81	248
	2	59	529	5092	8	24	72	27	77	236
	1	66	551	5159	9	29	89	29	85	260
5	5	49	497	4991	9	24	72	37	99	300
	4	53	509	5029	8	21	65	28	77	234
	3	56	520	5062	7	21	63	25	71	215
	2	60	532	5101	7	22	68	24	71	216
	1	67	553	5165	9	28	85	28	80	245

Trends in the positive rate for the Poisson distribution are displayed for a series of three measurements (additional figures noted when available). The probability density function and

cumulative distribution are displayed for a variety of source strengths for the Poisson distribution in Figure 37 at a background of 500.

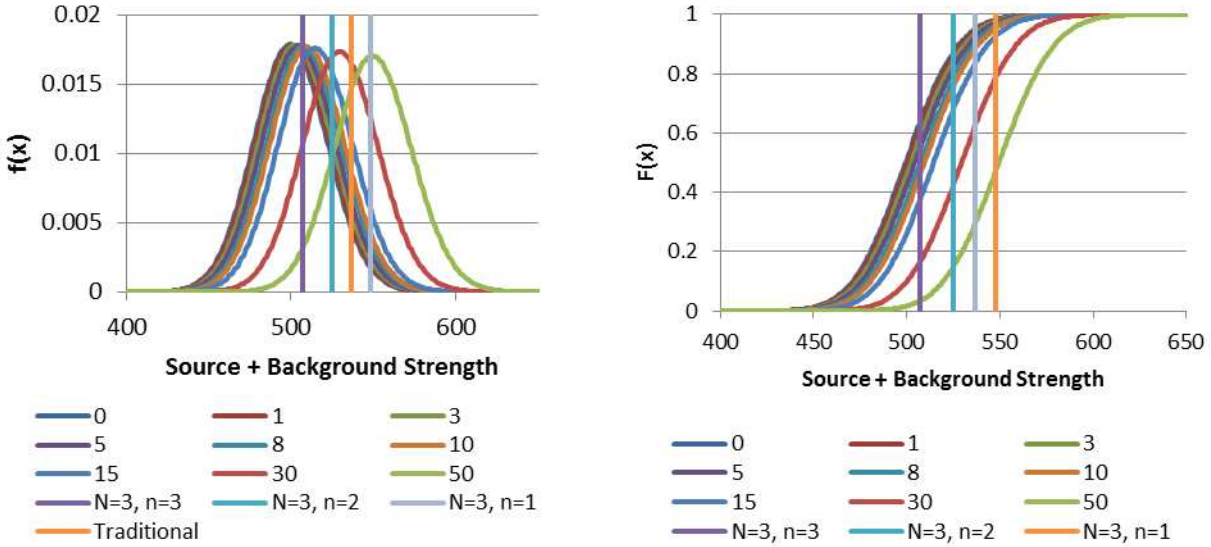

Figure 37 Probability Density Function and Cumulative Distribution for Different Source Strengths with Decision Threshold for Different n Values (Poisson, b=500, N=3, Deterministic)

Additional graphs of the probability density function and cumulative distribution for the Poisson distribution for different N are available in Figure 144 ($N = 2$), Figure 145 ($N = 3$), Figure 146 ($N = 4$), and Figure 147 ($N = 5$).

A graph of the positive rate for the Poisson distribution with source strength for a series of three measurements is in Figure 38. The positive rate for the Poisson distribution for all conditions has a similar shape to the positive rate for the triangular distribution and sinusoidal distribution, as well as the Poisson cumulative distribution function. The positive rate increases slowly at first, then more rapidly until it passes through an inflection, and finally slowly again. As seen in Figure 32, all three conditions for the Poisson distribution outperform the traditional method in terms of positive rate. Positive rates tend to be greatest for non-extreme conditions (for example $N = 3, n = 2$). Additional figures for other series lengths are in Figure 144 ($N = 2$), Figure 145 ($N = 3$), Figure 146 ($N = 4$), and Figure 147 ($N = 5$).

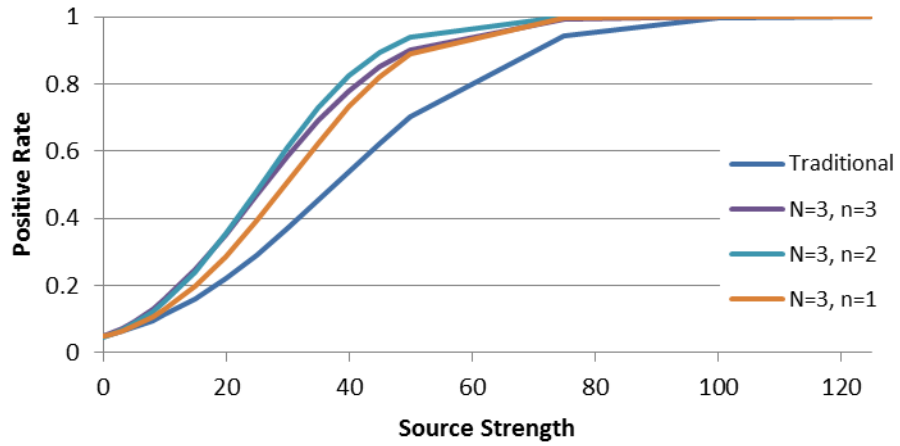

Figure 38 Positive Rate with Source Strength for Different n Values (Poisson, b=500, N=3, Deterministic)

The differences for the Poisson distribution positive rate for different conditions is shown in a bar graph in Figure 34 for $b = 500$ and $s = 10$. Unlike previously discussed distributions, the positive rate for the Poisson distribution is greatest for larger values of n. For the Poisson distribution, all conditions for a series of three measurements outperform the traditional method for positive rate.

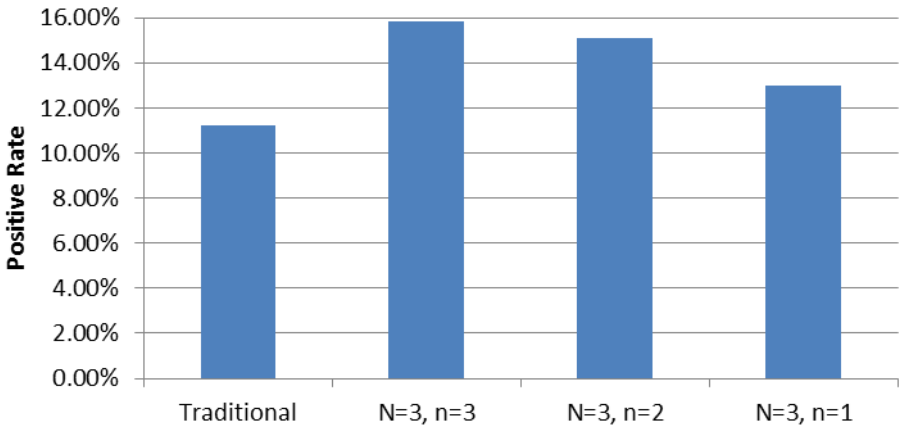

Figure 39 Positive Rate for Different n Values (Poisson, b=500, s=10, N=3, Deterministic)

A graph of the Poisson distribution positive rate with the source to background strength ratio is in Figure 40 for $N = 3, n = 2$. The shape of the graph is similar for all backgrounds. For larger backgrounds, 100% positive rate is achieved at lower source strength to background ratios

(as seen in Table 8). Additional figures for other N are located in Figure 139 (Traditional), Figure 140 ($N = 2$), Figure 141 ($N = 3$), Figure 142 ($N = 4$), and Figure 143 ($N = 5$).

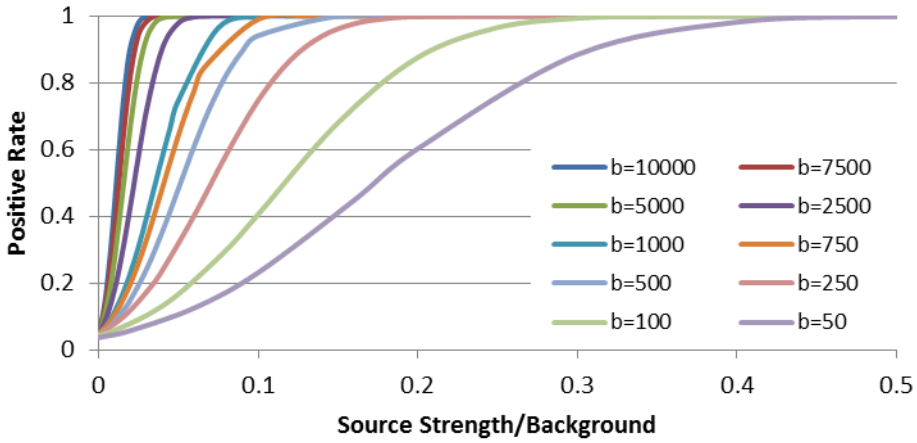

Figure 40 Positive Rate with Source/Background Strength at Different Background (Poisson, N=3, n=2, Deterministic)

Gaussian

The modeled Gaussian distribution is characterized by a mean value and a variance equal to the mean. The Gaussian probability density function for each background level is in Figure 41 for each background level.

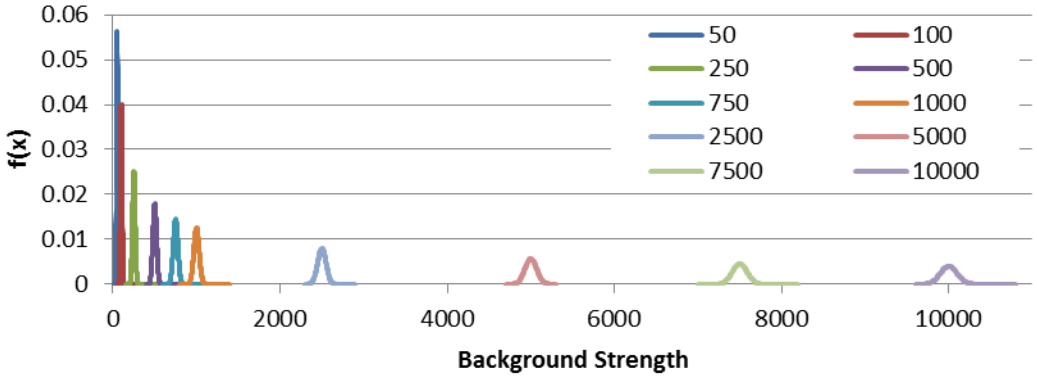

Figure 41 Probability Density Function for Different Background Levels (Gaussian, Deterministic)

The generated probability density function for the Gaussian source and background distribution for $b = 50$, $b = 500$, and $b = 5000$ is in Figure 42. The plotted distributions are for source strengths between 0 and 50.

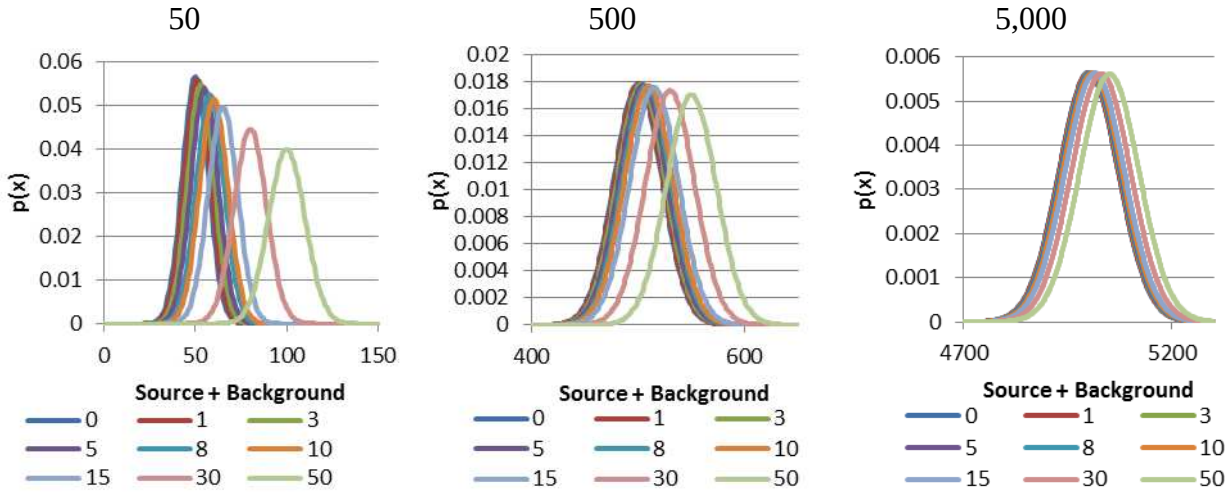

Figure 42 Probability Density Function at Different Source Strengths (Gaussian, b=50, 500, 5000, Deterministic)

As seen by Figure 42, the source and background distribution changed the most significantly for lower background levels. As the source strength increases, the distribution widens. The calculated values for the decision threshold (y^*) for the Gaussian distribution at a background of 50, 500, and 5000 are located in Table 9. Calculated Gaussian decision thresholds for all background strengths are contained in Table 16 within Appendix A.

Table 9 Calculated Values of y^* and Source Strength at 50% and 100% Detection (Gaussian, Deterministic)

		Background Strength			Background Strength			Background Strength		
N	n	50	500	5000	50	500	5000	50	500	5000
1	1	62	537	5116	12	37	117	58	135	403
2	2	55	517	5054	10	30	93	52	118	351
	1	64	544	5138	10	32	100	41	105	318
3	3	52	508	5024	9	27	83	49	110	327
	2	58	525	5078	8	25	78	36	89	270
	1	65	547	5150	9	29	92	35	91	280
4	4	50	502	5005	9	25	76	47	106	313
	3	55	515	5048	7	22	69	34	82	248
	2	59	529	5092	7	23	71	30	77	236
	1	66	550	5158	9	28	87	31	84	258
5	5	49	497	4991	8	24	72	46	102	302
	4	53	509	5029	7	21	64	32	78	235
	3	56	520	5062	7	20	63	28	71	215
	2	60	532	5101	7	21	67	27	70	216
	1	66	552	5164	8	26	84	29	79	243

As the series length increases, the calculated y^* for the Gaussian distribution increases for the same condition (larger N, but constant n). Additionally as the number of successes (times exceeding the decision threshold) approaches the series length, the calculated y^* decreases. Also listed in Table 9 is the source strength at which 50% and 100% detection is achieved for the Gaussian distribution. The ratio of the source strength to background strength for the same conditions and level of detection decreases as background strength increases.

Trends in the positive rate for the Gaussian distribution are illustrated through several representative figures for a series length of three (additional figures available in Appendix A and will be noted when available). Figure 43 contains a visual representative of the thresholds for the Gaussian distribution using a series of three measurements for $b = 500$, using the graphs of probability density function and cumulative distribution for a variety of source strengths with the threshold overlaid. Additional graphs of the Gaussian probability density function and cumulative distribution for different N are available in Figure 153 ($N = 2$), Figure 154 ($N = 3$), Figure 155 ($N = 4$), and Figure 156 ($N = 5$).

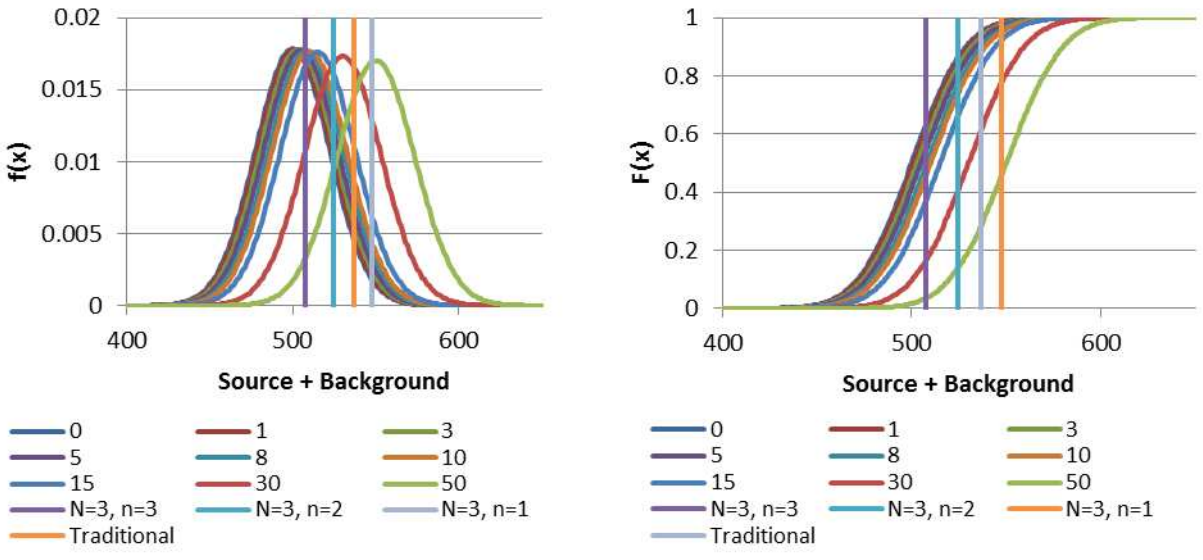

Figure 43 Probability Density Function and Cumulative Distribution for Different Source Strengths with Decision Thresholds for Different n Values (Gaussian, b=500, N=3, Deterministic)

Figure 44 contains a graph of the positive rate for the Gaussian distribution with source strength for a series of three measurements. The positive rate for the Gaussian distribution for all conditions has a similar shape to the positive rate for all distributions discussed (with the exception of the rectangular distribution) as well as the cumulative distribution function. The Gaussian positive rate increases slowly initially, more rapidly until it passes through an inflection, and then more slowly. As seen in Figure 44, all three conditions outperform the traditional method in terms of positive rate for the Gaussian distribution. Additional figures for different N are in Figure 153 ($N = 2$), Figure 154 ($N = 3$), Figure 155 ($N = 4$), and Figure 156 ($N = 5$).

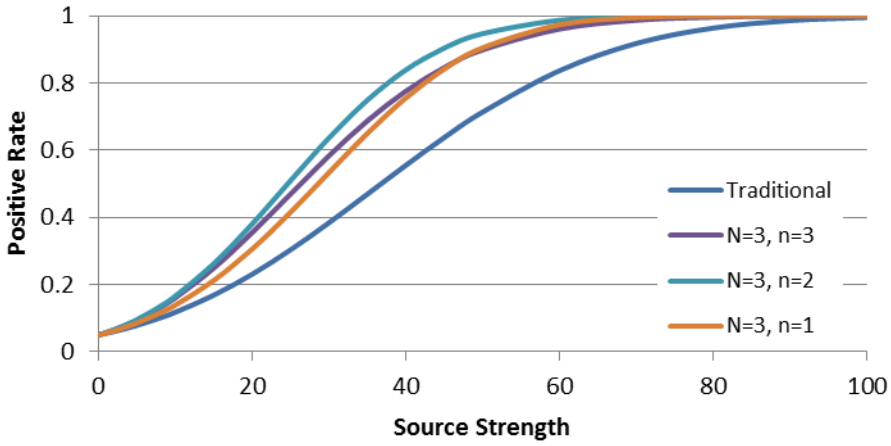

Figure 44 Positive Rate with Source Strength for Different n Values (Gaussian, b=500, N=3, Deterministic)

A graph of the positive rate with the source to background strength ratio for the Gaussian distribution is in Figure 45 for $N = 3, n = 2$. The shape of the graph is similar for all backgrounds. For the Gaussian distribution at larger backgrounds, 100% positive rate is achieved at lower source strength to background ratios (as seen in Table 9). Additional figures of other series lengths for the Gaussian distribution are located in Figure 148 (Traditional), Figure 149 ($N = 2$), Figure 150 ($N = 3$), Figure 151 ($N = 4$), and Figure 152 ($N = 5$).

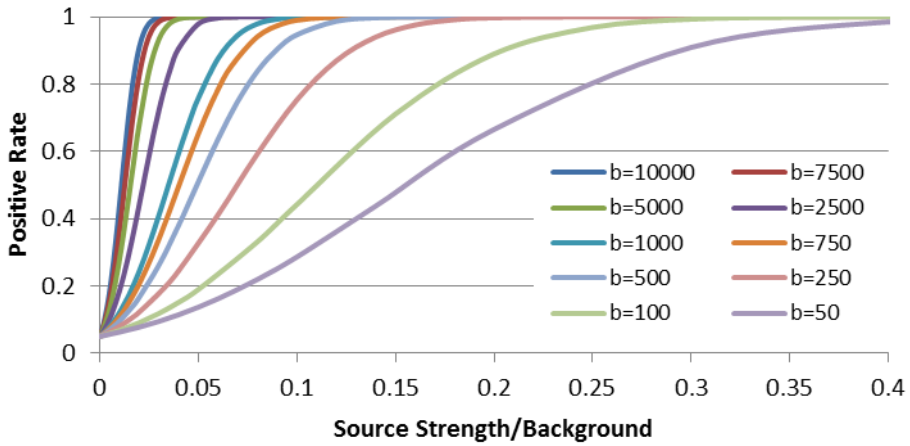

Figure 45 Positive Rate with Source/Background Strength at Different Background (Gaussian, N=3, n=2, Deterministic)

Stochastic

The stochastic method looked at five distributions: uniform, triangular, sinusoidal, Poisson, and Gaussian. The positive rate and time at first detection are looked at for the stochastic model. The stochastic method looked at the following scenarios:

Table 10 Scenarios Looked at for the Stochastic Method

Criteria	Values
Background Levels	500 50, 500, 5000 (Gaussian Distribution)
Source Strength	0, 1, 3, 5, 8, 10, 15, 30, 50 0, 1, 2, 3, 4, 5, 6, 7, 8, 9, 10, 15, 20, 25, 30, 35, 40, 45, 50 (Gaussian Distribution)
Series Length	1, 2, 3, 4, 5

The *at least* and *exact* conditions were compared for the Gaussian distribution. The probability density function for positives and time to first detection were also looked at for the Gaussian distribution.

At Least v. Exact

Using the Gaussian distribution at a background of 500, the two conditions of exactly n successes in a series of N measurements was compared to at least n successes in a series of N measurements. A comparison of the positive rate with source strength for the *exact* and *at least*

conditions using a series of two measurements is in Figure 46. There is no difference between techniques when $n = N$ as seen in Figure 46, as expected because when n is equal to N, Equations 89 and 90 converge resulting in the same values. For *exact* conditions when n does not equal N, the positive rate initially increases until reaching a maximum around 50% and then decreases. As source strength increases the likelihood of exceeding the decision threshold will increase, making the condition less likely. The difference in the *at least* and *exact* conditions for $N = 2, n = 1$ is most pronounced at higher source strengths. Additional information in Figure 157.

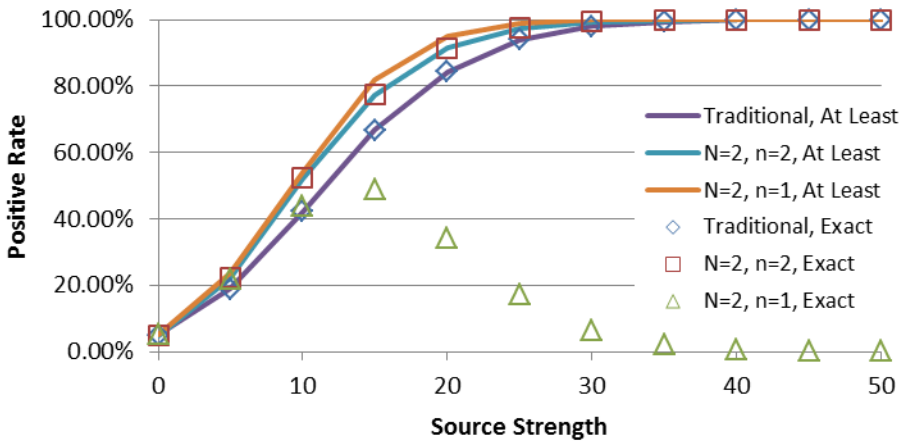

Figure 46 Positive Rate with Source Strength Comparison for At Least and Exact Conditions (Gaussian, N=2, Stochastic)

For the stochastic method, the time at first detection was also compared for when there are exactly n successes in a series of N measurements and when there are least n successes in a series of N measurements using a Gaussian distribution. Figure 47 contains a comparison of the time at first detection for the *exact* and *at least* conditions. There is very little difference between the two conditions for the time at first detection for the Gaussian distribution. Additional time at first detection information is in Appendix B in Figure 158. Future analysis will use the *at least* condition.

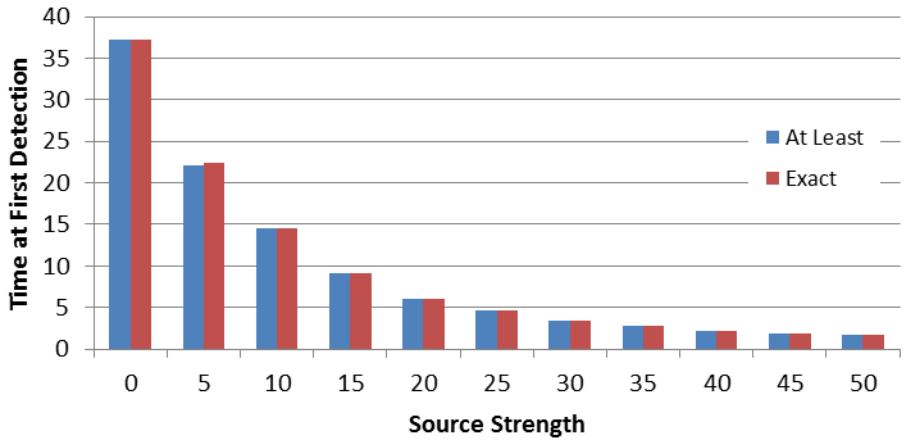

Figure 47 Time at First Detection with Source Strength Comparison for At Least and Exact Conditions (Gaussian, N=2, Stochastic)

Distribution of Positives and Time at First Detection

The probability density function for the number of positives and the time to first detection were investigated for the Gaussian distribution. The number of positives in 200 measurements was looked at for $b = 500$, $s = 10$, and $N = 3$. It was expected that the number of positives would approximate a Gaussian distribution. The measurement data was compared to the expected distribution for each value of n and is in Figure 48. The measurement data compares.

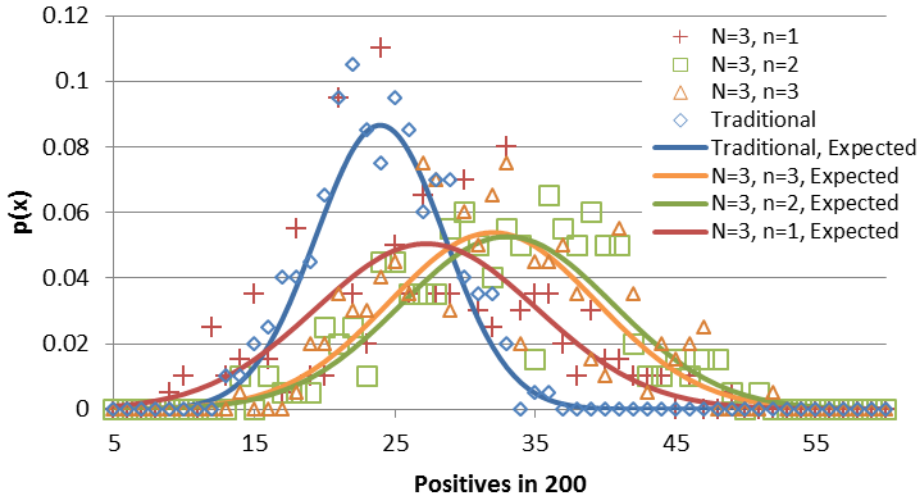

Figure 48 Probability Density Function for Positive Rate for Different n Values (Gaussian, N=3, b=500, s=10, Stochastic)

The probability density function for the time to first detection was also investigated. It was expected that the time to first detection would follow a geometric distribution. The

geometric distribution is a discrete probability distribution that represents the number of trials needed to get one success. The geometric distribution is characterized by a probability of success p. The probability of success on the k[th] trial can be described through the following equation, where k=1, 2, …, n.

$$P(X = k) = (1 - p)^{k-1}p \quad 91$$

The probability density function was compared to a geometric distribution for a Gaussian distribution. The p value for the geometric distribution was to be the positive rate. Figure 49 contains a comparison between the geometric distribution and measurement values for the traditional method and for $N = 3, n = 2$ for the Gaussian distribution.

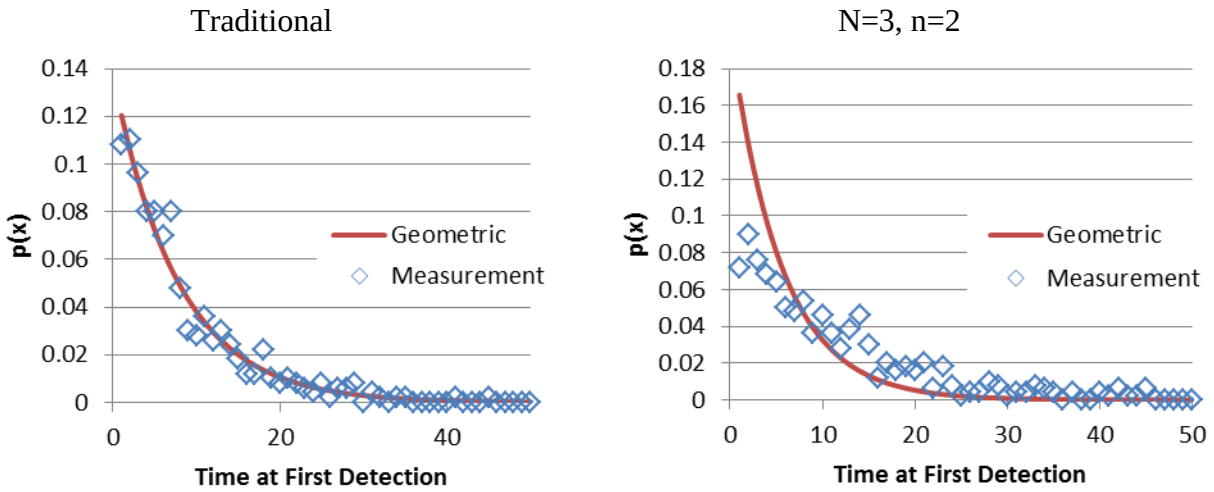

Figure 49 Time at First Detection Probability Density Function for Traditional Method and N=3, n=2, (Gaussian, b=500, s=10, Stochastic)

The measurement values compare well to the geometric distribution for the traditional method; however for $N = 3, n = 2$ the graph is a lot flatter than expected by the geometric distribution. Additional graphs for the time at first detection probability density function using the Gaussian distribution for different values of n is available in Appendix B in Figure 161. The probability density function for the time to first detection was compared for different measurement conditions using a Gaussian distribution for $N = 3$ for two different source values

in Figure 50 for $b = 500$. The density function peaks at a time equal to n. Additional probability density functions for different source strengths are available in Appendix B in Figure 159.

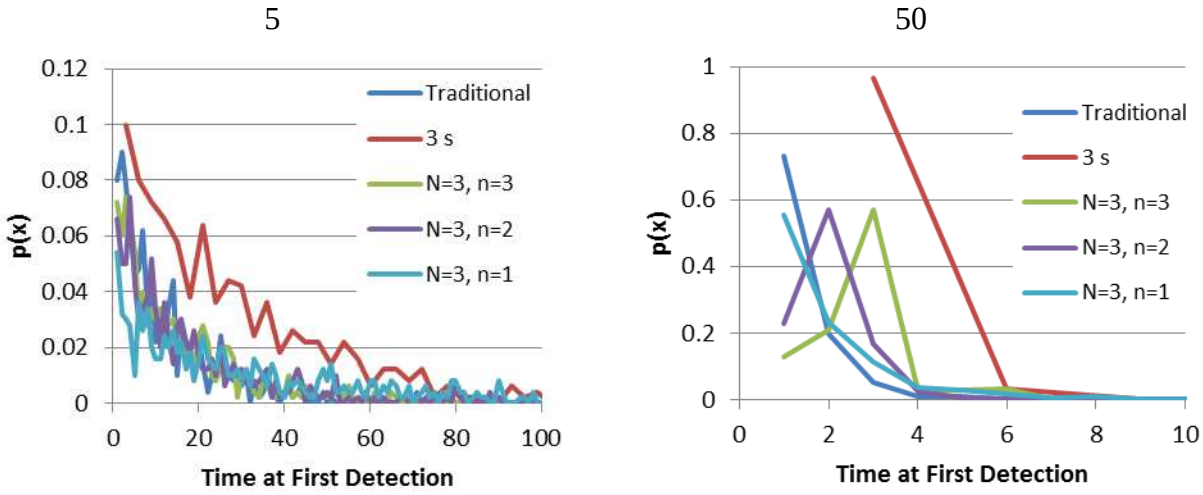

Figure 50 Time at First Detection Probability Density Function for Different n Values (Gaussian, b=500, Gaussian, Stochastic)

The probability density function for time at first detection was also looked at for different source strengths using a Gaussian distribution. Figure 51 contains a graph of the probability density function for $N = 3, n = 2$ for different source strengths. Additional graphs for the Gaussian distribution using different values of N and n is available in Figure 160.

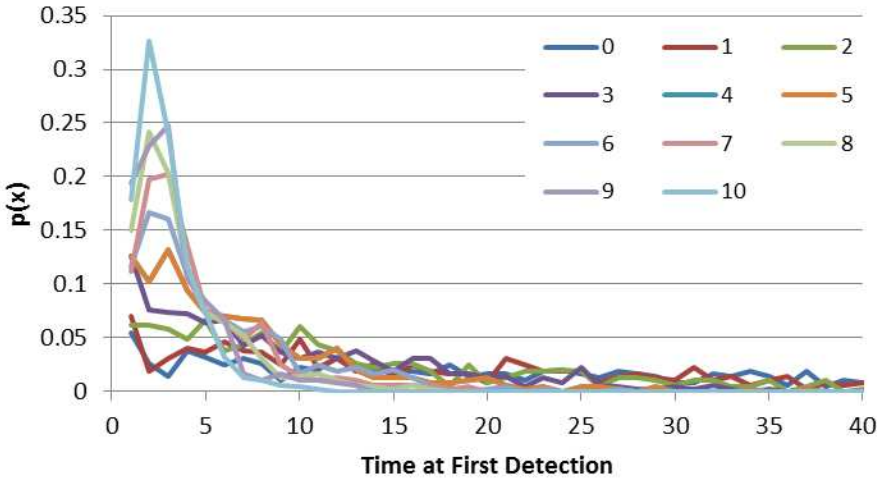

Figure 51 Probability Density Function for Time at First Detection for Different Source Strength (Gaussian, b=500 N=3, n=2, Stochastic)

Rectangular

Two different background and source spectra simulation techniques were used for the stochastic methodology. One methodology assumes that the source is known and adds the source to background using two random numbers. The second methodology involves sampling off of a source and background distribution (one distribution).

When using one distribution, the mean value for the rectangular distribution was at the sum of the background and source and the width of the distribution was chosen such that the variance for the rectangular distribution was equal to mean. For example for a background of 500 and a source value of 50, the mean of the single distribution would be at 550; and the variance would be chosen at 550.

When the data was generated by summing a source and a background distribution, one value was sampled off of a rectangular background distribution with a mean equal to the mean background and a second value was sampled off of a rectangular source distribution with a mean equal to the mean of the sample; the variance of each distribution was equal to the respective mean. For the previous example, one number would be generated off of a rectangular background distribution with a mean and variance of 500, a second number would be generated off of a rectangular source distribution with a mean value and variance of 50, and the two numbers would be summed to create the source and background distribution.

The differences in using one distribution and the sum of two distributions are illustrated for the rectangular distribution through the probability density function for a background of 500 at different source strengths in Figure 52. The probability density function for the rectangular distribution using each technique is the same for a source strength of zero and resembles a

rectangle. However as the source strength increases the probability density function for the rectangular distribution using the two distribution method begins to take a trapezoidal shape.

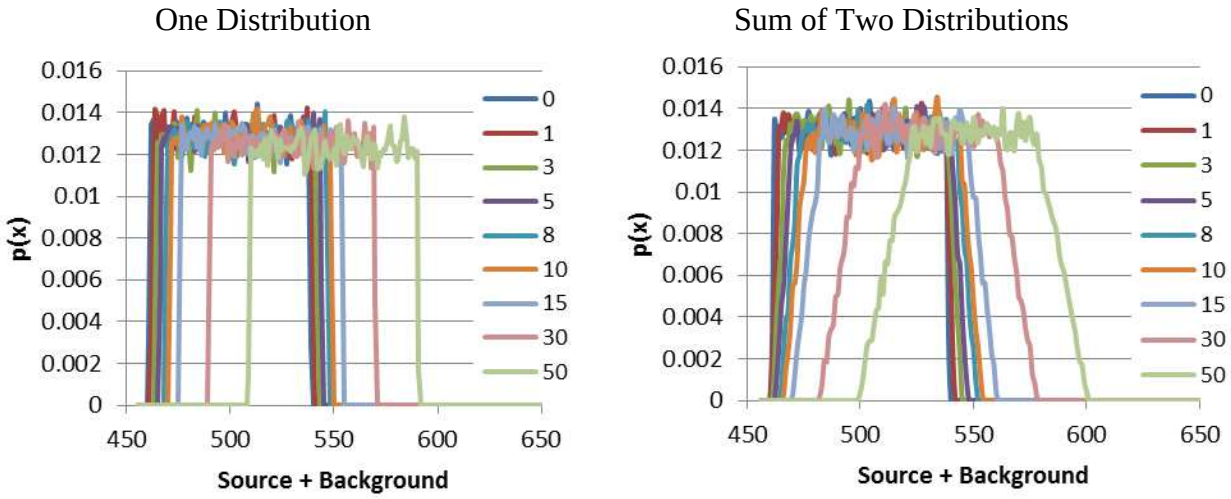

Figure 52 Probability Density Function for Different Source Strengths Comparison for Two Measurement Simulation Techniques (Rectangular, b=500, Stochastic)

The differences in the two measurement simulation techniques are illustrated on the same plot for the rectangular distribution at source strengths of 0, 5, and 50 in Figure 53 for $b = 500$. The differences in probability density functions are most prominent for higher source strength.

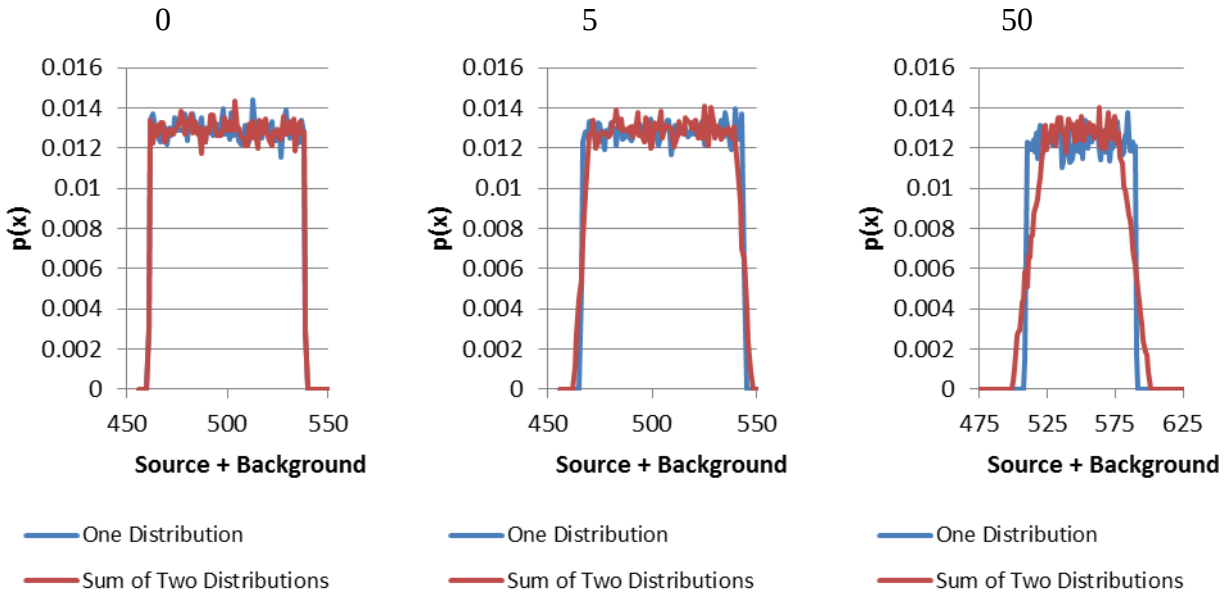

Figure 53 Probability Density Function Comparison for Two Measurement Simulation Techniques for Several Source Strengths (Rectangular, s=0, 5, 50, b=500, Stochastic)

Additional plots for other source strengths for the rectangular distribution are available in Appendix B in Figure 162 ($s = 1, 3, 5, 8$) and Figure 163 ($s = 10, 15, 30, 50$). In addition to the comparison of the probability density function, the positive rate and time at first detection for the rectangular distribution are compared in Figure 54 for $N = 2, n = 2$.

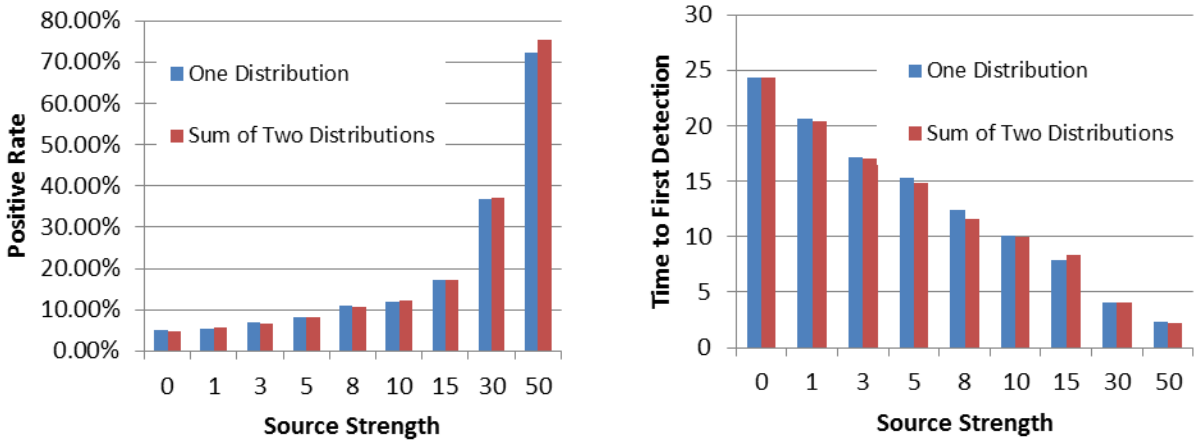

Figure 54 Positive Rate and Time at First Detection with Source Strength Comparison for Two Measurement Simulation Techniques (Rectangular, N=2, n=2, b=500, Stochastic)

For certain source strengths, the values for generating off of one distribution are greater than for two distributions. Values for the positive rate are within 5% and values for detection time are within 10%. Additional graphs for different values of n for the rectangular distribution are available in Appendix B for positive rate (Figure 164) and time at first detection (Figure 165). All future data discussed for the rectangular distribution is generating by using two random numbers.

A comparison of the positive rate and time to first detection for different combinations of n ($N = 3$) for the rectangular distribution is in Figure 55 for $b = 500$. The error bars displayed are for one standard deviation; due to the inherent properties of the time to first detection (geometric distribution), the standard deviation is large compared to the mean. As the source strength increases the positive rate increases for the rectangular distribution, while the time at

first detection decreases. The positive rate increases most rapidly for $n = 1$, while it increases slowest for a three second long measurement. The smallest time at first detection occurs for the rectangular using the traditional method ($N = 1, n = 1$) and the three second long measurement (3 s). Additional graphs for different series lengths for the rectangular distribution are in Figure 166 (Positive Rate) and Figure 167 (Time at First Detection).

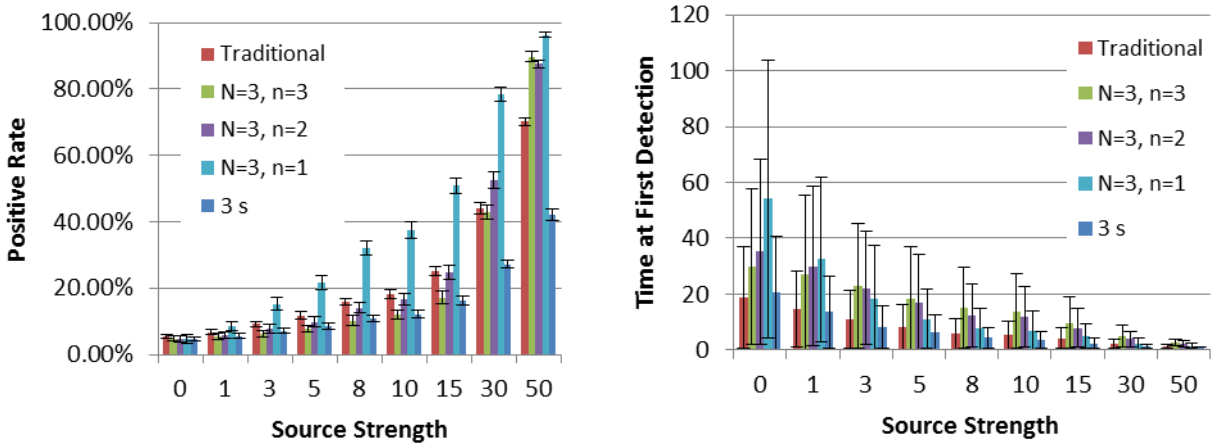

Figure 55 Positive Rate and Time at First Detection with Source Strength for Different n Values (Rectangular, N=3, b=500, Stochastic)

For $b = 500$ and $s = 10$, the trends for positive rate and time at first detection are shown for the rectangular distribution in Figure 56 using $N = 3$. The error bars displayed are for one standard deviation.

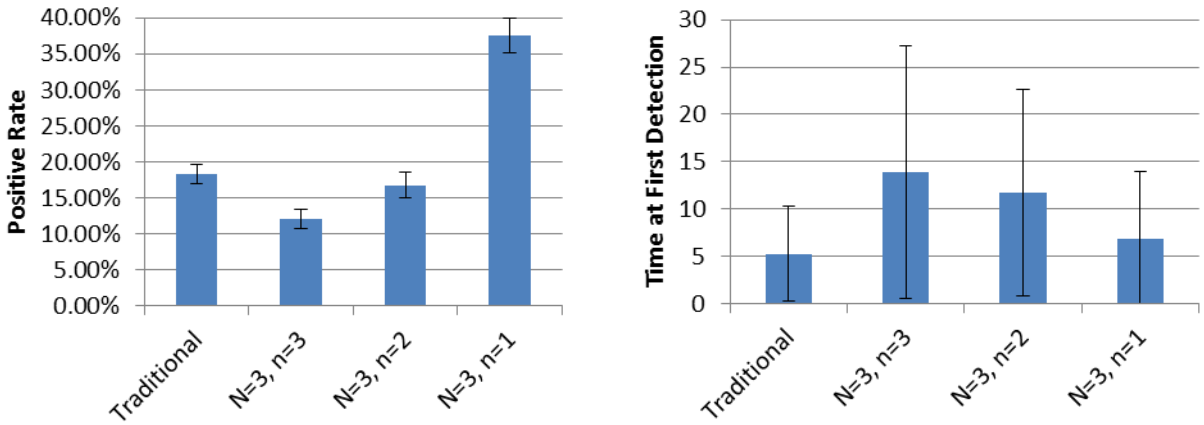

Figure 56 Positive Rate and Time at First Detection for Different n Values (Rectangular, b=500, N=3, s=10, Stochastic)

The positive rate for the rectangular distribution is greatest for the traditional method and when $n = 1$. As n increases, the positive rate decreases for the rectangular distribution. Similarly the traditional method and $n = 1$ has the shortest time to first detection (for the rectangular distribution), while the larger n results in a longer time at first detection.

Trends in the data (positive rate and time at first detection) for different series lengths for the rectangular distribution were looked at for three conditions: all successes ($N = n$), at least one success in a series ($n = 1$), and for different measurement lengths. Figure 57 contains a graph of the positive rate with source strength and time at first detection with source strength, when $n = N$ for different series lengths for the rectangular distribution.

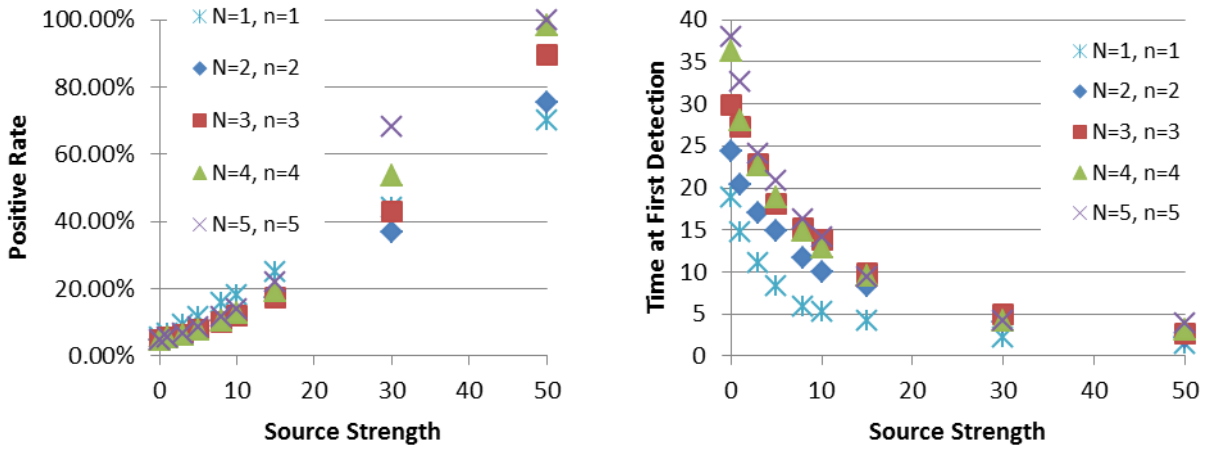

Figure 57 Positive Rate and Time at First Detection with Source Strength Comparison for Different N Values (Rectangular, b=500, n=N, Stochastic)

As seen in Figure 57, the positive rate for all five measurement lengths begins at 5%, as expected for the rectangular distribution. The shape of the curve for positive rate with source strength for the rectangular distribution is characterized by slow increase of positive rate at first with source strength and then more rapid increase as the source strength becomes larger. Initially the positive rate increases most rapidly with source strength for shorter series lengths (example $N = 1, n = 1$), but after a source strength of 15, the positive rate for longer series increases more

rapidly with the condition $N = 5, n = 5$ reaching 100% positive rate by a source strength of 50. For the rectangular distribution the time at first detection, the drop in time at first detection with increased source strength is largest for small source strengths and then become less significant for higher source strengths. The time at first detection for the rectangular distribution is largest for larger series lengths for all source strengths; however, the difference in time at first detection becomes less as source strength increases.

Figure 58 contains a graph of the positive rate with source strength and time at first detection with source strength, when $n = 1$ for different series lengths for the rectangular distribution. The shape of the positive rate graph for the rectangular distribution with increased source strength for $n = 1$ has a different shape than for $n = N$. Rather than increasing slowly at low source strength then rapidly at high source strength, the positive rate for the rectangular distribution at $n = 1$ increases rapidly at lower source strengths and slower at high source strengths. The plot of the time at first detection with source strength is similar for $n = N$ and $n = 1$ for the rectangular distribution; however, the differences between the five measurements length is less significant, especially after a source strength of around 5.

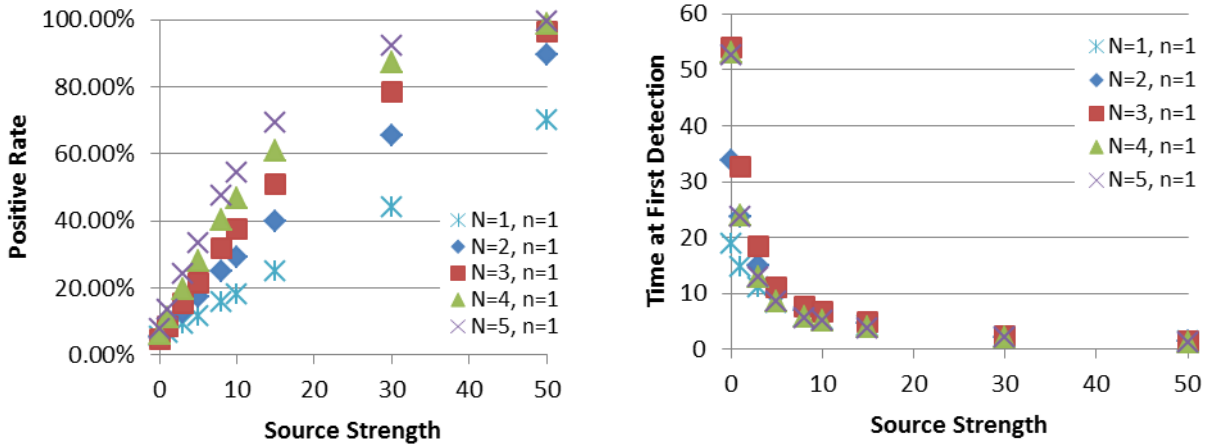

Figure 58 Positive Rate and Time at First Detection with Source Strength Comparison for Different N Values (Rectangular, n=1, b=500, Stochastic)

A comparison of positive rate and time at first detection for different measurement lengths for the rectangular distribution is in Figure 59. The positive rate with source strength is greatest for a measurement length of 5 s, the least for a measurement length of 3 s, with a measurement length of 1 s falling in between. The shape of the positive rate with source strength for the rectangular distribution is similar to $n = 1$, but closer to a straight line. The time at first detection has a similar shape to the other conditions described. The time at detection for the rectangular distribution is largest for 5 s and smallest for 1 s.

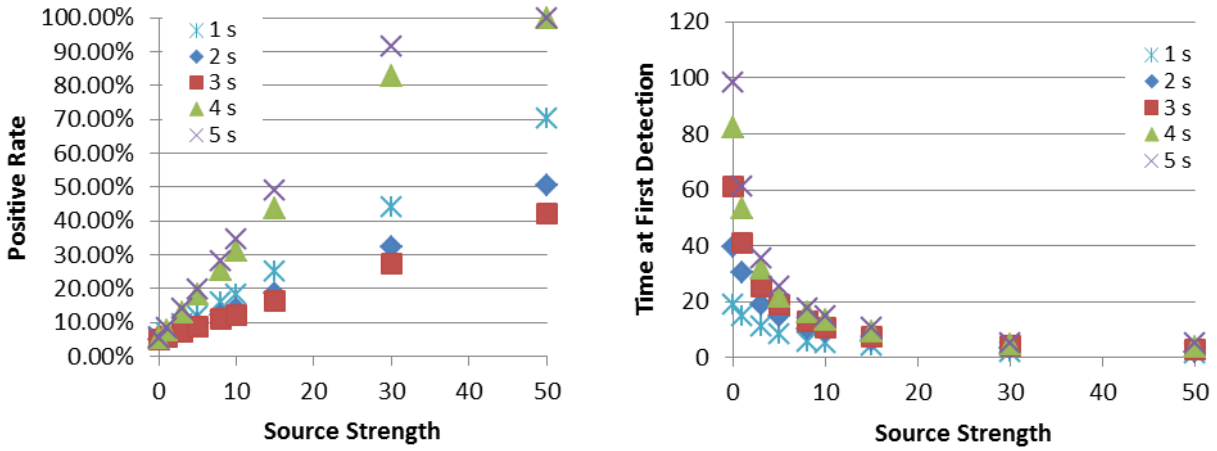

Figure 59 Positive Rate and Time at First Detection with Source Strength Comparison for Different N Values (Rectangular, b=500, Stochastic)

Triangular

As with the rectangular distribution, two different source and background spectra simulation techniques were used for the triangular distribution. One methodology uses one distribution to generate the source and background distribution, and the second method uses two distributions – a source distribution and a background distribution – and sums them to generate the source and background distribution. As with the deterministic method, the triangular distribution created is symmetric.

When using one distribution, the mean value ($c = \mu$) was chosen to be the sum of the background and source distribution, while the width of the triangle was chosen to keep a similar

width to the Gaussian distribution. The limits of the triangle were chosen to be $a = c - 3\sqrt{c}$ and $b = c + 3\sqrt{c}$. For example for a background of 500 and a source value of 50, the mean c would equal 550, while $a = 550 - 3\sqrt{550} = 480$ and $b = 550 + 3\sqrt{550} = 620$.

When the data was generated by summing a source distribution and a background distribution, one value was sampled off of a triangular background distribution with a mean c equal to the mean background and a second value was sampled off of a triangular source distribution with a mean c equal to the mean of the sample; the limits of each triangular distribution were chosen to be $a = c - 3\sqrt{c}$ and $b = c + 3\sqrt{c}$. For the previous example, one number would be generated off of a triangular background distribution with a mean of 500 and limits at $a = 500 - 3\sqrt{500} = 433$ and $b = 500 + 3\sqrt{500} = 567$, a second number would be generated off of a triangular source distribution with a mean of 50 and limits at $a = 50 - 3\sqrt{50} = 43$ and $b = 50 + 3\sqrt{50} = 57$. The differences in the two source and background simulation techniques for the triangular distribution by comparing the probability density function at $b = 500$ and several source strengths in Figure 60.

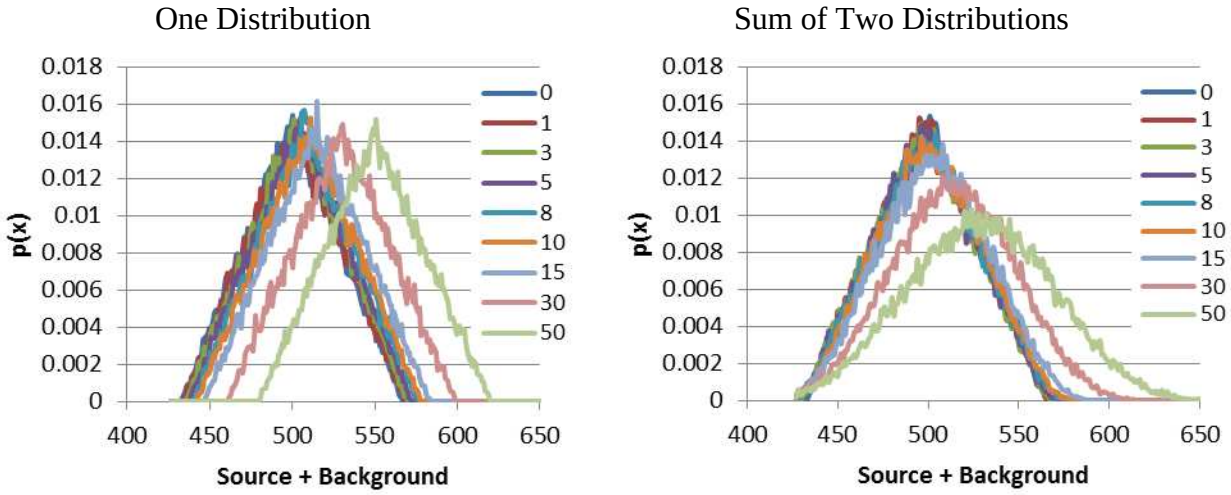

Figure 60 Probability Density for Different Source Strengths Comparison for Two Measurement Simulation Techniques (Triangular, b=500, Stochastic)

The distribution for each technique is the same for source strength of zero, but changes significantly at higher source strengths. As seen in Figure 60, the resulting shape from generating off of two distributions for the triangular distribution at higher source strengths has a more rounded shape, wider shape, and significantly reduced peak probability. These differences in the measurement simulation techniques for the triangular distribution are also illustrated by plotting probability density functions for each measurement technique on the same plot for source strengths of 0, 5, and 50 in Figure 61 for a background of 500.

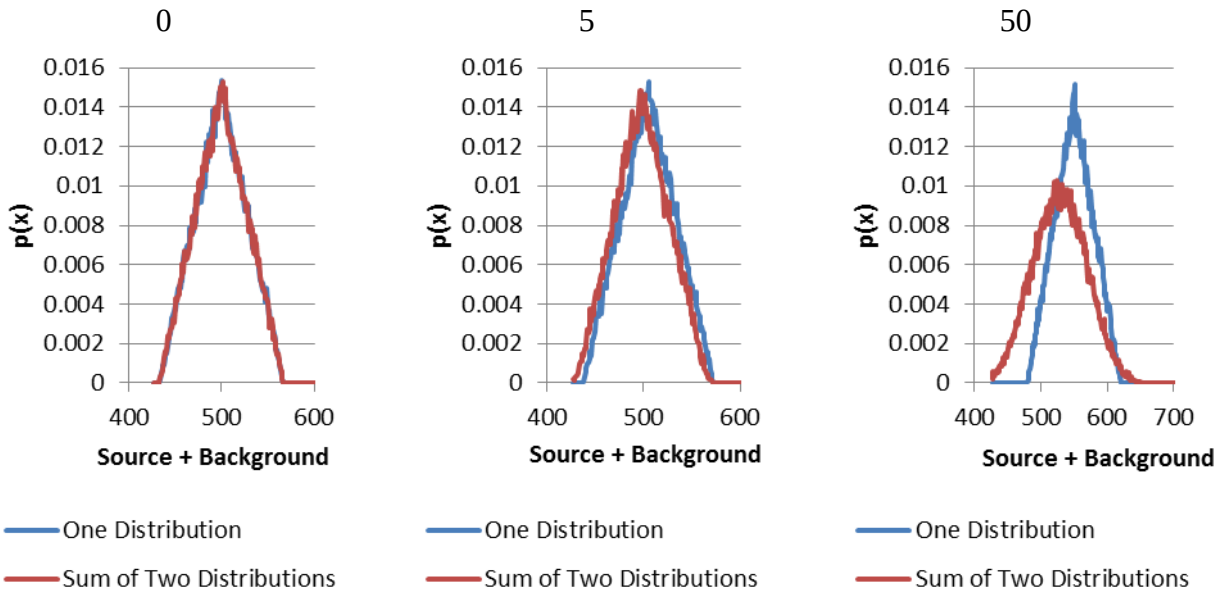

Figure 61 Probability Density Function Comparison for Two Measurement Simulation Techniques for Several Source Strengths (Triangular, b=500, Stochastic)

The differences in probability density functions for the triangular distribution are most prominent for higher source strength, as also seen for the rectangular distribution. Additional comparison for the triangular distribution at different source strengths is available in Figure 168 ($s = 1, 3, 5, 8$) and Figure 169 ($s = 10, 15, 30, 50$). In addition to the comparison of the probability density function for the triangular distribution, the positive rate and time at first detection are compared in Figure 62 for $N = 2, n = 2$.

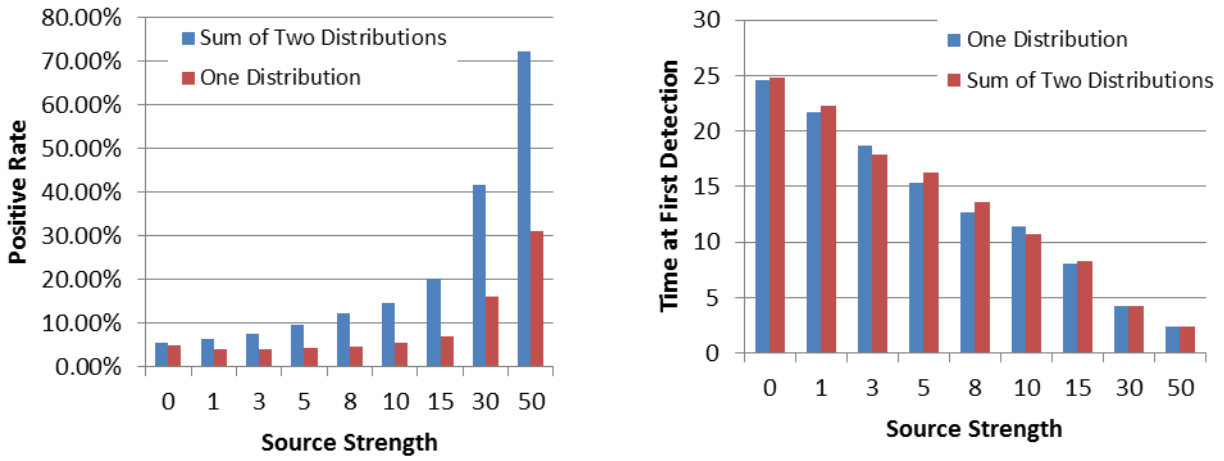

Figure 62 Positive Rate and Time at First Detection with Source Strength Comparison for Two Measurement Simuation Techniques (Triangular, N=2, n=2, b=500, Stochastic)

For the triangular distribution, generating values off of two distributions consistently produces consistently larger positive values. However for the time at first detection, for certain source strengths, the values for generating off of one distribution are greater than for two distributions. Values for the positive rate for the triangular distribution vary significantly for the two source simulation techniques are within 50% for the traditional method, while they are within 70% for $n = 1$ and $n = 2$. The difference in time to first detection values is much less – within 10% for the traditional method and $n = 1$, and 15% for $n = 2$. Additional comparison graphs using the two measurement simulation techniques for the triangular distribution are available in Appendix B in Figure 170 (positive rate) and Figure 171 (time at first detection). All future data discussed for the triangular distribution is generated using two random numbers.

A comparison of the positive rate and time to first detection for the triangular distribution for $N = 3$ and $b = 500$ is in Figure 63. The error bars are for one standard deviation. As seen with the rectangular distribution, as the source strength increases, the positive rate increases and the time at first detection decreases for the triangular distribution. The positive rate is the greatest for a measurement length of 3 s with $n = 1$ yielding the second highest positive rate. The smallest time at first detection is for the traditional method ($N = 1, n = 1$). Additional graphs for

different N values of the triangular distribution are available in Figure 172 (positive rate) and Figure 173 (time at first detection).

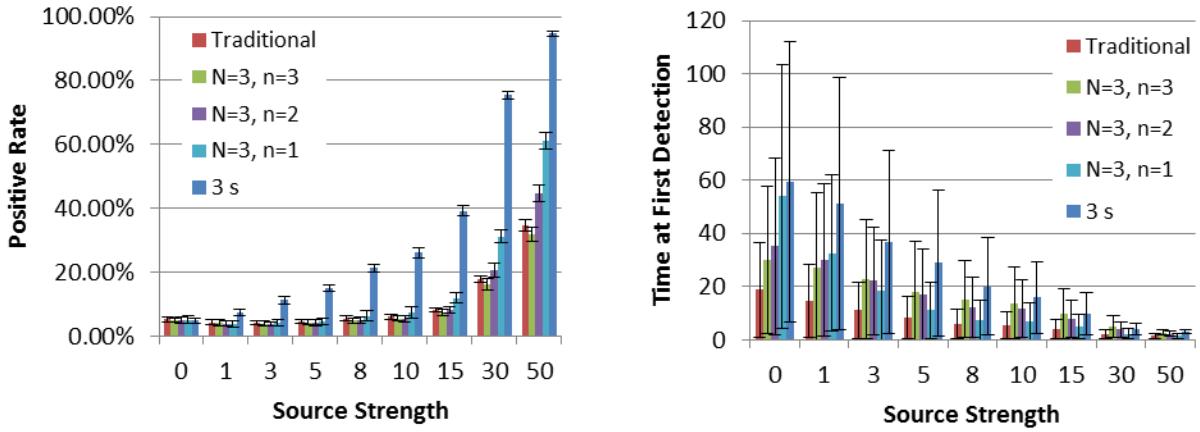

Figure 63 Positive Rate and Time at First Detection with Source Stnregth for Different n Values (Triangular, N=3, b=500, Stochastic)

The trends for the positive rate and time at first detection between different conditions for the triangular distribution are illustrated in Figure 64 for $N = 3$, $b = 500$, and $s = 10$. The error bars displayed are for one standard deviation.

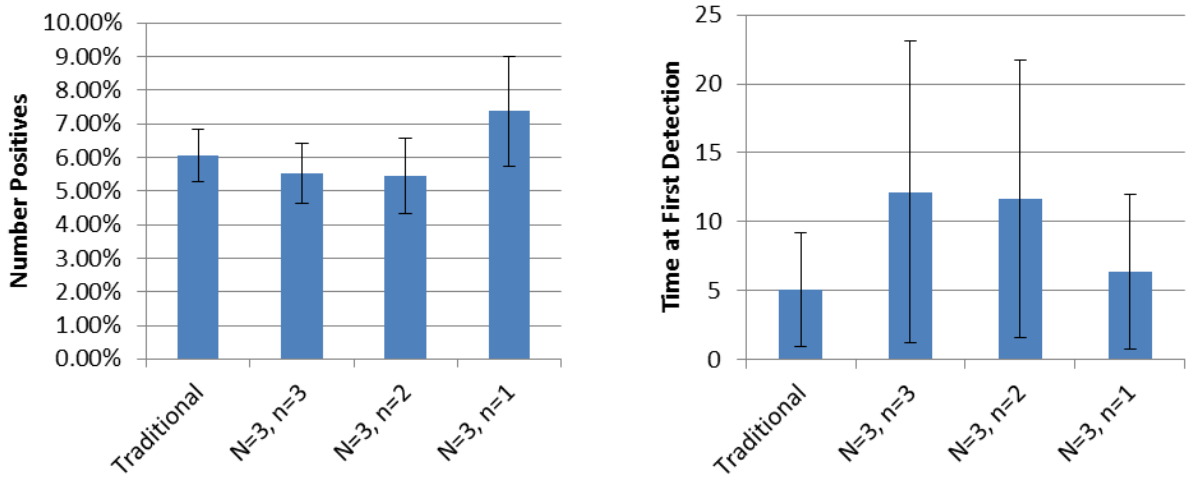

Figure 64 Positive Rate and Time to First Detection for Different n Values (Triangular, b=500, N=3, s=10, Stochastic)

The positive rate is smallest for non-extreme conditions (for example here, $n = 2$) for the triangular distribution. While the time at first detection for the triangular distribution is the lowest for the traditional method and when $n = 1$ and the largest is for when $n = N$. Similar to

the rectangular distribution, trends in the data for different series lengths for the triangular distribution were looked at for three conditions: all successes ($N = n$), at least one success ($n = 1$), and for different measurement lengths.

Figure 65 contains a graph of the positive rate and time at first detection with source strength, when $n = N$ for different series lengths. The positive rate for all five measurement lengths begins at 5%, and increases approximately linearly with source strength for the triangular distribution. The greatest positive rate is seen for longer measurement series. The longest time at first detection for the triangular distribution was seen for the longer measurement series, with $N = 5$ being consistently largest and $N = 1$ being consistently the smallest. As source strength increases the difference in detection time for the different series becomes less pronounced.

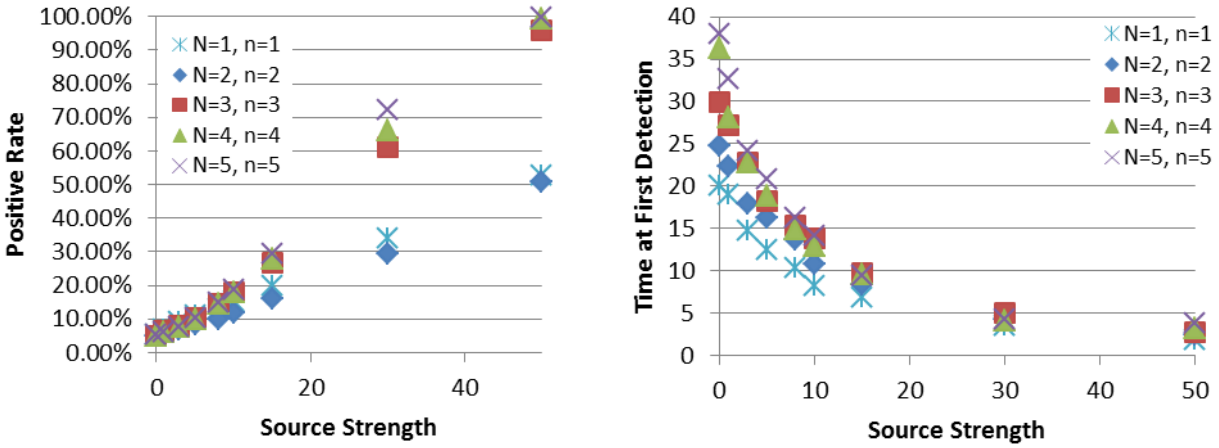

Figure 65 Positive Rate and Time at First Detection with Source Strength Comparison for Different N Values (Triangular, n=N, b=500, Stochastic)

Figure 66 contains a graph of the positive rate with source strength and time at first detection with source strength, when $n = 1$ for the triangular distribution at different series lengths. The shape of the positive rate graph with increased source strength for $n = 1$ has a different shape than for $n = N$, as also seen for the rectangular distribution. For $n = 1$, the triangular distribution positive rate increases rapidly at lower source strengths and slower at high

source strengths. The plot of the time at first detection for the triangular distribution with source strength is similar for $n = N$ and $n = 1$; however, the differences between the five measurements length is less significant with the exception of $N = 2$.

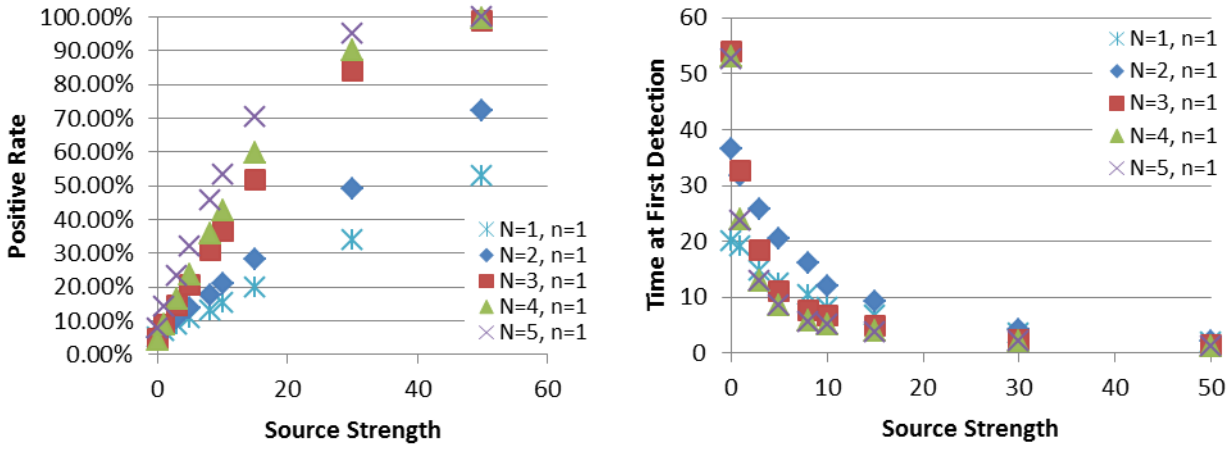

Figure 66 Positive Rate and Time at First Detection with Source Strength Comparison for Different N Values (Triangular, n=1, b=500, Stochastic)

A comparison of positive rate and time at first detection for different measurement lengths for the triangular distribution is in Figure 67.

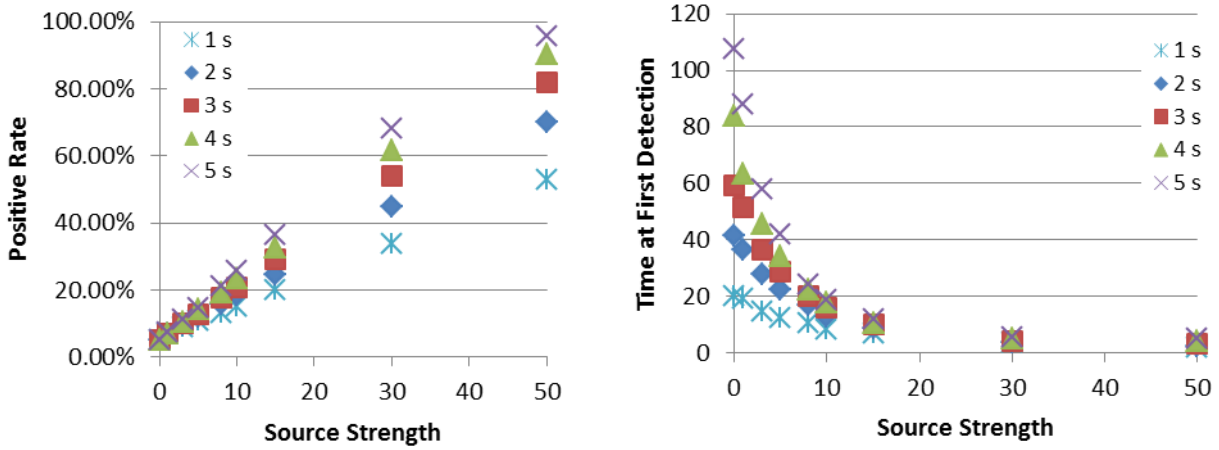

Figure 67 Positive Rate and Time at First Detection with Source Strength Comparison for Different N Values (Triangular, b=500, Stochastic)

The positive rate with source strength is greatest for a measurement length of 5 s, the least for a measurement length of 1 s. The shape of the triangular distribution positive rate with

source strength is close to a straight line, similar to $n = 1$. The time at first detection has a similar shape to the other conditions described. However, the differences between the initial time at first detection at $s = 0$ is a lot more significant. The largest time at first detection for the triangular distribution is for 5 s and the smallest is for 1 s.

Sinusoidal

Two different source and background spectra simuation techniques were used for the sinusoidal distribution and compared. One methodology generated measurement values off of a single source and background distribution, while the second method generates a value off of a source distribution and a value off of background distribution, summing them. As with the deterministic method, the sinusoidal distribution is equal to one half of the sine wave.

When using one distribution, the mean value of the sinusoidal distribution was chosen to be the sum of the background and source mean, while the width of sinusoidal distribution was chosen to keep a similar width to the Gaussian distribution. The characteristic values of the sinusoidal are $a = \mu - 3\sqrt{\mu}$ and $b = \mu + 3\sqrt{\mu}$, with a period of $T = 12\sqrt{\mu}$. For example for a background of 500 and a source value of 50, the mean μ would equal 550, while $a = 480$, $b = 620$, and $T = 12\sqrt{550} = 280$.

When the data was generated by summing a source distribution and a background distribution, one value was sampled off of a sinusoidal background distribution with a mean μ equal to the mean background and a second value was sampled off of a sinusoidal source distribution with a mean μ equal to the mean of the sample with the same characteristic a and b values as previous. For the previous example, one number would be generated off of a sinusoidal background distribution with a mean of 500 characterized by $a = 433$, $b = 567$, and $T =$

$12\sqrt{500} = 268$; a second number would be generated off of a sinusoidal source distribution with a mean of 50, $a = 43$, $b = 57$, and $T = 12\sqrt{50} = 28$.

The differences in the two measurement simulation techniques for the sinusoidal distribution are highlighted by comparing the probability density function in Figure 68 for $b = 500$ and a few source strengths. The distribution for each technique is the same for source strength of zero. The differences in the two techniques for the sinusoidal distribution are less significant than those for the rectangular and triangular distributions.

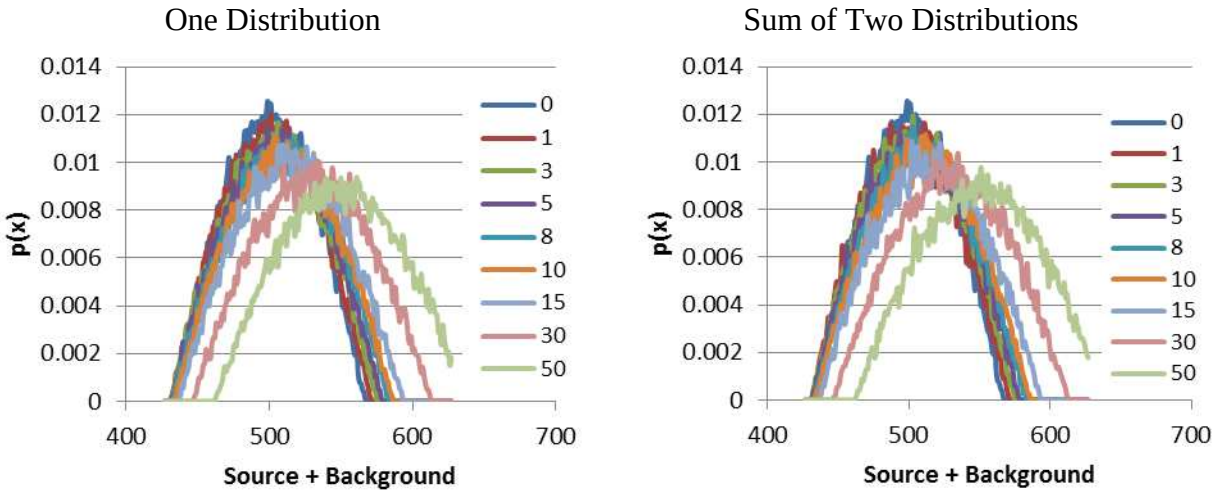

Figure 68 Probability Density Function for Different Source Strengths Comparison for Two Measurement Simulation Techniques (Sinusoidal, b=500, Stochastic)

The differences in the two measurement simulation techniques are illustrated on the same plot for several source strengths in Figure 69 for $b = 500$. There are little visual differences for the two measurement simulation techniques for the sinusoidal distribution. Graphs for additional source strengths are in Appendix B in Figure 174 ($s = 1, 3, 5, 8$) and Figure 175 ($s = 10, 15, 30, 50$).

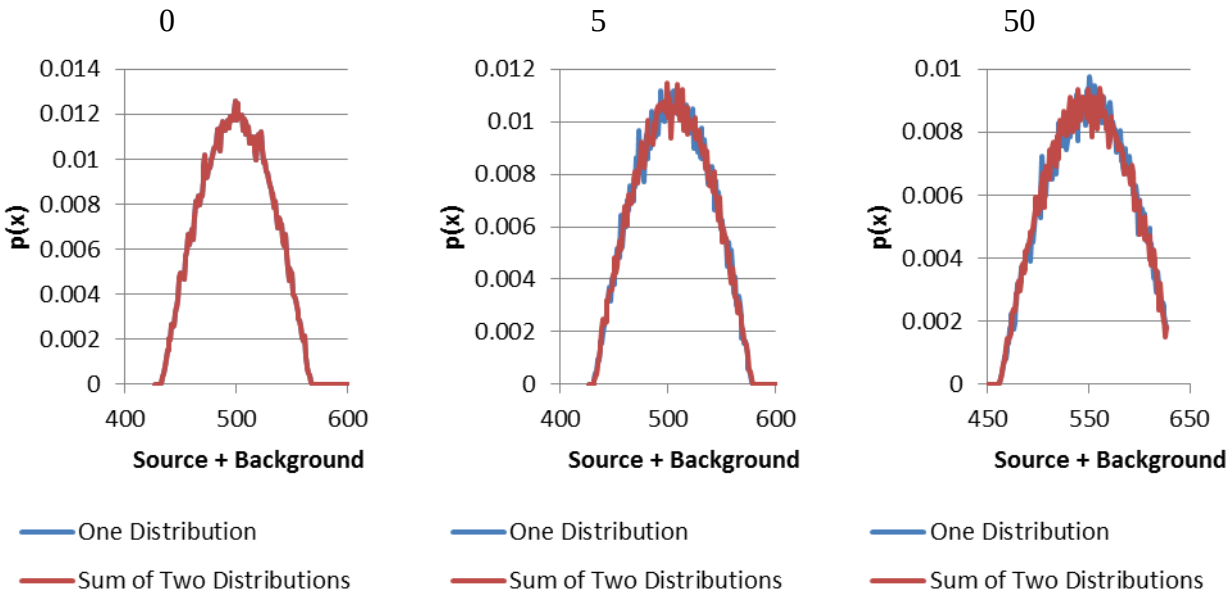

Figure 69 Probability Density Function Comparison for Measurement Simulation Techniques for Several Source Strengths (Sinusoidal, b=500, Stochastic)

The positive rate and time at first detection are compared in addition to the probability density function; a comparison of the positive rate and time at first detection for the sinusoidal distribution is in Figure 70 for $N = 2, n = 2$. For the sinusoidal distribution the main differences are in the positive rate for $N = 2$.

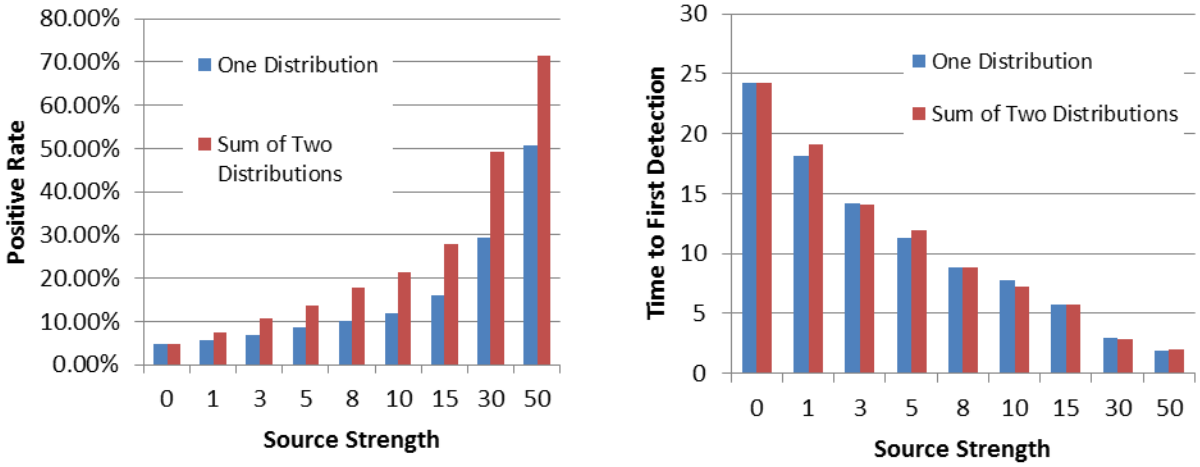

Figure 70 Positive Rate and Time at First Detection with Source Strength Comparison for Two Measurement Simulation Techniques (Sinusoidal, N=2, n=2, b=500, Stochastic)

Generating measurement values off of two distributions consistently yields a higher positive rate for the sinusoidal distribution. For the traditional method positive rate values are

within 5%, however for $n = 1$ and $n = 2$, positive rates vary by as much as 80% for the two measurement simulation techniques. The calculated time to first detection for the two measurement techniques are similar for all conditions (within 10%). Additional graphs with other values of n are available for the sinusoidal distribution in Figure 176 (positive rate) and Figure 177 (time to first detection). All future data discussed for the sinusoidal distribution is generating by using two random numbers.

A comparison of the positive rate and time to first detection for different combinations of n for the sinusoidal distribution for $N = 3$ and $b = 500$ is in Figure 71. Error bars displayed are for one standard deviation. Additional graphs for different series lengths for the sinusoidal distribution are in Figure 177 (positive rate) and Figure 178 (time at first detection).

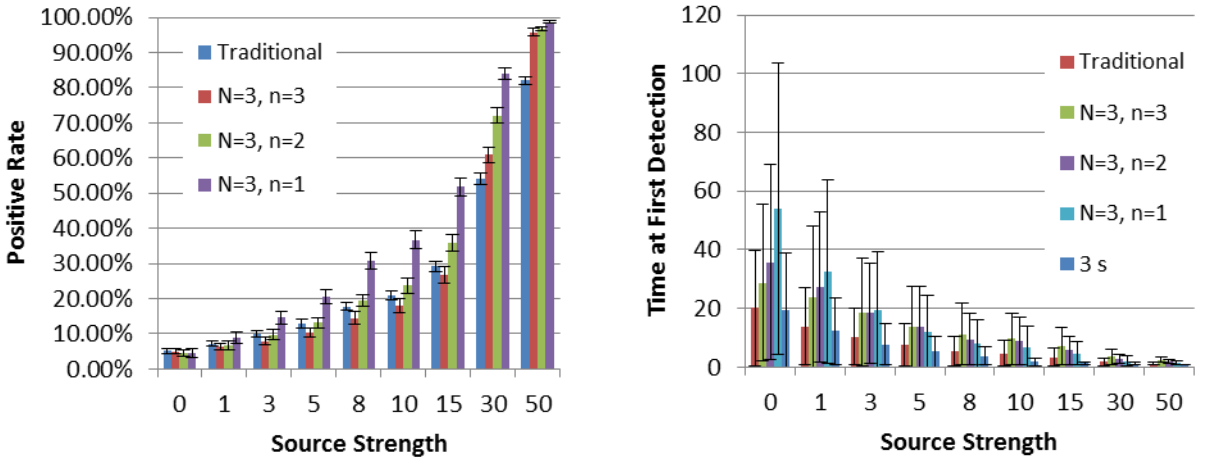

Figure 71 Positive Rate and Time at First Detection with Source Strength for Different n Values (Sinusoidal, N=3, b=500, Stochastic)

As seen in Figure 71 and for the other distributions discussed, as the source strength increases the positive rate increases and the time at first detection decreases. The positive rate for the sinusoidal distribution increases most rapidly for $n = 1$. The smallest time at first detection for the sinusoidal distribution occurs for the traditional method ($N = 1, n = 1$) and the three second long measurement.

For $b = 500$ and $s = 10$, the trends for positive rate and time at first detection are illustrated for the sinusoidal distribution in Figure 72 using $N = 3$. Error bars displayed are for one standard deviation. The positive rate for the sinusoidal distribution tends to be greatest when $n = 1$. As the number of successes required increases, the positive rate decreases for the sinusoidal distribution. The traditional method yields a higher positive rate than when $n = N$, as also seen with the rectangular distribution. For the sinusoidal time to first detection, traditional method and 1+ measurements exceeding the decision threshold in a series has the shortest time to first detection, while the larger number of required measurements exceeding the decision threshold results in a longer time at first detection.

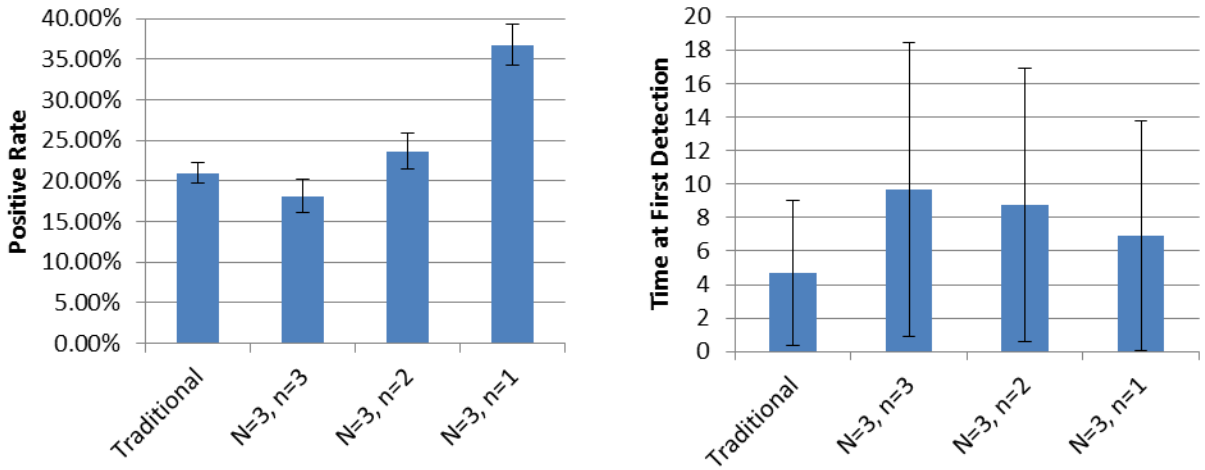

Figure 72 Positive Rate and Time to First Detection for Different n Values (Sinusoidal, b=500, N=3, s=10, Stochastic)

Trends in the data (positive rate and time at first detection) for different series lengths for the sinusoidal distribution were looked at for three conditions: all successes ($N = n$), at least one success in a series ($n = 1$), and for different measurement lengths. Figure 73 contains a graph of the positive rate with source strength and time at first detection with source strength for the sinusoidal distribution, when $n = N$ for different series lengths.

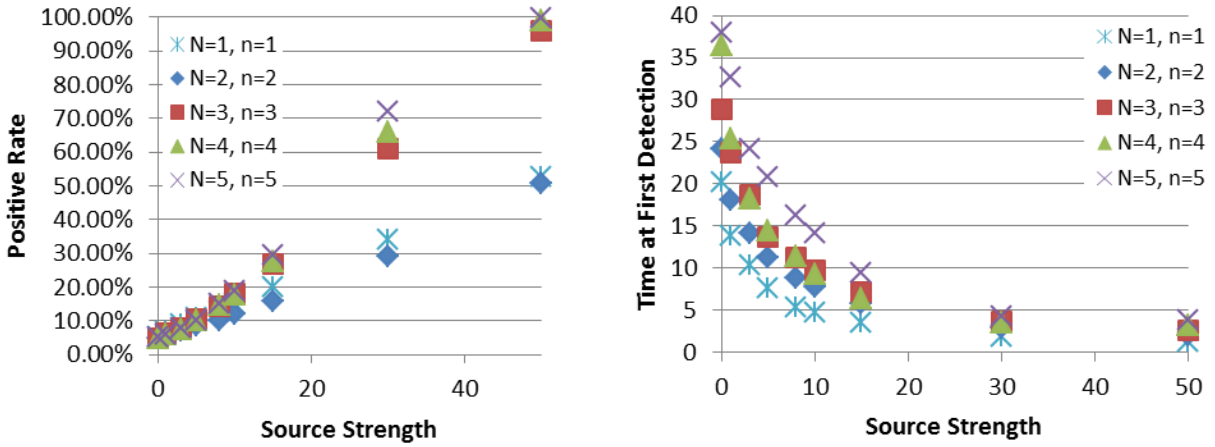

Figure 73 Positive Rate and Time at First Detection with Source Strength Comparison for Different N Values (Sinusoidal, n=N, b=500, Stochastic)

The positive rate for all five measurement lengths begins at 5% and increases approximately linearly with source strength. The positive for larger measurement lengths for the sinusoidal distribution is larger than for shorter series lengths. For the sinusoidal time at first detection, the larger measurement lengths have larger time at first detection, while shorter measurement lengths have shorter times at first detection; this remains constant for all source strengths.

Figure 74 has a graph of the positive rate with source strength and time at first detection with source strength, when $n = 1$ for different series lengths for the sinusoidal distribution.

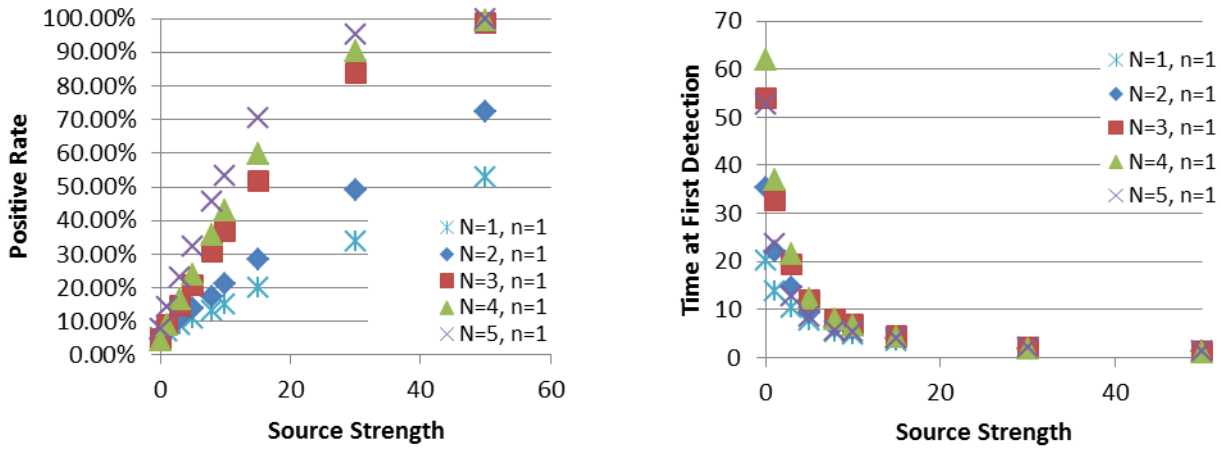

Figure 74 Positive Rate and Time at First Detection with Source Strength Comparison for Different N Values (Sinusoidal, n=1, b=500 Stochastic)

The shape of the positive rate graph with increased source strength for $n = 1$ has a different shape than for $n = N$ (as seen for other distributions discussed); the positive rate for $n = 1$ increases rapidly at lower source strengths and slower at high source strengths. The plot of the time at first detection with source strength for the sinusoidal distribution is similar for $n = N$ and $n = 1$; however, the differences between the five measurements length is less significant, especially after a source strength of around 5.

Figure 75 contains a comparison of positive rate and time at first detection for different measurement lengths for the sinusoidal distribution. The positive rate with source strength is greatest for a measurement length of 5 s, and smallest for a measurement length of 1 s. The shape of the positive rate with source strength for the sinusoidal distribution is approximately a straight line, similar to $n = 1$. The time at first detection has a similar shape to other conditions and distributions discussed. The time at detection is largest for 5 s and smallest for 1 s for the sinusoidal distribution.

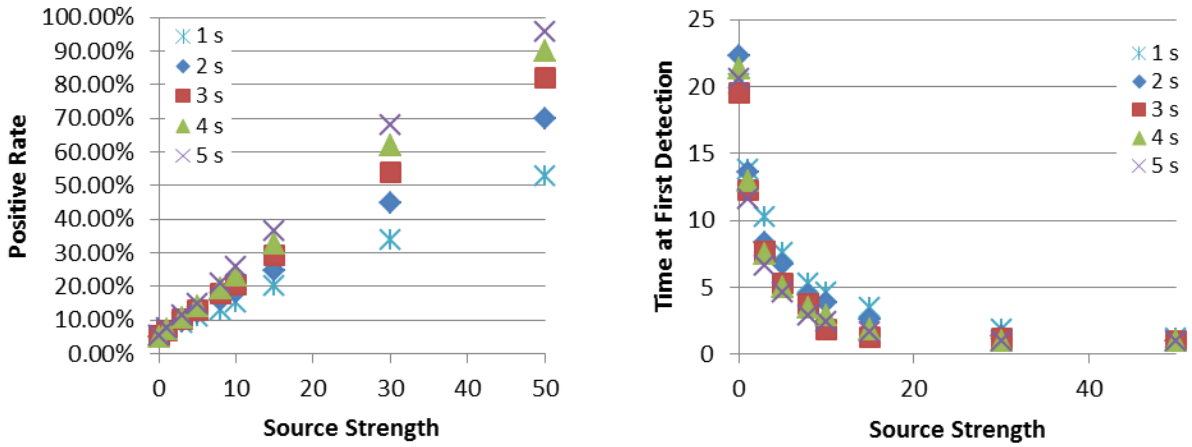

Figure 75 Positive Rate and Time at First Detection with Source Strength Comparison for Different N Values (Sinusoidal, b=500, Stochastic)

Poisson

Measurements for the Poisson distribution were generated using two different source and background spectra simulation techniques and compared. The first method generates

measurement values off of a single source and background distribution, while the second method generates a value off of a source distribution and a value off of background distribution, summing them. The Poisson distribution is characterized by only a mean value. When using one distribution, the mean value was chosen to be the sum of the background and source mean. When the data was generated by summing two distributions, one value was sampled off of a Poisson background distribution with a mean equal to the mean background and a second value was sampled off of a Poisson source distribution with a mean equal to the mean of the source. The generated probability density functions are compared for the Poisson distribution in Figure 76 for a background of 500 and a few source strengths. For the Poisson distribution, there is very little difference between techniques, as also seen for the sinusoidal distribution.

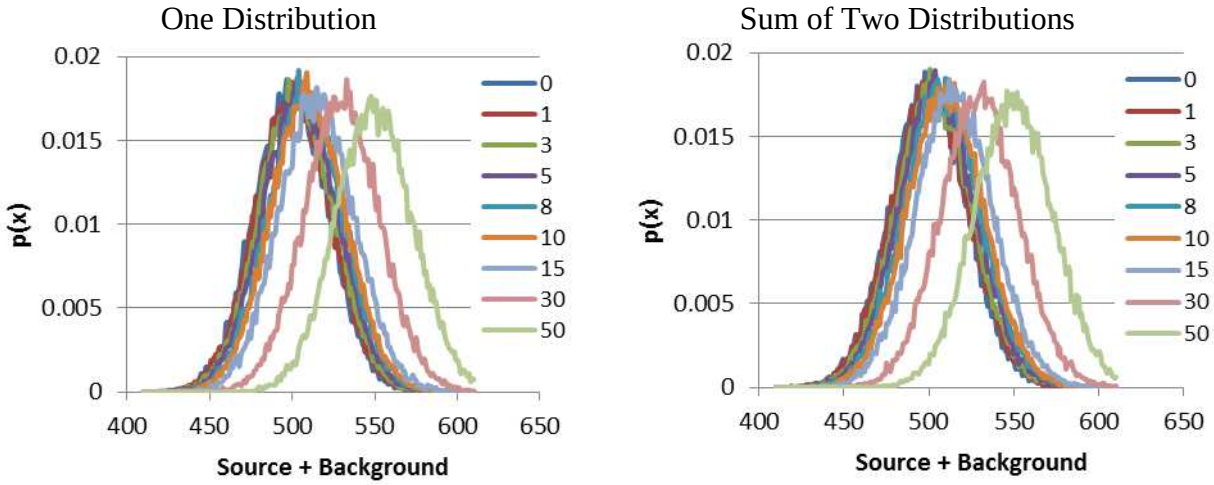

Figure 76 Probability Density Function for Different Source Strengths Comparison for Two Measurement Simulation Techniques (Poisson, b=500, Stochastic)

The differences in the two measurement simulation techniques are illustrated on the same plot in Figure 77 for $b = 500$ for the Poisson distribution. There are little differences between the measurement simulation techniques for the Poisson distribution. Additional comparisons for other source strengths are in Figure 180 ($s = 1, 3, 5, 8$) and Figure 181 ($s = 10, 15, 30, 50$).

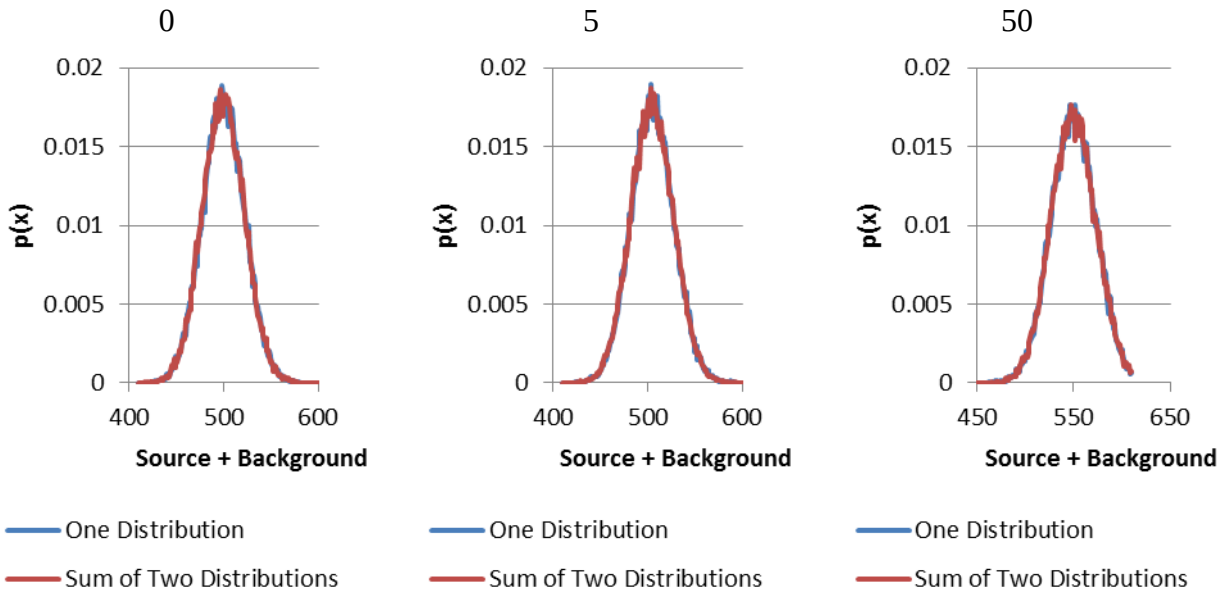

Figure 77 Probability Density Function Comparison for Two Measurement Simulation Techniques For Several Source Strengths (Poisson, b=500, Stochastic)

In addition to the comparison of the probability density function, the positive rate and time at first detection are compared for the Poisson distribution in Figure 78 for $N = 2, n = 2$.

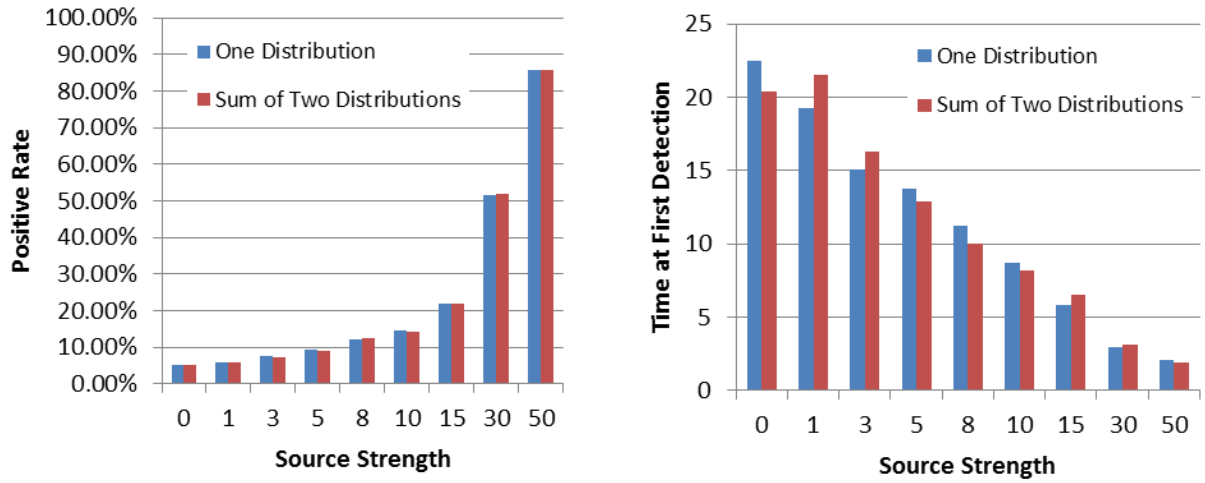

Figure 78 Positive Rate and Time at First Detection with Source Strength Comparison for Measurement Simulation Techniques (Poisson, N=2, n=2, b=500, Stochastic)

Values for the positive rate are within 10% and values for detection time are within 15%. Comparisons for additional n values are in Figure 182 (positive rate) and Figure 183 (time at first detection). All future Poisson data discussed is generating using two random numbers.

A comparison of the Poisson positive rate and time to first detection for different combinations of n ($N = 3$) is in Figure 79 for a background of 500. Error bars displayed are for one standard deviation. As the source strength increases the positive rate increases and the time at first detection decreases. The positive rate for larger values of n and for a 3 s measurement time increase the most rapidly; however positive rate for all conditions increase at a similar rate with source strength. The time at first detection is longest for the 3 s measurement and decreases as n and N decrease. Additional graphs for different series lengths are in Figure 184 (positive rates) and Figure 185 (time at first detection).

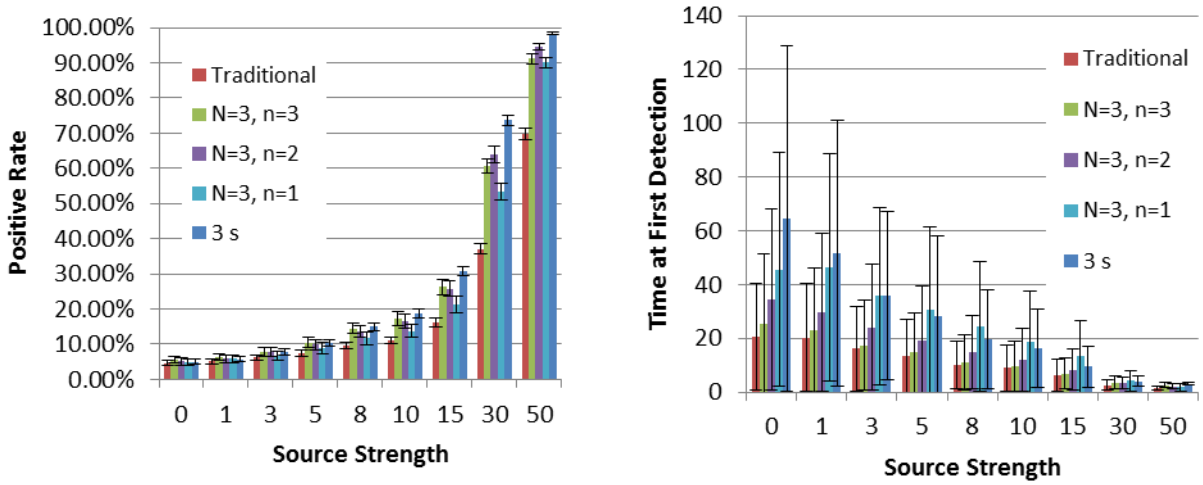

Figure 79 Positive Rate and Time at First Detection with Source Strength for Different n Values (Poisson, N=3, b=500, Stochastic)

For $b = 500$ and $s = 10$, the trends for positive rate and time at first detection between different conditions for the Poisson distribution are illustrated in Figure 80 for $N = 3$. Displayed error bars are for one standard deviation. The positive rate for the Poisson distribution tends to increase as n increases. The time at first detection also tends to decrease as n increases for the Poisson distribution. Trends in the data (positive rate and time at first detection) for different series lengths for the Poisson distribution were looked at for three conditions: $N = n$, $n = 1$, and for different measurement lengths.

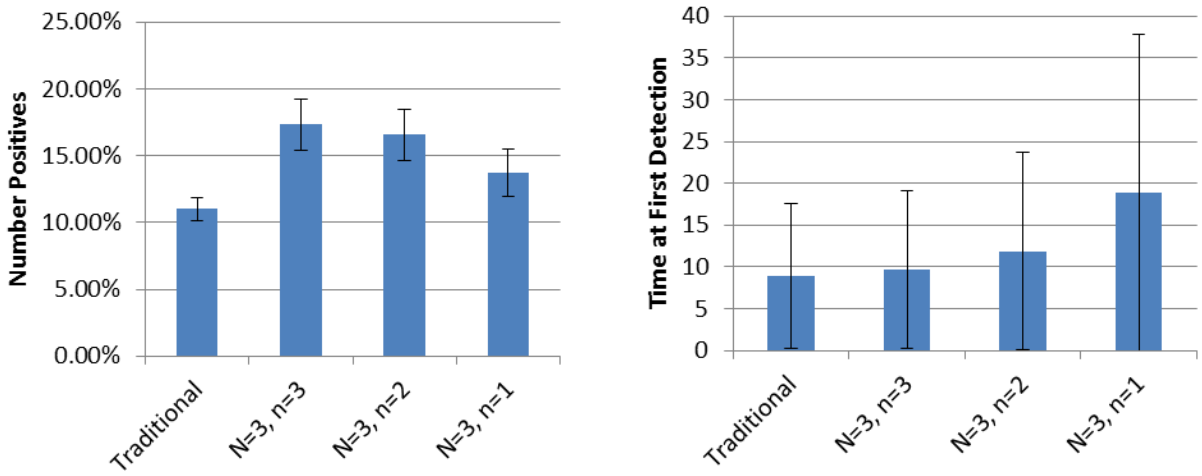

Figure 80 Positive Rate and Time at First Detection for Different n Values (Poisson, b=500, N=3, s=10, Stochastic)

Figure 81 contains a graph of the Poisson positive rate with source strength and time at first detection with source strength, when $n = N$ for different series lengths.

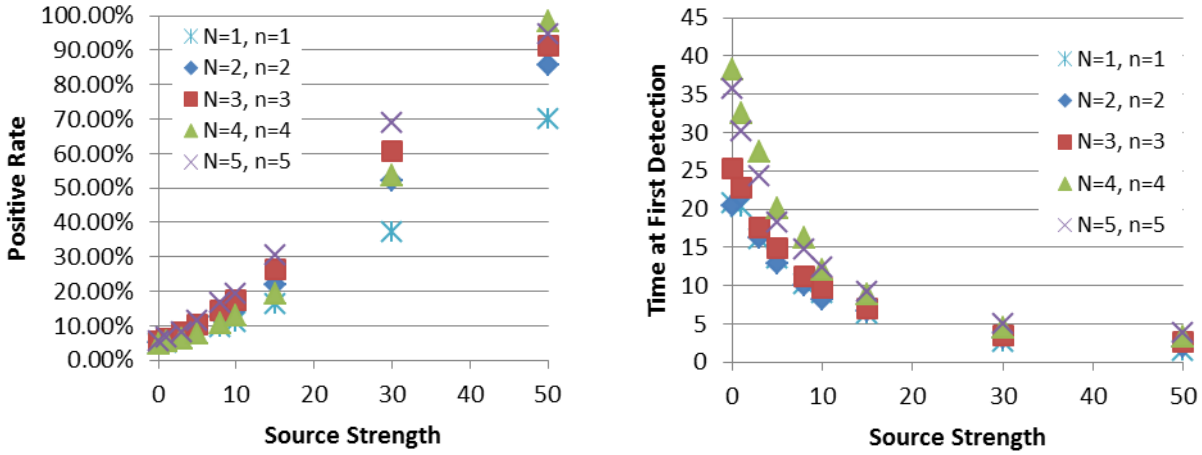

Figure 81 Positive Rate and Time at First Detection with Source Strength Comparison for Different N Values (Poisson, n=N, b=500, Stochastic)

The positive rate for all five measurement lengths begins at 5% and increases approximately linearly with source strength. The largest positive rate is for a series of 5 measurements and smallest for the traditional method for the Poisson distribution. For the time at first detection, the drop in time at first detection with increased source strength is largest for small source strengths and then become less significant for higher source strengths. The time at

first detection is largest for the Poisson distribution for $N = 4$ and $N = 5$, and smallest for $N = 2$ and $N = 1$.

Figure 82 contains a graph for the Poisson distribution of the positive rate with source strength and time at first detection with source strength, when $n = 1$ for different series lengths. The shape of the positive rate with source strength is different for $N = 4$ for the Poisson distribution. The positive rate for $N = 4, n = 1$ initially increases rapidly and slows with additional source strength; the other measurement lengths exhibit an initial slow growth in positive rate with source strength until larger source strengths.

Based on other distributions for the $n = 1$ condition, the shape of $N = 4$ is more expected. This should be investigated further for the Poisson distribution. The plot of the time at first detection for the Poisson distribution with source strength is similar for $n = N$ and $n = 1$; however, $N = 3$ exhibits the largest time at first detection, while $N = 4, 5, 1$ exhibit the lowest.

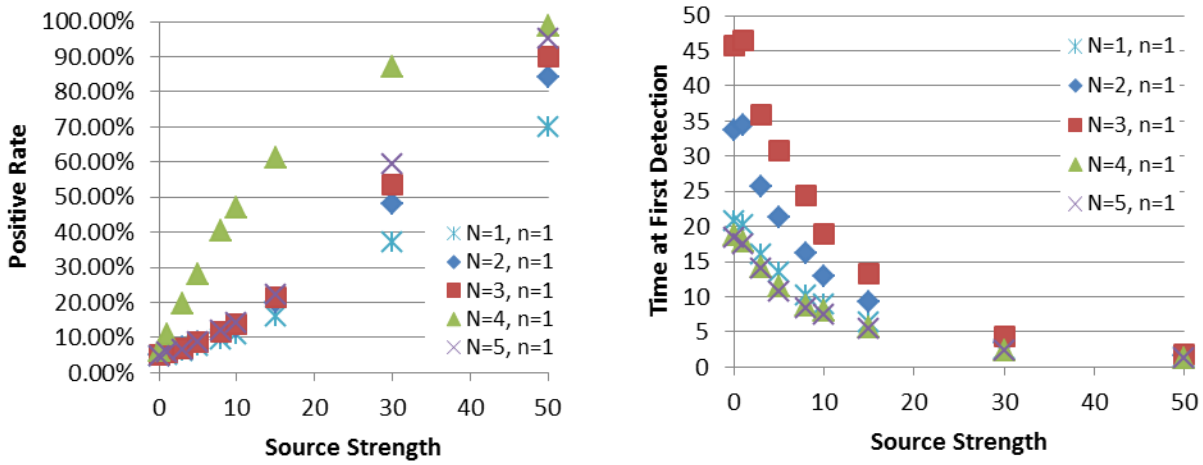

Figure 82 Positive Rate and Time at First Detection with Source Strength Comparison for Different N Values (Poisson, n=1, b=500, Stochastic)

Figure 83 contains a comparison of positive rate and time at first detection for different measurement lengths for the Poisson distribution. The positive rate with source strength is greatest for 5 s and least for 1 s. The positive rate with source strength is close to a straight line.

The time at first detection has a similar shape to the other conditions described. The time at detection is largest for 5 s and smallest for 1 s.

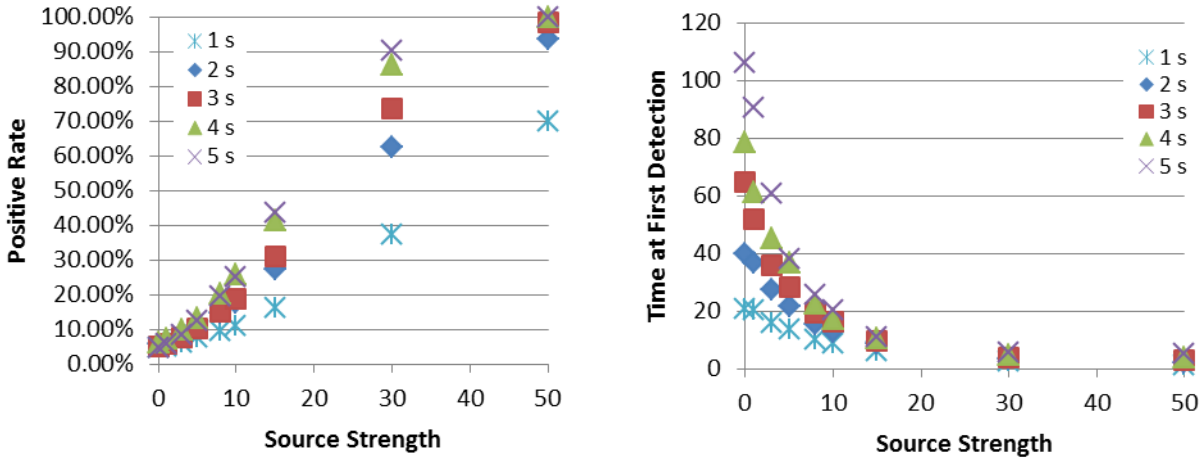

Figure 83 Positive Rate and Time at First Detection with Source Strength Comparison for Different N Values (Poisson, b=500, Stochastic)

Gaussian

Measurements for the Gaussian distribution were generated using two different source and background spectra simulation techniques and compared. The first method generates data off of a single source and background distribution, while the second method sums a value generated off of a source distribution and a value generated off of background distribution. The Gaussian distribution is characterized by a mean value and a variance. The variance was chosen to be the mean, as with the Poisson distribution.

When using one distribution, the mean value of the Gaussian distribution was the sum of the background and source mean with an equivalent variance. When data was generated of two distributions, one distribution had a mean and variance equivalent to the background mean, while the second distribution had a mean and variance equivalent to the source mean. The two source and background simulation techniques are compared through the probability density function in

Figure 84 for $b = 500$. As with the Poisson distribution, there is little difference between the measurement simulation techniques for the Gaussian distribution.

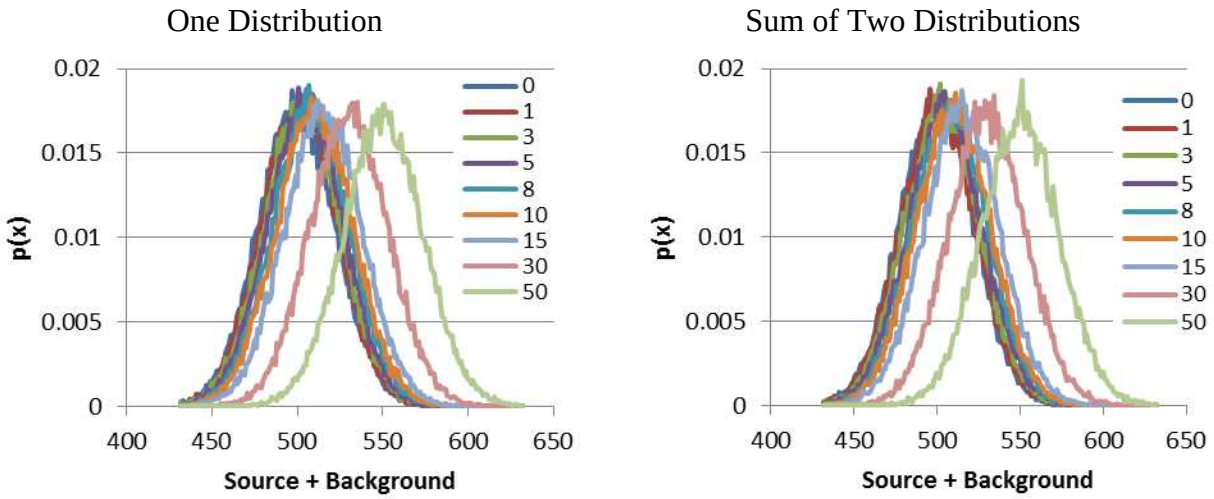

Figure 84 Probability Density Function for Different Source Strengths Comparison for Two Measurement Simulation Techniques (Gaussian, b=500, Stochastic)

The two measurement simulation techniques are also compared for the Gaussian distribution on the same plot for source strengths of 0, 5, and 50 for a background of 500 in Figure 85.

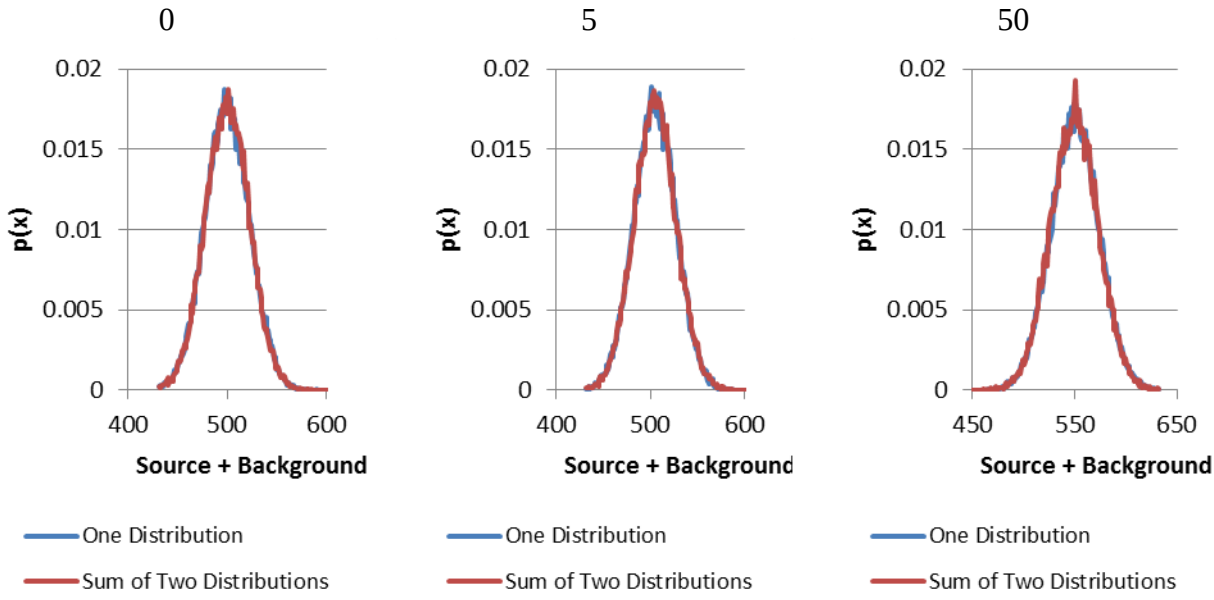

Figure 85 Probability Density Function Comparison for Two Measurement Simulation Techniques For Several Source Strengths (Gaussian, b=500, Stochastic)

There are little differences in the distributions for the Gaussian distribution. Additional comparisons of the probability density function for the two measurement techniques for the Gaussian distribution using other source strengths are in Appendix B in Figure 186 ($s = 1, 3, 5, 8$) and Figure 187 ($s = 10, 15, 30, 50$).

The Gaussian positive rate between the two measurement simulation techniques are compared for $N = 2, n = 2$ in Figure 86. Values for the positive rate are within 10%. Additional comparisons for the Gaussian distribution are available for other values of n in Appendix B in Figure 188. All future data discussed for the Gaussian distribution is generating by using two random numbers.

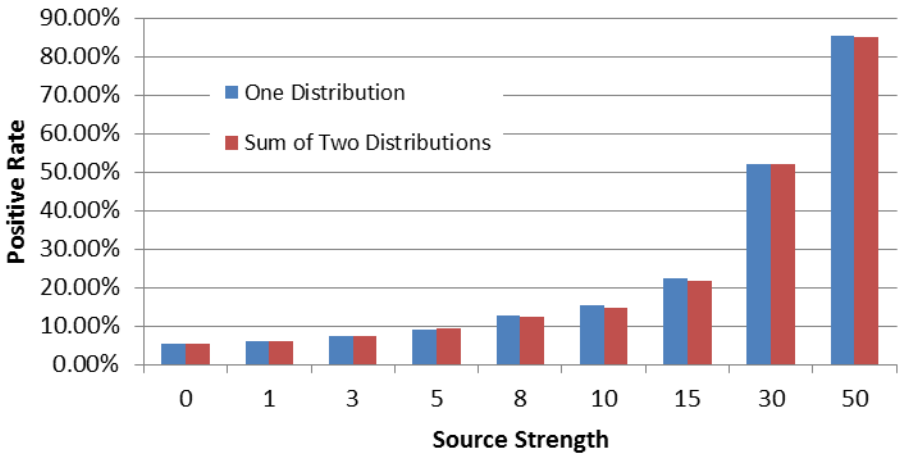

Figure 86 Positive Rate with Soruce Strength for Two Measurement Simulation Techniques (Gaussian, N=2, n=2, b=500, Stochastic)

A comparison of the positive rate and time to first detection for the Gaussian distribution for different n ($N = 3$) is in Figure 87 for $b = 500$. The error bars are one standard deviation. As seen by Figure 87, the Gaussian positive rate increases as the source strength increases, while the time at first detection decreases. The positive rate tends to be the largest for non-extreme values of n (example $N = 3, n = 2$) for the Gaussian distribution. The time at first detection is the largest for a three second long measurement and $n = 1$ and smallest for the traditional

method. Additional graphs for the Gaussian different series lengths and background levels are available for the positive rate: Figure 189 ($N = 2$), Figure 190 ($N = 3$), Figure 191 ($N = 4$), Figure 192 ($N = 5$), and time at first detection: Figure 193 ($N = 2$), Figure 194 ($N = 3$), Figure 195 ($N = 4$), Figure 196 ($N = 5$).

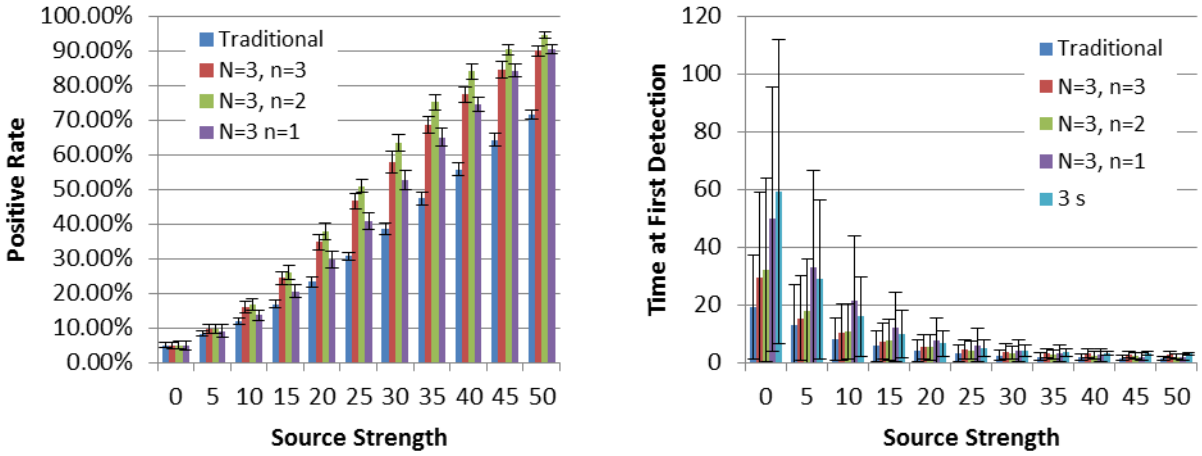

Figure 87 Positive Rate and Time at First Detection for Different n Values (Gaussian, N=3, b=500, Stochastic)

Figure 88 contains a bar graph for the positive rate and time to first detection for different number of successes for $N = 3$ for the Gaussian distribution ($b = 500$ and $s = 10$). The error bars displayed are for one standard deviation.

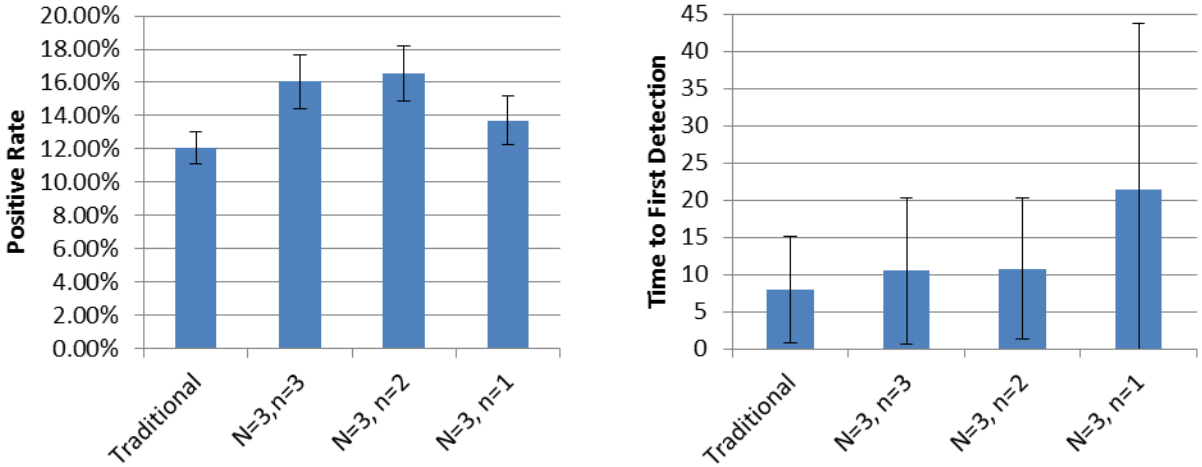

Figure 88 Positive Rate and Time to First Detection for Different n Values (Gaussian, b=500, N=3, s=10, Stochastic)

The positive rate for the Gaussian distribution tends to be greatest for non-extreme values of n, as seen in Figure 87, and smallest for $n = 1$. The smallest time to first detection correlates to the largest values of the positive rate, being the largest for $n = 1$. Trends in the data (positive rate and time at first detection) for different series lengths for the Gaussian distribution were looked at for three conditions: all successes ($N = n$), at least one success in a series ($n = 1$), and for different measurement lengths.

Figure 89 contains a graph for the Gaussian distribution of the positive rate with source strength and time at first detection with source strength, when $n = N$ for different series lengths. The positive rate for all conditions begins at 5% and increases approximately linearly with source strength. The largest positive rate for the Gaussian distribution is for $N = 5$ and the smallest is for $N = 1$. The time at first detection initially decreases rapidly with added source strength and then slows at higher source strengths. The time at first detection for the Gaussian distribution is largest for larger series lengths; however, the difference in time at first detection becomes less as source strength increases.

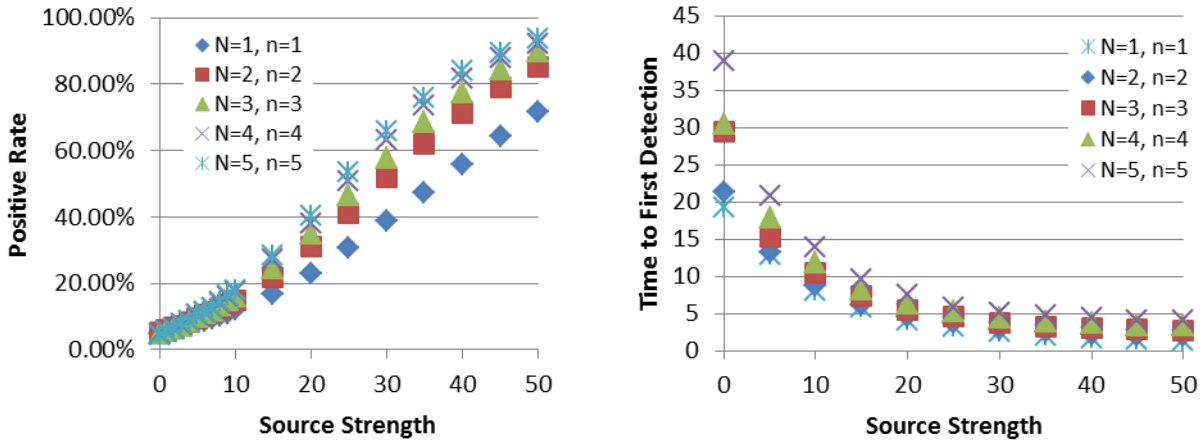

Figure 89 Positive Rate and Time at First Detection with Source Strength Comparison for Different N Values (Gaussian, n=N, b=500, Stochastic)

Figure 90 contains a graph for the Gaussian distribution of the positive rate with source strength and time at first detection with source strength, when $n = 1$. The positive rate for $n = 1$ increases rapidly at lower source strengths and slower at high source strengths. The plot of the Gaussian time at first detection with source strength is similar for $n = N$ and $n = 1$; however, the differences between the five measurements length is less significant.

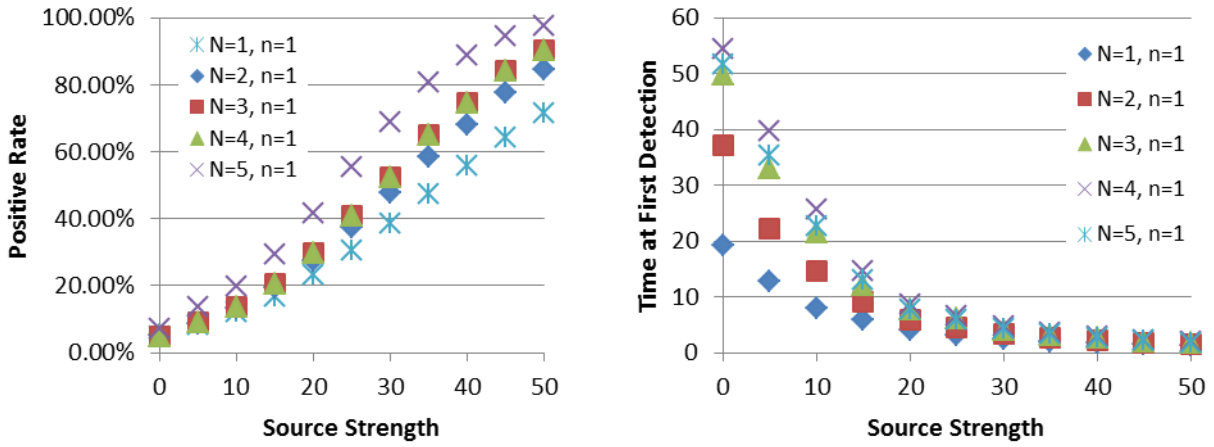

Figure 90 Positive Rate and Time at First Detection with Source Strength Comparison for Different N Values (Gaussian, n=1, b=500, Stochastic)

Figure 91 contains a comparison of the positive rate and time at first detection for the Gaussian distribution for different measurement lengths.

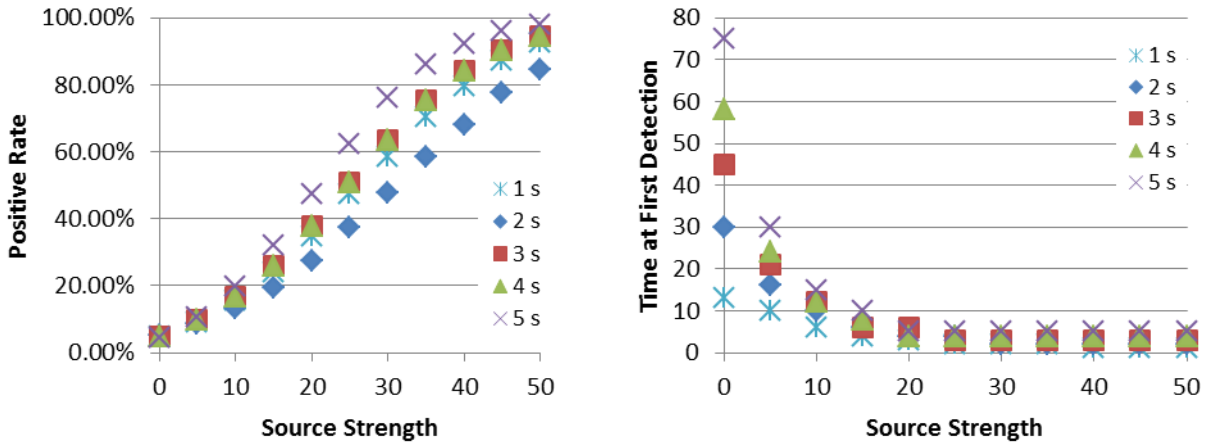

Figure 91 Positive Rate and Time at First Detection with Source Strength Comparison for Different N Values (Gaussian, b=500, Stochastic)

The positive rate with source strength has a similar shape to the cumulative distribution function for the Gaussian distribution. The positive rate is the greatest for 5 s, the least for 1 s. The time at first detection for the Gaussian distribution has a similar shape to the other conditions and distributions described. The time at detection is largest for 5 s and smallest for 1 s.

Comparison of Deterministic and Stochastic Methods and Discussion

Two methodologies for analyzing the series of measurements were investigated: looking at exactly n values exceeding the decision threshold in N measurements, and looking at least n values exceeding the decision threshold in N measurements. The two methodologies were looked at for both the deterministic and stochastic methods and showed similar trends. The comparison was investigated for the Gaussian distribution, but observations should hold for other distributions as well.

A value of $N = 2$ was investigated for the stochastic method, while $N = 3, 4, 5$ were also investigated for the deterministic method. All N values showed similar trends. There are no differences when $n = N$, because Equation 89 and 90 converge for $n = N$. For other values of n for the *exact* condition as the source strength increases, eventually the positive rate increases to a maximum at around 50% and decreases. This is likely because as the source strength increases, the probability density function is shifted to the right beyond the threshold. It becomes more likely that greater than n successes will occur and eventually only N successes is possible. The *at least* methodology takes this into account and as the source strength increases the positive rate increases to eventually 100%.

For the stochastic method, two different measurement generating techniques were investigated. One technique generated off of one distribution using one random number where

the mean of that distribution was equal to the sum of the source and the background. The second method generated off of a source and a background distribution using two random numbers and summed the values. The probability density functions were compared visually and the positive rate and time to first detection were compared. There were significant visual differences for the rectangular and triangular distributions, but weren't for the sinusoidal, Poisson, and Gaussian distributions. For the positive rate, there was less than 5% variation for the rectangular distribution, less than 10% variation for the Poisson and Gaussian, and up to 80% error for the sinusoidal and triangular distributions. For the time at first detection, there was less than 10% variation for the rectangular distribution and sinusoidal distribution, and less than 15% variation for the Poisson and triangular distribution. Overall, the time at first detection showed less variation between the two techniques than the positive rate. There was significant difference in the positive rate data for the triangular and sinusoidal distributions.

The probability density function for the positive rates and the time to first detection were also looked at for the stochastic method. The distribution of positive rates followed closely to a normal distribution, while the time to first detection followed closely to a geometric distribution. Both of these agreed better when $n = N$. For values of n less than N, the probability density function for the measurement data is larger at higher times at first detection than expected for the geometric distribution with p equal to the positive rate. The positive rate may not be the best predictor for the time at first detection for conditions where n is not equal to N.

For the deterministic distribution, the probability density function was looked at for different background levels. For each distribution as the mean background increased the distribution widened and the peak probability decreased. Additionally, as source strength

increased the distribution widened; the widening of the distribution is most significant when the source strength is large compared to the mean background.

Values for the decision threshold were calculated for $N = 1, 2, 3, 4, 5$ and for corresponding n values between 1 and N. For larger N values with constant n, the decision threshold increased. Additionally as n approaches N, the decision threshold decreases. If n and N become large enough, the decision threshold can decrease lower than the mean of the distribution. For the deterministic method, the source strength for 50% and 100% detection was calculated for each condition. As the background strength increases, the positive rate is larger for the same source to background ratio. This is because although the background probability density function widens as the background increases it does not scale 1:1. For example, the probability density function for a mean of 50 will not be twice as wide as for a mean of 100.

Behavior of the positive rates and time at first detection with N was investigated by looking at a couple circumstances: $n = N$, $n = 1$, and the measurement length. In general, the behavior for the positive rate with source strength agreed well for all distributions. For the all conditions the positive rate tended to be largest for $N = 5$ and lowest for $N = 1$. The same applied for the time at first detection. This indicates that a higher positive rate does not always coincide with a lower time at first detection, as would be expected with the geometric distribution.

The positive rates are compared for each distribution for the deterministic and stochastic methodologies. Additionally, positive rates (for stochastic and deterministic) and time at first detection (for stochastic) are compared between distributions. The distributions will be discussed in the same order that they appeared in the text. The positive rate for the rectangular distribution is compared for the stochastic and deterministic methods in two ways in Figure 92 for $b = 500$

and $N = 3$. The left side of Figure 92 contains a plot of the positive rate with source strength for each condition of n for $N = 3$. The deterministic method is displayed using a solid line with individual stochastic data points over laid. For the rectangular distribution, the calculated positive rate for stochastic and deterministic methods agrees well with source strength. The right side of Figure 92 contains a bar graph for the different conditions of n at a source strength of 10. The deterministic and stochastic methods agree well with each other for $N = 3$.

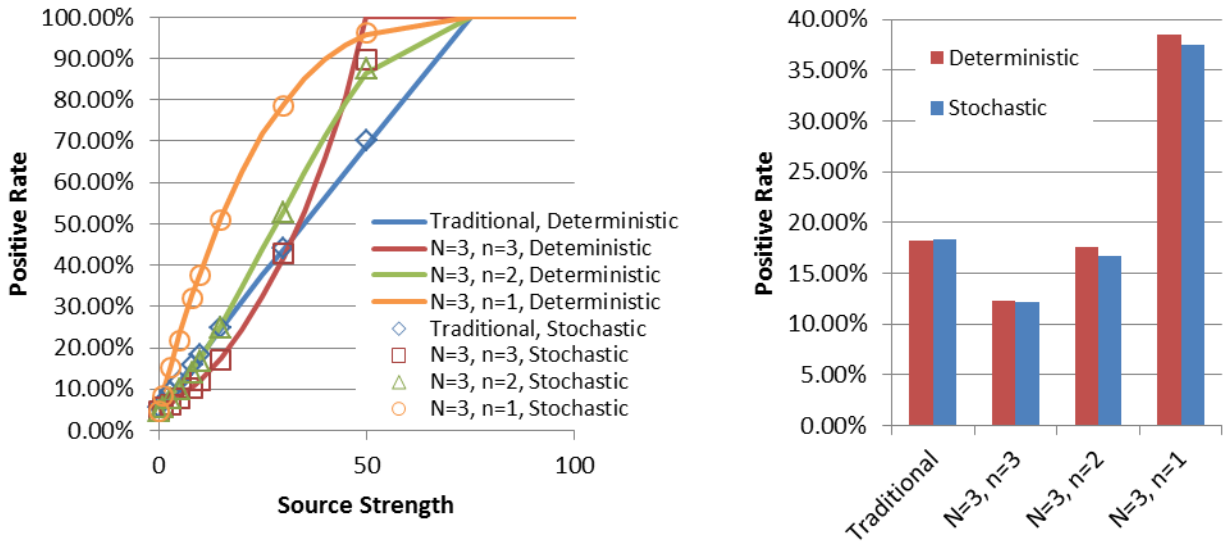

Figure 92 Deterministic and Stochastic Positive Rate with Source Strength Comparison for Different n Values (Rectangular, b=500, N=3)

Figure 93 contains two comparisons of the positive rate for the triangular distribution using the stochastic and deterministic methods for a background of 500 and $N = 3$. On the left side of Figure 93 is a plot of the positive rate with source strength for each condition of n for $N = 3$, while the right side has a bar graph for the different conditions of n at a source strength of 10. The deterministic and stochastic methods do not agree with each other as well as for the rectangular distribution. Either the deterministic method overestimates the positive rate by about two times or the stochastic method underestimates the positive rate by a factor of two at $N = 3$.

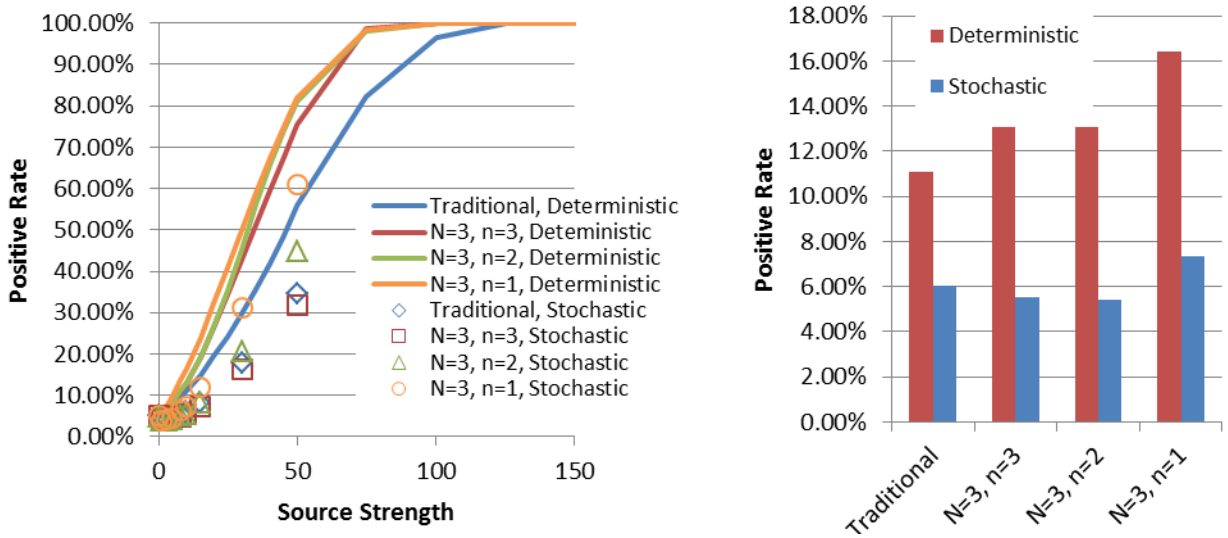

Figure 93 Deterministic and Stochastic Positive Rate with Source Strength Comparison for Different n Values (Triangular, b=500, N=3)

The positive rate for the sinusoidal distribution is compared for the stochastic and deterministic methods in two ways in Figure 94 for a background of 500 and $N = 3$.

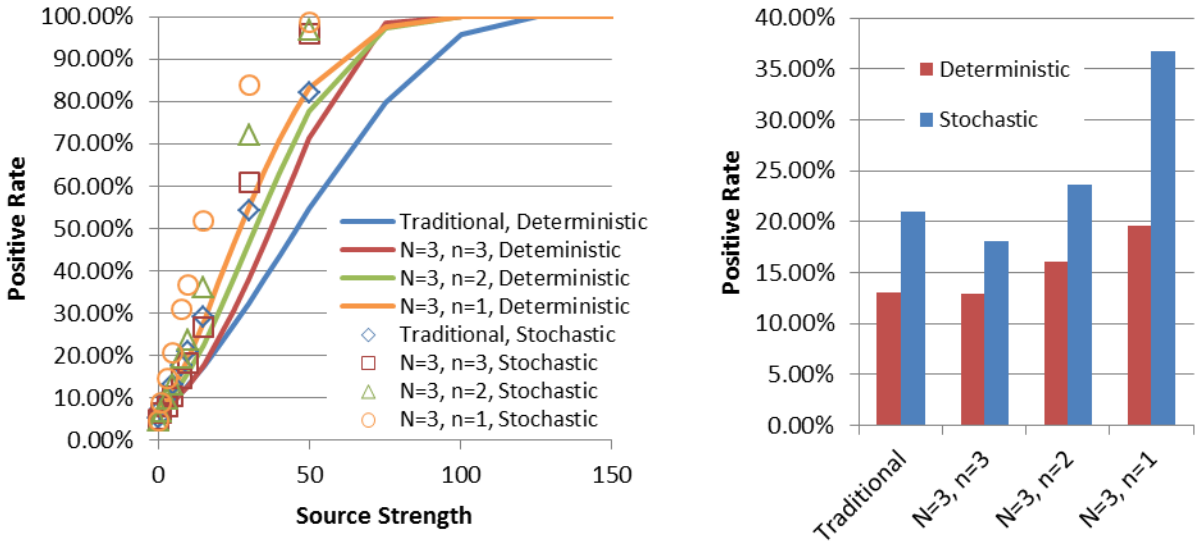

Figure 94 Deterministic and Stochastic Positive Rate with Source Strength Comparison for Different n Values (Sinusoidal, b=500, N=3)

The left side of Figure 94 contains a plot of the positive rate with source strength for each condition of n for $N = 3$. For the sinusoidal distribution, the calculated positive rate for stochastic method tends to agree with the deterministic method for smaller source strengths, but begins to become larger than the deterministic method of larger source strengths. The right side

of Figure 94 contains a bar graph for the different conditions of n at a source strength of 10. The stochastic method predicts a higher positive rate than the deterministic method. The most significant difference in positive rate for the two methods is for $N = 3, n = 1$.

The positive rate for the stochastic and deterministic methods is also compared in two ways for the Poisson distribution in Figure 95 for a background of 500 and $N = 3$. The left side of Figure 95 contains a plot of the positive rate with source strength for each condition of n for $N = 3$, while the right side of Figure 95 contains a bar graph for the different conditions of n at a source strength of 10. For the Poisson distribution, the calculated positive rate for stochastic and deterministic methods agree well with source strength, as well as for different n for $N = 3$.

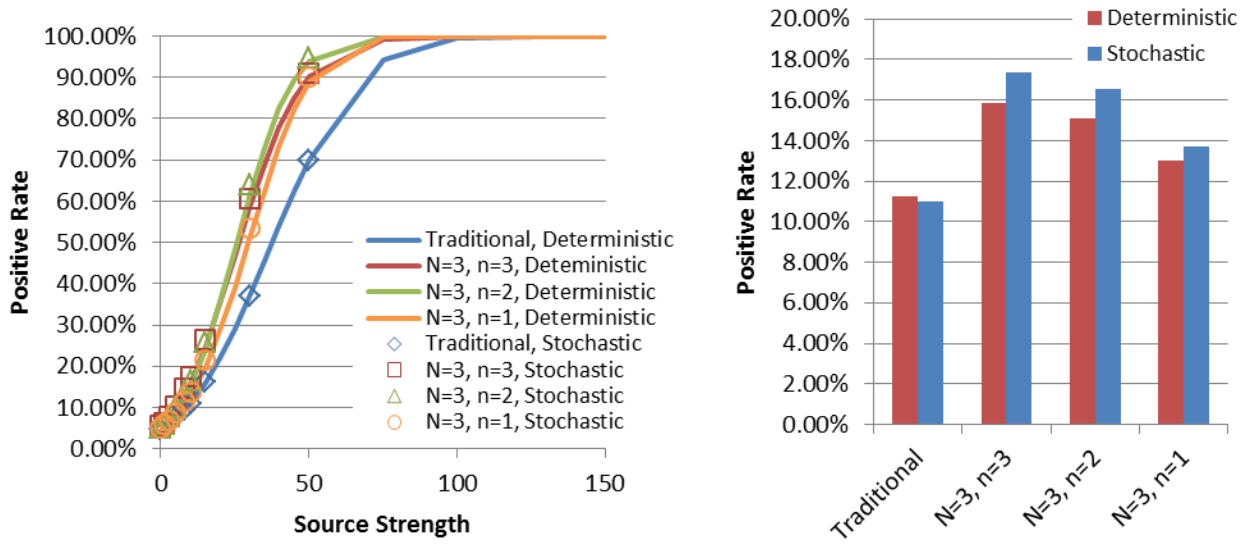

Figure 95 Deterministic and Stochastic Positive Rate with Source Strength Comparison for Different n Values (Poisson, b=500, N=3)

The positive rate for the stochastic and deterministic methods is also compared for the Gaussian distribution in two ways in Figure 96 for a background of 500 and $N = 3$. The left side of Figure 96 contains a plot of the positive rate with source strength for each condition of n for $N = 3$. For the Gaussian distribution, the calculated positive rate for stochastic and deterministic methods agree well with source strength. The right side of Figure 96 contains a bar graph for the

different conditions of n at a source strength of 10. The deterministic method tends to over-predict the stochastic methods at a source strength of 10 by a couple of percent.

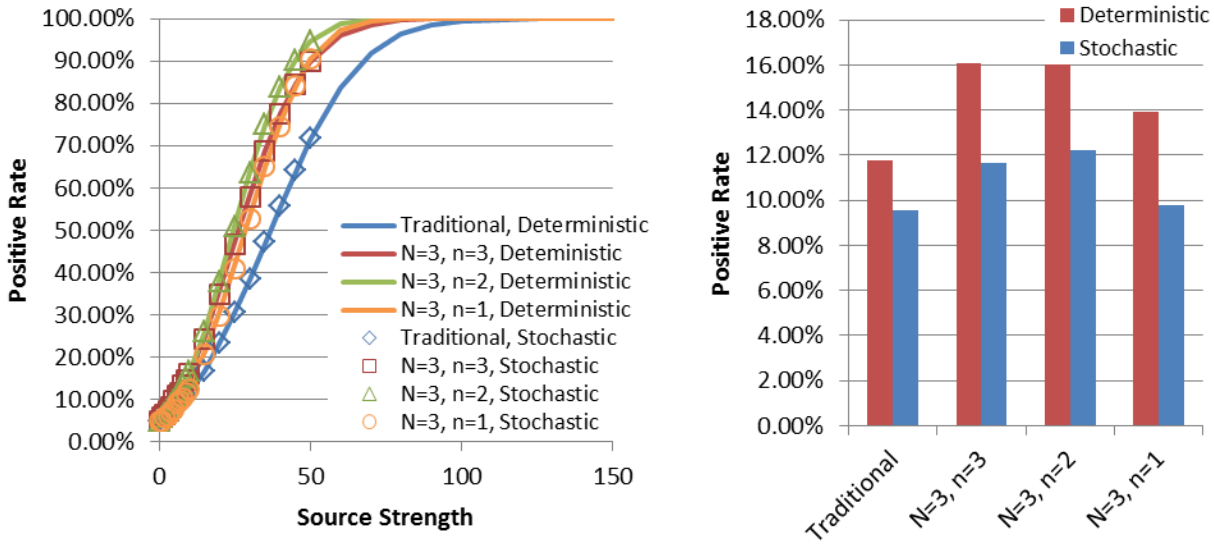

Figure 96 Deterministic and Stochastic Positive Rate with Source Strength Comparison for Different n Values (Gaussian, b=500, N=3)

The trends in positive rate for the deterministic and stochastic methods are also compared between distributions in Figure 97 for a series of three measurements at a background of 500 and source strength of 10.

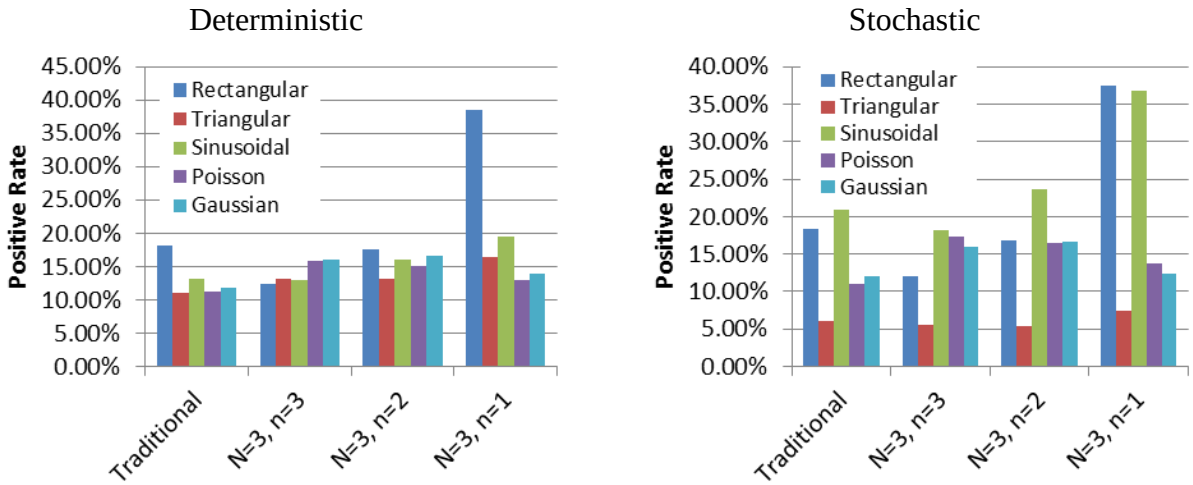

Figure 97 Stochastic and Deterministic Positive Rate Comparison for Different Distributions with Different n Values (N=3, b=500)

For the deterministic method the positive rates are comparable for all conditions except for the rectangular distribution. For the stochastic method there is more variability. The positive rates for the triangular distribution tend to be a lot lower than for other distributions. For both the stochastic and deterministic methods, the Poisson distribution and Gaussian distribution estimate similar positive rates for all conditions.

The trends in time at first detection between distributions for the stochastic methods are compared in Figure 98 for a series of three measurements at a background of 500 and source strength of 10. The time at first detection of all distributions is comparable except for $n = 1$. For $n = 1$, the Gaussian and Poisson distributions exhibit much higher times at first detection.

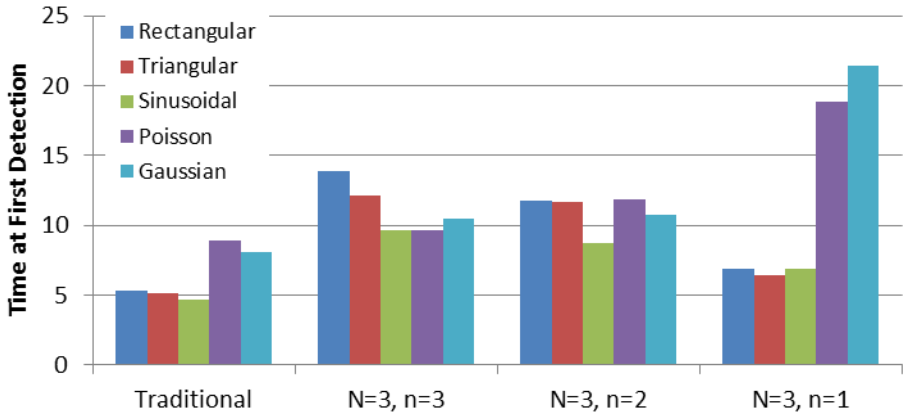

Figure 98 Stochastic Time at First Detection Comparison for Different Distributions with Different n Values (b=500, s=10, Stochastic)

The probability density function for the time at first detection was also compared for the different distributions used. The probability density functions for the traditional method and $N = 3, n = 2$ are displayed in Figure 99 for $b = 500$ and $s = 10$. Additional graphs for different values of n are in Appendix B in Figure 197. For the traditional method, the probability at a time of 1 is greater for the rectangular, triangular and sinusoidal distribution than for the Poisson and Gaussian distributions. This could explain why the calculated mean time at first detection for $s = 10$ is larger for the Poisson and Gaussian distribution. The probabilities for the traditional

distribution with time at first detection compare well otherwise. For $N = 3, n = 2$, the probability peaks around 2, corresponding to the n value. The peak probability is greatest for the sinusoidal and triangular distributions.

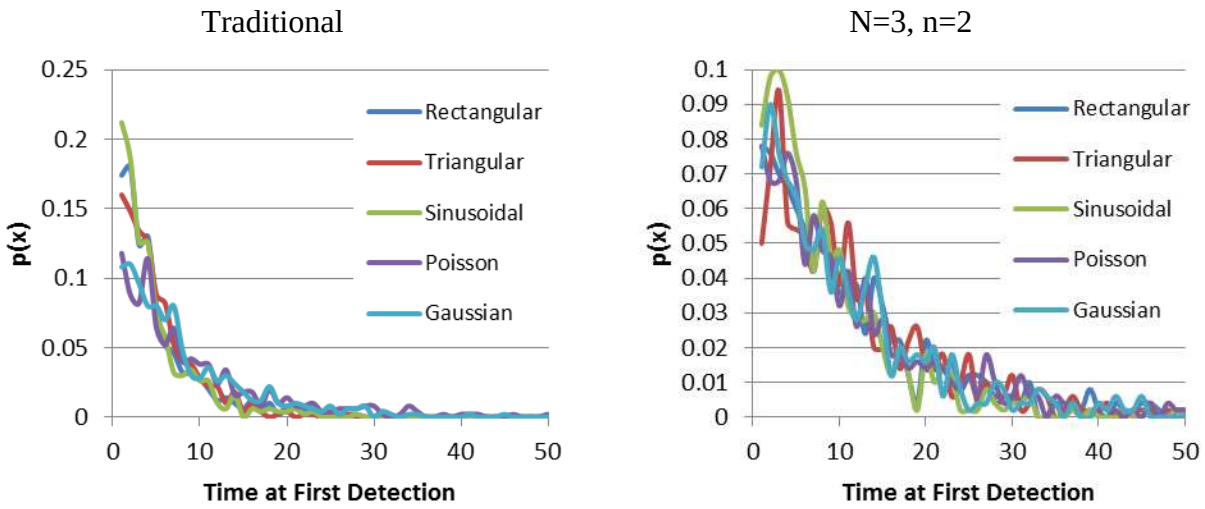

Figure 99 Probability Density Function for Time at First Detection for Different Distribution for Traditional and N=3, n=2 (b=500, s=10,Stochastic)

Implementation into a Detection System

In addition to simulation data, data and analysis was also performed for data taken in the Room 119 of the MRB at Colorado State University (Fort Collins, CO). The background in the room was assessed by taking a background measurement to assess the average count rate and energy spectrum, several repeated 15 minute background measurements to assess time behavior, and a short background measurement prior to the measurement with source data.

The background measurement was performed for 300 s. The energy spectrum for the background radiation is in

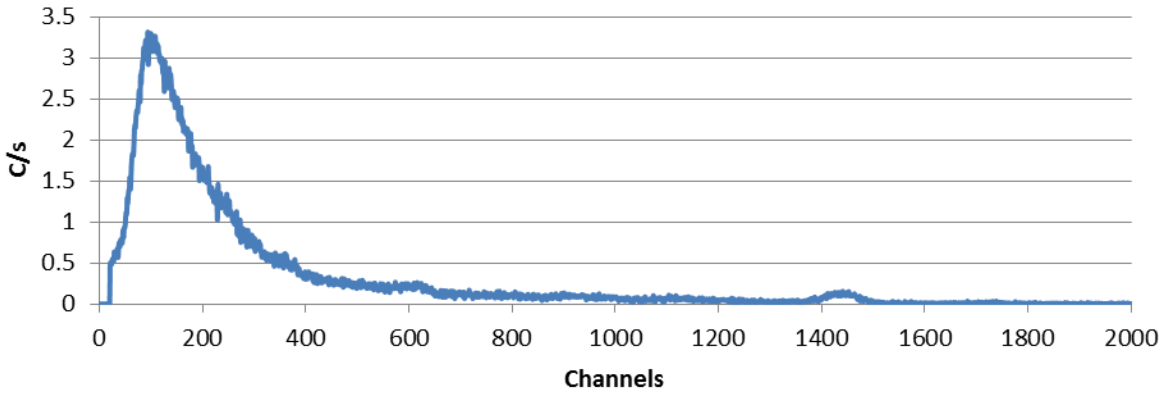

Figure 100. The average count rate was determined to be 669.27 C/s for the full energy window. The energy spectrum is characterized by a low energy Compton background. As seen in

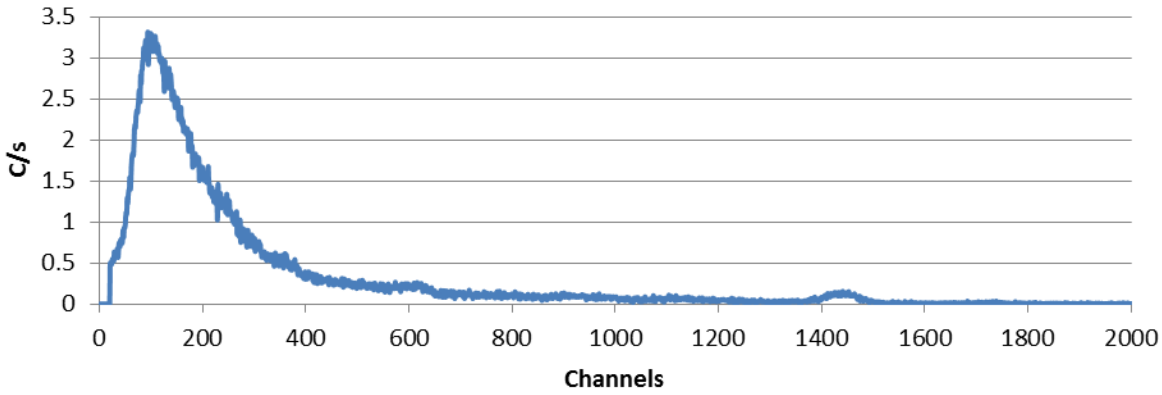

Figure 100, there is a peak around channel 1450 corresponding to the 1.46 MeV gamma from Potassium-40.

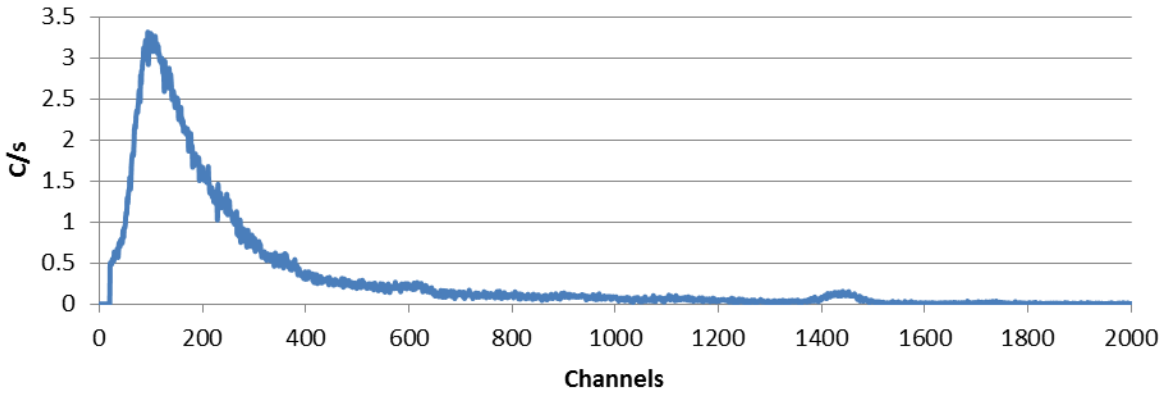

Figure 100 Energy Spectrum for Background

The time behavior for the background in Room 119 was determined by taking repeated 10 minute samples over 24 hours. Due to the large amounts of natural terrestrial background in Colorado it was anticipated that there might variation in dose rate due to variation in radon concentrations. Figure 101 contains a graph of the count rate with the time the measurement was taken. Fluctuations in the count rate are similar to what would be expected due to changes in radon from night to day.

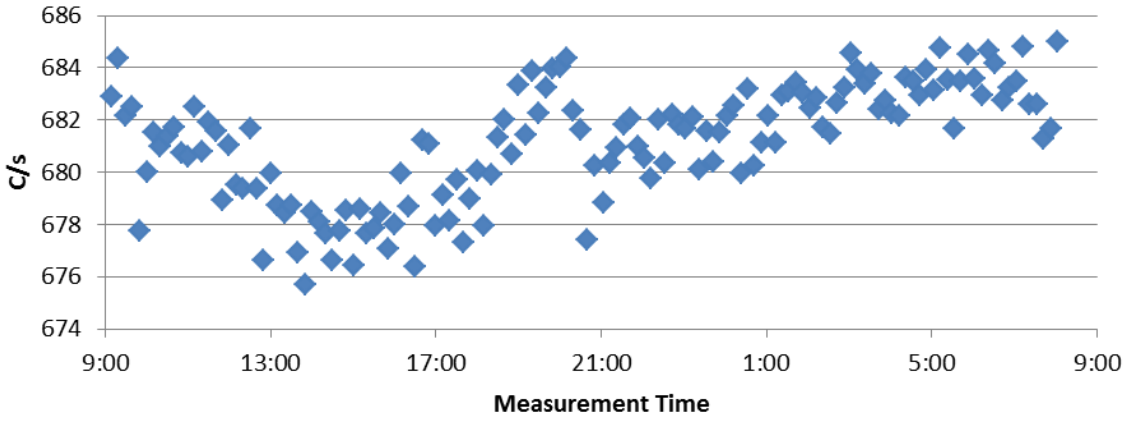

Figure 101 Time Behavior for Background in Room 119

The source used was a Cesium-137 button source. The location of the source was determined by looking at the count rate above background at several source distances. It was desired that the count rate would be large enough to see differences in different analysis techniques, but small enough to not cause 100% positives. The count rate above background was

determined for the full energy window. A graph of the count rate above background with source distance is in Figure 102.

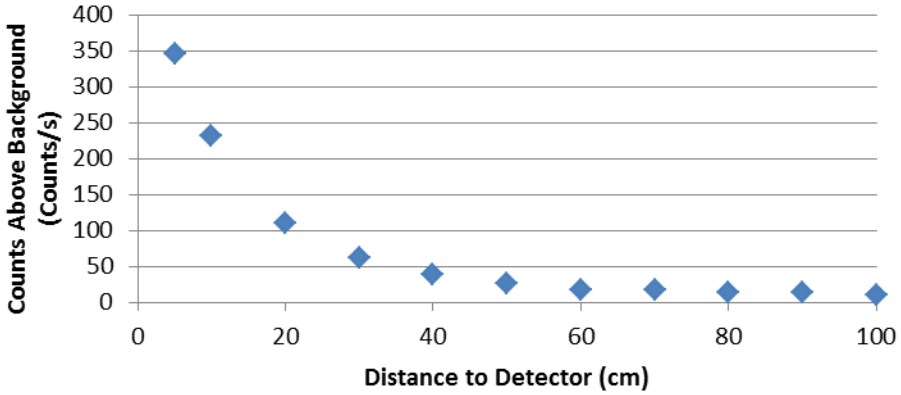

Figure 102 Count Rate vs. Distance for a Cesium-137 Source

The counts above background drop off rapidly with distance, as expected from the inverse-square law. The source distance was chosen at 40 cm, which yields a count rate of 13.84 C/s. The energy spectrum for the source was also taken and is displayed in Figure 104. The full energy deposition peak is observed around channel 650 in the energy spectrum. The counts in smaller channels are due to the Compton spectrum, and counts in channels after the peak are due to background.

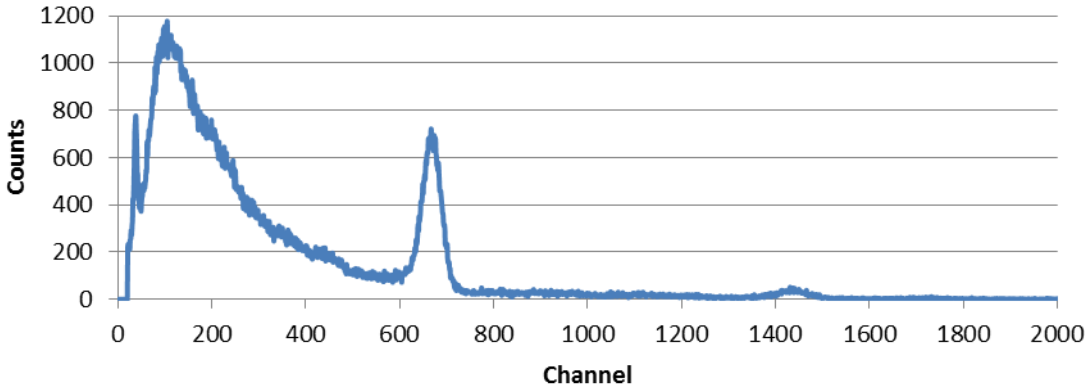

Figure 103 Energy Spectrum at 5 cm for Source and Background

Repeated measurements were performed for 1 s, 2 s, 3 s, 4 s, and 5 s. For each measurement length 10 repeated measurements were taken of 120, for 1200 total measurements.

The positive rate and time at first detection is calculated for N values between 1 and 5. The measurement data is compared to simulation data for a Gaussian distribution. For $N = 3$, the positive rate and time at first detection are compared for measurement and simulation data in Figure 104. Additional graphs for other values of N is available in Appendix C in Figure 198 ($N = 2$), Figure 199 ($N = 3$), Figure 200 ($N = 4$), and Figure 201 ($N = 5$).

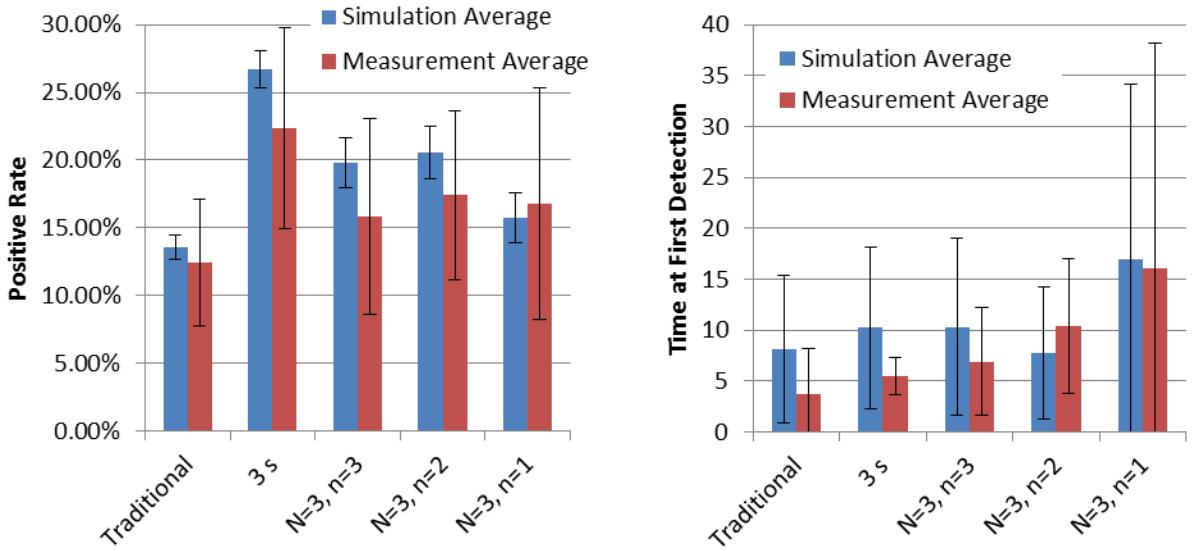

Figure 104 Positive Rate and Time at First Detection Comparison for Simulation and Measuement Using Different n Values (N=3, b=669.27, s=13.84)

The probability density function was also looked at for the positive rate and the time at first detection for measurement and simulation (Gaussian) data. The probability density function for the positive rate for measurement and simulation data is in Figure 105 for $N = 3$. The data is compared to a Gaussian distribution. The average positive rate for $b = 669.27$ and s=13.84 is fairly small and as a result a large portion of the predicted distribution is the left of 0%. For this case, the predicted distribution does not match the measurement values well. Additional figures for the probability density function are in Appendix C in Figure 202 ($N = 2$), Figure 203 ($N = 2$), Figure 204 ($N = 3$), Figure 205 ($N = 3$), Figure 206 ($N = 4$), Figure 207 ($N = 4$), Figure 208 ($N = 5$), and Figure 209 ($N = 5$).

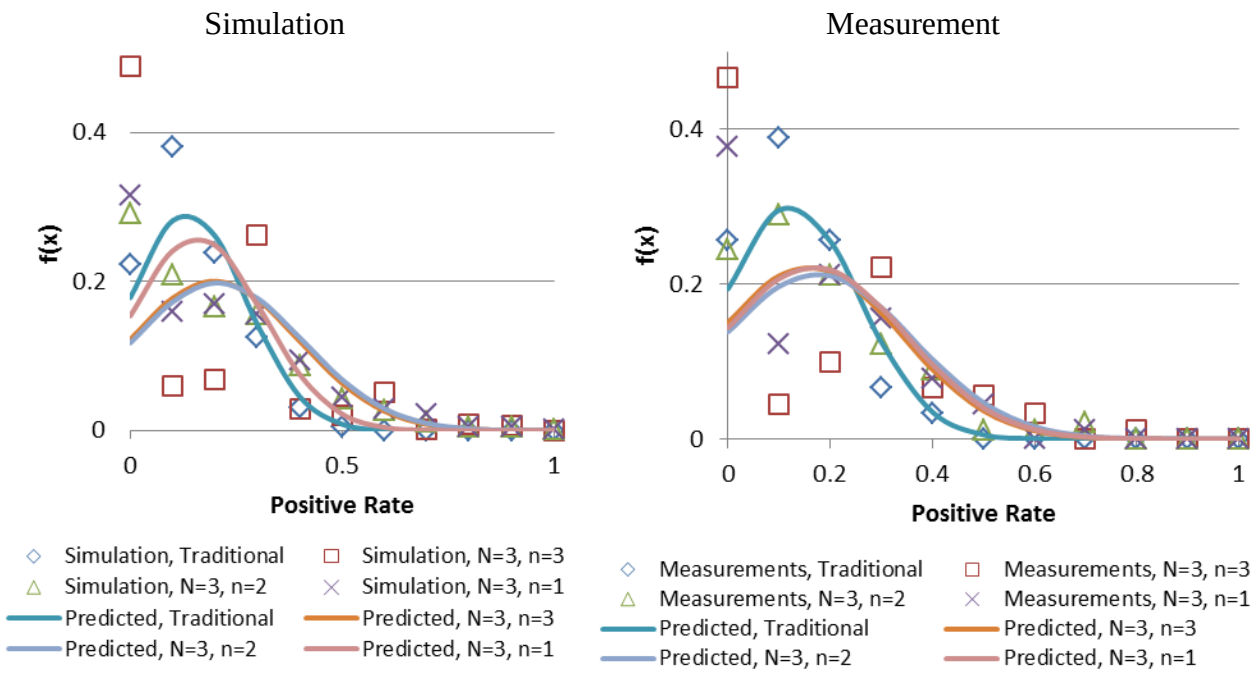

Figure 105 Positive Rate Probability Density Function Comparison for Measurement and Simulation for Different n Values (Gaussian, N=3, b=669.27, s=13.84)

The probability density function for the time at first detection for measurement and simulation data is in Figure 106 for $N = 3$. The data is compared to a geometric distribution.

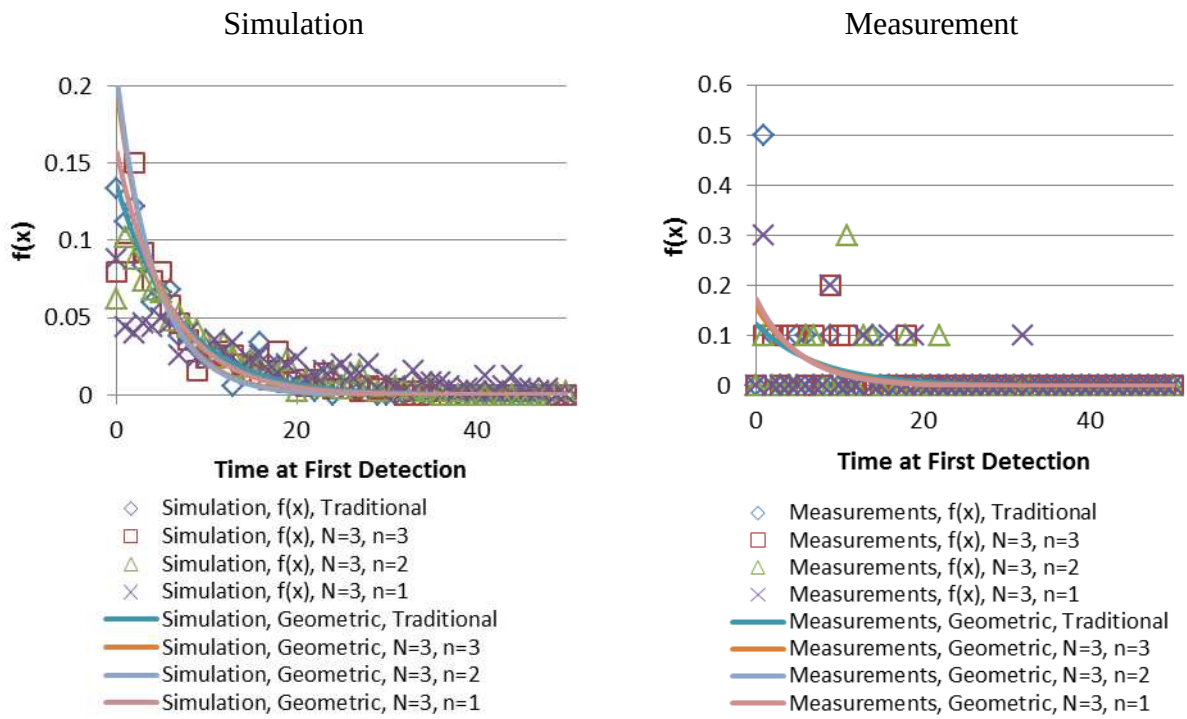

Figure 106 Time at First Detection Probability Density Function Comparison for Measurement and Simulation for Different n Values (Gaussian, N=3, b=669.27, s=13.84)

The predicted geometric distributions for all the conditions are similar to each other. The simulation data fits better to the predicted data, since more simulation data could be created. Additional figures for the probability density function are in Appendix C in Figure 215 ($N = 2$), Figure 216 ($N = 3$), Figure 217 ($N = 3$), Figure 218 ($N = 4$), Figure 219 ($N = 4$), Figure 220 ($N = 5$), and Figure 221 ($N = 5$).

Trends in the data (positive rate and time at first detection) for different series lengths for the measurement and simulation (Gaussian) data were looked at for three conditions: all successes ($N = n$), at least one success in a series ($n = 1$), and for different measurement lengths. The positive rate and time at first detection for $n = N$ for measurement and simulation data is in Figure 107. Error bars displayed are for one standard deviation.

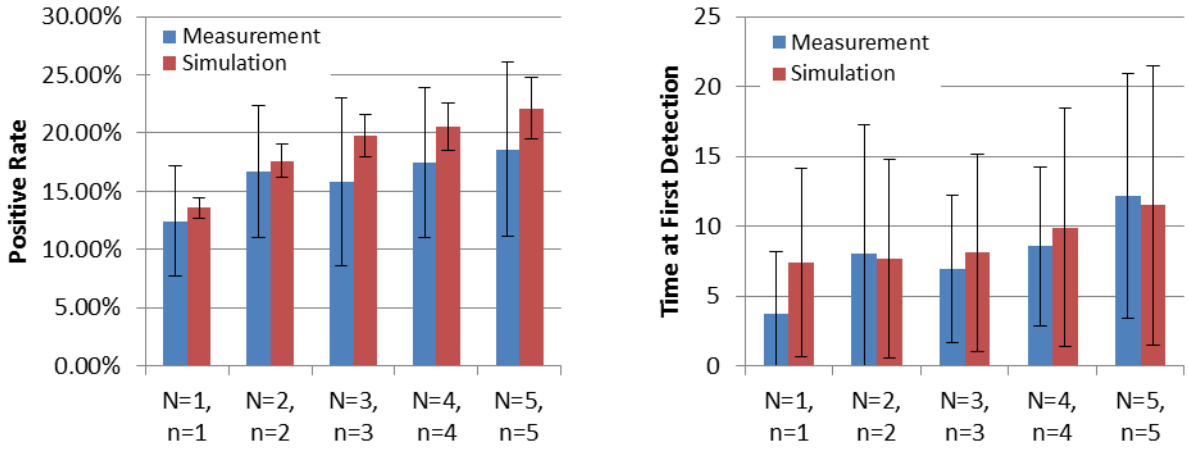

Figure 107 Positive Rate and Time at First Detection for Simulation and Measuement (n=N, b=669.27, s=13.84)

Large values of n tend to correlate with higher positive rates and time at first detection while small values of n tend to correlate to lower positive rates and time at first detection. The positive rate and time at first detection for $n = 1$ for measurement and simulation data is in Figure 108. Error bars are for one standard deviation. Larger N tend to correlate to higher positive rates and detection time while smaller N correlate to lower positive rates and detection time. The value for $N = 5$ appears to be small compared to other values.

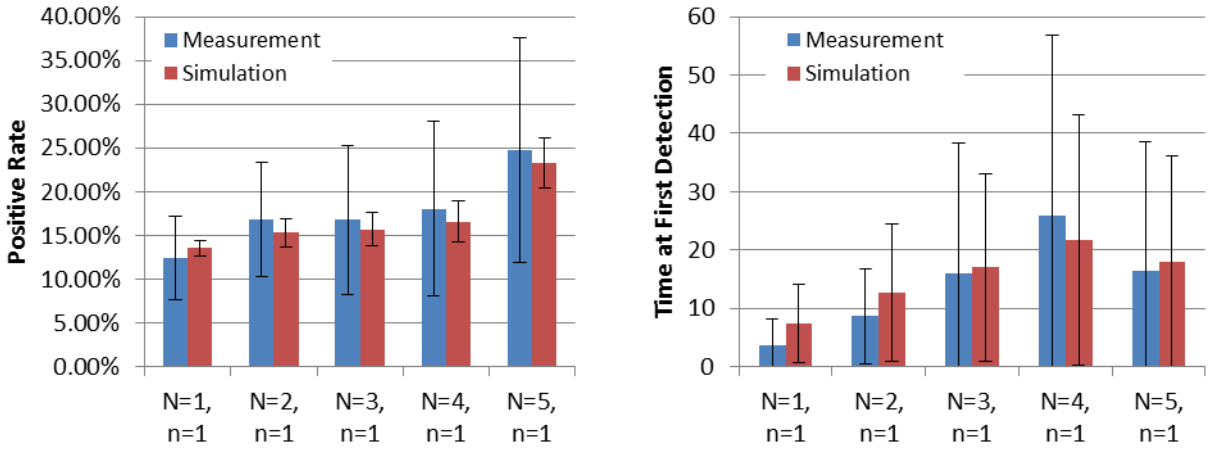

Figure 108 Positive Rate and Time at First Detection for Simulation and Measuement (n=1, b=669.27, s=13.84)

The positive rate and time at first detection for different measurement lengths for measurement and simulation data is in Figure 109. Error bars are for one standard deviation.

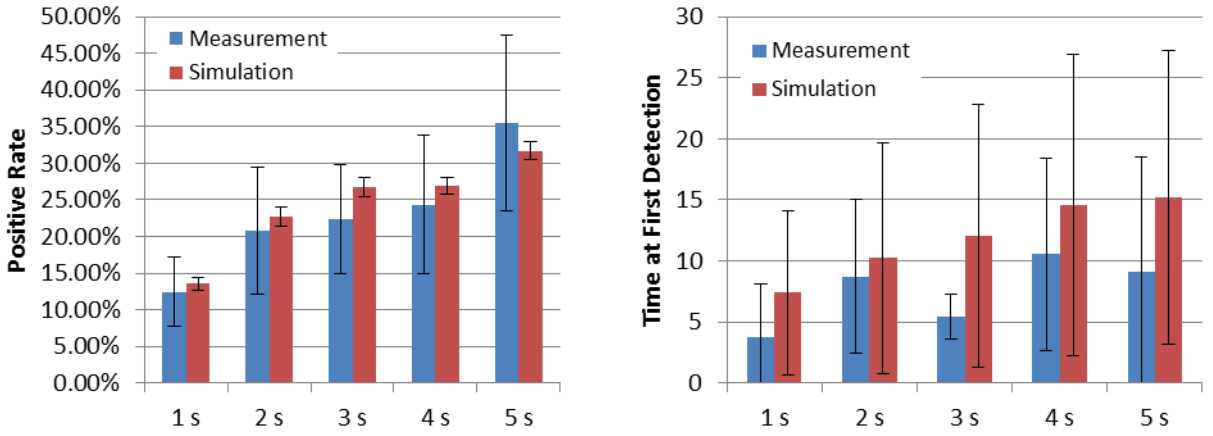

Figure 109 Positive Rate and Time at First Detection for Simulation and Measuement for Measurement Length (b=669.27, s=13.84)

Large measurement lengths tend to correlate with higher positive rates and time at first detection while small values of n tend to correlate to lower positive rates and time at first detection.

Table 11 contains a comparison for the positive rate and time at first detection using several techniques. The positive rate is calculated using the deterministic and stochastic methods and is compared to measurement data. The time at first detection is calculated using the

stochastic method and compared to measurement data. The measurement data positive rate and time at first detection tend to be smaller than predicted for the deterministic and stochastic methods. The measurement data overall compare well to deterministic and stochastic methods.

Table 11 Positive Rate and Time at First Detection Comparison for Different Calculation Techniques

	Positive Rate			Time at First Detection	
	Deterministic	Stochastic	Measurement	Stochastic	Measurement
Traditional	13.60%	13.57%	12.43%	7.41	3.73
N=2, n=2	16.96%	17.60%	16.72%	7.68	8
N=2, n=1	15.36%	15.33%	16.80%	12.64	8.64
N=3, n=3	19.31%	19.78%	15.84%	8.12	6.9
N=3, n=2	20.04%	20.57%	17.40%	10.38	10.36
N=3, n=1	16.46%	15.72%	16.76%	17	16.09
N=4, n=4	21.13%	20.57%	17.47%	9.91	8.55
N=4, n=3	23.26%	24.20%	21.16%	9.69	8.55
N=4, n=2	22.17%	22.59%	18.54%	12.34	10.82
N=4, n=1	17.27%	16.57%	18.04%	21.68	25.82
N=5, n=5	22.61%	22.14%	18.61%	11.51	12.18
N=5, n=4	25.77%	26.24%	21.24%	10.71	6.27
N=5, n=3	26.07%	25.17%	20.81%	12.12	12.18
N=5, n=2	23.83%	22.79%	20.10%	13.52	10.45
N=5, n=1	17.92%	23.22%	24.79%	18.06	16.45

The methodology described in this thesis to examine a series of measurements rather than just one measurement (as is done traditionally) can be easily implemented into a detection system. The measurement series length, number of successes required and false positive rate (number of positives due to background) can be optimized for the detection system. For example, consider the scenario where a portal monitor is used in exiting the secured area of the power plant. The system uses a 5 second long counting interval to determine if contamination is present. The background count rate on average is 500 counts per second. Currently the system operates by developing a decision threshold based on a 5 s long count, the average background count rate, and assuming a Gaussian distribution of counts.

If a 5 s count is taken, 2500 counts will be recorded on average with a standard deviation of 50 (assuming Poisson counting statistics). The decision threshold for $\alpha = 0.05$ can be

calculated at 2598 counts in 5 s or 519.6 counts per second. If a 1 s measurement in considered, 500 counts will be recorded on average with a standard deviation of 22.4 (assuming Poisson counting statistics); the resulting decision threshold is at 543.9 counts per second. However, if a series of five measurements is looked at and it is desired that all five measurements exceed the decision threshold ($n = N$), the decision threshold for a series of measurements can be calculated for a p value of 0.549280 as 497. The algorithm can be implemented into the portal monitor by counting the amount of times in the last five measurements that the decision threshold for a series of measurements was exceeded. In this case if the decision threshold for a series of measurements is exceeded five times in the last five measurements, the portal monitor would alarm.

CONCLUSIONS

The decision threshold for a series of measurements can be easily implemented into a detection system. First an appropriate decision threshold for the series of measurements needs to be calculated given the values of N, n, and α. Secondly, the amount of times the decision threshold for a series of measurements is exceeded in the last N measurements needs to be calculated and compared to n. If the number of measurements exceeding the decision threshold for a series of measurements is greater than n, an alarm would occur.

Several trends and criteria were investigated for the analysis of a series of N measurements. The goal of this project was to assess the effectiveness of using data from a series of measurements, rather than one individual measurement to define a suitable decision threshold. A series of N measurements varying between 1 and 5 was studied, with n of those measurements exceeding a threshold designed to exhibit no more than 5% false positives when no source is present.

It was determined that due to the shift in the probability density function when a source is added, it is more effective to utilize considerations of at least n of N measurements exceeding a threshold rather than exactly n measurements. If the *exact* condition is used, 100% detection can never be achieved because due to the shift in the probability density function it is impossible for only n measurements to exceed the decision threshold in a series of N unless $n = N$.

Also investigated was the simulation of measurement data. Two methodologies were used: sampling off of one combined source and background distribution and sampling off of two separate source and background distributions and summing the values. It was found that sampling off of two distribution of one shape does not always yield a distribution in the same

shape. Differences in the shapes of the two distributions were especially pronounced for high source strength data. The rectangular and triangular distributions showed significant differences in the probability density functions between the two simulation techniques. However, visual inspection of the similarities between the distributions does not always correlate with degree of differences in detection probability and time at first detection. For instance, the rectangular distribution which had significant visual differences in the probability density functions between the two methods had the least variation between the two methodologies for the positive rate and time at first detection data. The technique used to simulate the measurement data should be chosen so that it matches the actual source and background data observed.

The probability density functions for the positive rate and time at first detection were investigated for the Gaussian distribution. The probability distribution for positive rate follows well to a Gaussian distribution, except at small values for the source, because the distribution becomes negative. Additional studies into a distribution that exhibit negative values are necessary. The probability distribution for time at first detection closely follows a geometric distribution when $n = N$, but does not follow as closely for other values of n. One problem is that for a series of measurements, at least n measurements need to be performed before an alarm can occur. If an alarm occurs at less than n measurements, one of the positives was due to a false positive signal from the background. So although exceeding the decision threshold at a time less than n, it is less likely than would be predicted by the geometric distribution. Another complication is that although longer time series tend to yield higher positive rates for equivalent conditions, they also yield longer times to first detection. If a geometric distribution was used, the time at first detection would be predicted as lower due to the higher positive rate.

Several distributions were investigated for this project. For a given source strength and background strength, the same trends between conditions are not apparent for all distributions. In the case of $N = 3, n = 2$, this value of n outperformed other n values for the Gaussian distribution, but did the poorest for the rectangular and sinusoidal distributions, and was somewhere in the middle for the other distributions. Each distribution appears to be unique and it is difficult to state general trends between conditions. However, for all conditions and distributions as source strength increased the positive rate increased and the time at first detection decreased, approaching n. More investigation is necessary into the root causes for the differences in the distributions.

Finally, measurement data were taken for one background and source level. Overall, the measurement data agreed well with values calculated using the deterministic and stochastic techniques. As seen for simulated data, a high positive rate does not always indicate a small time at first detection. More data should be taken to assess trends for the probability density function for the time at first detection and positive rate.

REFERENCES

[1] H. Cember and T. Johnson, Introduction to Health Physics, McGraw-Hill Companies, Inc, 2009.

[2] J. Turner, Atoms, Radiation, and Radiation Protection, Weinheim: Wiley-VCH, 2009.

[3] G. Knoll, Radiation Detection and Measurement, Hoboken: John Wiley & Sons, Inc, 2000.

[4] United States Nuclear Regulatory Commission, "Sources of Radiation," 17 October 2014. [Online]. Available: http://www.nrc.gov/about-nrc/radiation/around-us/sources.html. [Accessed 13 October 2015].

[5] M. Kalos and P. Whitlock, Monte Carlo Methods, Weinheim: Wiley-VCH, 2008.

[6] D. Wackerly, W. Mendenhall and R. Scheaffer, Mathematical Statistics with Applications, Belmont: Brppls/Cole, 2008.

[7] J. Klumpp, G. Miller and A. Brandl, "Characterisation of Non-Constant Background in Counting Measurements," *Radiation Protection Dosimetry,* vol. 164, no. 3, pp. 408-421, 2015.

[8] J. Klumpp and A. Brandl, "Bayesian Analysis of Energy and Count Rate Data for Detection of Low Count Rate Radioactive Sources," *Health Physics Journal,* vol. 108, no. 3, pp. 364-370, 2015.

[9] A. Brandl and A. Jimenez, "Stastical Criteria to Set Alarm Levels for Continuous

Measurement of Ground Contamination," *Health Physics Journal*, vol. 95, no. 2, pp. 128-132, 2008.

[10] A. Brandl, "Statistical Considerations for Improved Signal Identification from Repeated Measurements at Low Signal-to-background Ratios," *Health Physics Journal*, vol. 104, no. 3, pp. 256-263, 2013.

[11] Teledyne Lecroy, "WaveSurfer 3000 Oscilloscopes," 2015. [Online]. Available: http://cdn.teledynelecroy.com/files/pdf/wavesurfer-3000-datasheet.pdf. [Accessed 30 October 2015].

[12] Teledyne LeCroy, "ArbStudio," 11 June 2014. [Online]. Available: http://cdn.teledynelecroy.com/files/pdf/arbstudio_factsht.pdf. [Accessed 30 October 2015].

[13] Canberra Industries, "Scintillation Detectors & Options," February 2009. [Online]. Available: http://www.canberra.com/products/detectors/pdf/Model-802-SS-CSP0232.pdf. [Accessed 2 November 2015].

[14] Canberra Industries, "Digital Signal Processing," 2012. [Online]. Available: http://www.canberra.com/products/radiochemistry_lab/pdf/Lynx-SS-C38658.pdf. [Accessed 2 November 2015].

APPENDIX A

Deterministic

Exact v. At Least

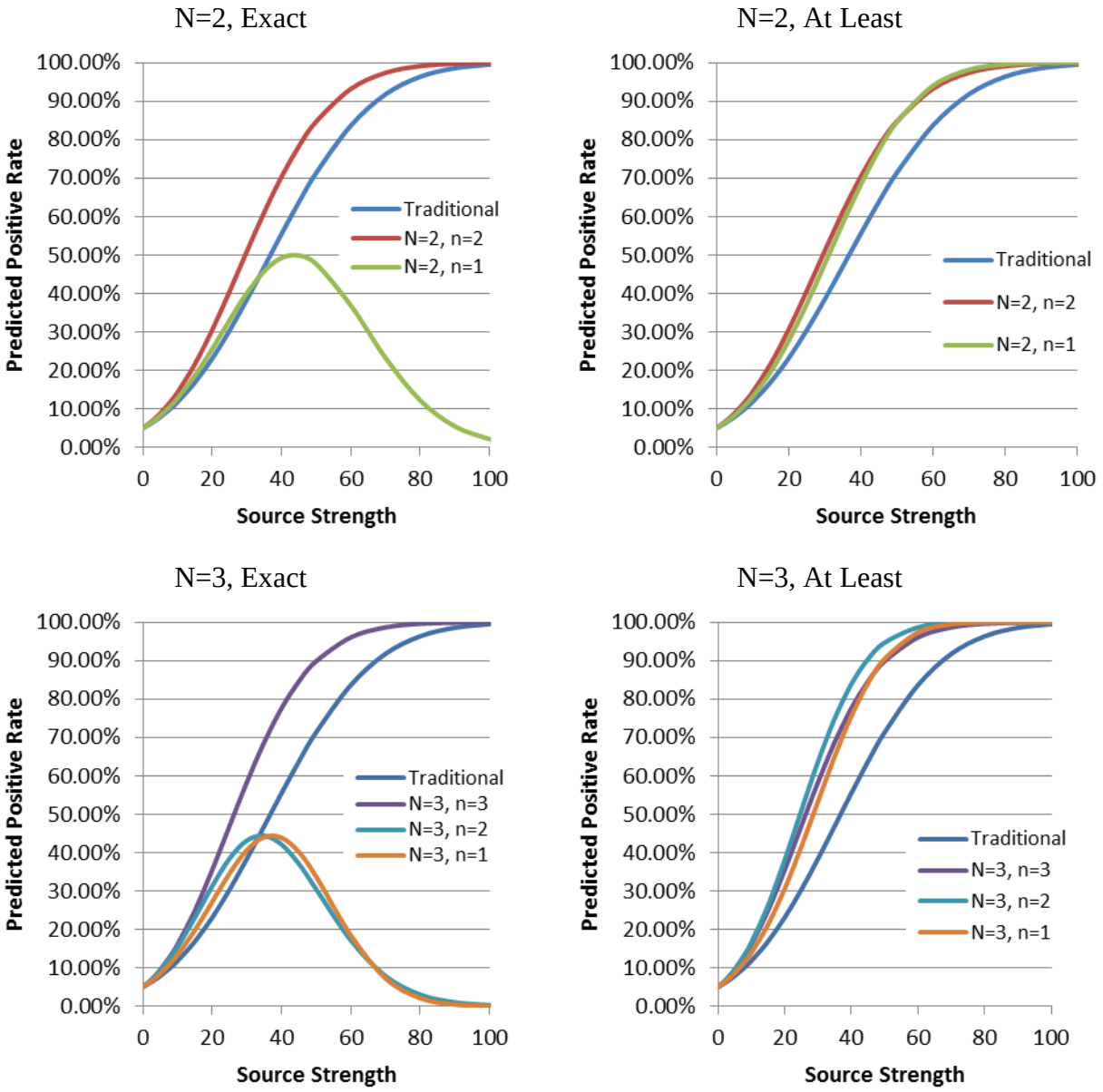

Figure 110 Positive Rate with Source Strength Comparison for Exact and At Least Conditions with Different n Values (Gaussian, b=500, N=2, N=3)

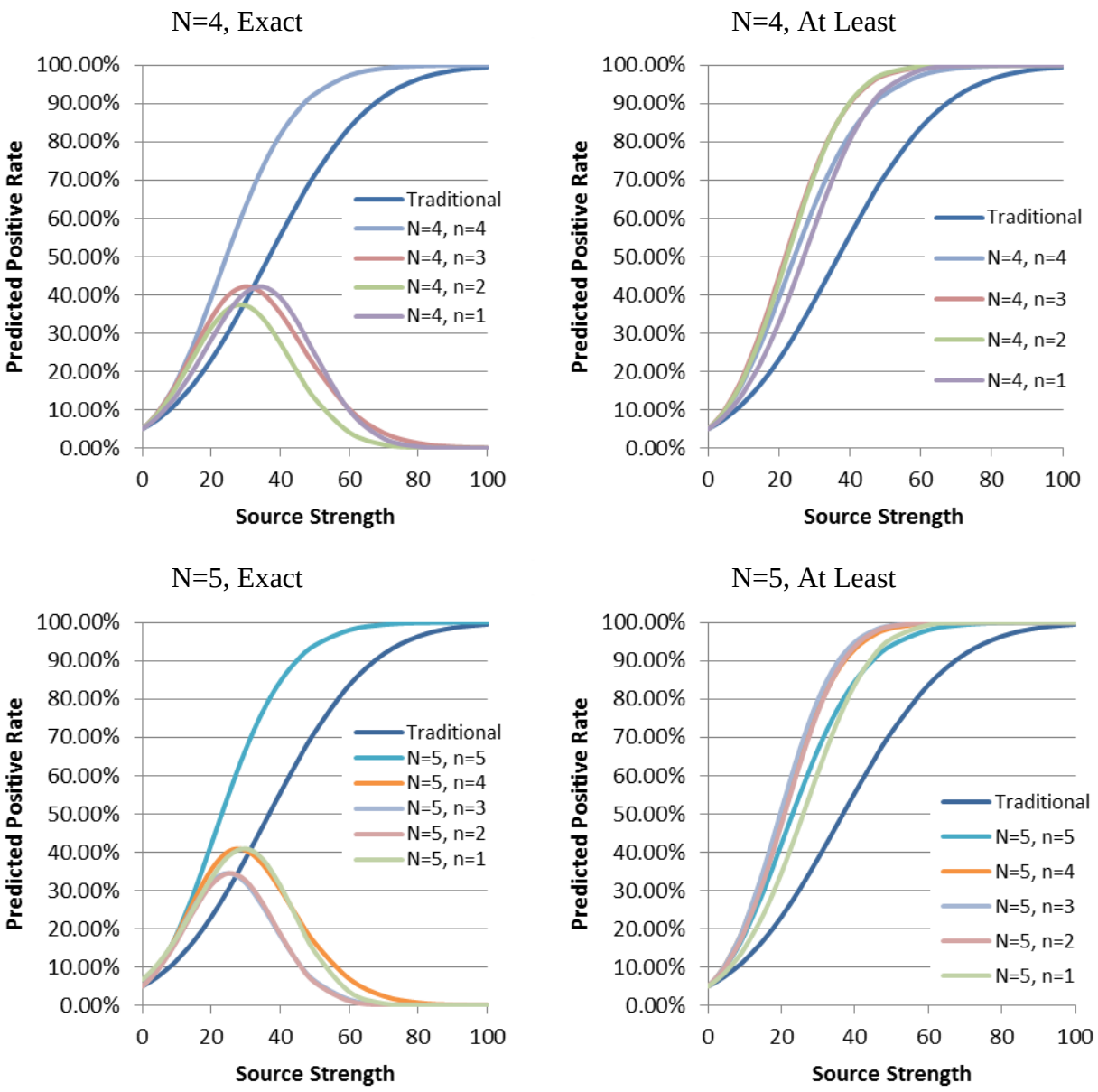

Figure 111 Positive Rate with Source Strength Comparison for Exact and At Least Conditions with Different n Values (Gaussian, b=500, N=4, N=5)

Rectangular

Table 12 Calculated Values of y* at Different Background Strengths (Rectangular, Deterministic)

		Background Strength									
N	n	50	100	250	500	750	1000	2500	5000	7500	10000
1	1	61	116	275	535	793	1049	2578	5110	7642	10156
2	2	57	110	265	521	776	1030	2548	5068	7583	10096
	1	62	116	276	537	795	1052	2582	5116	7642	10164
3	3	53	105	257	510	762	1014	2523	5032	7539	10046
	2	59	113	270	528	785	1040	2563	5089	7609	10126
	1	62	117	276	537	796	1053	2584	5118	7645	10167
4	4	51	101	251	502	753	1003	2505	5007	7508	10009
	3	56	109	264	519	774	1028	2544	5062	7575	10087
	2	60	114	272	531	788	1044	2570	5099	7621	10139
	1	62	117	277	538	796	1053	2584	5119	7646	10169
5	5	49	98	247	496	745	995	2491	4988	7485	9983
	4	54	105	259	512	765	1017	2527	5039	7547	10055
	3	58	111	267	524	779	1034	2554	5076	7593	10108
	2	60	115	273	533	790	1046	2573	5104	7627	10147
	1	62	117	277	538	796	1054	2585	5120	7647	10170

Positive Rate

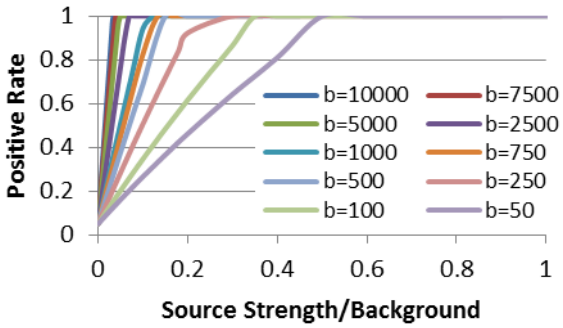

Figure 112 Positive Rate with Source Strength/Background for Different Values of b (Rectangular, Traditional, Deterministic)

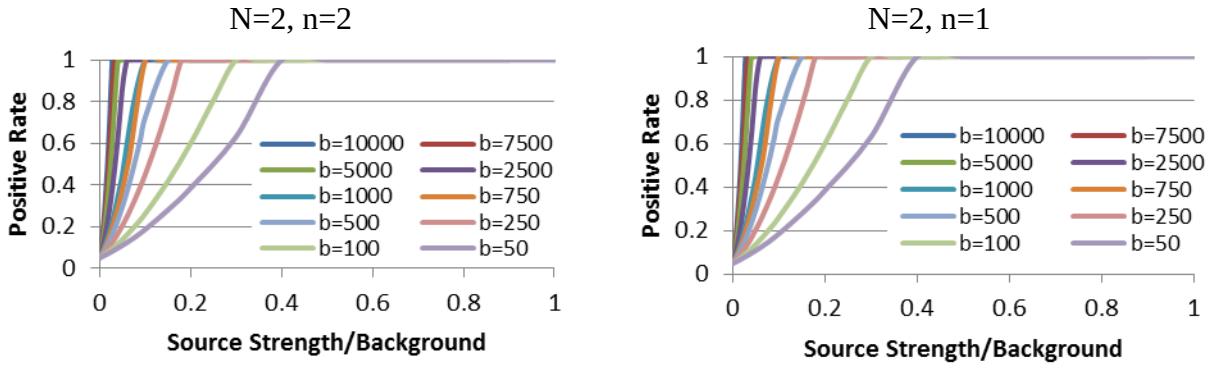

Figure 113 Positive Rate with Source Strength/Background for Different Values of n and b (Rectangular, N=2, Deterministic)

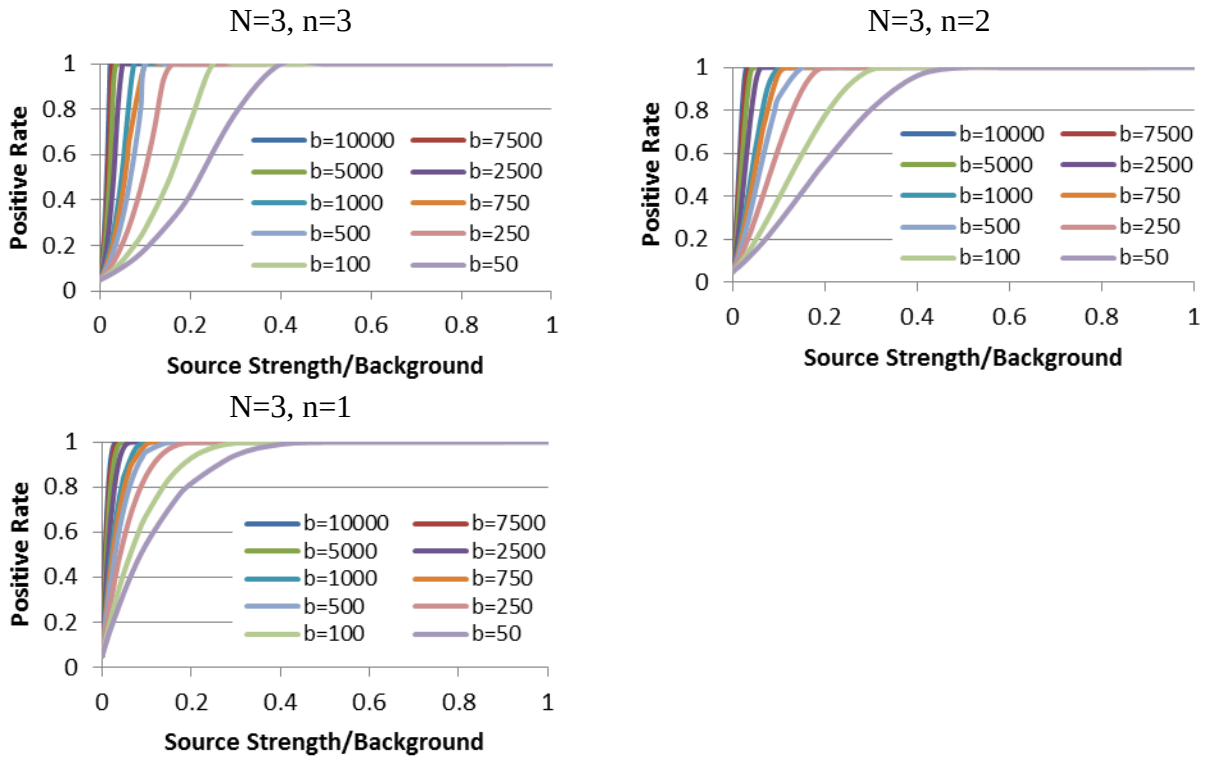

Figure 114 Positive Rate with Source Strength/Background for N=3 for Different Values of b (Rectangular, N=3, Deterministic)

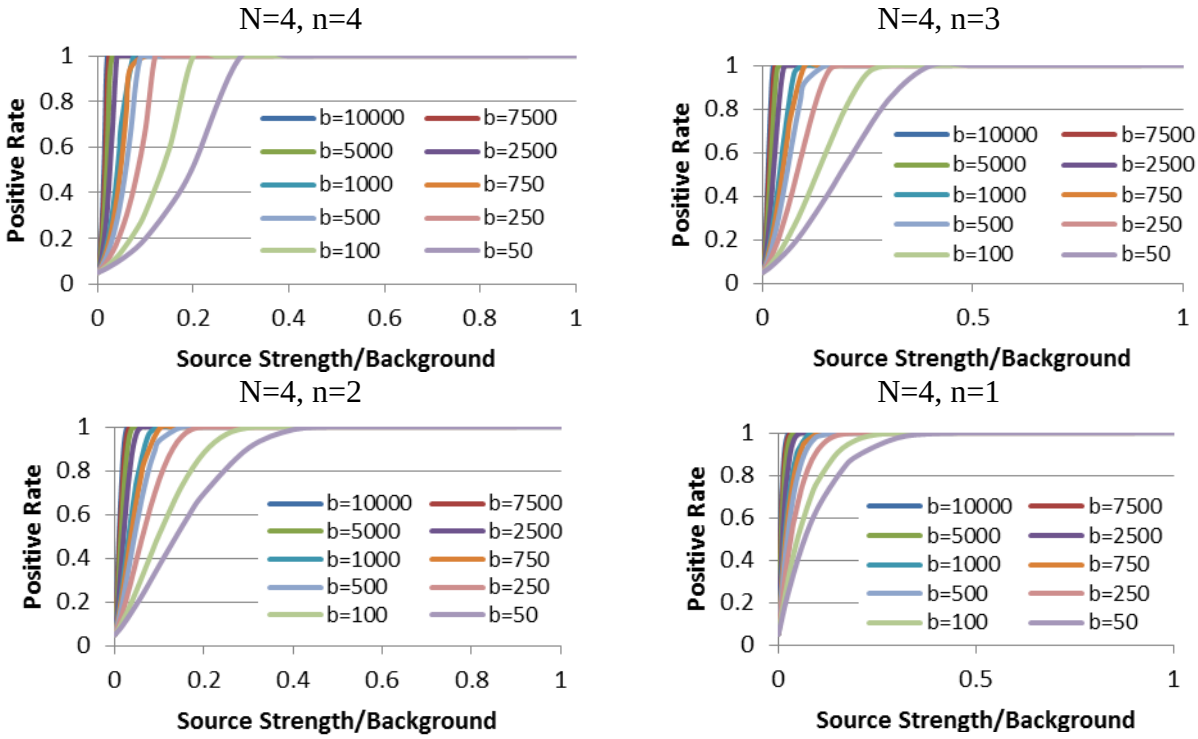

Figure 115 Positive Rate with Source Strength/Background for Different Values of n and b (Rectangular, N=4, Deterministic)

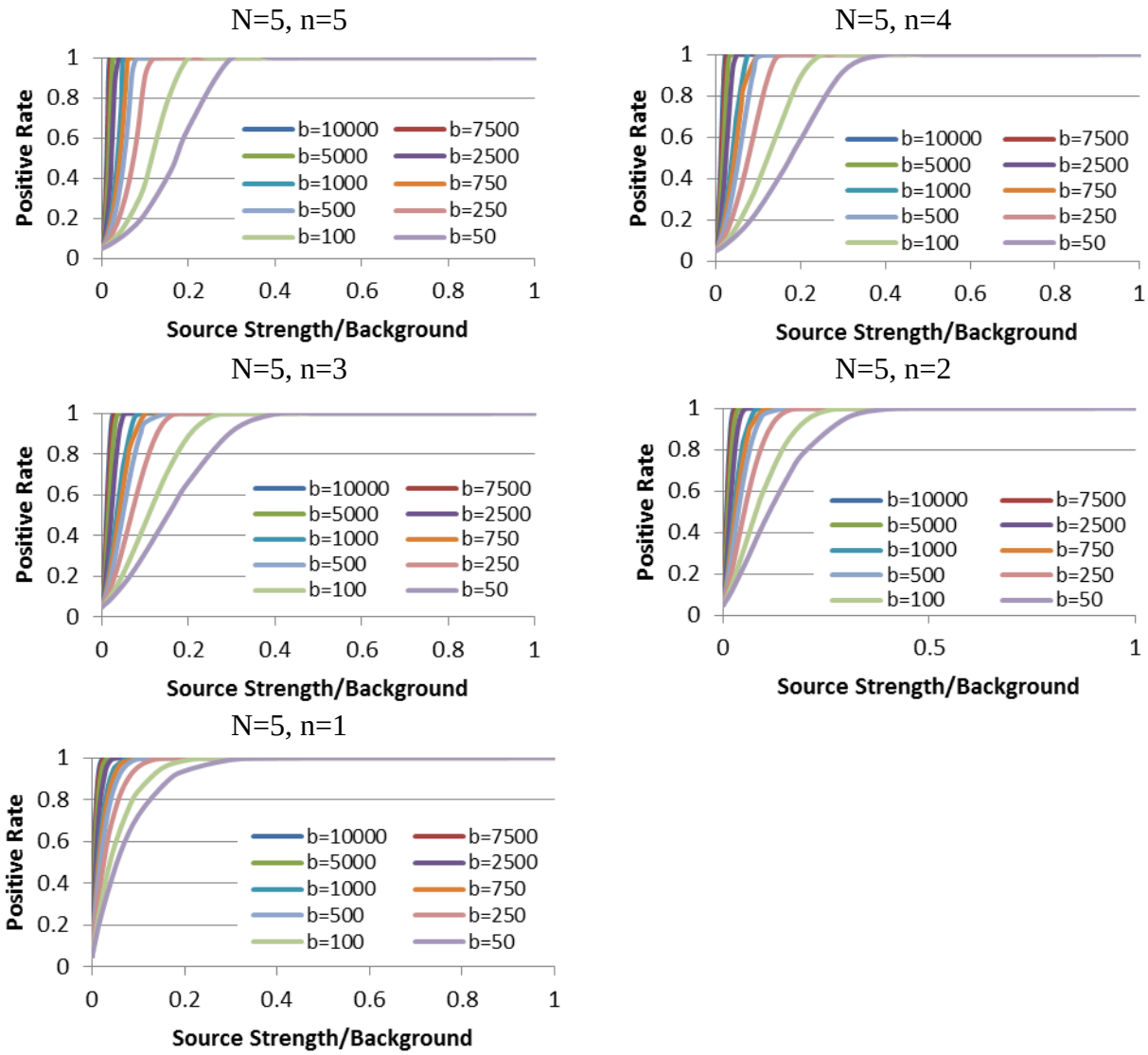

Figure 116 Positive Rate with Source Strength/Background for Different Values of n and b (Rectangular, N=5, Deterministic)

N=2
b=50

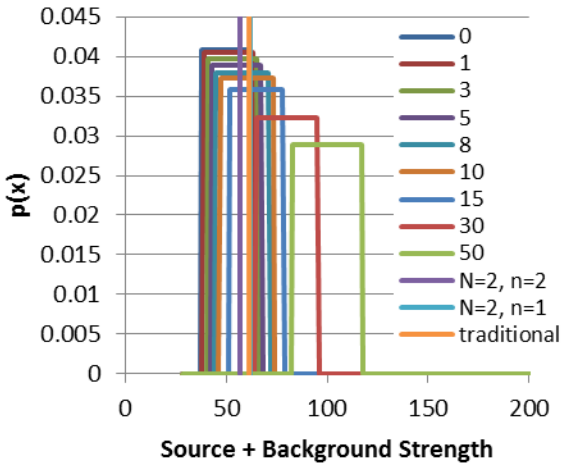

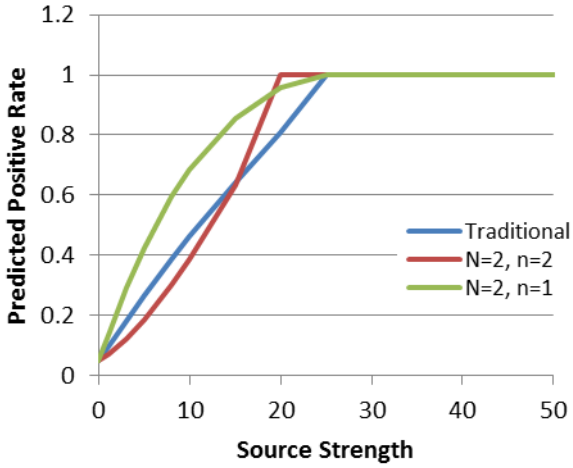

b=500

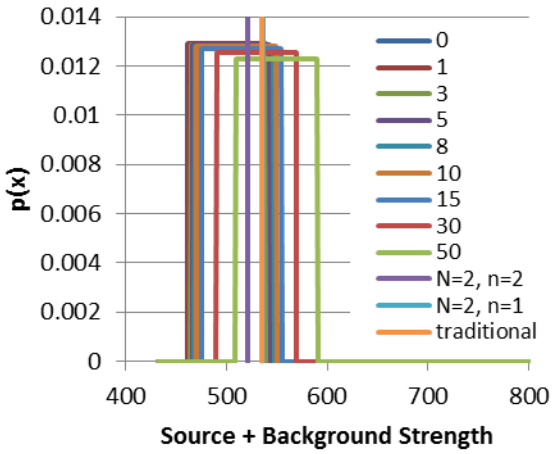

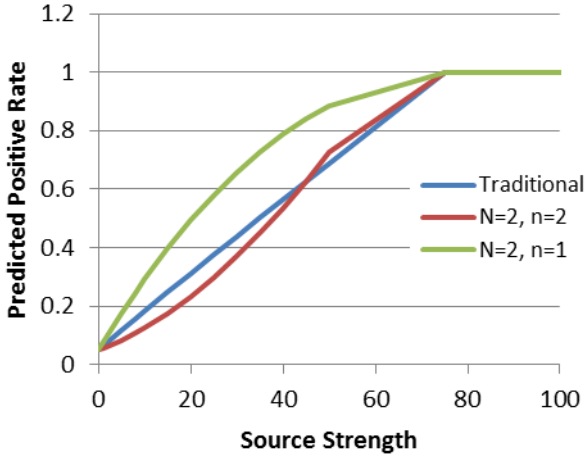

b=5000

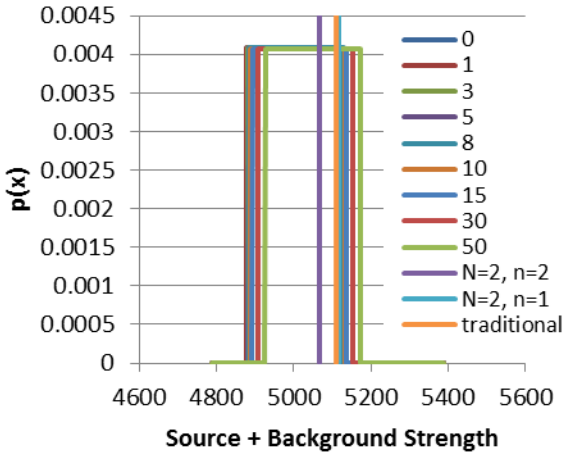

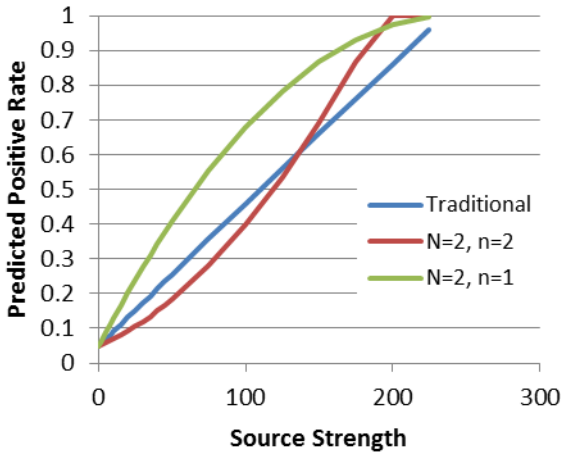

Figure 117 Positive Rate for Source Strength for Different Values of n and Constant b (Rectangular, N=2, Deterministic)

N=3

b=50

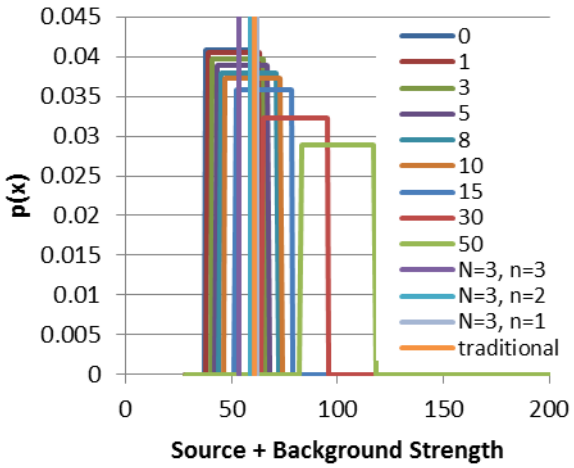

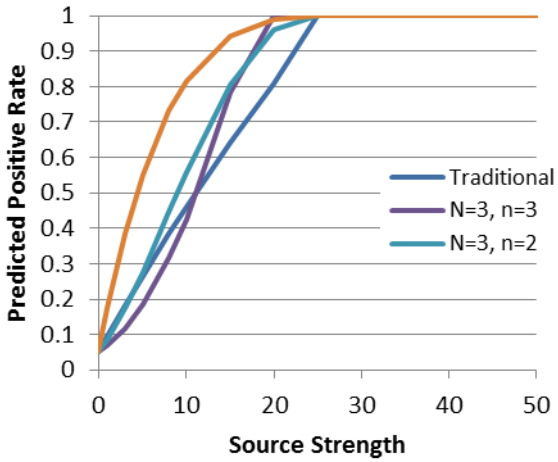

b=500

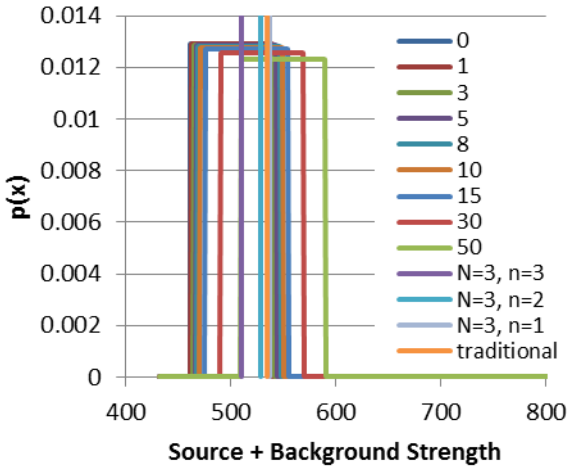

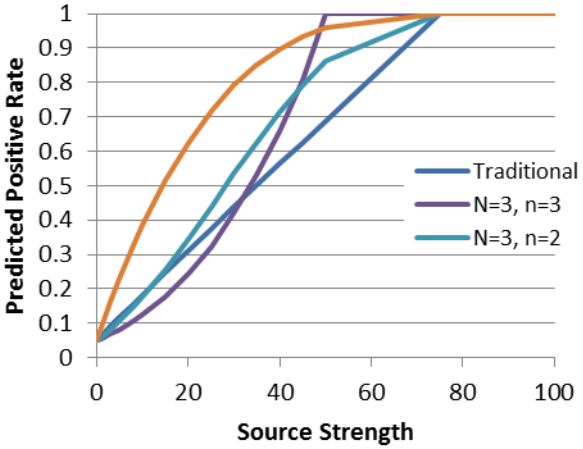

b=5000

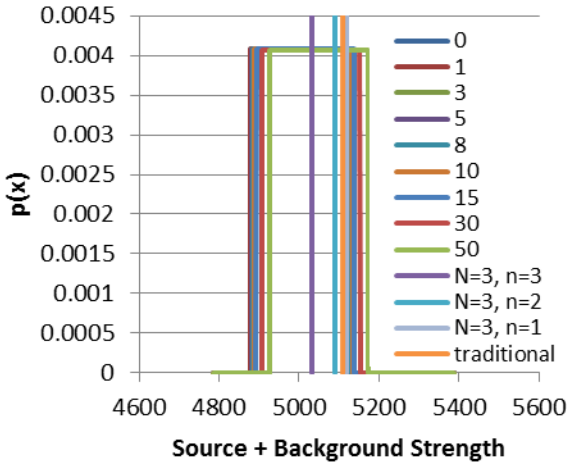

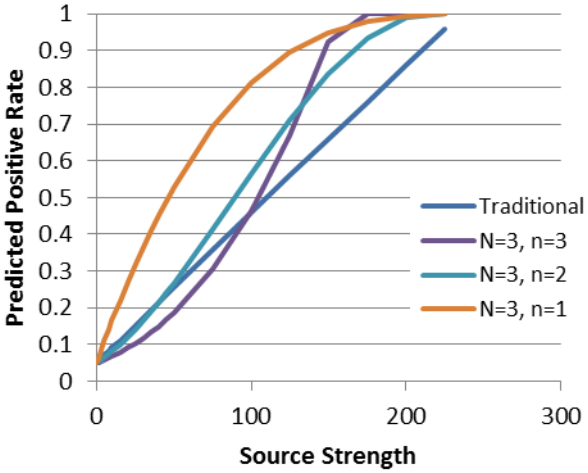

Figure 118 Positive Rate with Source Strength for Different Values of n and Constant b (Rectangular, N=3, Deterministic)

N=4

b=50

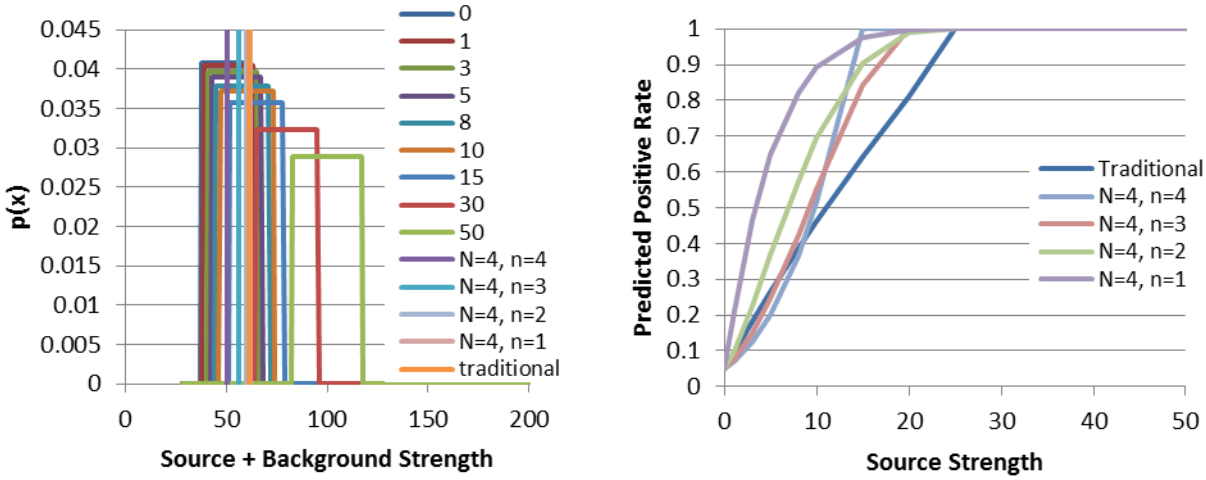

b=500

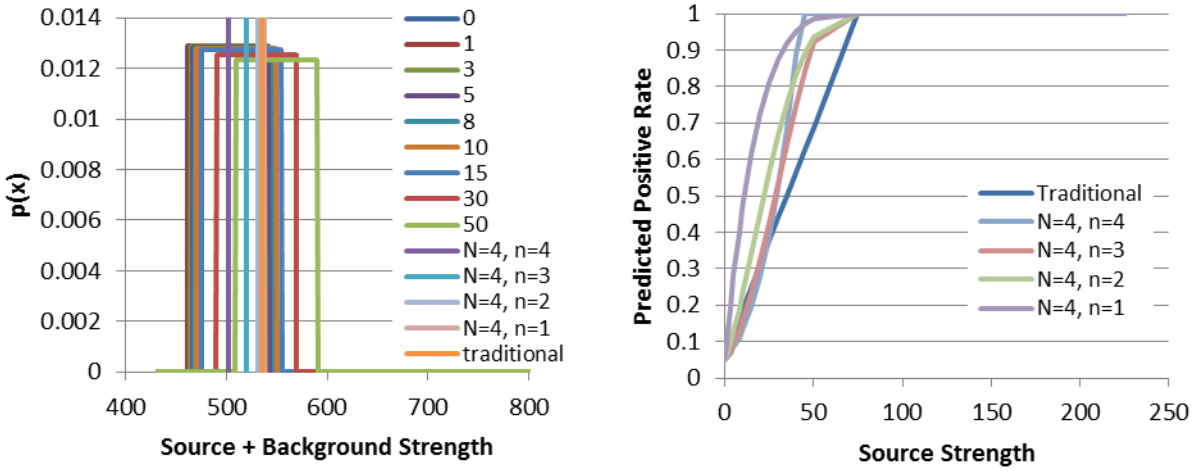

b=5000

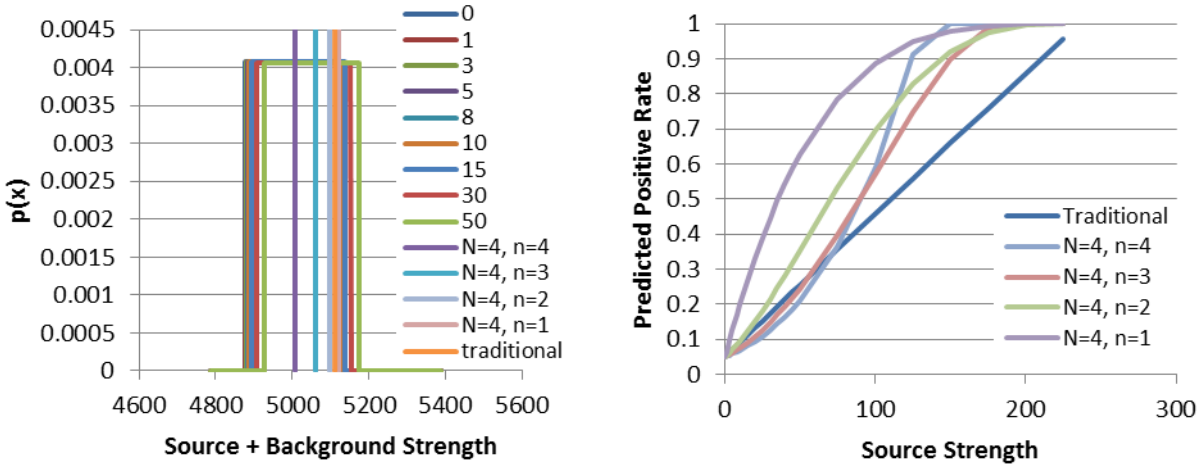

Figure 119 Positive Rate with Source Strength for Different Values of n and Constant b (Rectangular, N=2, Deterministic)

N=5

b=50

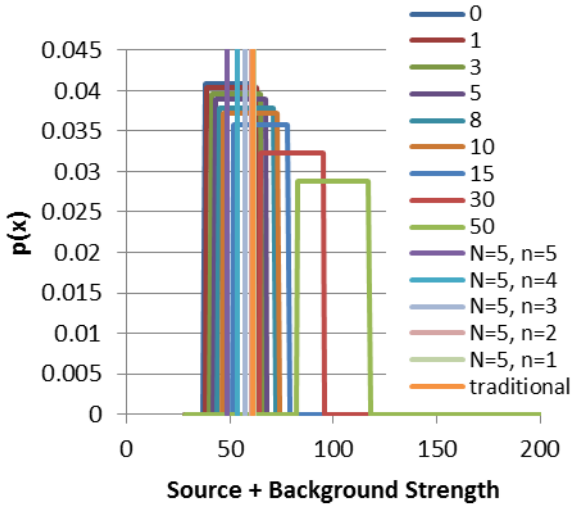

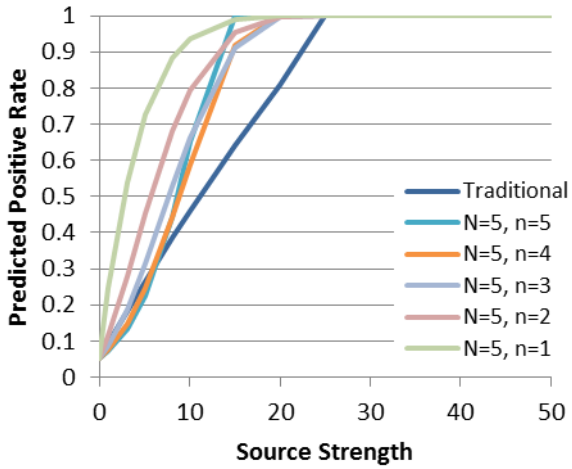

b=500

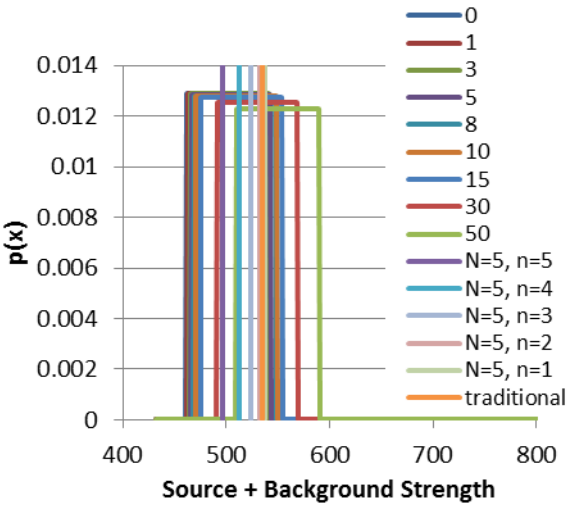

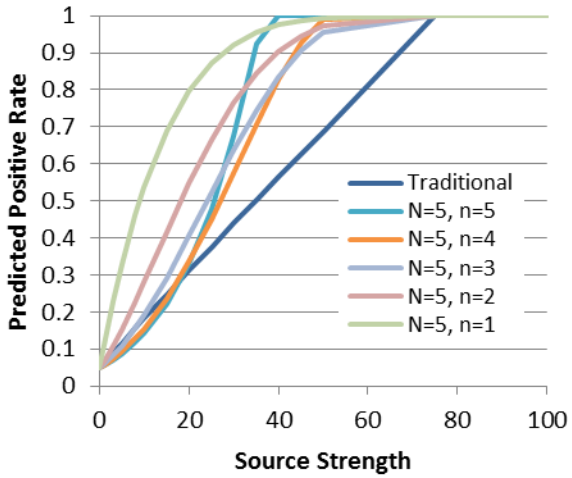

b=5000

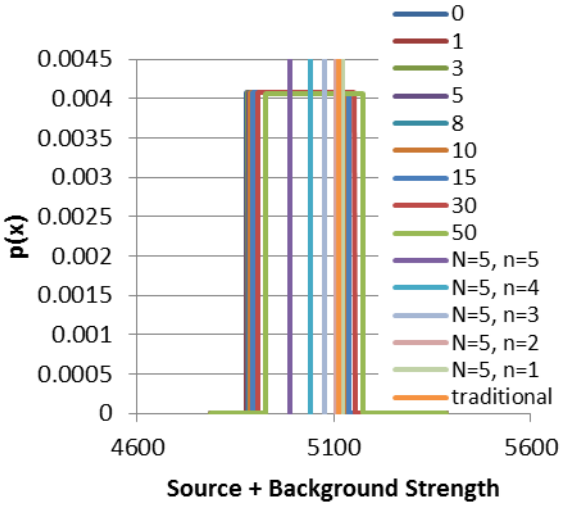

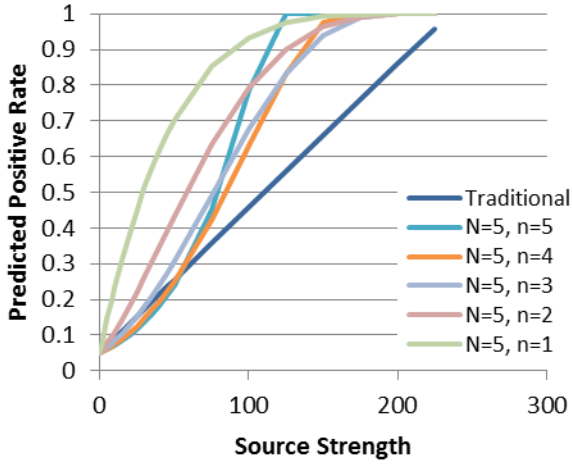

Figure 120 Positive Rate with Source Strength for Different Values of n and Constant b (Rectangular, N=5, Deterministic)

Triangular

Table 13 Calculated Values of y* at Different Backgrounds Strengths (Triangular, Deterministic)

		Background Strength									
N	n	50	100	250	500	750	1000	2500	5000	7500	10000
1	1	64	121	282	586	806	1065	2603	5145	7678	10205
2	2	57	110	266	522	777	1031	2550	5070	7586	10099
	1	66	123	286	552	814	1074	2616	5164	7701	10232
3	3	53	104	257	509	762	1013	2521	5030	7537	10042
	2	60	114	273	532	789	1046	2572	5102	7625	10144
	1	67	124	288	555	817	1078	2622	5173	7712	10245
4	4	51	101	251	502	752	1003	2504	5006	7507	10008
	3	56	109	264	520	774	1028	2544	5063	7577	10088
	2	62	117	276	537	796	1053	2584	5118	7645	10167
	1	68	125	289	556	819	1080	2626	5178	7718	10252
5	5	49	98	248	497	746	995	2492	4989	7487	9985
	4	54	105	258	512	764	1016	2526	5037	7545	10052
	3	58	112	268	526	782	1037	2558	5082	7600	10115
	2	63	118	279	541	800	1058	2591	5129	7658	10183
	1	68	126	290	557	820	1081	2629	5182	7723	10257

Positive Rate

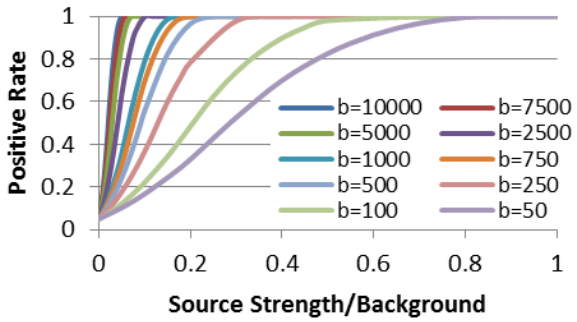

Figure 121 Positive Rate with Source Strength/Background with Different Values of b (Triangular, Traditional, Deterministic)

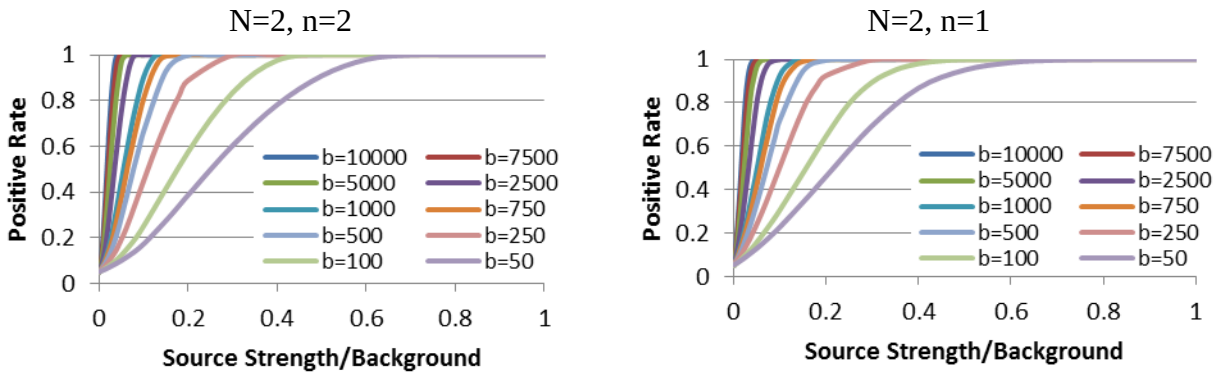

Figure 122 Positive Rate with Source Strength/Background with Different Values of n and b (Triangular, N=2, Deterministic)

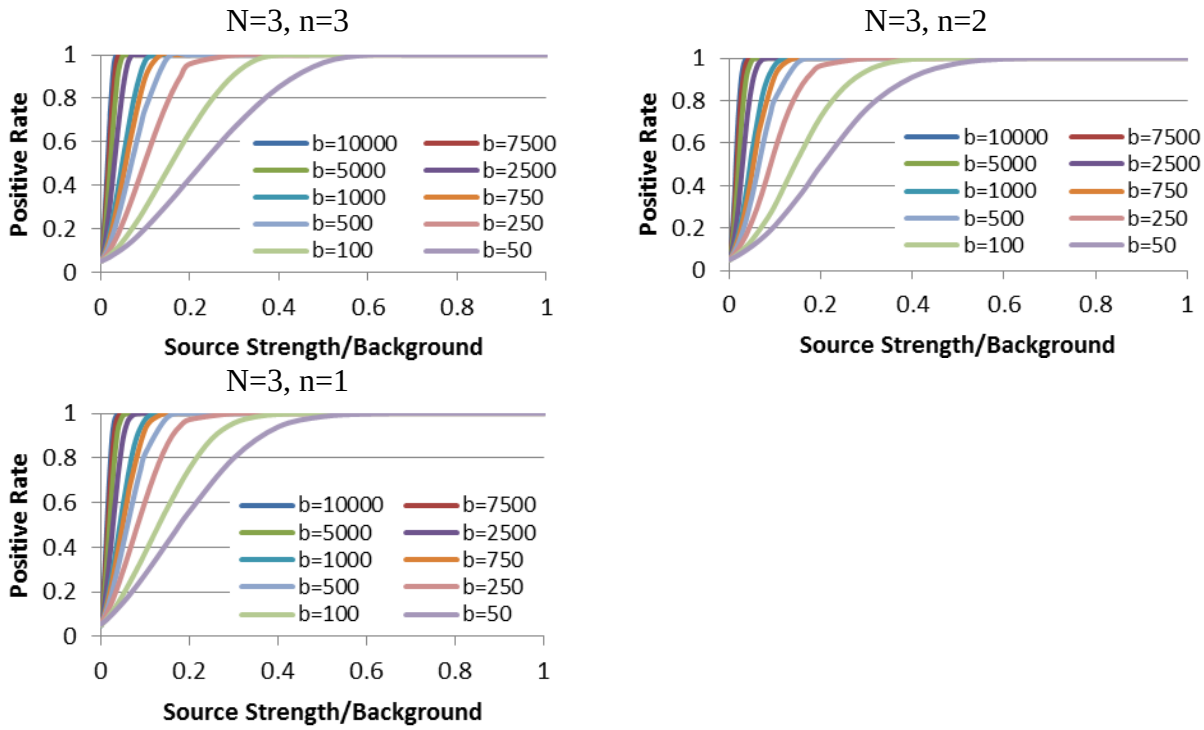

Figure 123 Positive Rate with Source Strength/Background with Different Values of n and b (Triangular, N=3, Deterministic)

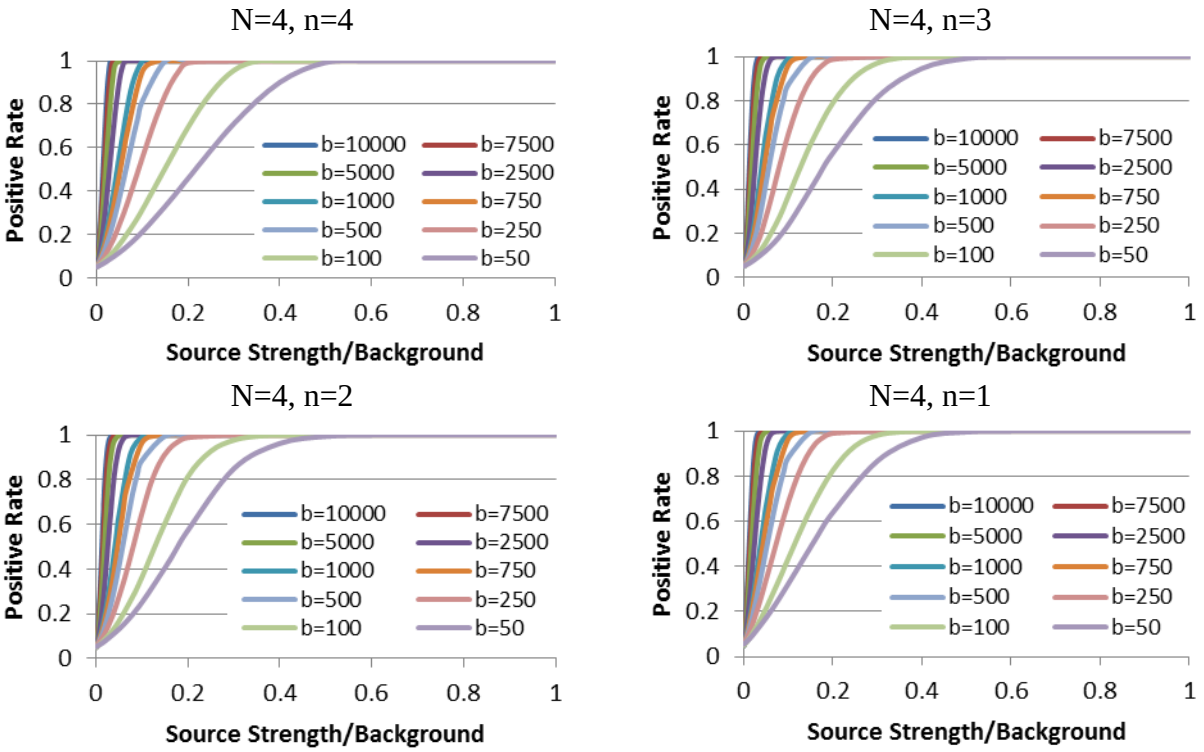

Figure 124 Positive Rate with Source Strength/Background with Different Values of n and b (Triangular, N=4, Deterministic)

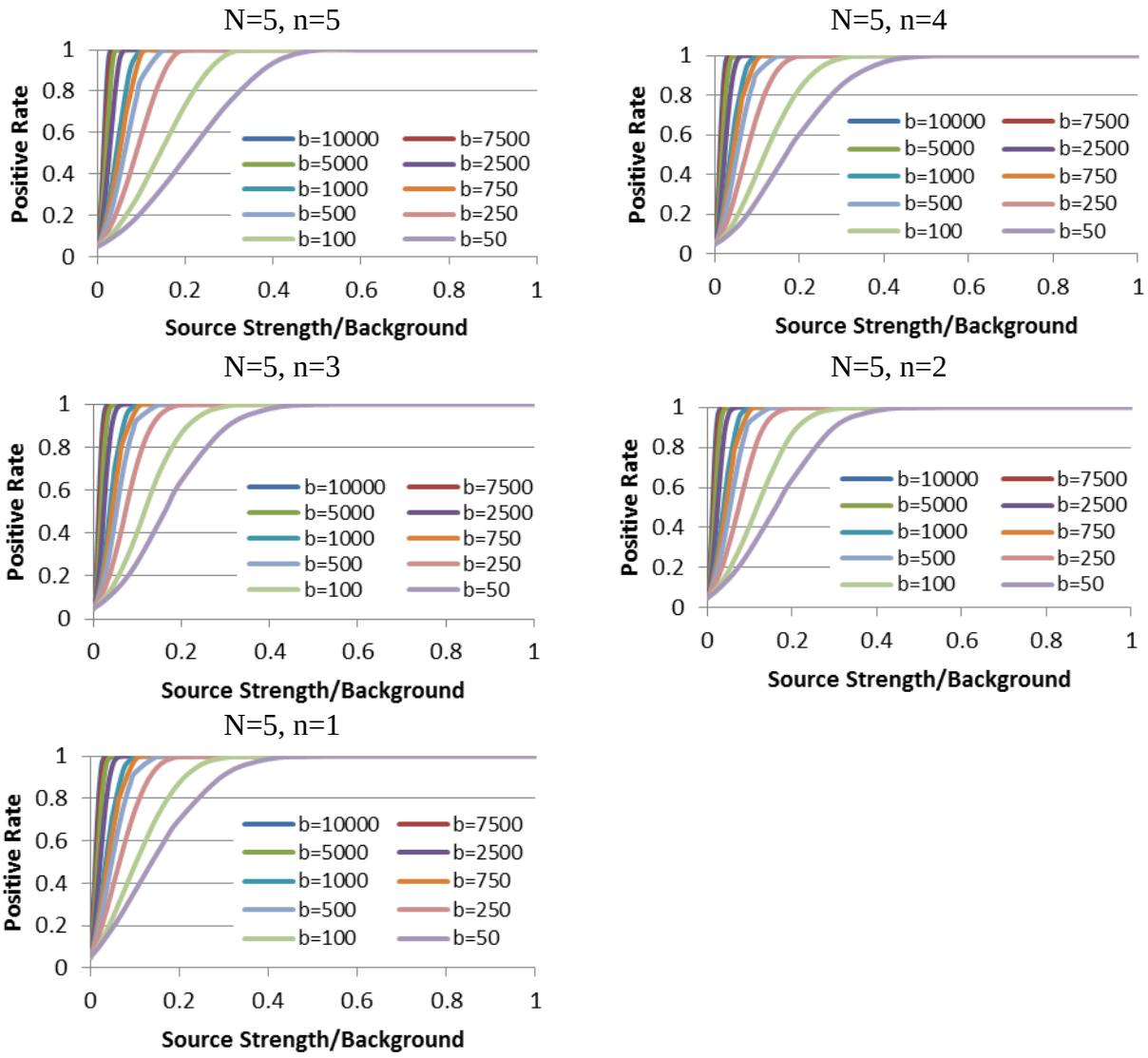

Figure 125 Positive Rate with Source Strength/Background with Different Values of n and b (Triangular, N=5, Deterministic)

N=2

b=50

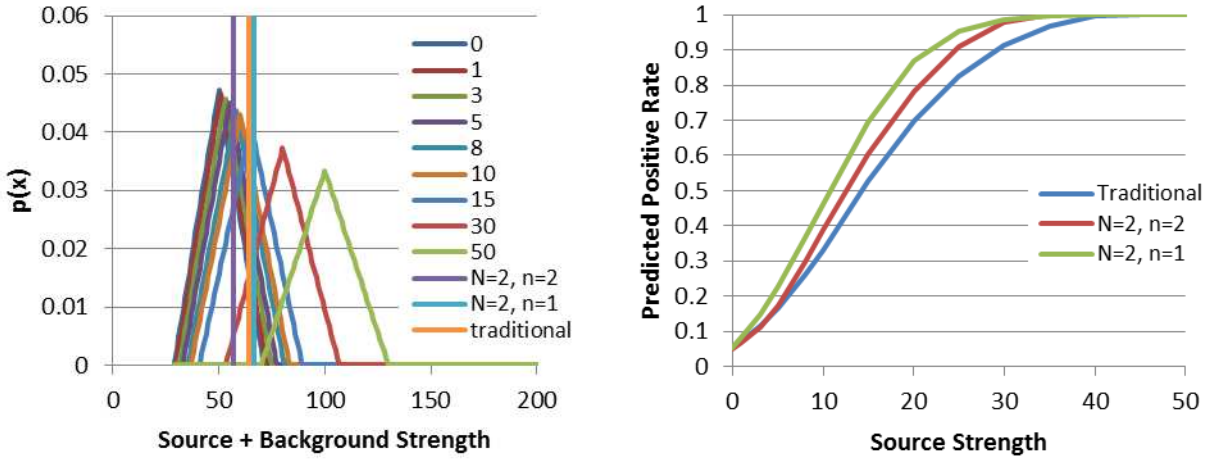

b=500

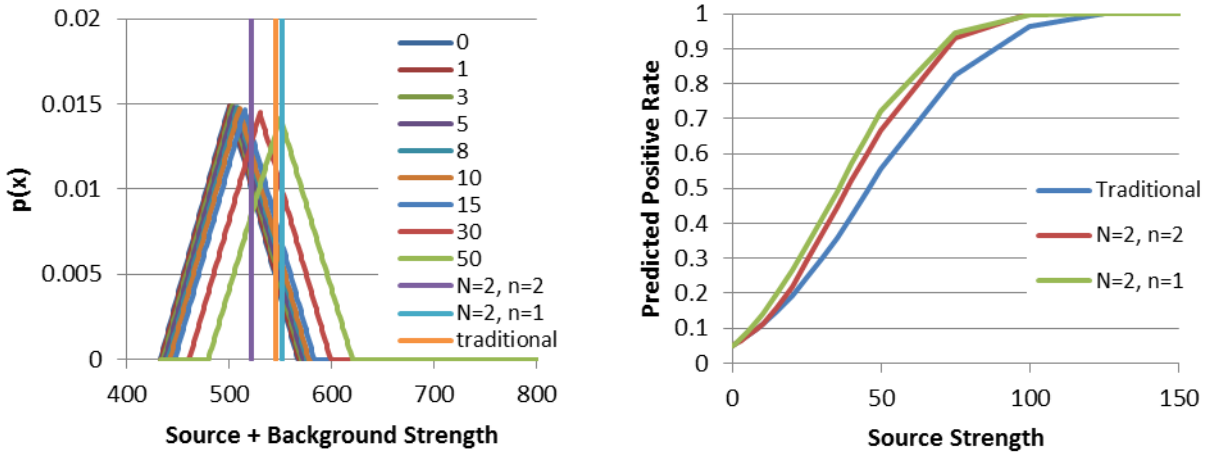

b=5000

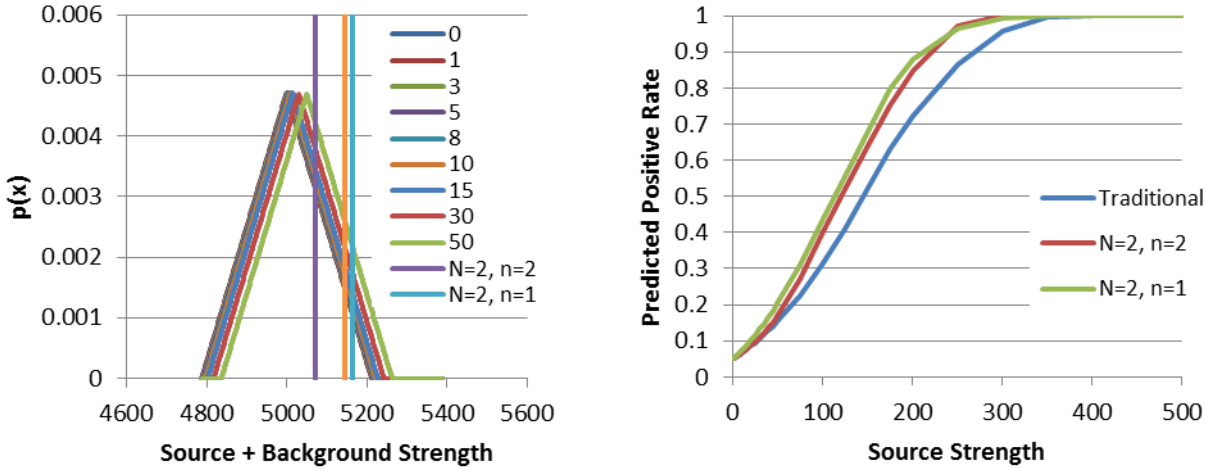

Figure 126 Positive Rate with Source Strength for Different Values of n and Constant b (Triangular, N=2, Deterministic)

N=3

b=50

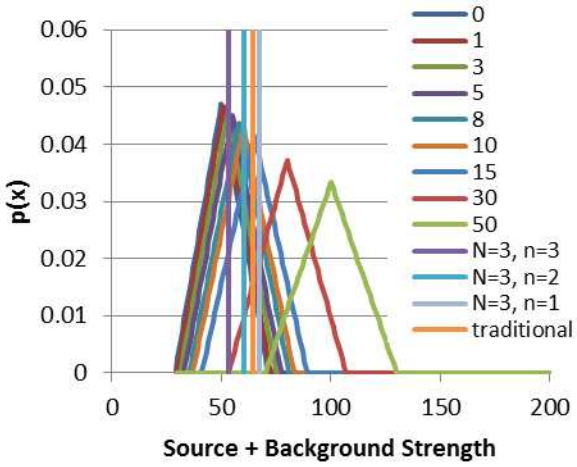

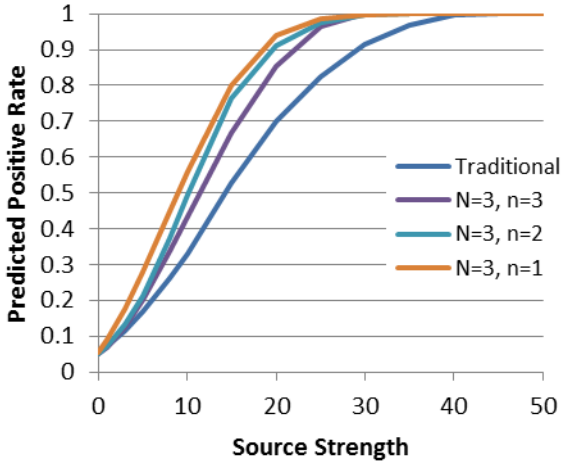

b=500

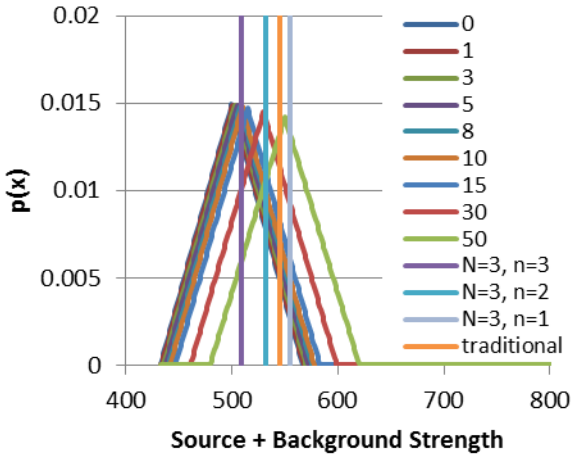

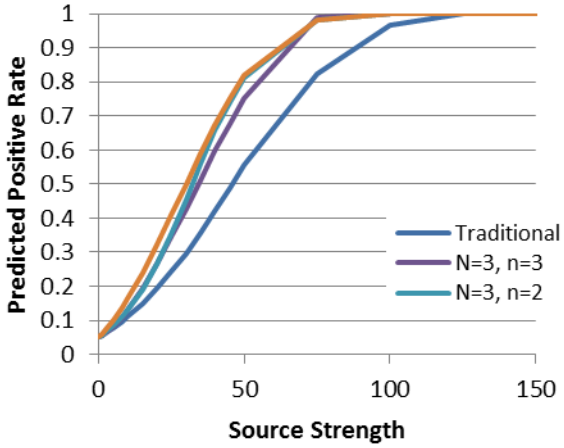

b=5000

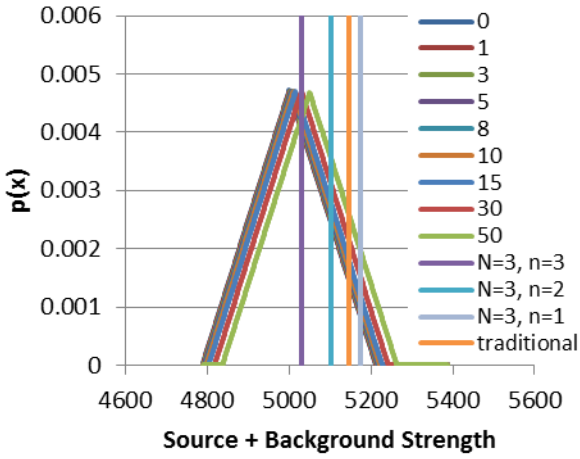

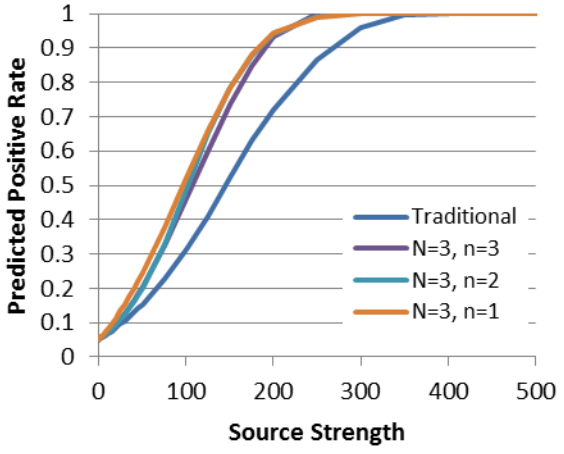

Figure 127 Positive Rate with Source Strength for Different Values of n and Constant b (Triangular, N=3, Deterministic)

N=4
b=50

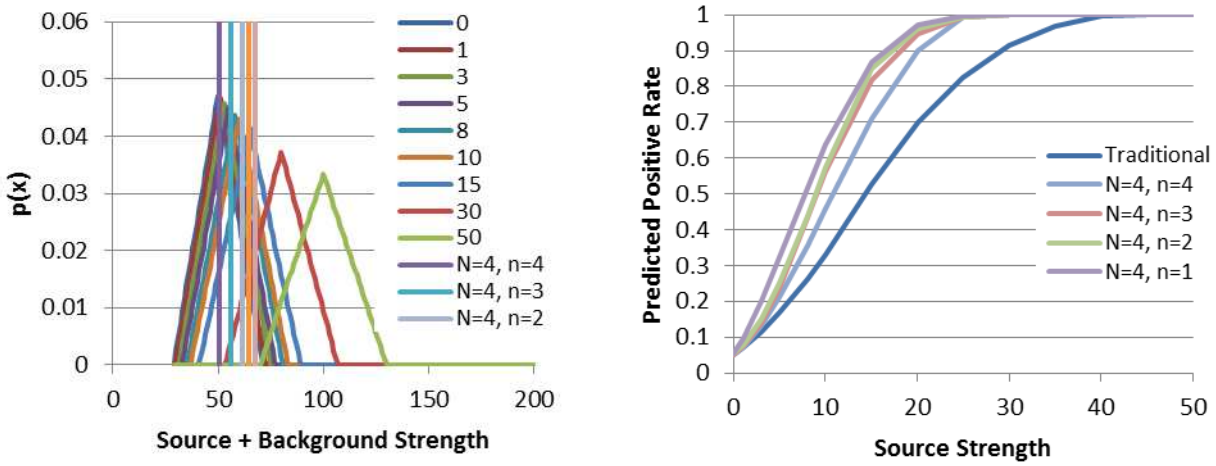

b=500

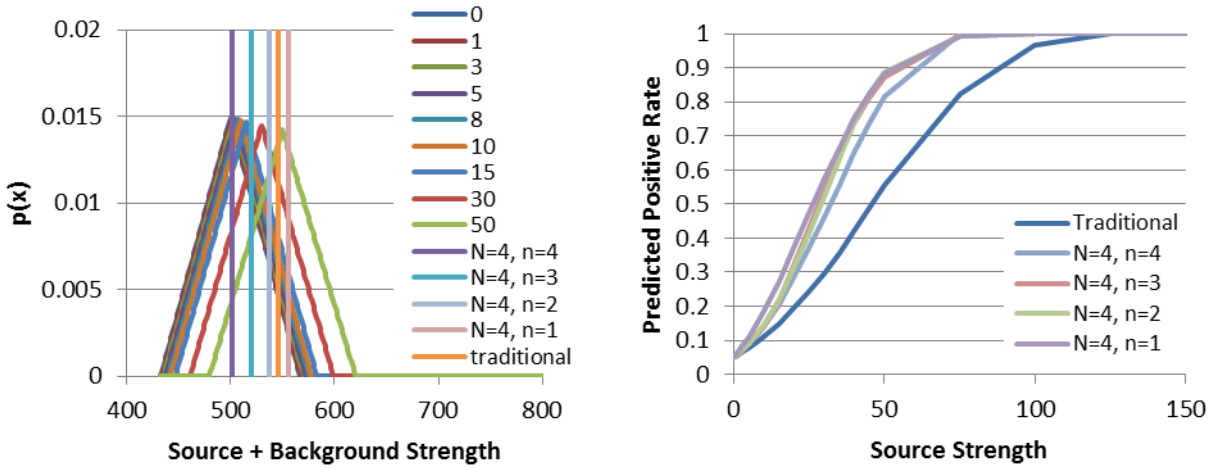

b=5000

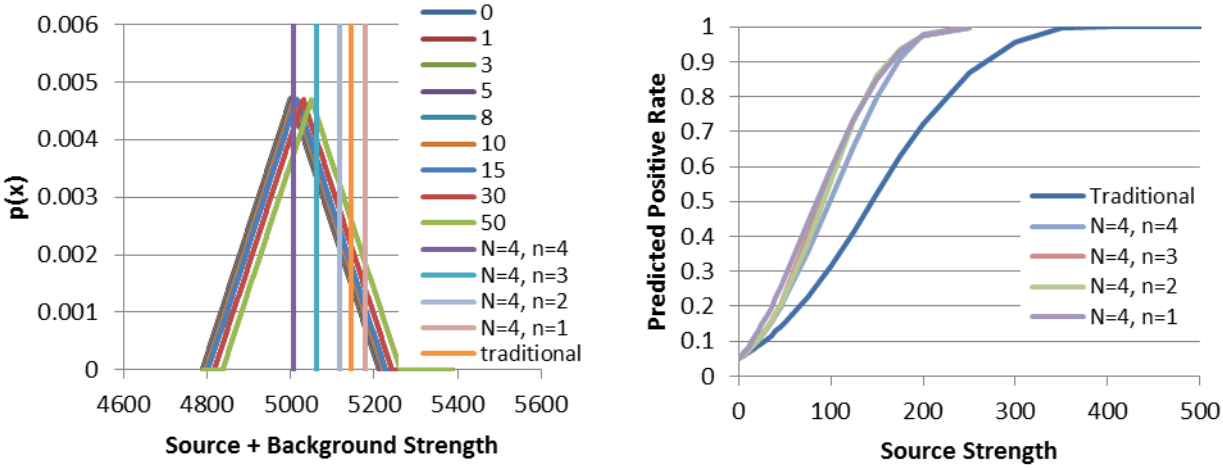

Figure 128 Positive Rate with Source Strength for Different Values of n and Constant b (Triangular, N=4, Deterministic)

N=5

b=50

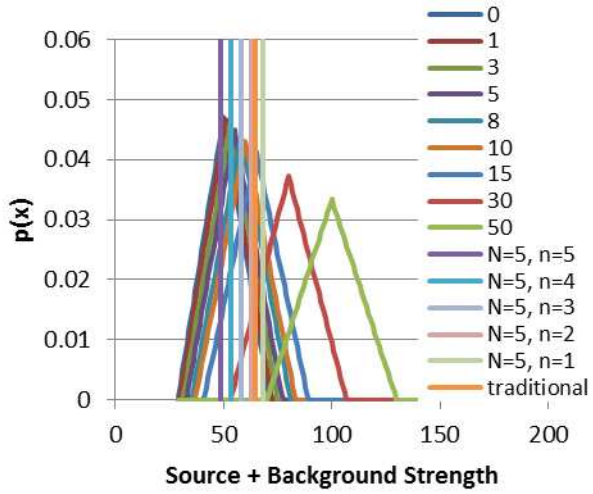

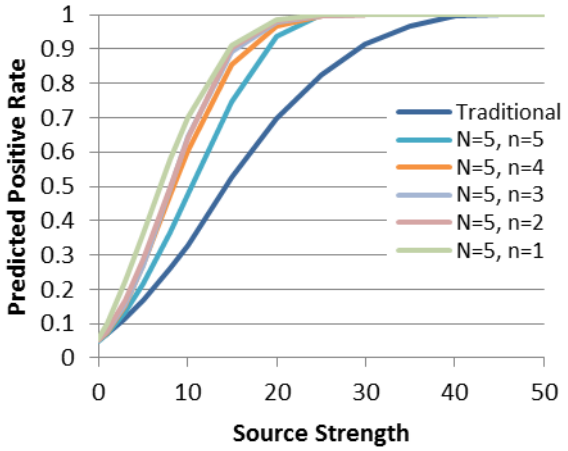

b=500

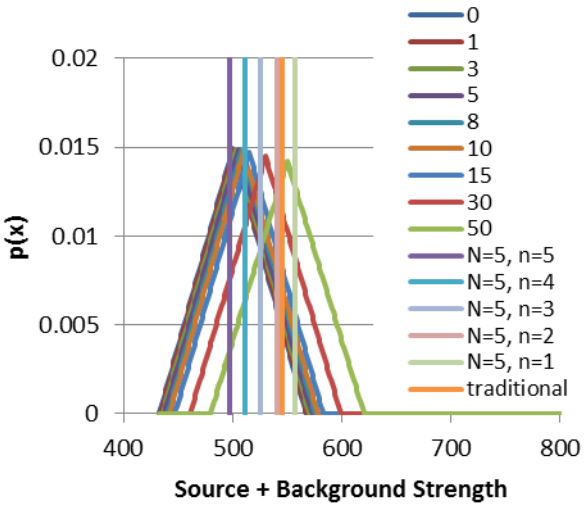

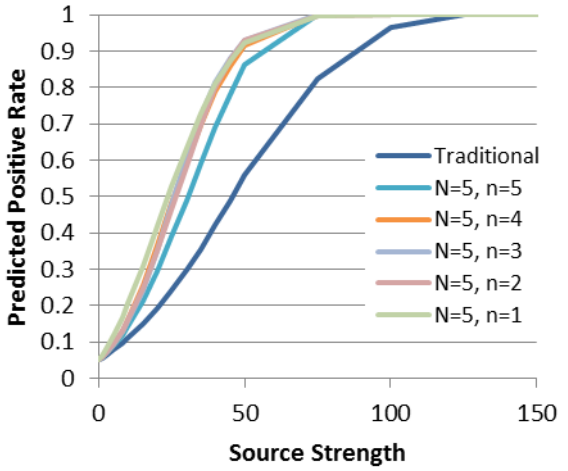

b=5000

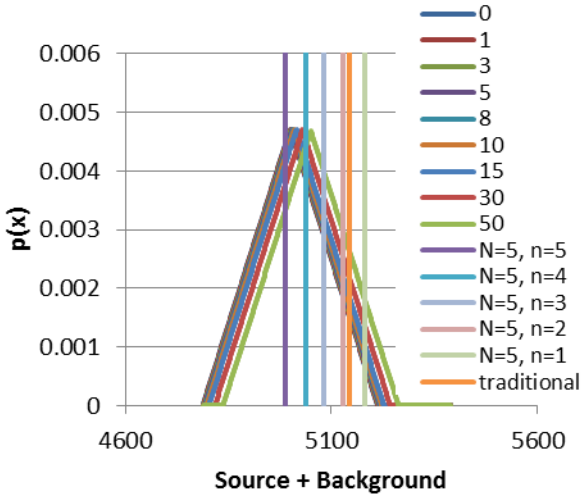

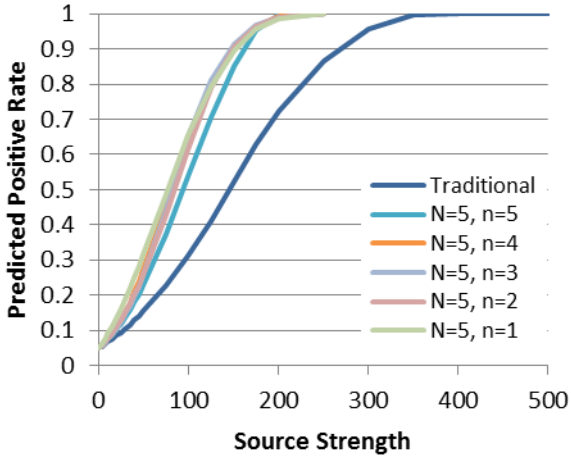

Figure 129 Positive Rate with Source Strength for Different Values of n and Constant b (Triangular, N=5, Deterministic)

Sinusoidal

Table 14 Calculated Values of y* at Backgrounds Strengths (Sinusoidal, Deterministic)

		Background Strength									
N	n	50	100	250	500	750	1000	2500	5000	7500	10000
1	1	64	121	282	546	806	1065	2603	5145	7678	10205
2	2	57	110	266	522	777	1031	2550	5070	7586	10099
	1	66	123	286	552	814	1074	2616	5164	7701	10232
3	3	53	104	257	509	762	1013	2521	5030	7537	10042
	2	60	114	273	532	789	1046	2572	5102	7625	10144
	1	67	124	288	555	817	1078	2622	5173	7712	10245
4	4	51	101	251	502	752	1003	2504	5006	7507	10008
	3	56	109	264	520	774	1028	2544	5063	7577	10088
	2	62	117	276	537	796	1053	2584	5118	7645	10167
	1	68	125	289	556	819	1080	2626	5178	7718	10252
5	5	49	98	248	497	746	995	2492	4989	7487	9985
	4	54	105	258	512	764	1016	2526	5037	7545	10052
	3	58	112	268	526	782	1037	2558	5082	7600	10115
	2	63	118	279	541	800	1058	2591	5129	7658	10183
	1	68	126	290	557	820	1081	2629	5182	7723	10257

Positive Rate

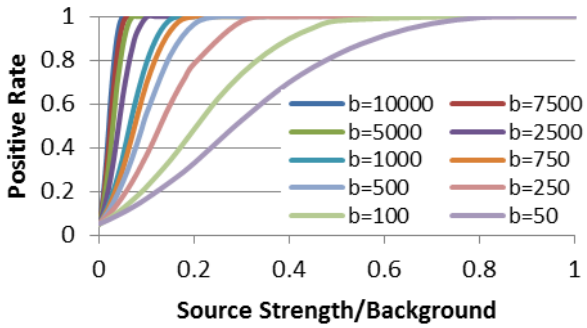

Figure 130 Positive Rate with Source Strength/Background with Different Values of b (Sinusoidal, Traditional, Deterministic)

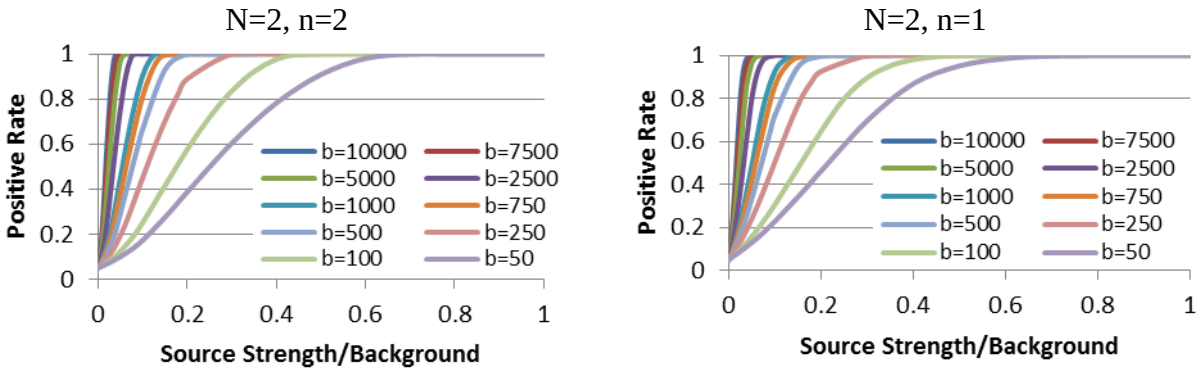

Figure 131 Positive Rate with Source Strength/Background with Different Values of n and b (Sinusoidal, N=2, Deterministic)

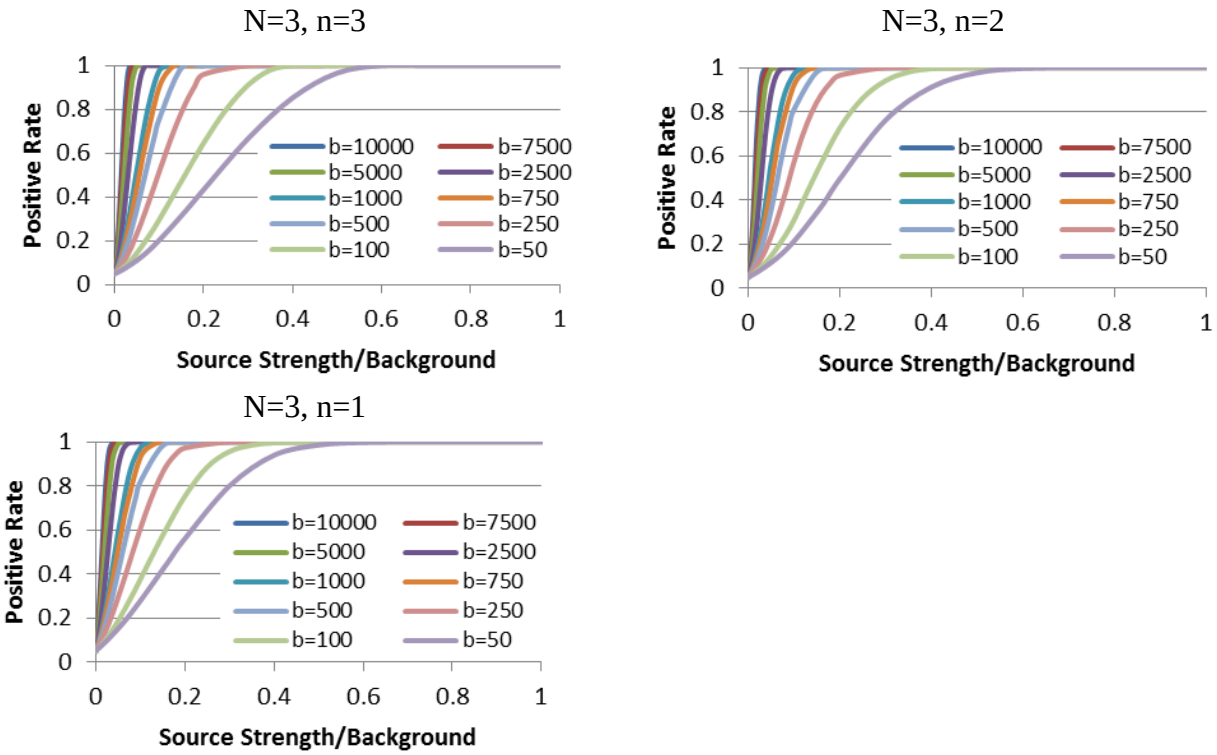

Figure 132 Positive Rate with Source Strength/Background with Different Values of n and b (Sinusoidal, N=3, Deterministic)

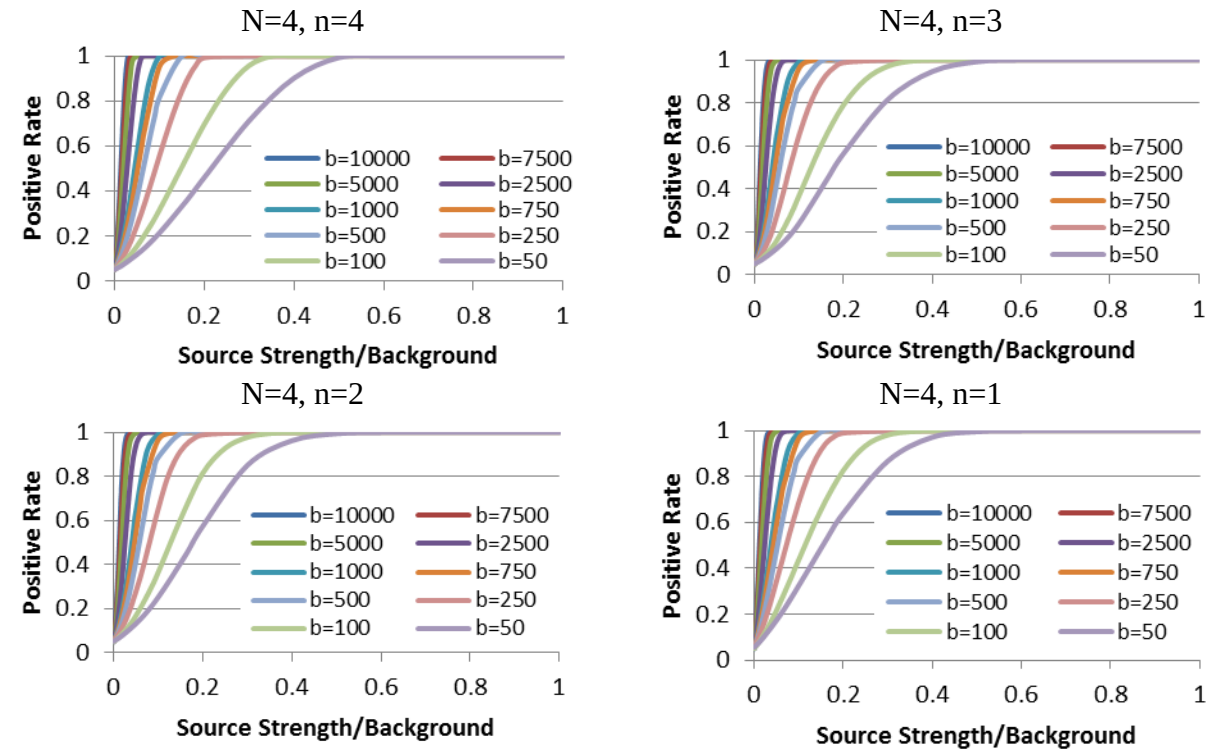

Figure 133 Positive Rate with Source Strength/Background with Different Values of n and b (Sinusoidal, N=4, Deterministic)

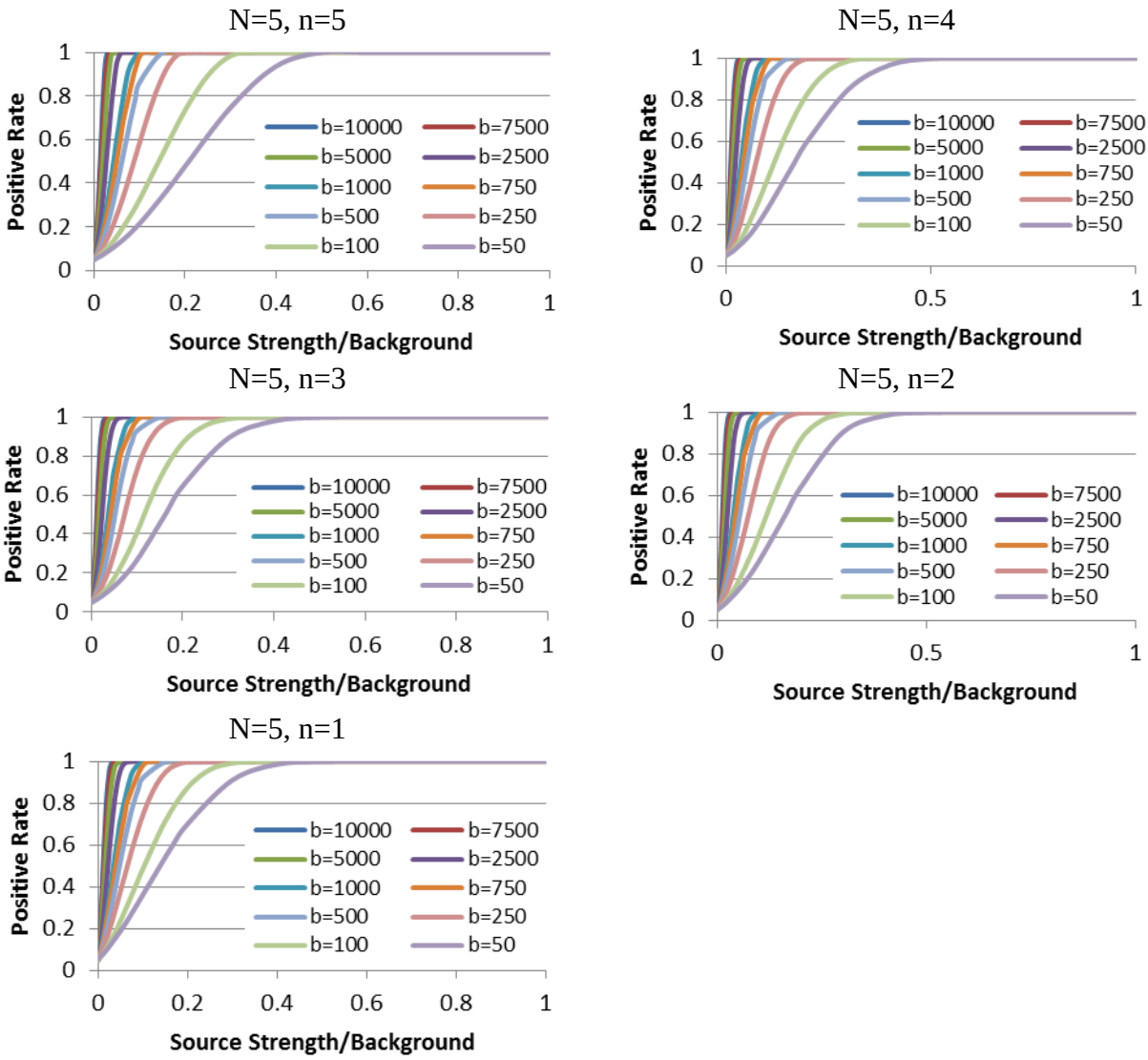

Figure 134 Positive Rate with Source Strength/Background with Different Values of n and b (Sinusoidal, N=5, Deterministic)

N=2

b=50

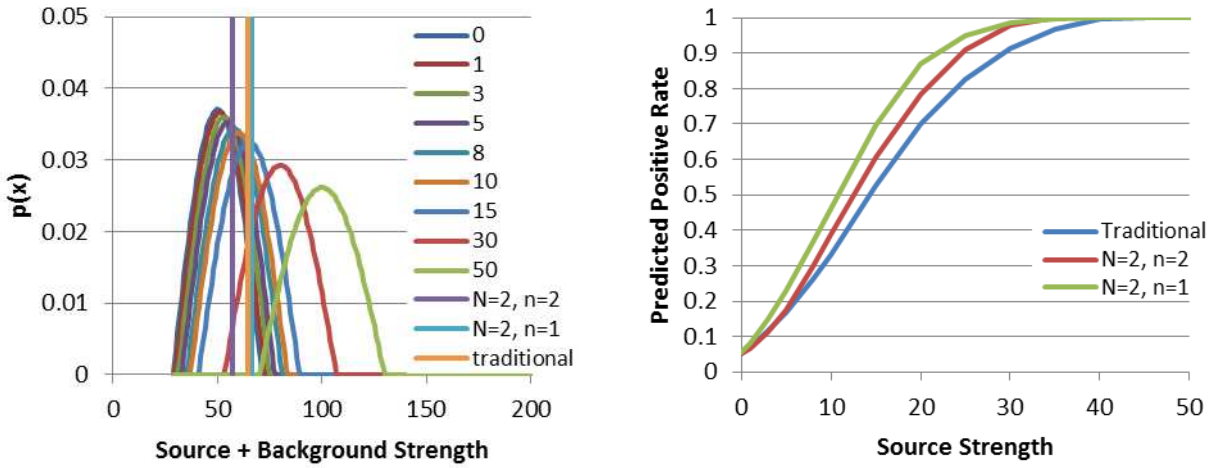

b=500

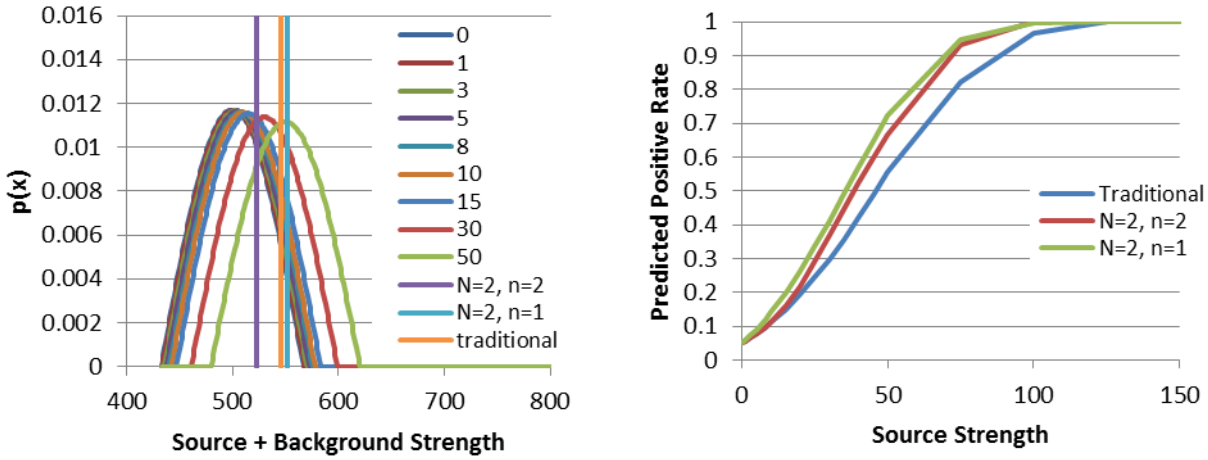

b=5000

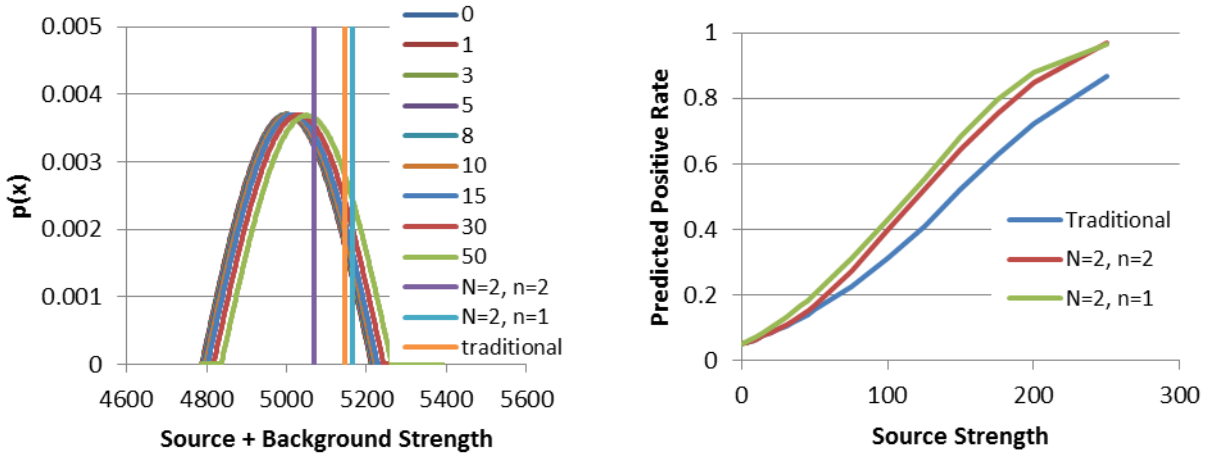

Figure 135 Positive Rate with Source Strength for Different Values of n and Constant b (Sinusoidal, N=2, Deterministic)

N=3

b=50

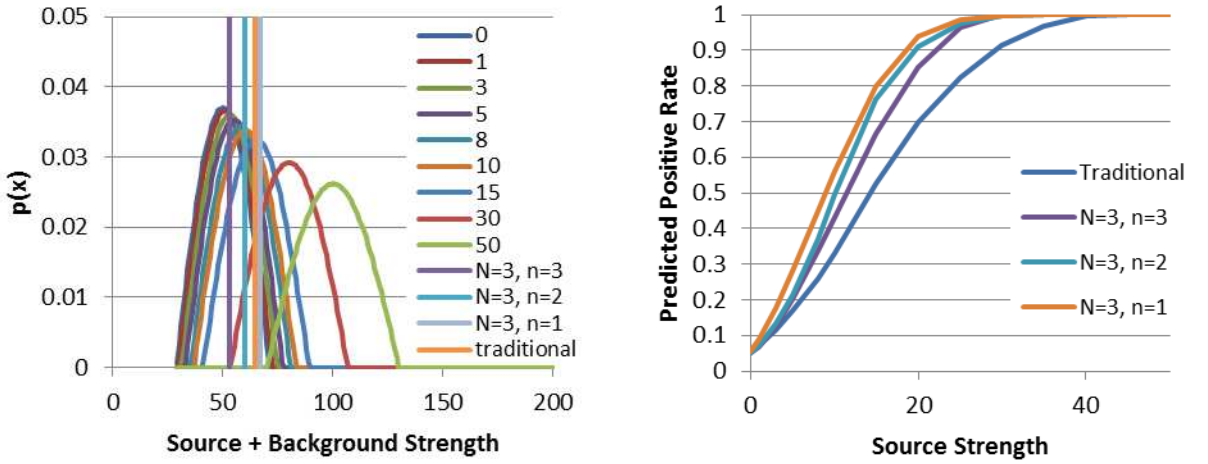

b=500

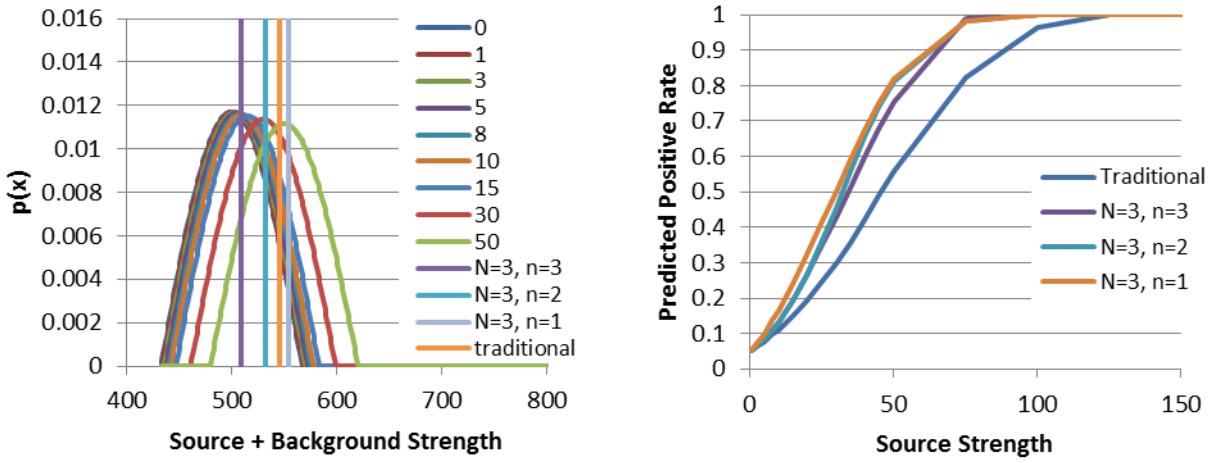

b=5000

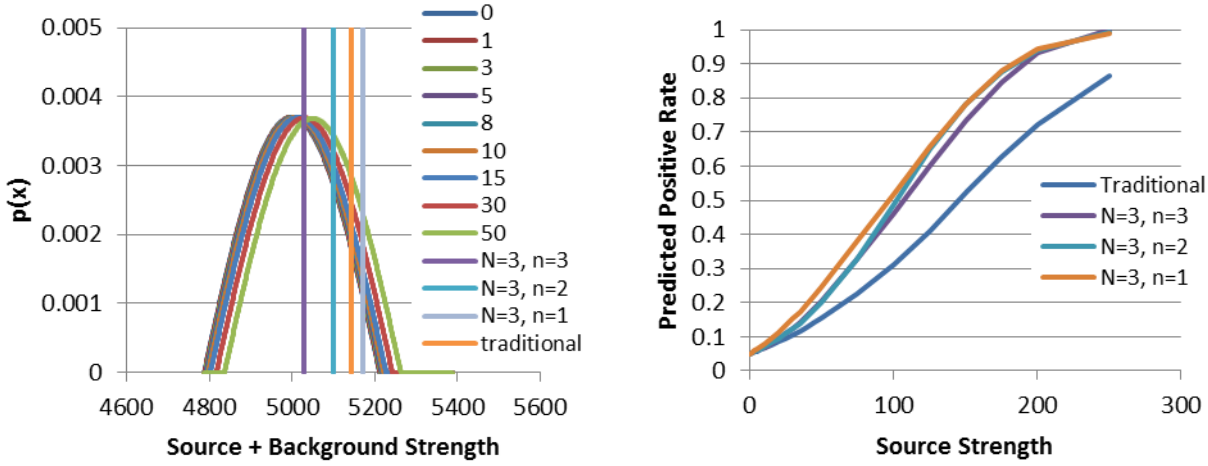

Figure 136 Positive Rate with Source Strength for Different Values of n and Constant b (Sinusoidal, N=3, Deterministic)

N=4

b=50

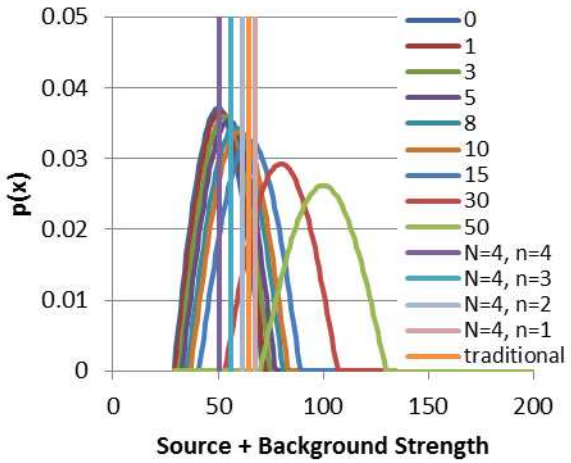

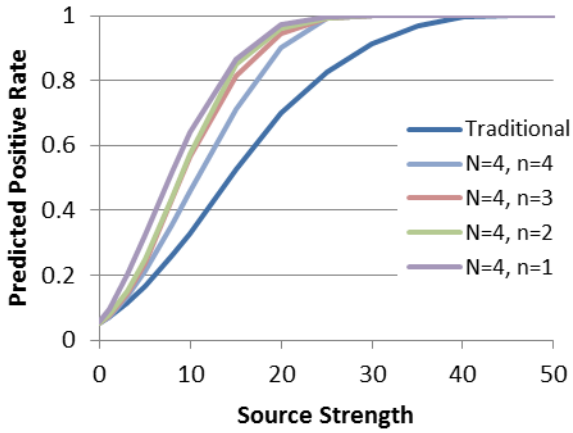

b=500

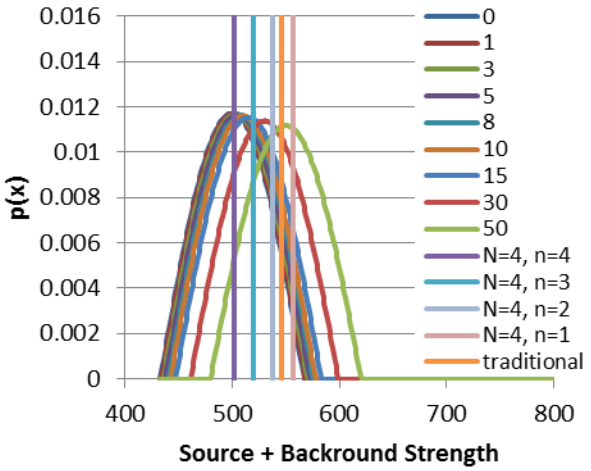

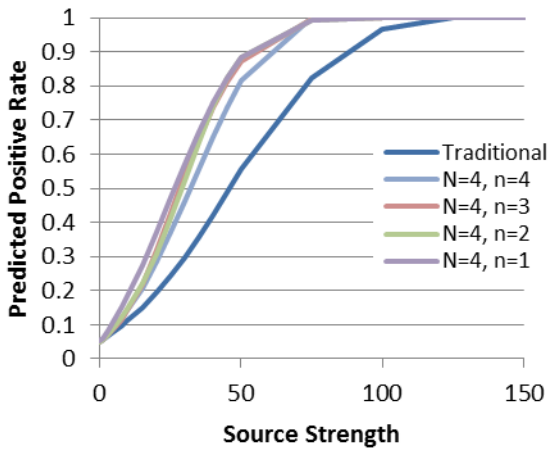

b=5000

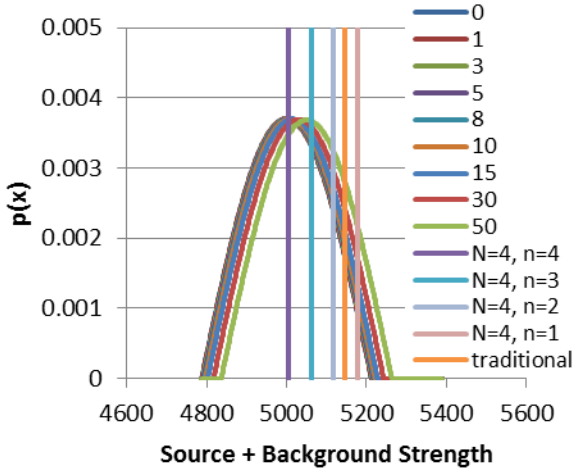

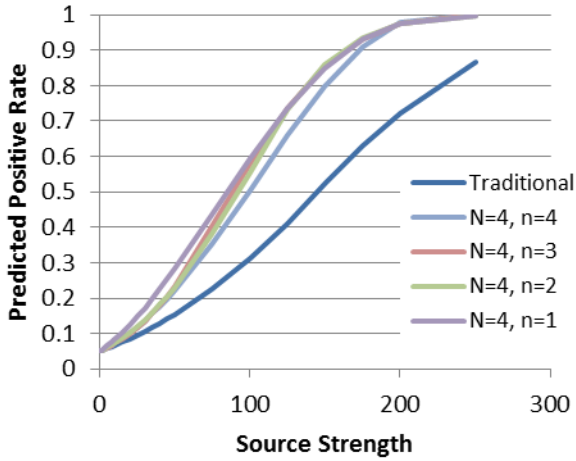

Figure 137 Positive Rate with Source Strength for Different Values of n and Constant b (Sinusoidal, N=4, Deterministic)

N=5

b=50

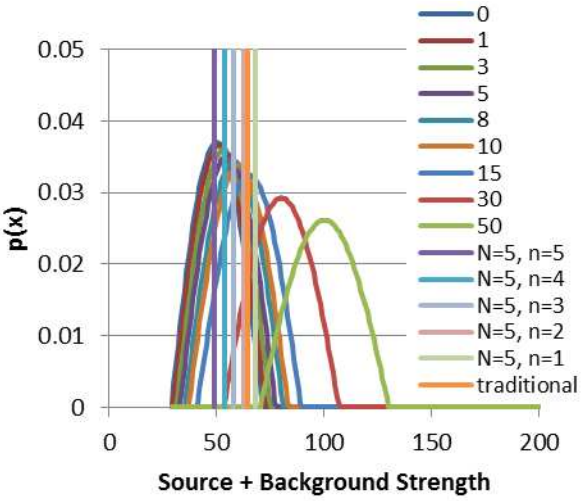

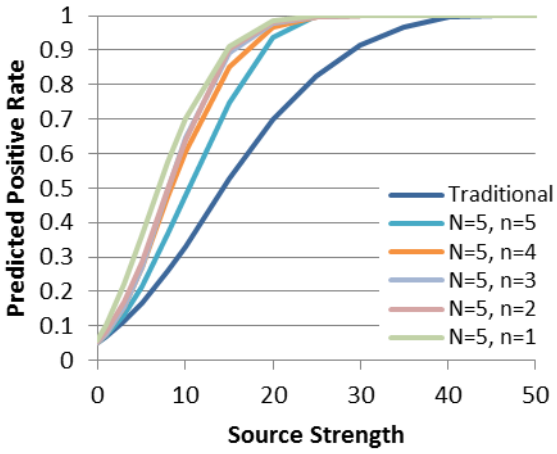

b=500

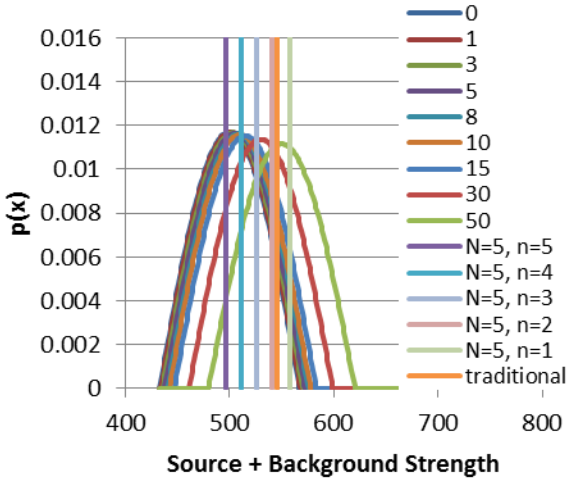

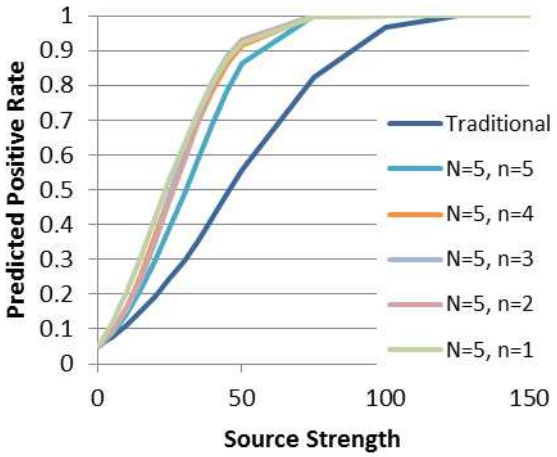

b=5000

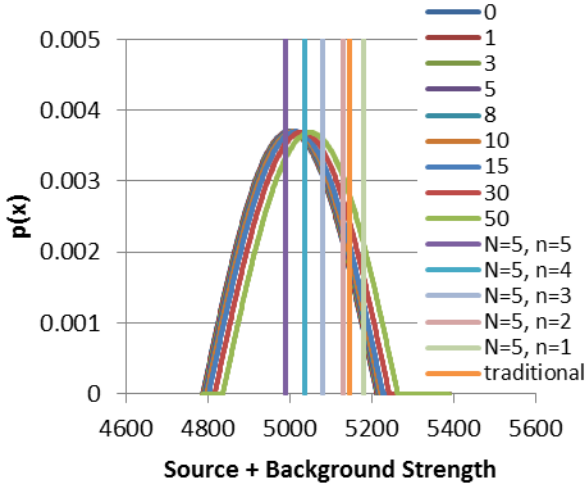

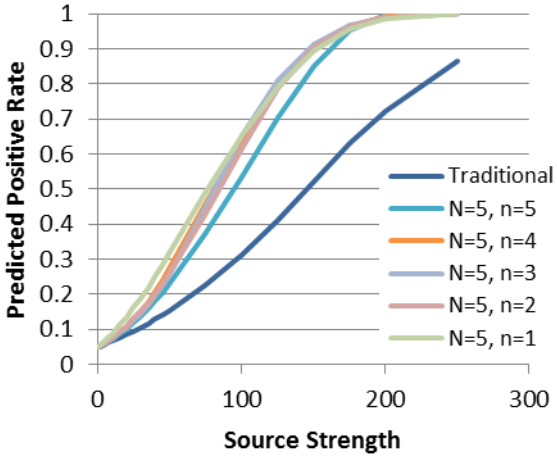

Figure 138 Positive Rate with Source Strength for Different Values of n and Constant b (Sinusoidal, N=5, Deterministic)

Poisson

Table 15 Calculated Values of y* at Backgrounds Strength (Poisson, Deterministic)

		Background Strength									
N	n	50	100	250	500	750	1000	2500	5000	7500	10000
1	1	62	117	276	537	795	1052	2583	5117	7643	10165
2	2	55	108	262	517	771	1024	2538	5054	7566	10076
	1	64	120	281	544	804	1062	2598	5139	7670	10196
3	3	52	103	255	507	759	1010	2517	5024	7529	10033
	2	58	111	267	525	780	1035	2555	5078	7595	10110
	1	66	122	284	548	809	1068	2607	5151	7684	10213
4	4	50	101	251	501	752	1002	2503	5005	7506	10007
	3	55	107	261	515	769	1021	2534	5048	7559	10068
	2	59	113	271	529	786	1041	2565	5092	7612	10130
	1	66	123	286	551	812	1071	2612	5159	7694	10224
5	5	49	99	248	497	746	996	2494	4991	7489	9987
	4	53	104	256	509	761	1013	2520	5029	7535	10040
	3	56	109	264	520	774	1028	2544	5062	7576	10088
	2	60	114	273	532	789	1045	2572	5101	7624	10143
	1	67	124	287	553	814	1074	2617	5165	7702	10233

Positive Rate

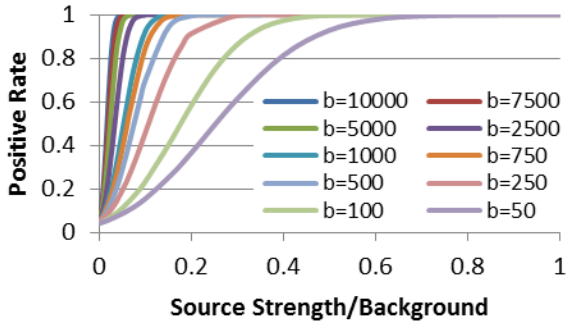

Figure 139 Positive Rate with Source Strength/Background with Different Values of b (Poisson, Traditional, Deterministic)

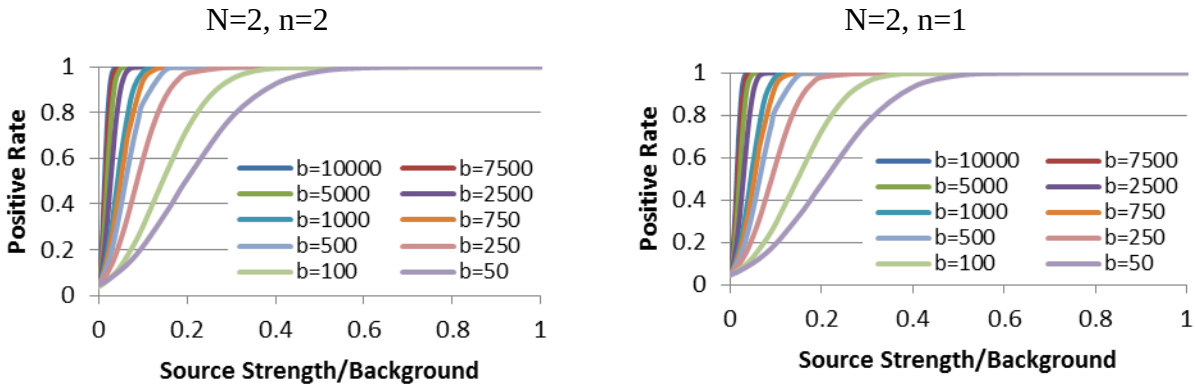

Figure 140 Positive Rate with Source Strength/Background with Different Values of n and b (Poisson, N=2, Deterministic)

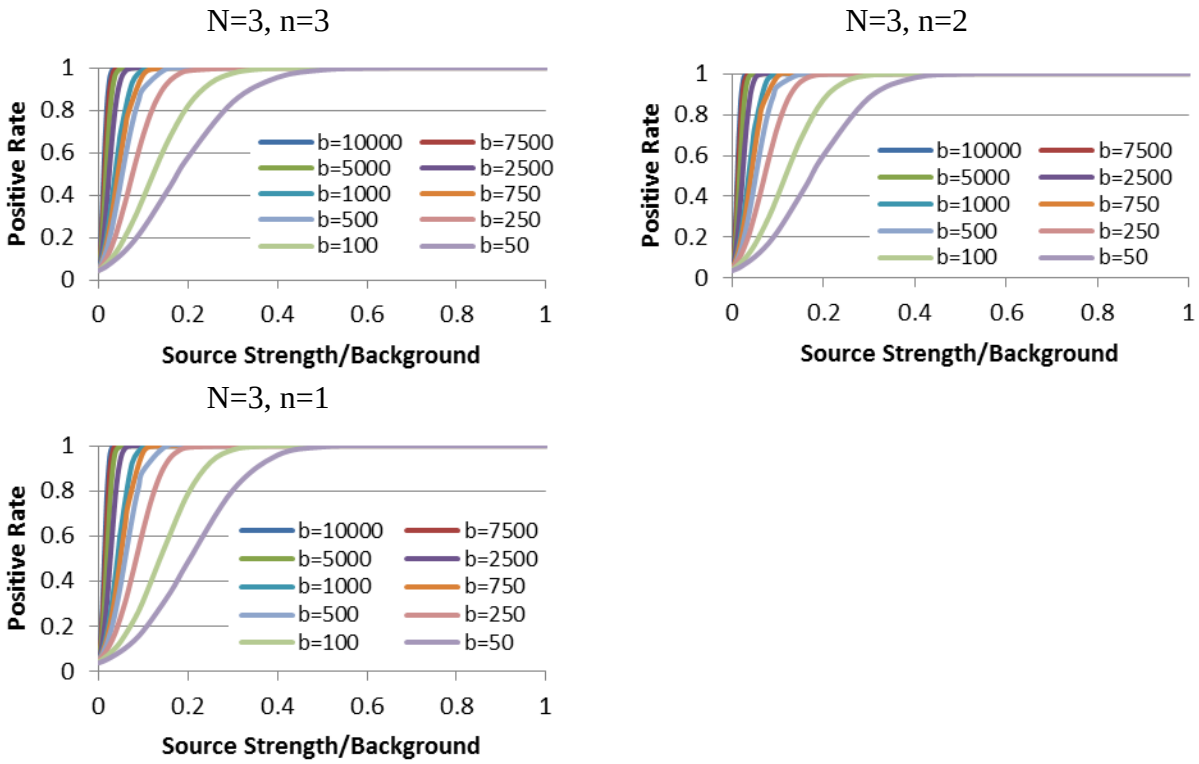

Figure 141 Positive Rate with Source Strength/Background with Different Values of n and b (Poisson, N=3, Deterministic)

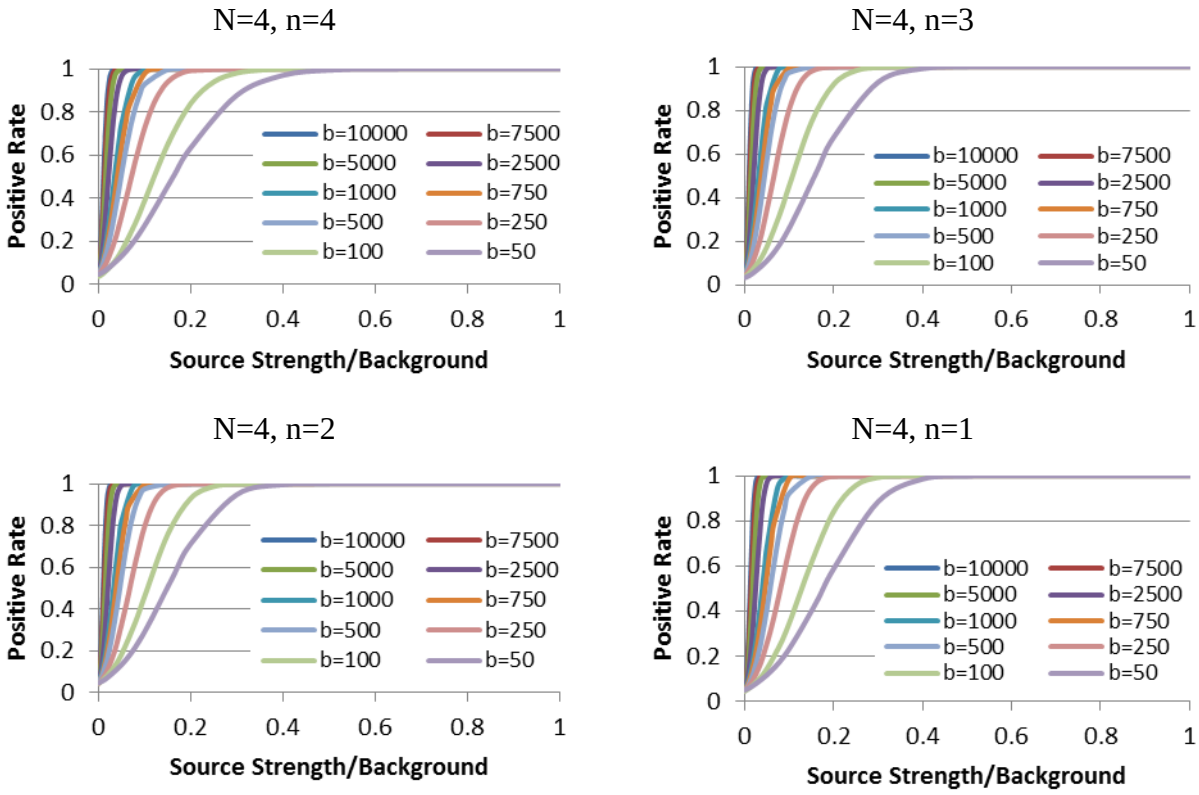

Figure 142 Positive Rate with Source Strength/Background with Different Values of n and b (Poisson, N=4, Deterministic)

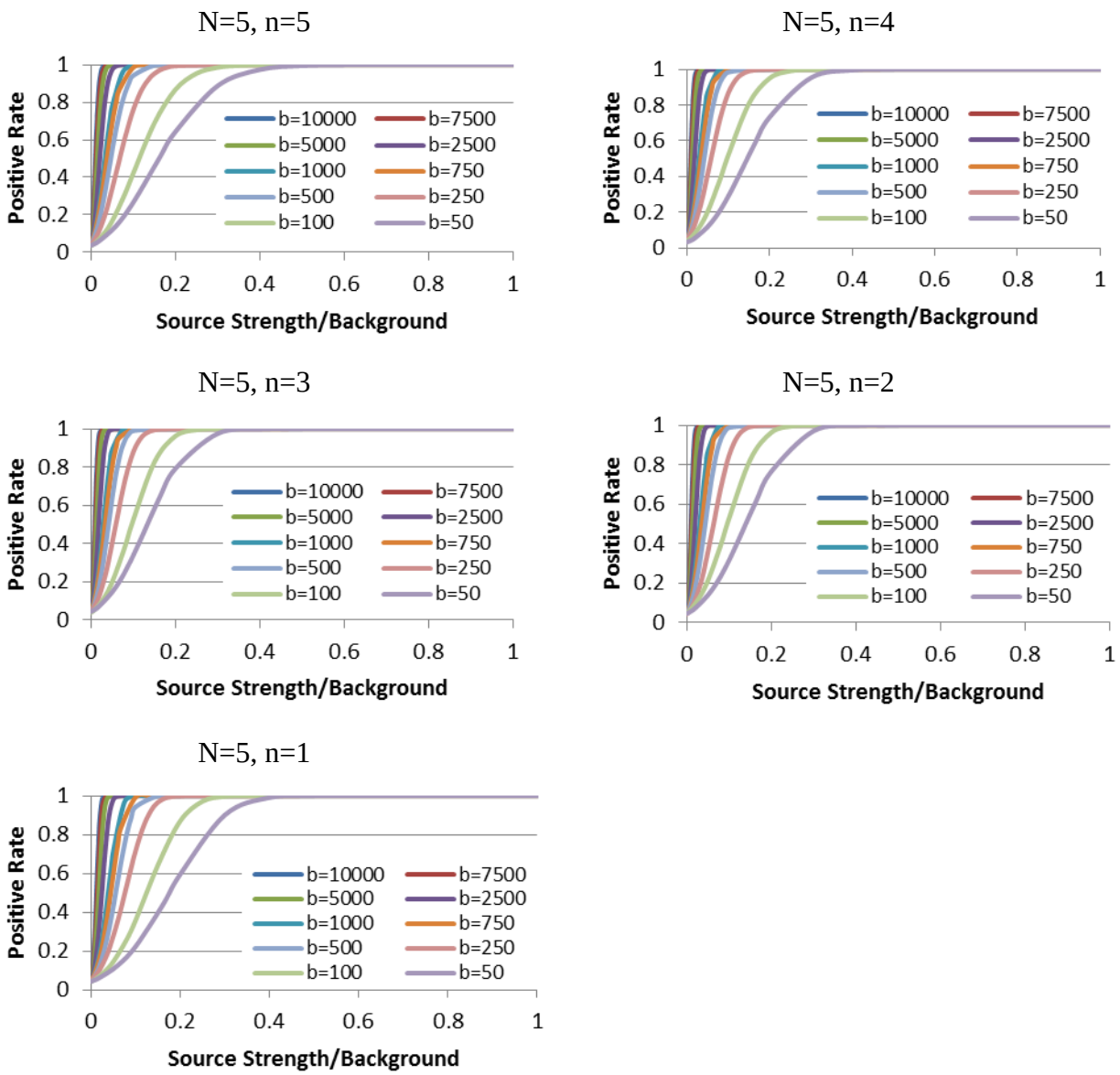

Figure 143 Positive Rate with Source Strength/Background with Different Values of n and b (Poisson, N=5, Deterministic)

N=2

b=50

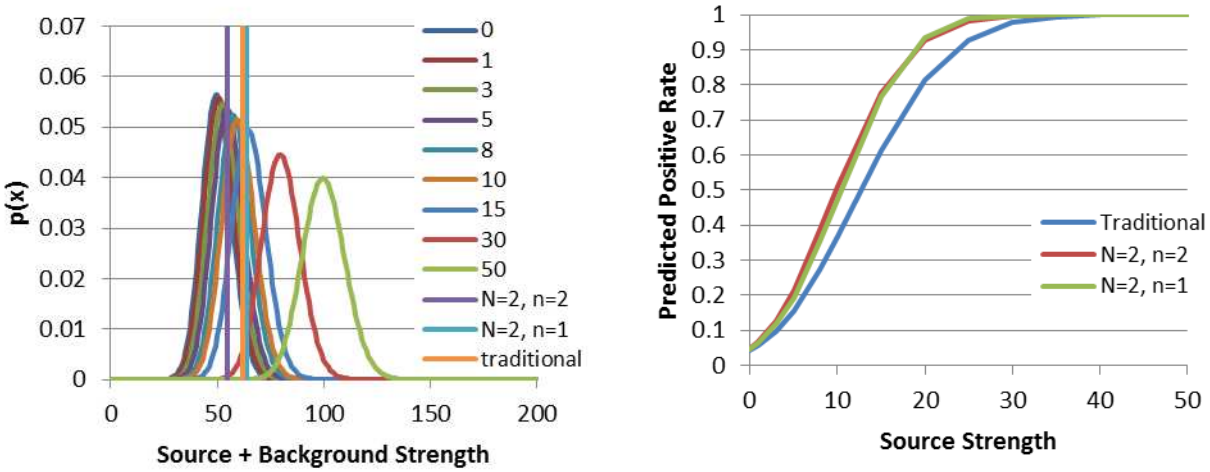

b=500

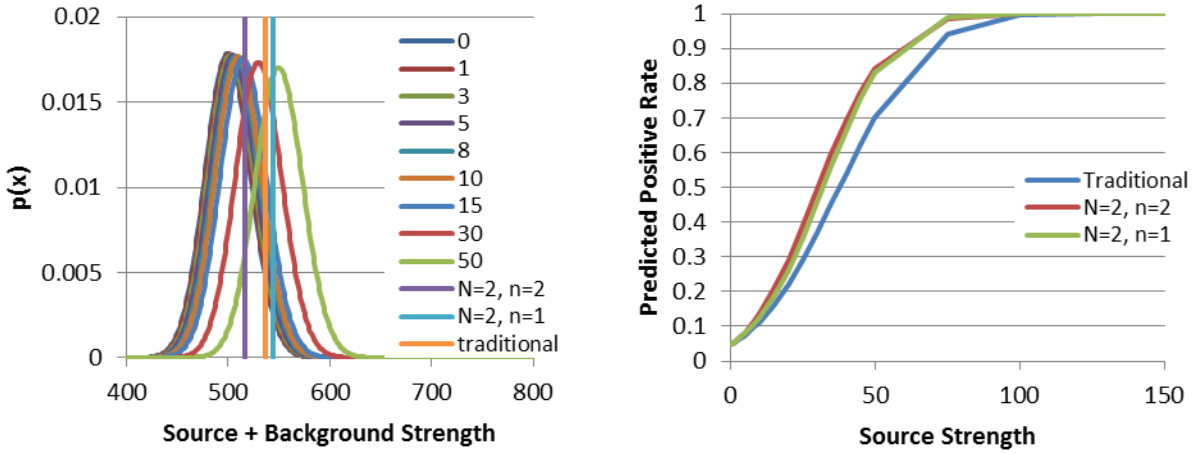

b=5000

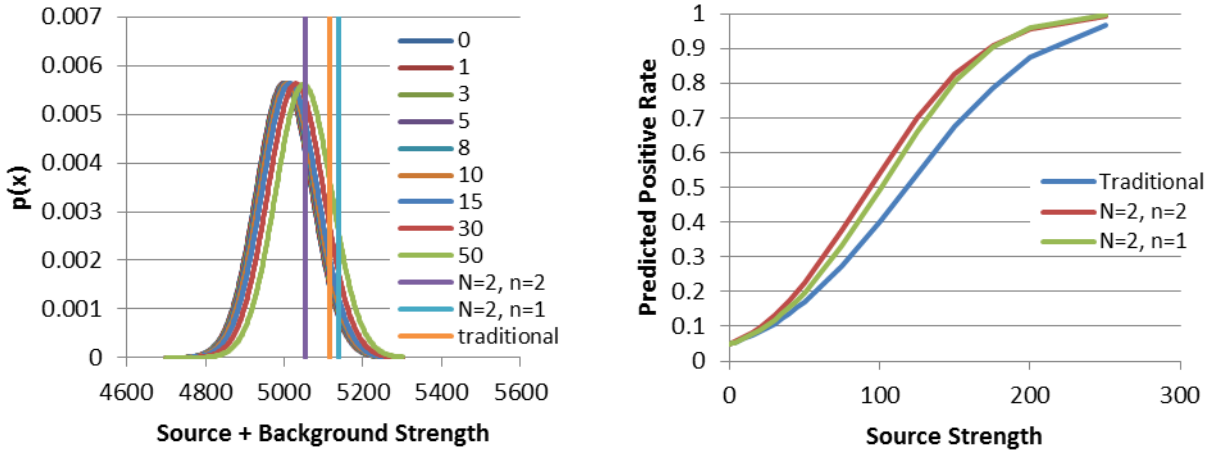

Figure 144 Positive Rate with Source Strength for Different Values of n and Constant b (Poisson, N=2, Deterministic)

N=3

b=50

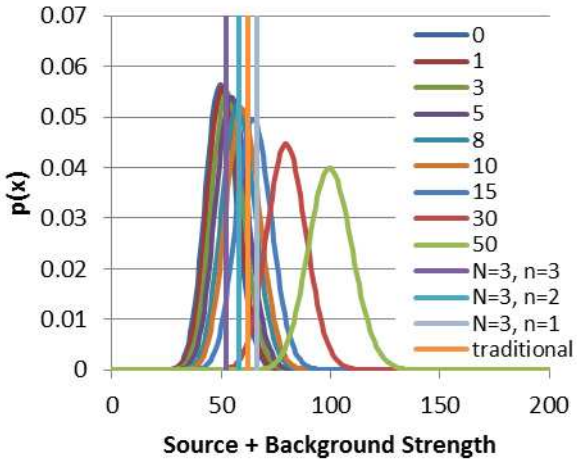

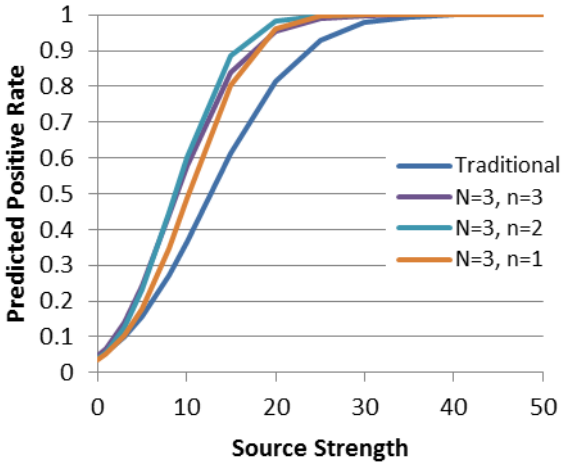

b=500

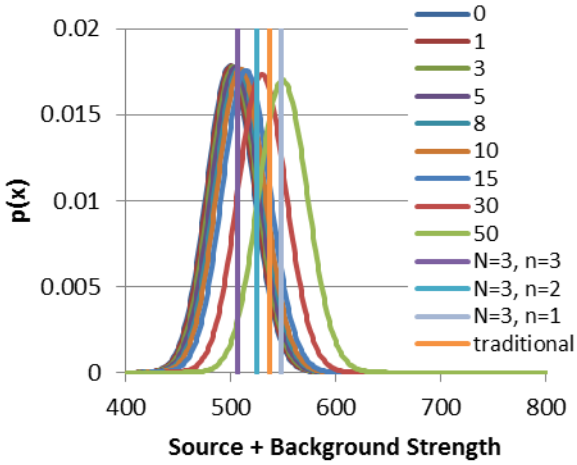

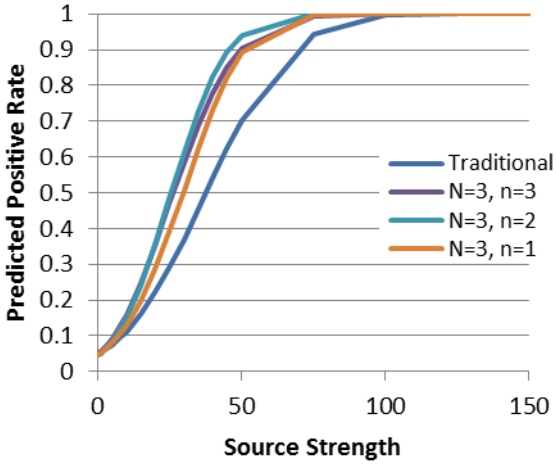

b=5000

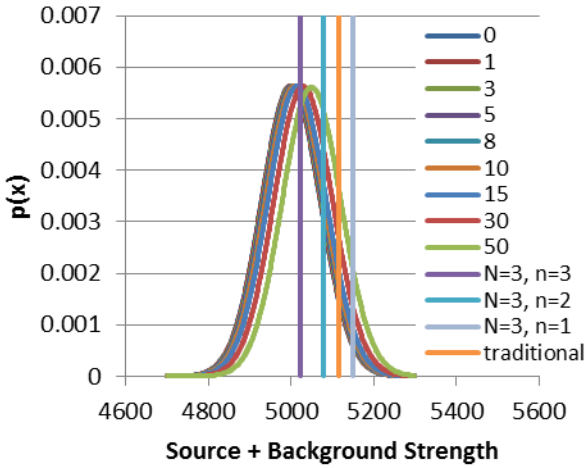

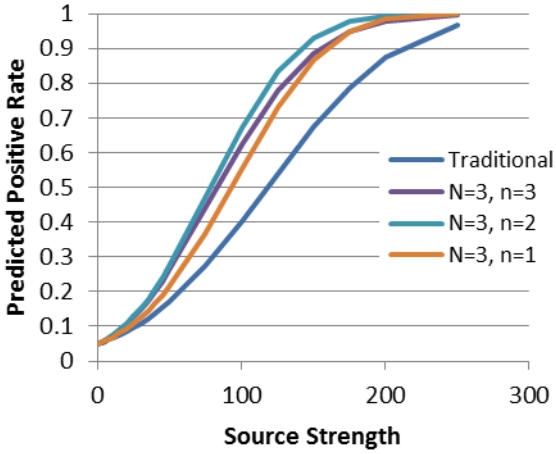

Figure 145 Positive Rate with Source Strength for Different Values of n and Constant b (Poisson, N=3, Deterministic)

N=4

b=50

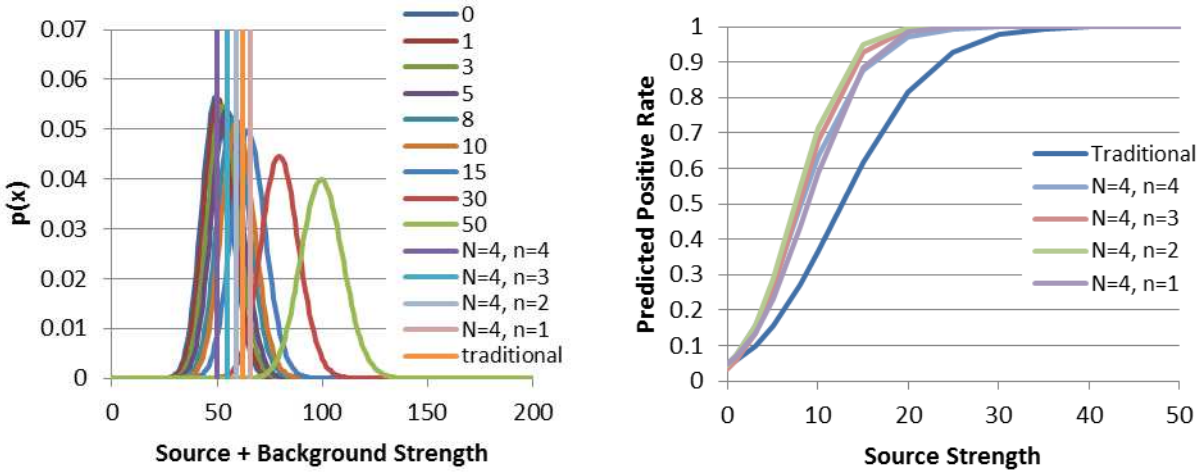

b=500

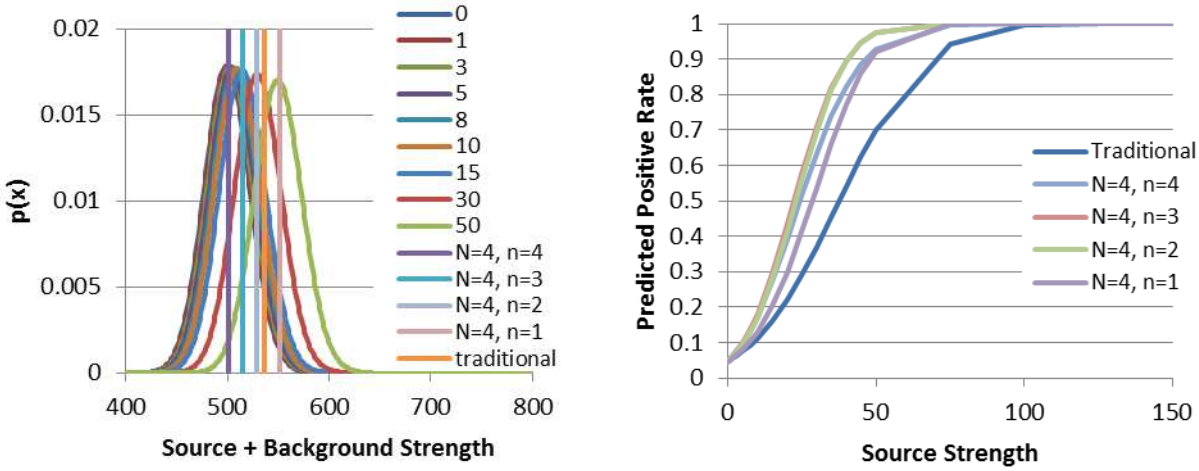

b=5000

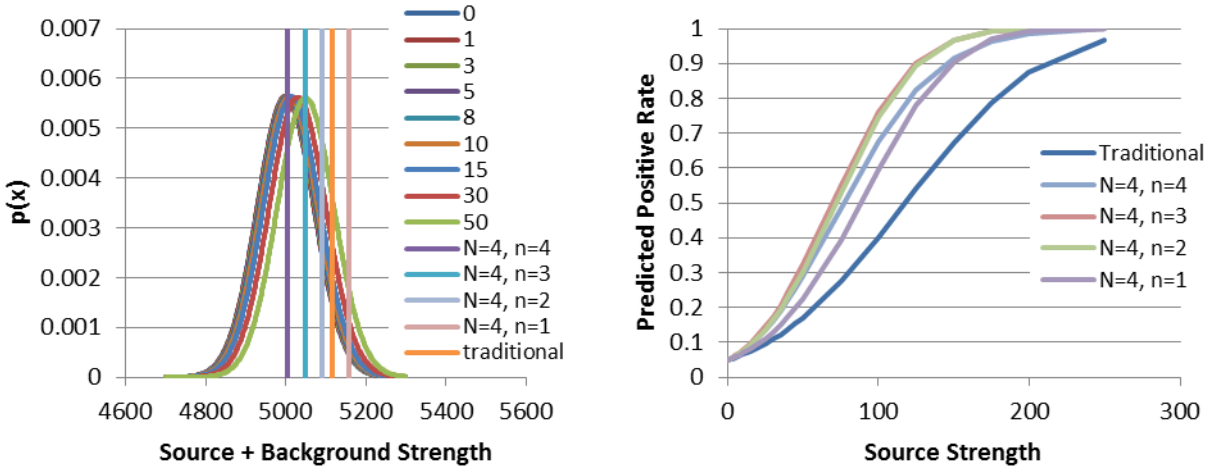

Figure 146 Positive Rate with Source Strength for Different Values of n and Constant b (Poisson, N=4, Deterministic)

N=5

b=50

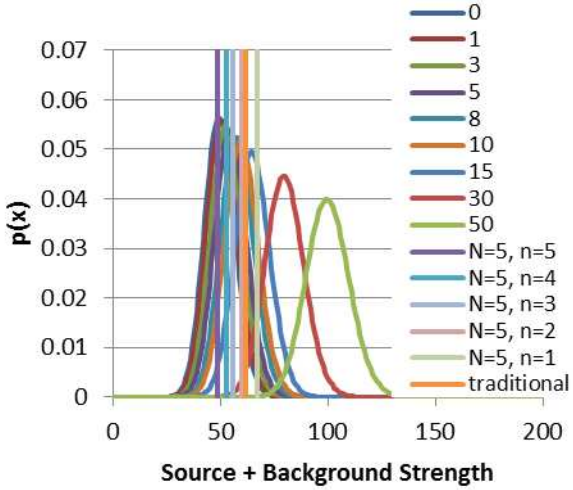

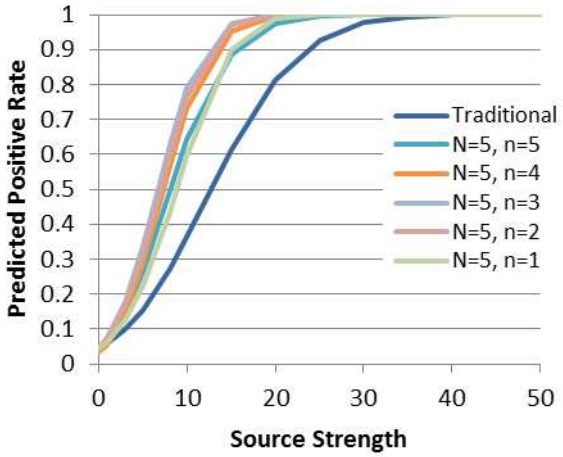

b=500

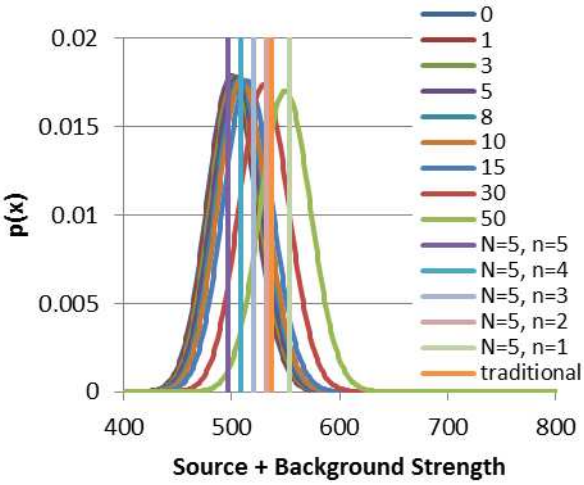

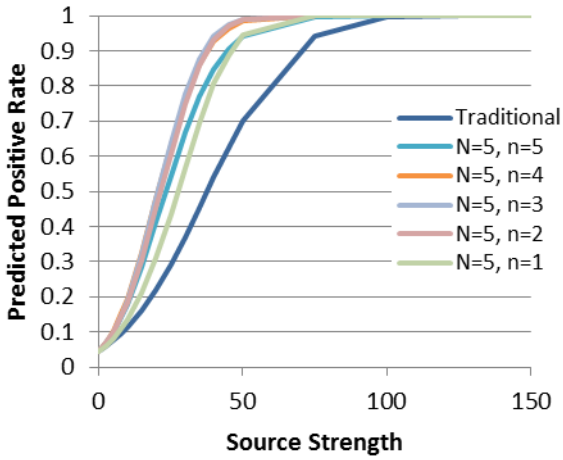

b=5000

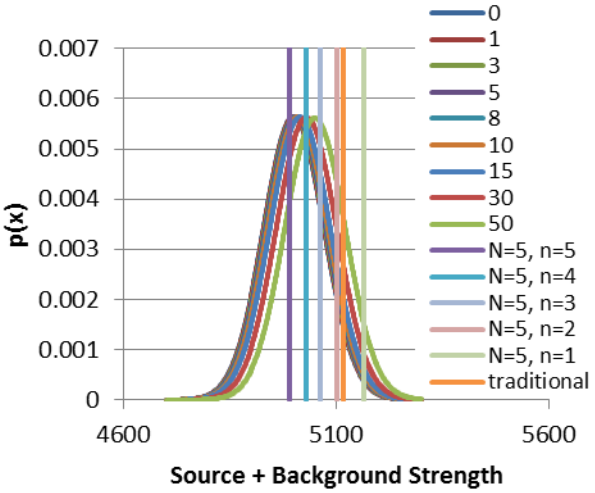

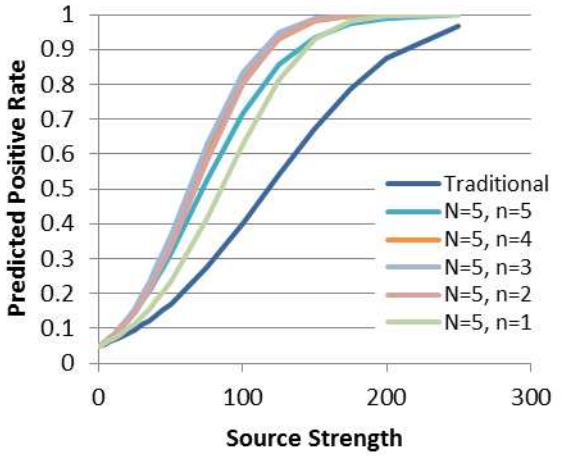

Figure 147 Positive Rate with Source Strength for Different Values of n and Constant b (Poisson, N=5, Deterministic)

Gaussian

Table 16 Calculated Values of y* at Backgrounds Strengths (Gaussian, Deterministic)

		Background Strength									
N	n	50	100	250	500	750	1000	2500	5000	7500	10000
1	1	62	116	277	537	795	1052	2582	5116	7642	10164
2	2	55	108	262	517	771	1024	2538	5054	7566	10076
	1	64	120	281	544	804	1062	2598	5138	7669	10195
3	3	52	103	255	508	759	1011	2517	5024	7529	10034
	2	58	111	267	525	780	1035	2555	5078	7595	10110
	1	65	121	284	547	808	1067	2606	5150	7684	10212
4	4	50	101	251	502	752	1002	2503	5005	7506	10007
	3	55	107	261	515	769	1021	2534	5048	7559	10068
	2	59	113	270	529	785	1041	2565	5092	7612	10130
	1	66	122	285	550	811	1071	2612	5158	7693	10223
5	5	49	99	248	497	747	996	2494	4991	7489	9988
	4	53	104	256	509	761	1013	2520	5029	7535	10041
	3	56	109	264	520	774	1028	2544	5062	7576	10088
	2	60	114	273	532	789	1045	2571	5101	7624	10143
	1	66	123	287	552	813	1073	2616	5164	7701	10232

Positive Rate

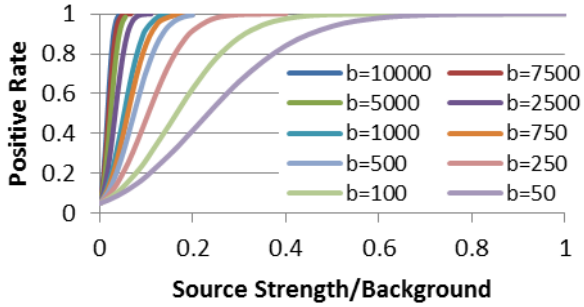

Figure 148 Positive Rate with Source Strength/Background with Different Values of b (Gaussian, Traditional, Deterministic)

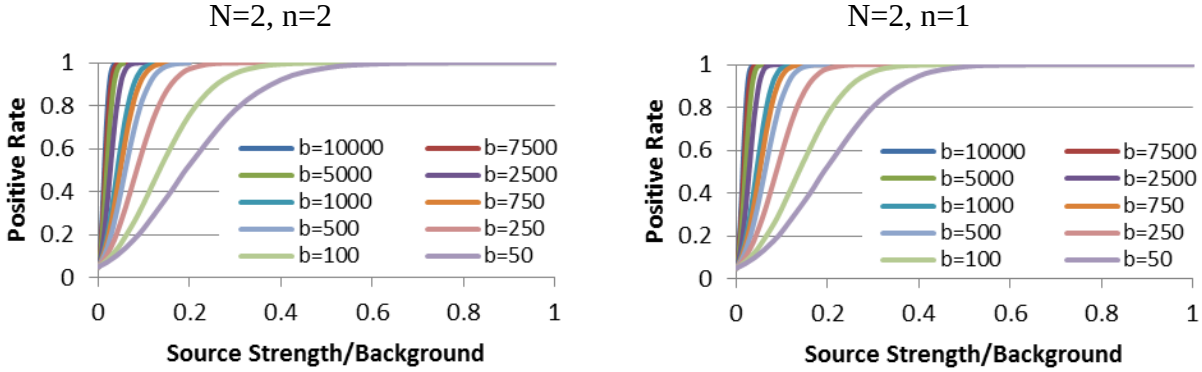

Figure 149 Positive Rate with Source Strength/Background with Different Values of n and b (Gaussian, N=2, Deterministic)

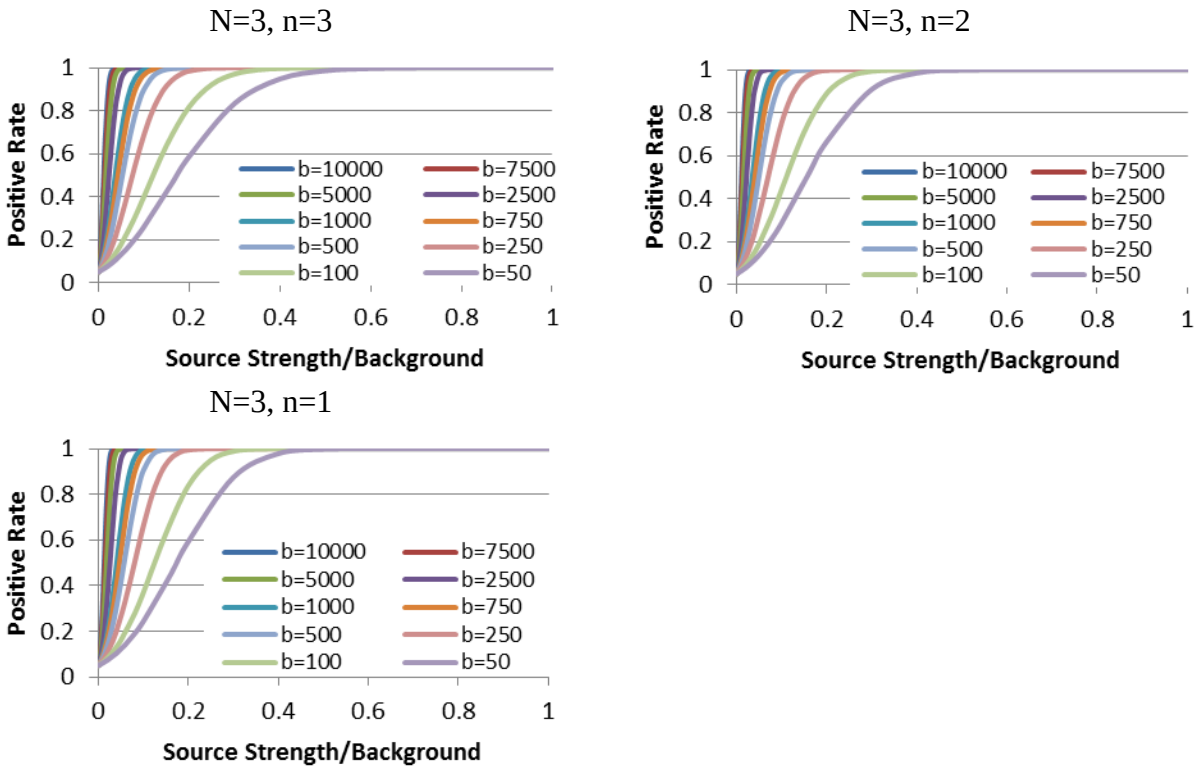

Figure 150 Positive Rate with Source Strength/Background with Different Values of n and b (Gaussian, N=3, Deterministic)

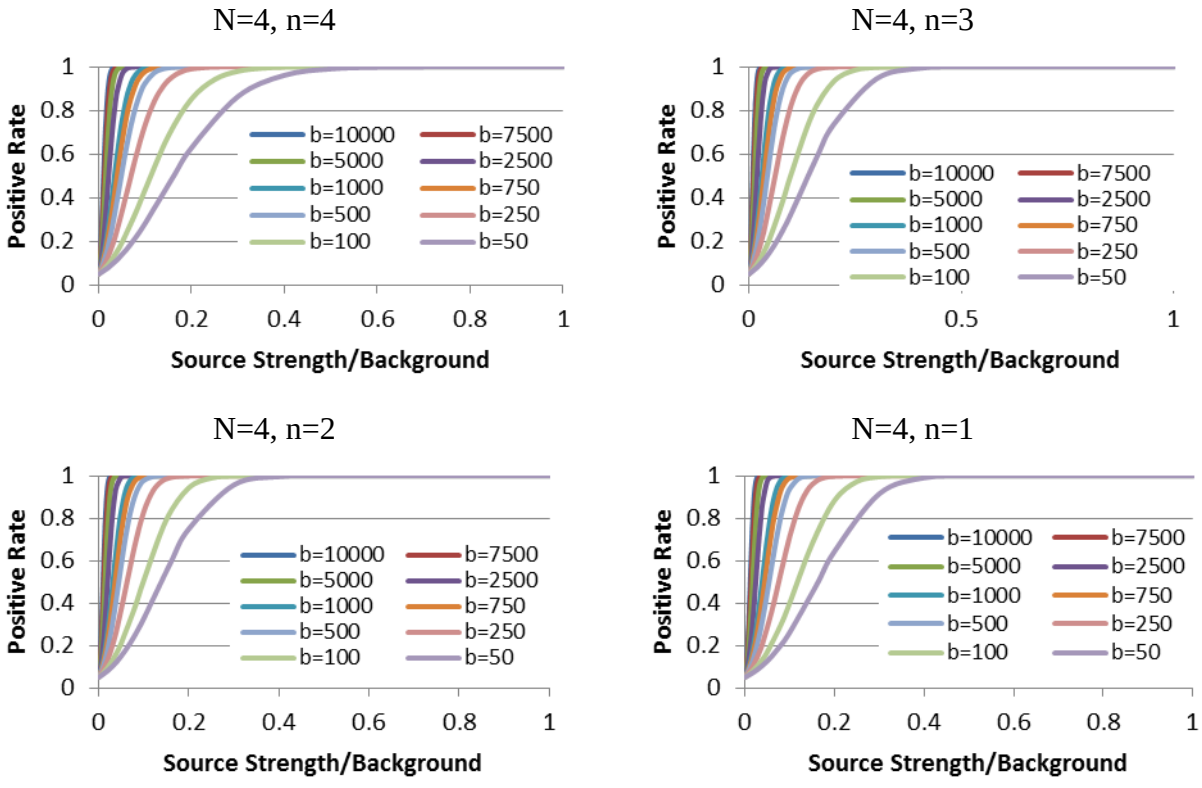

Figure 151 Positive Rate with Source Strength/Background with Different Values of n and b (Gaussian, N=4, Deterministic)

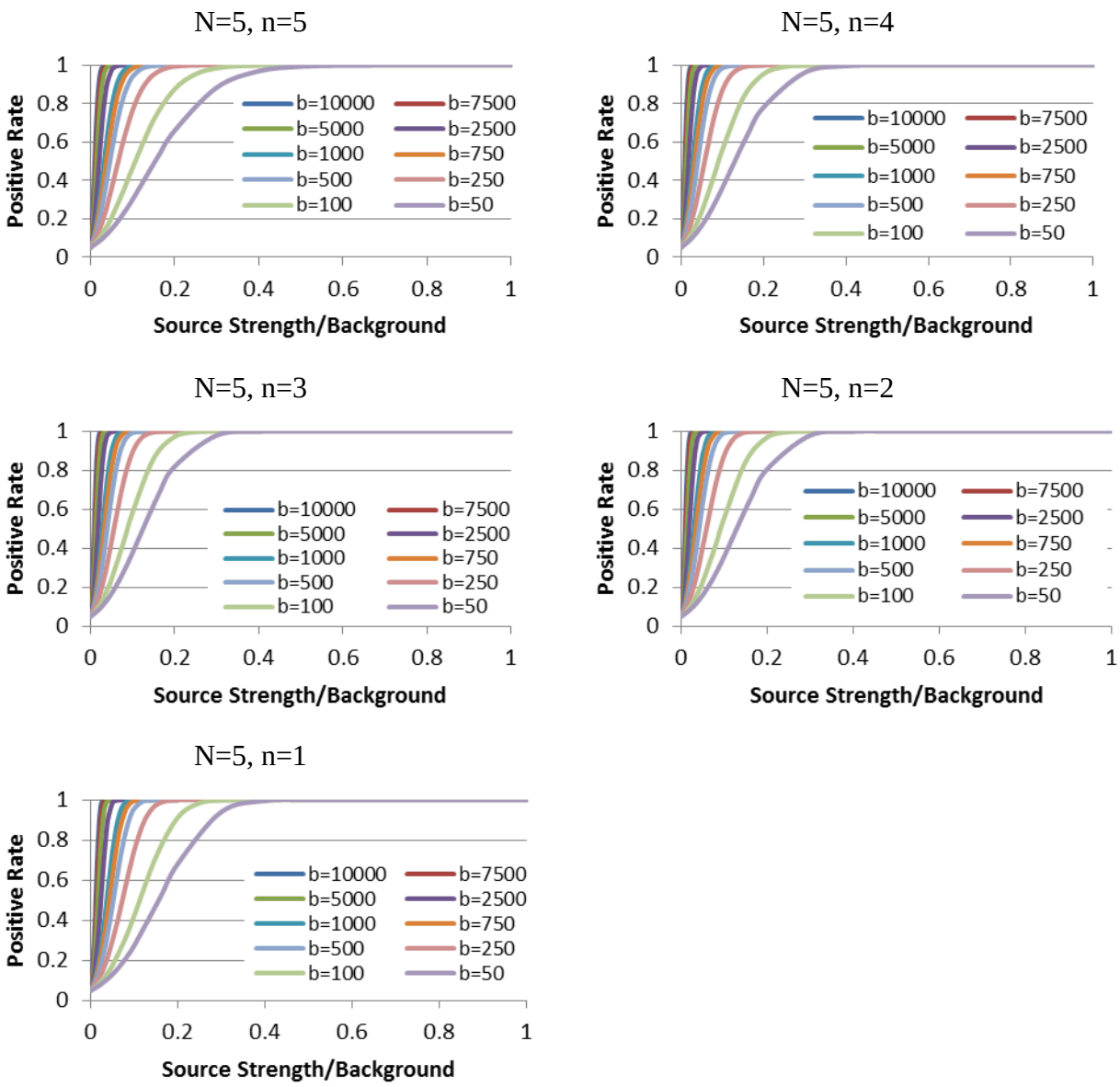

Figure 152 Positive Rate with Source Strength/Background with Different Values of n and b (Gaussian, N=5, Deterministic)

N=2

b=50

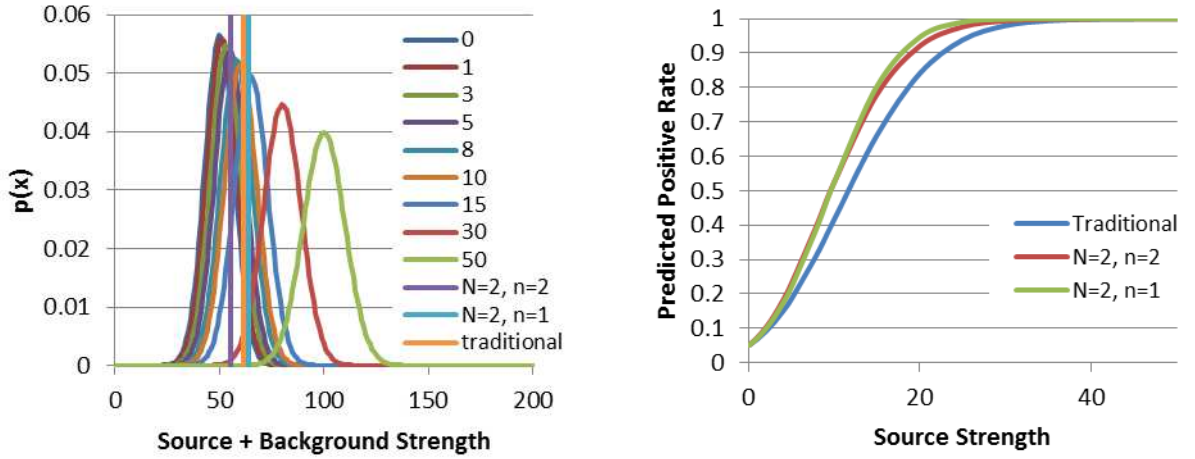

b=500

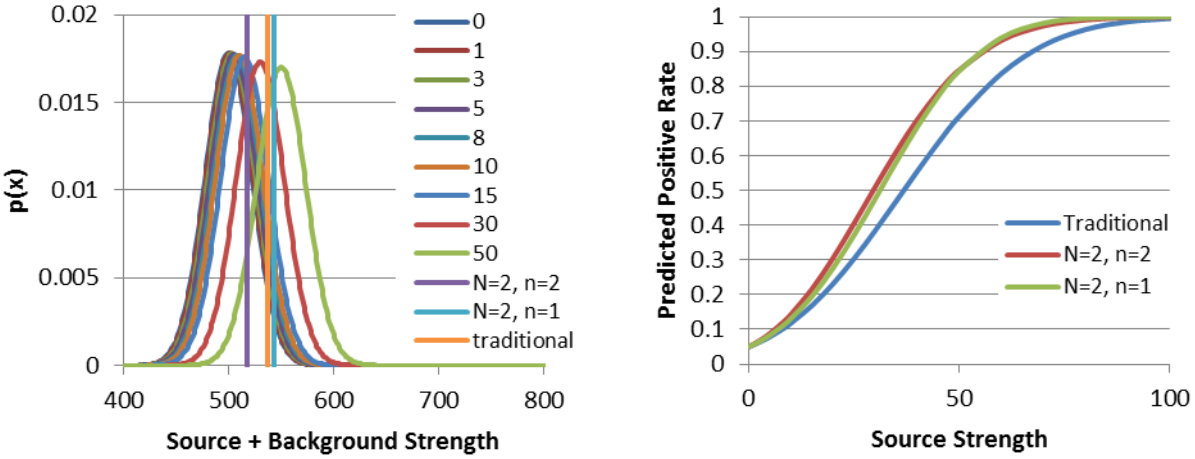

b=5000

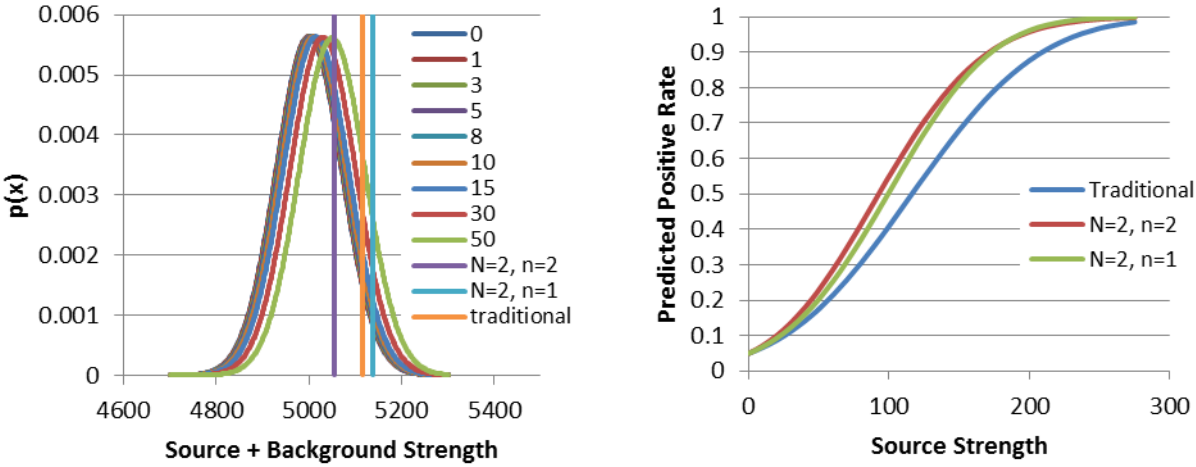

Figure 153 Positive Rate with Source Strength for Different Values of n and Constant b (Gaussian, N=2, Deterministic)

N=3

b=50

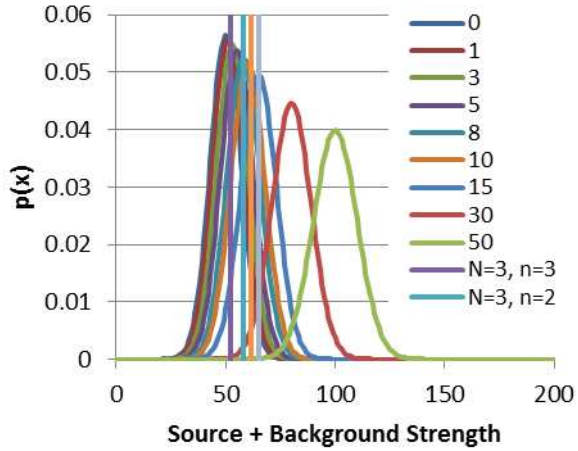

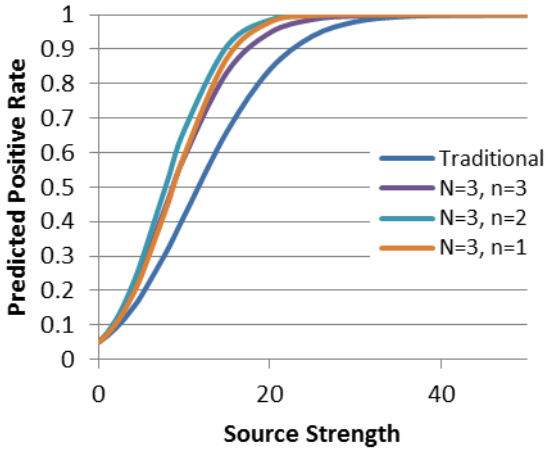

b=500

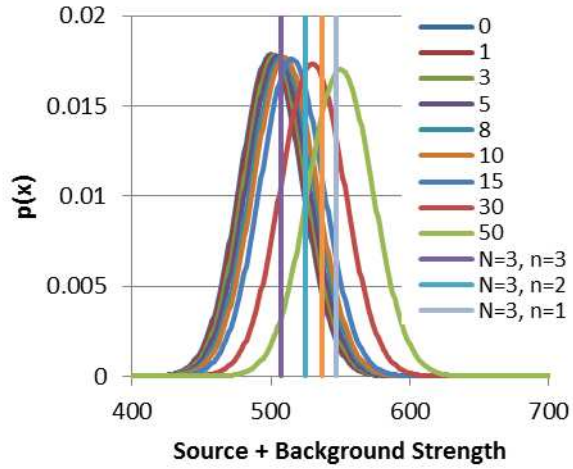

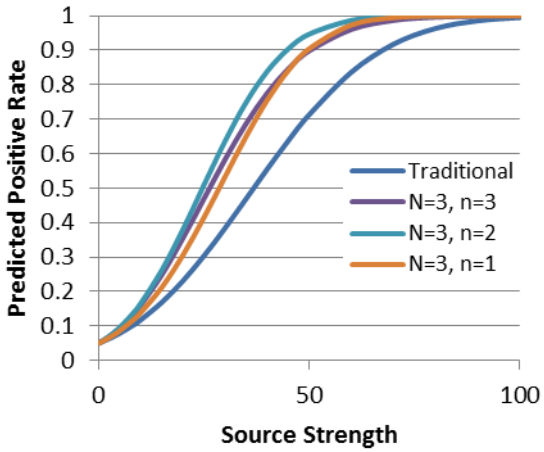

b=5000

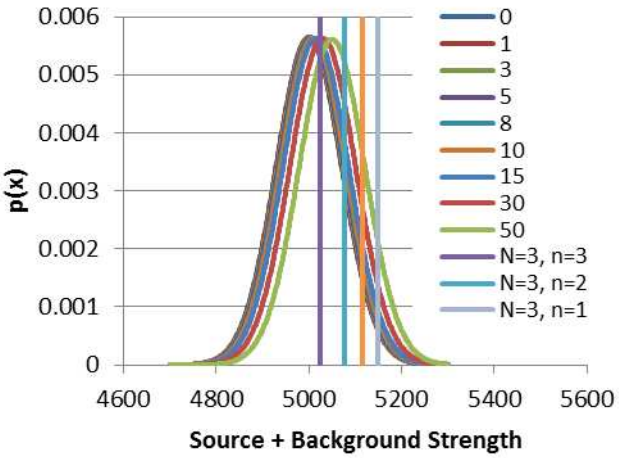

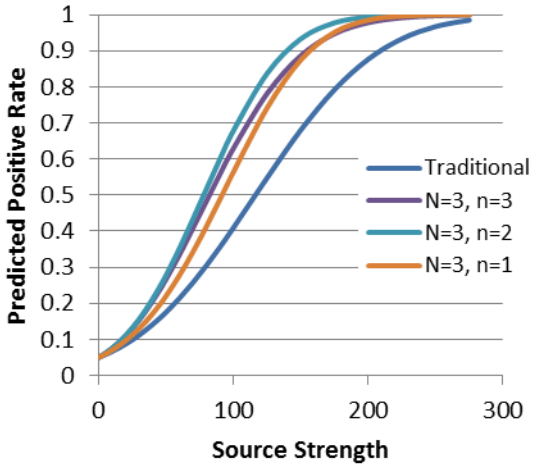

Figure 154 Positive Rate with Source Strength for Different Values of n and Constant b (Gaussian, N=3, Deterministic)

N=4

b=50

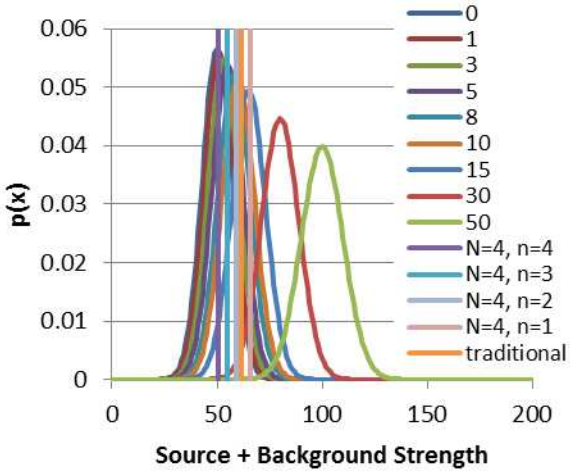

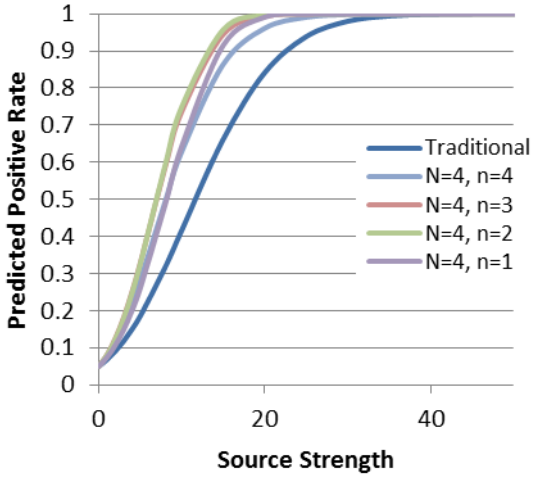

b=500

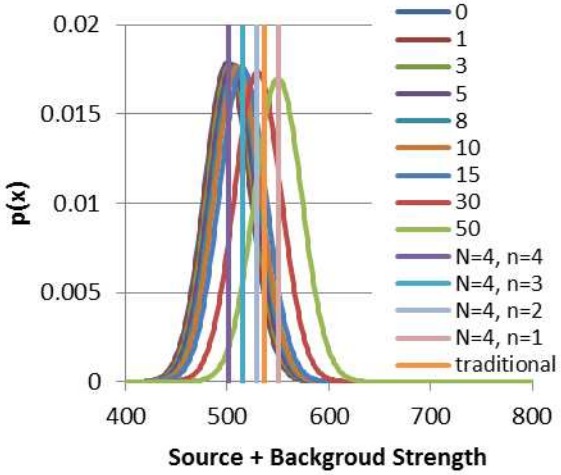

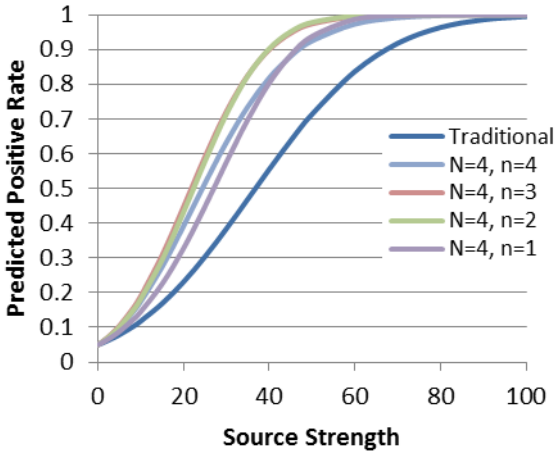

b=5000

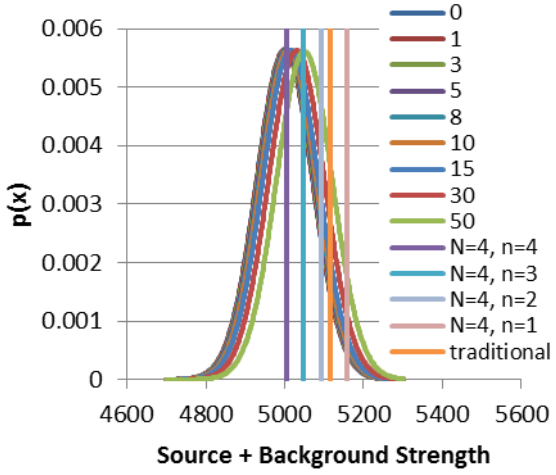

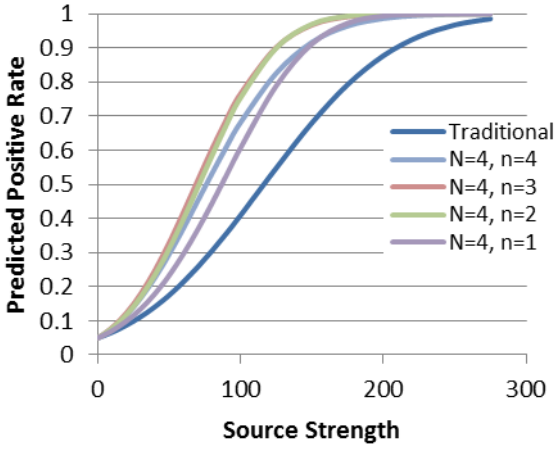

Figure 155 Positive Rate with Source Strength for Different Values of n and Constant b (Gaussian, N=4, Deterministic)

N=5

b=50

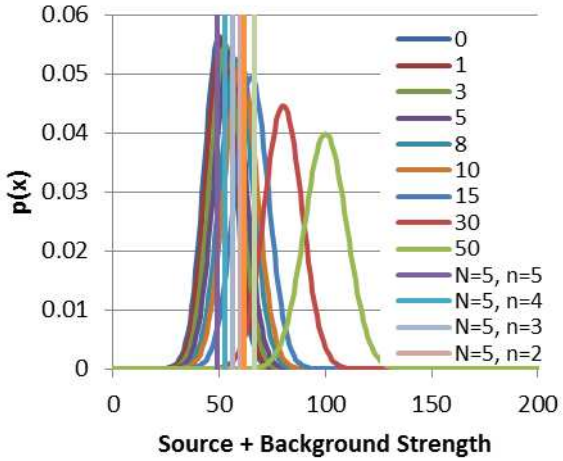

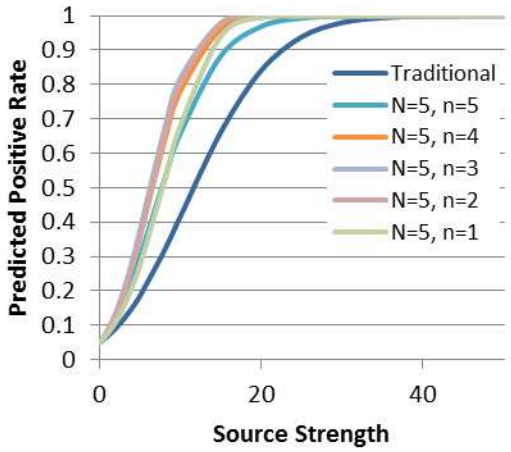

b=500

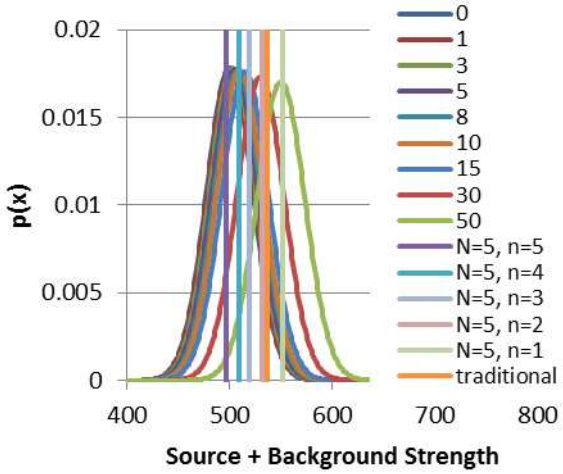

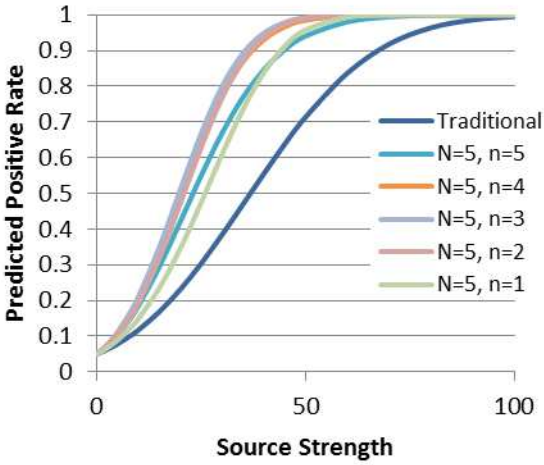

b=5000

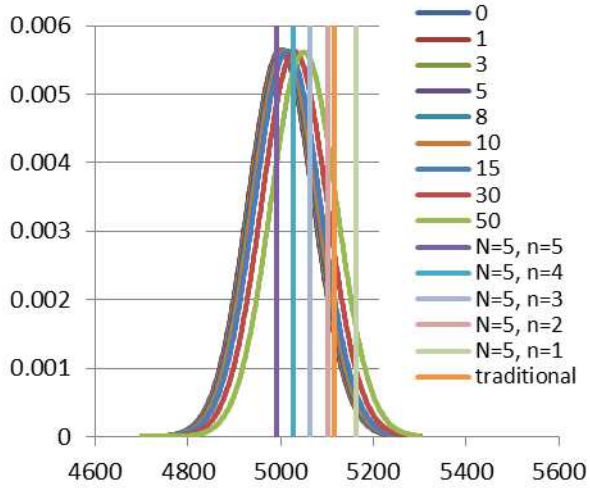

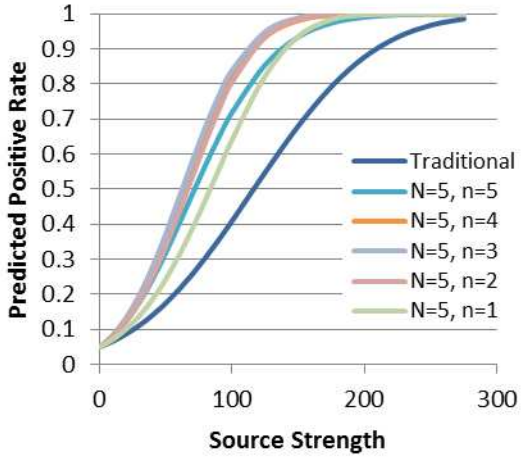

Figure 156 Positive Rate with Source Strength for Different Values of n and Constant b (Gaussian, N=5, Deterministic)

APPENDIX B

Stochastic

At Least v. Exact

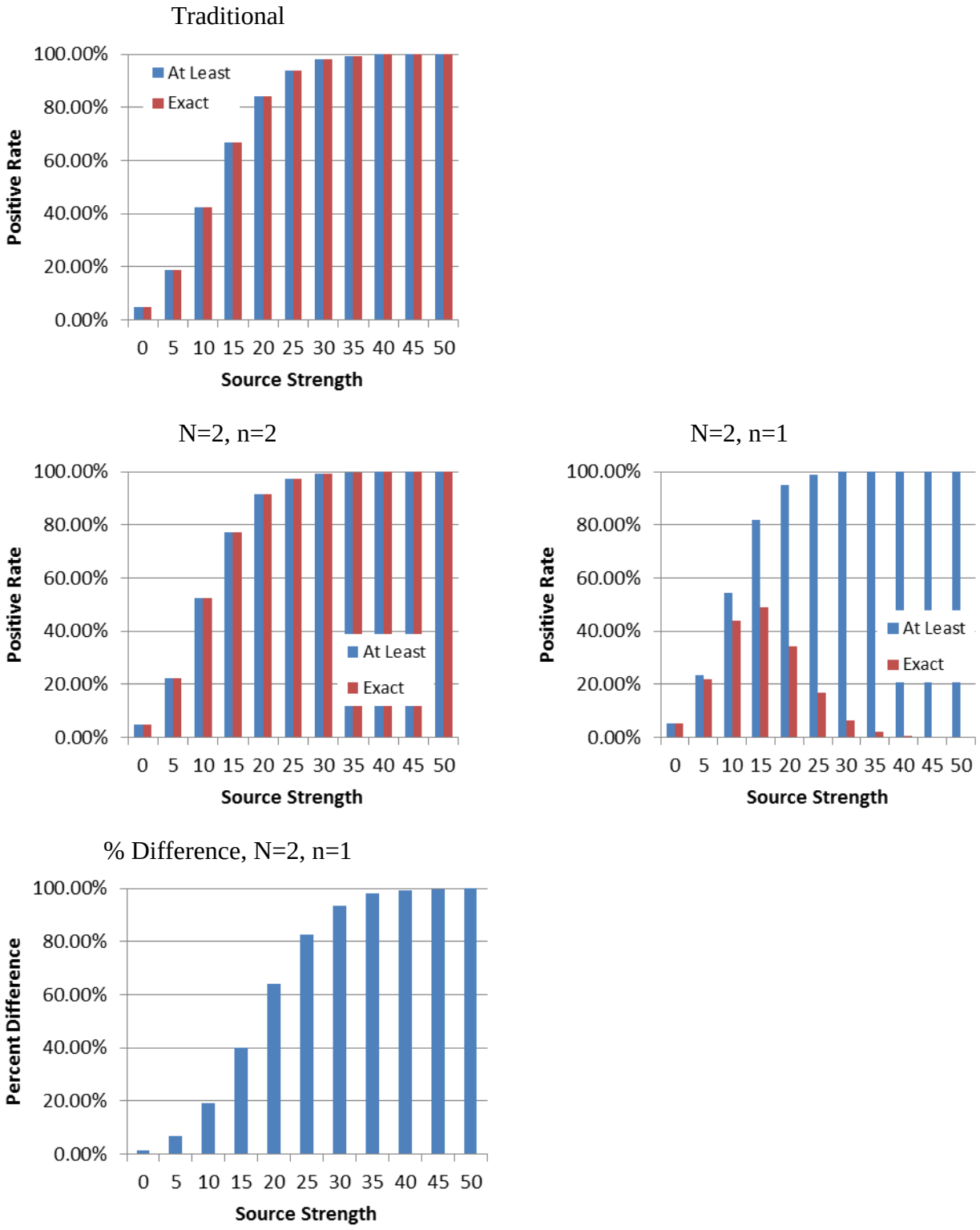

Figure 157 Positive Rate with Source Strength Comparison of Exact and At Least Conditions for Different n Values (Gaussian, N=2, b=500, Stochastic)

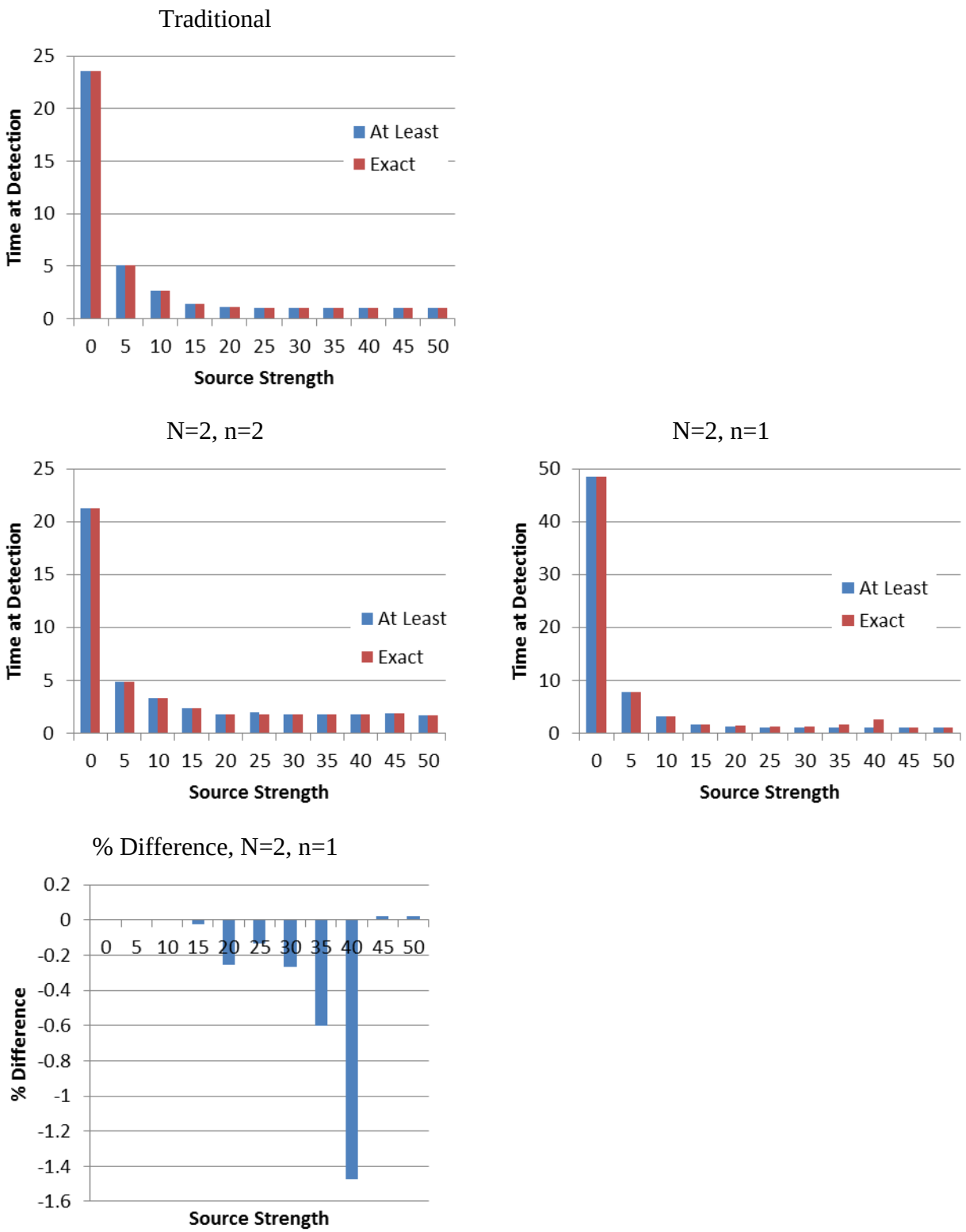

Figure 158 Time at First Detection with Source Strength Comparison of Exact and At Least Conditions for Different n Values (Gaussian, N=2, b=500, Stochastic)

Distribution of Positive and Time at First Detection

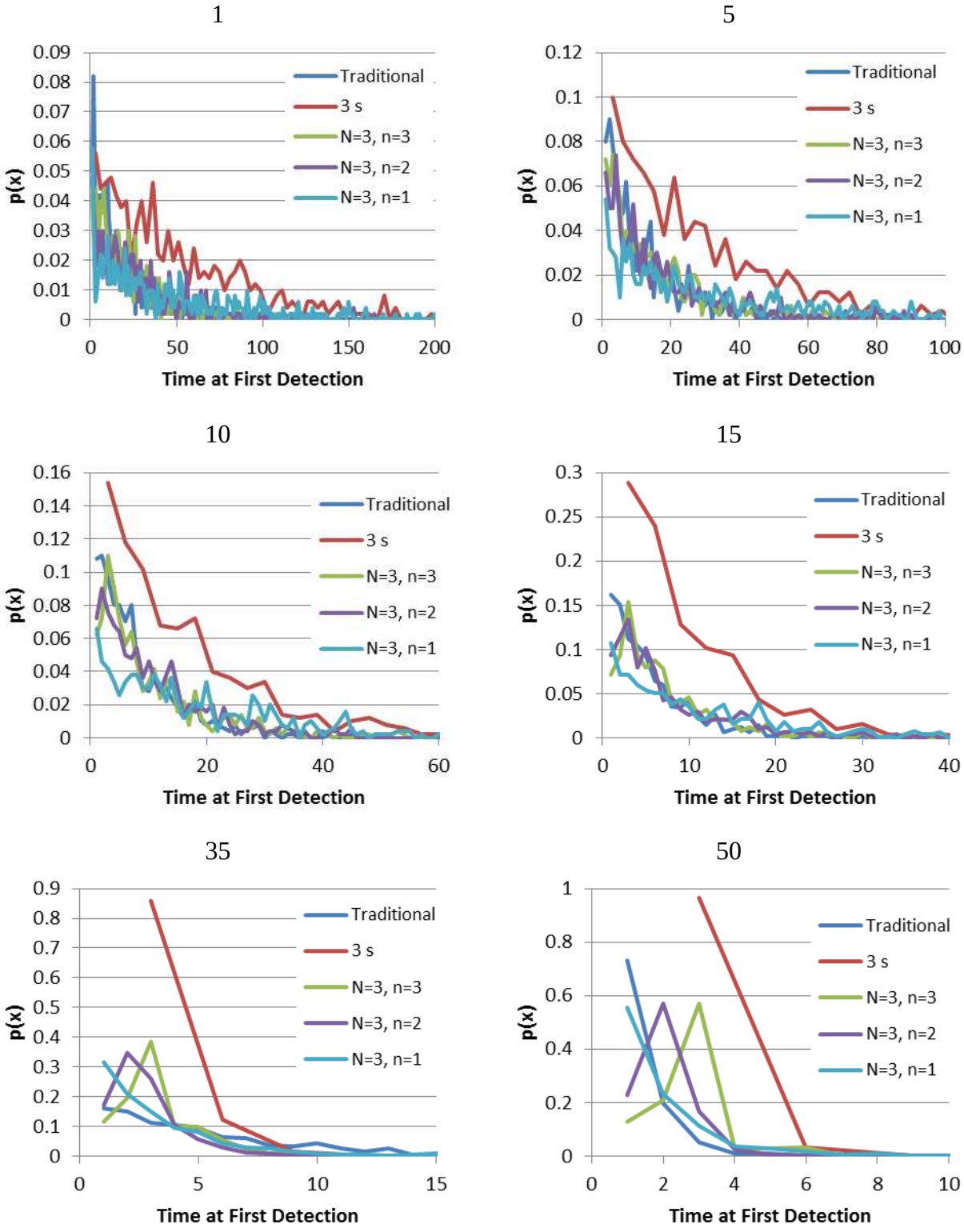

Figure 159 Probability Density Function for Time at First Detection for Different Source Strengths (Gaussian, N=3, b=500, Stochastic)

Traditional

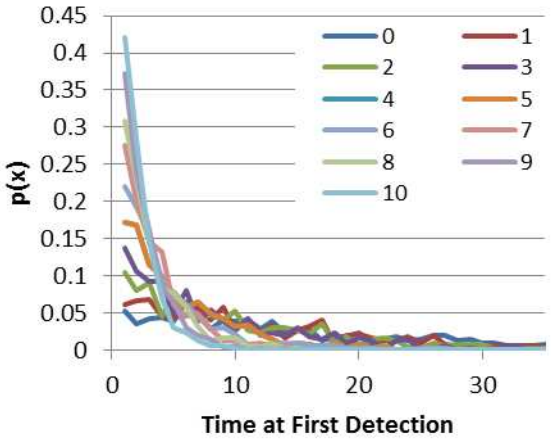

3 s

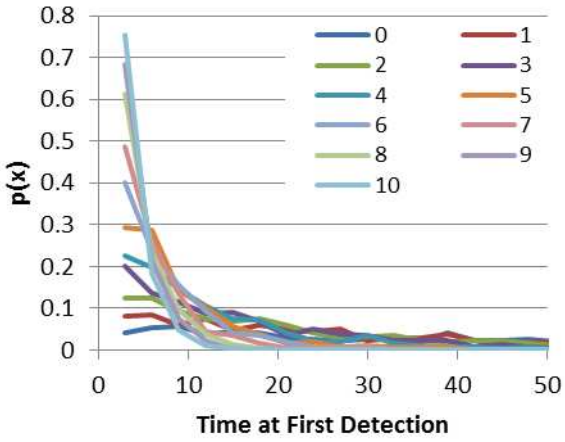

N=3, n=3

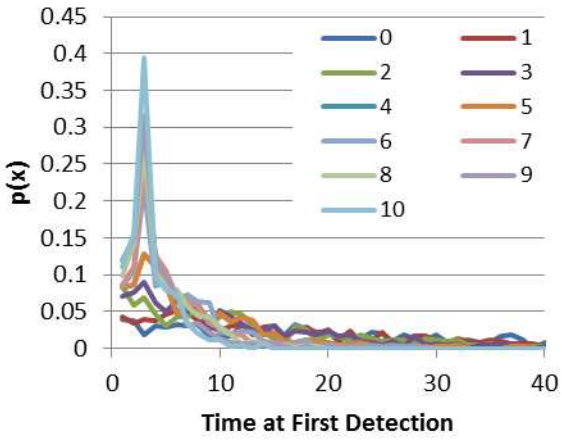

N=3, n=2

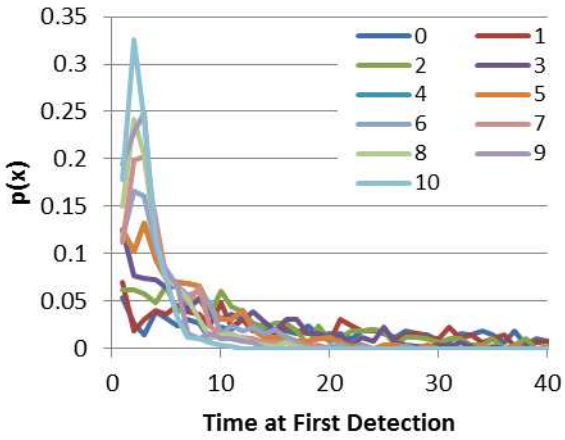

N=3, n=1

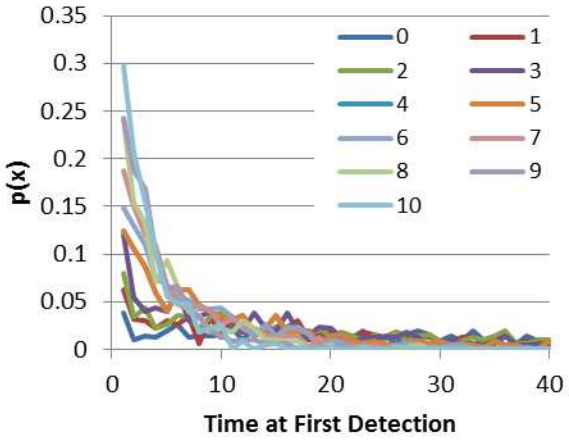

Figure 160 Probaility Density Function for Time at First Detection for Different n Values (Gaussian, N=3, b=500, Stochastic)

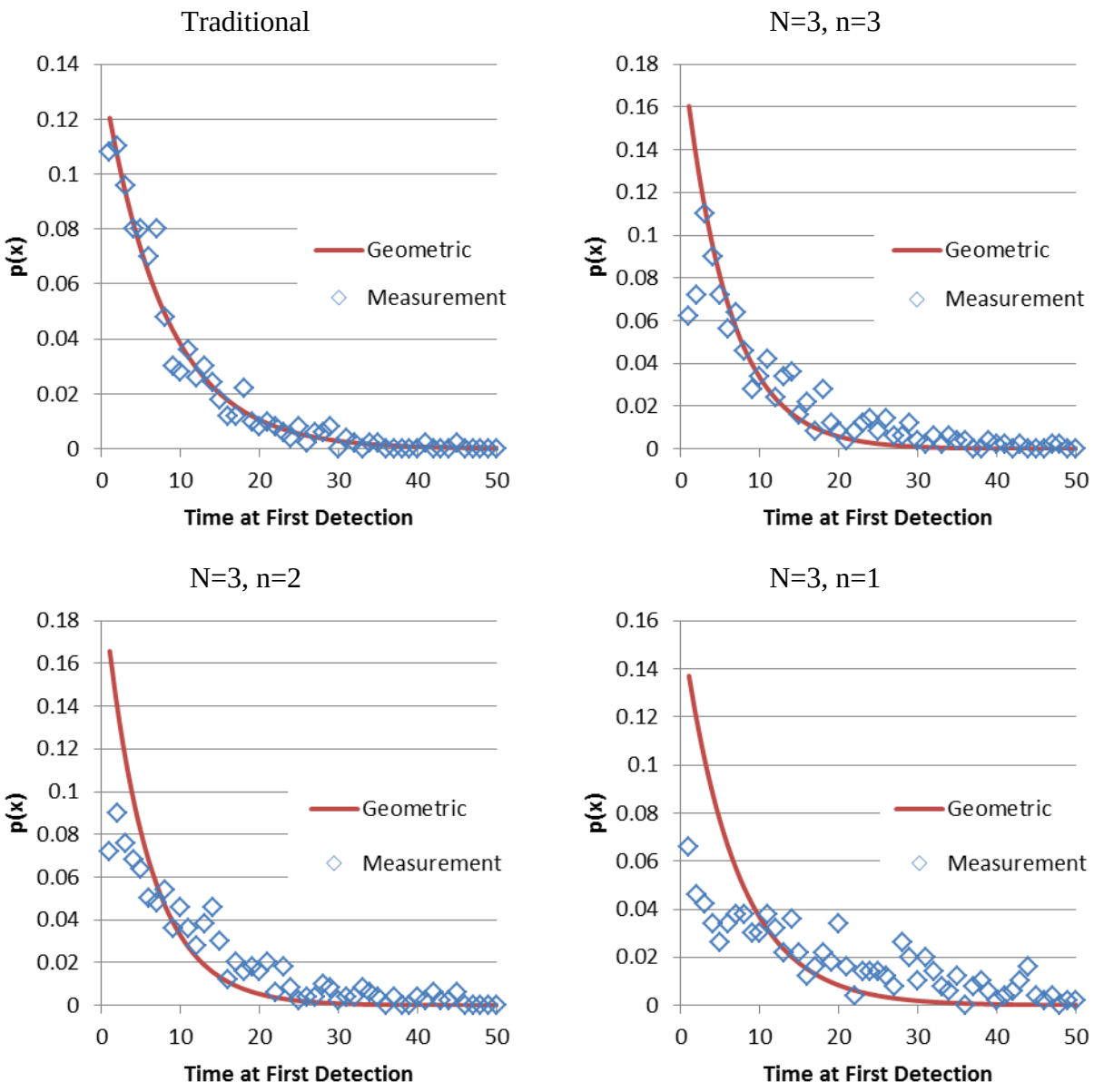

Figure 161 Probability Density Function Comparison for Time at First Detection between Measurement and Geometric Distribution (Gaussian, N=3, b=500, Stochastic)

Uniform

Comparison of Measurement Simulation Techniques

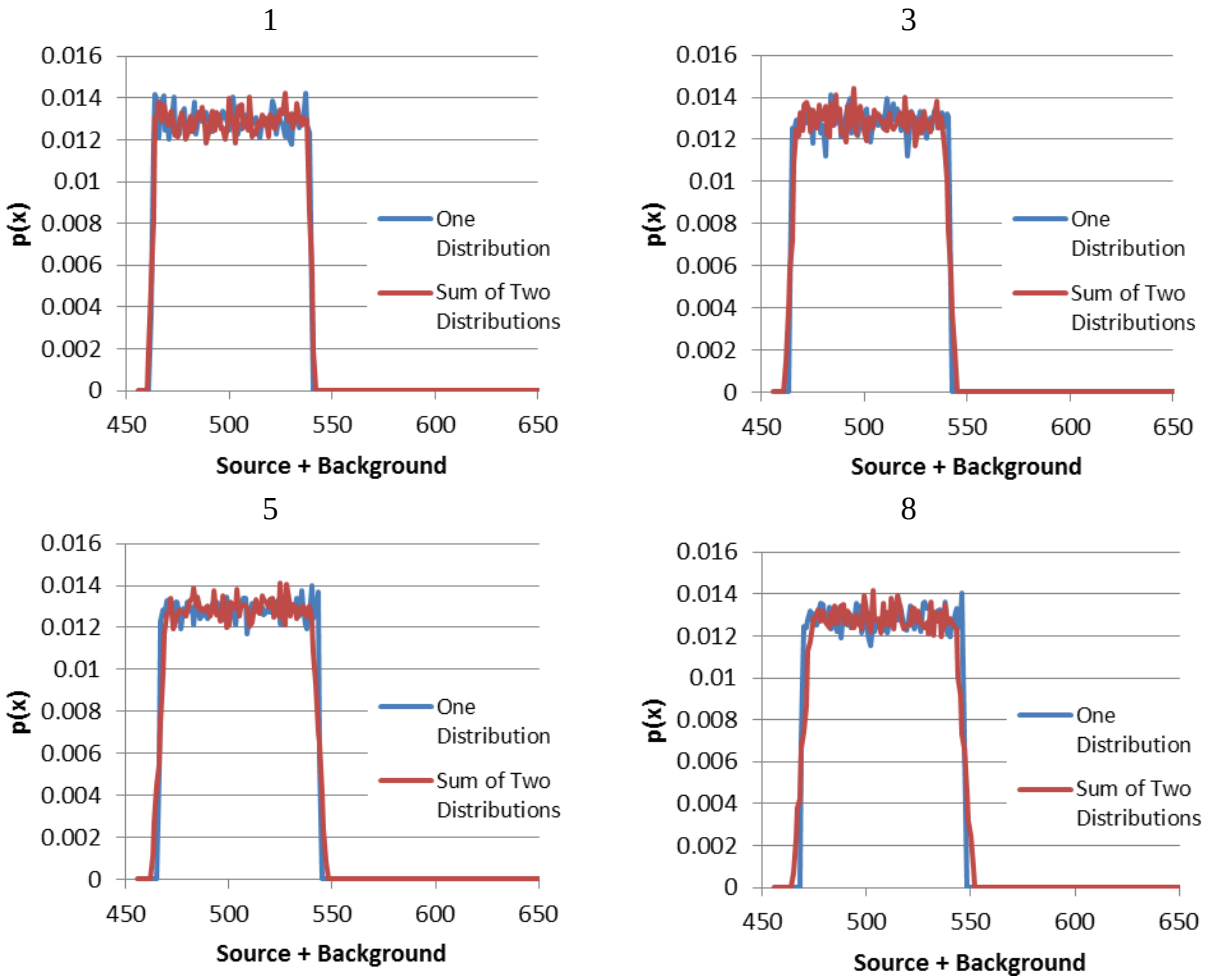

Figure 162 Probability Density Function Comparison for Two Measurement Simulation Techniques for Different Source Strengths (Rectangular, b=500, s=1, 3, 5, 8, Stochastic)

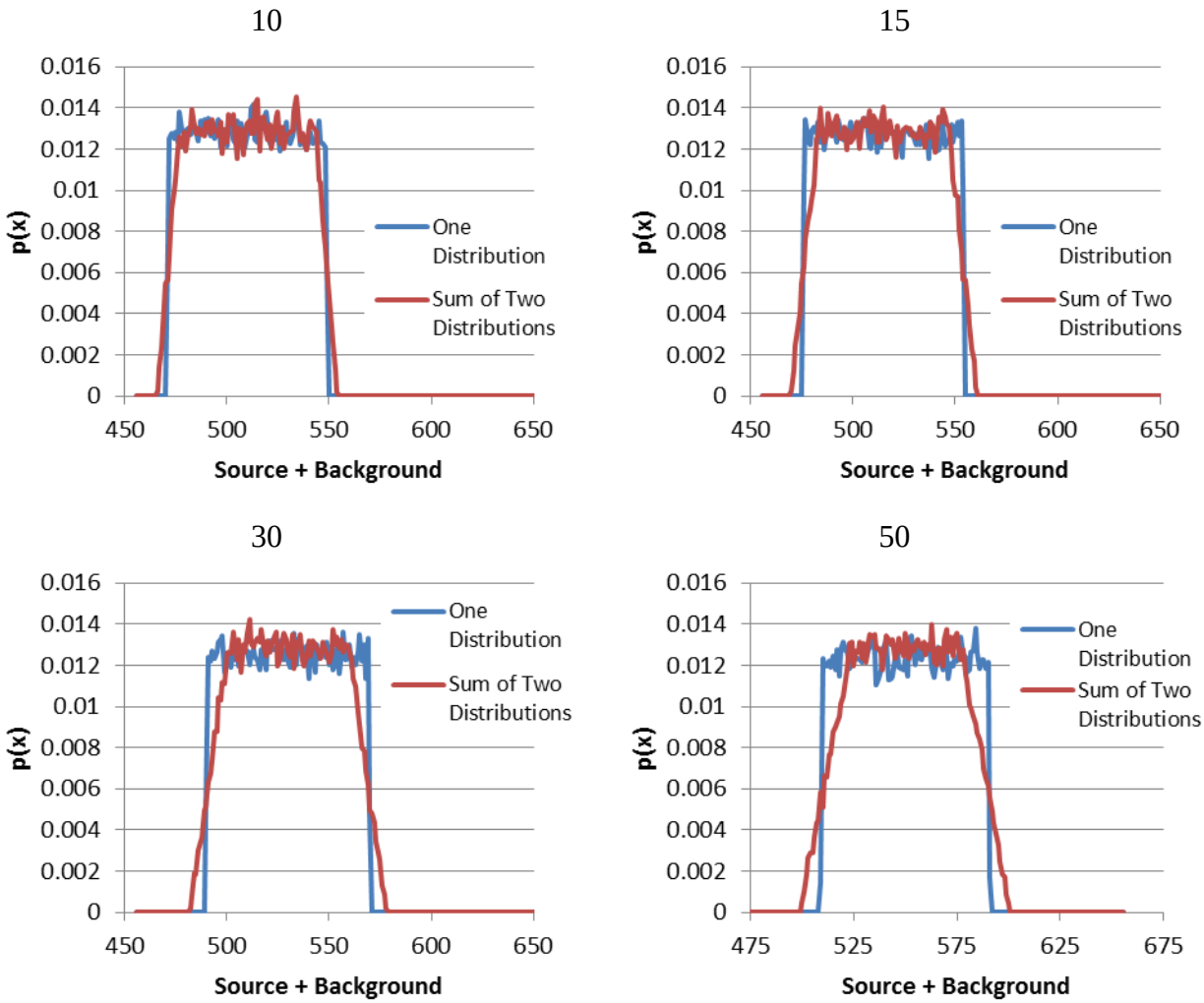

Figure 163 Probability Density Function Comparison for Two Measurement Simulation Techniques for Different Source Strengths (Rectangular, b=500, s=10, 15, 30, 50, Stochastic)

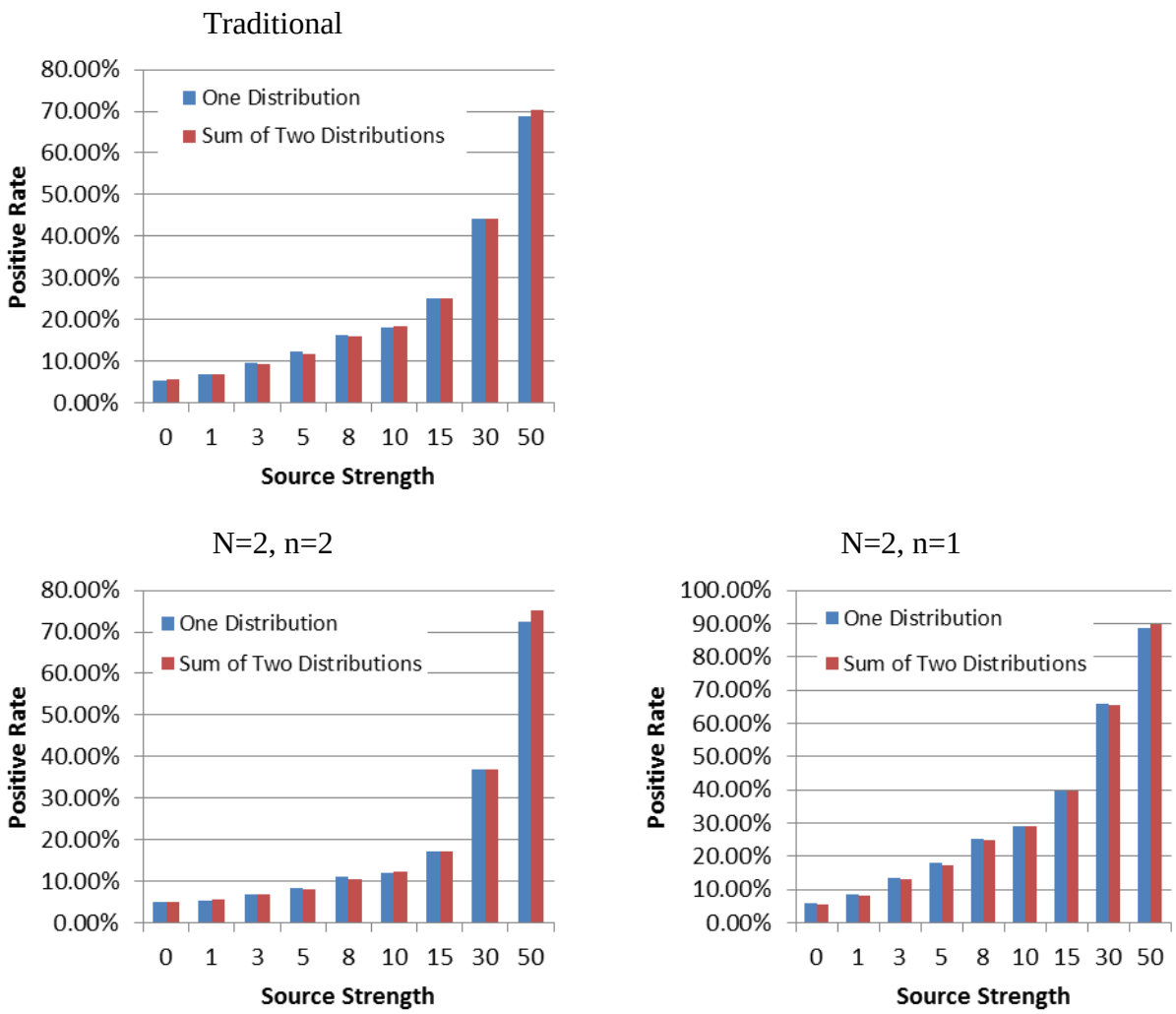

Figure 164 Positive Rate with Source Strength Comparison for Two Measurement Simulation Techniques (Rectangular, b=500, Stochastic)

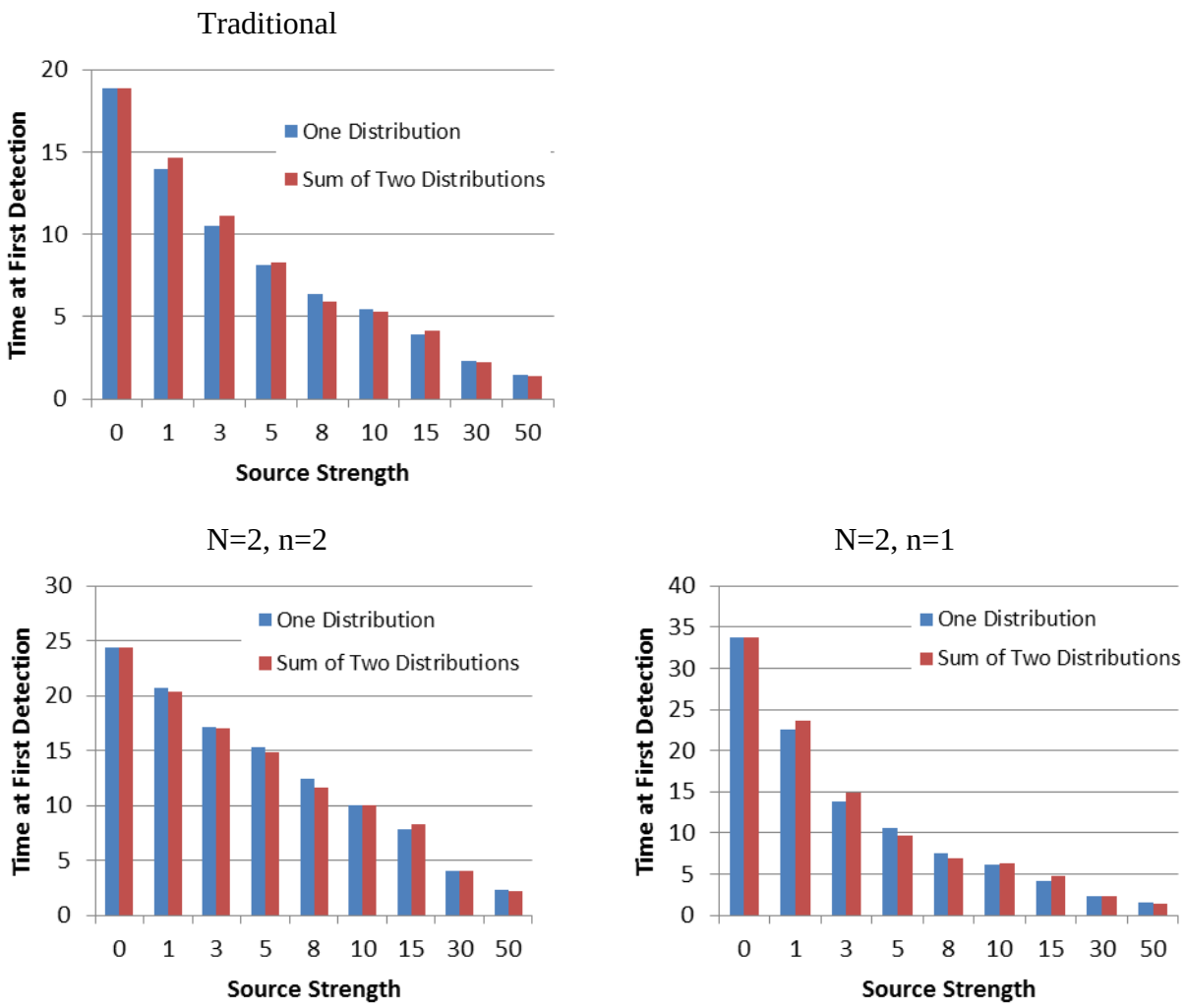

Figure 165 Time at First Detection with Source Strength Comparison for Two Measurement Simulation Techniques (Rectangular, b=500, Stochastic)

Positive Rate

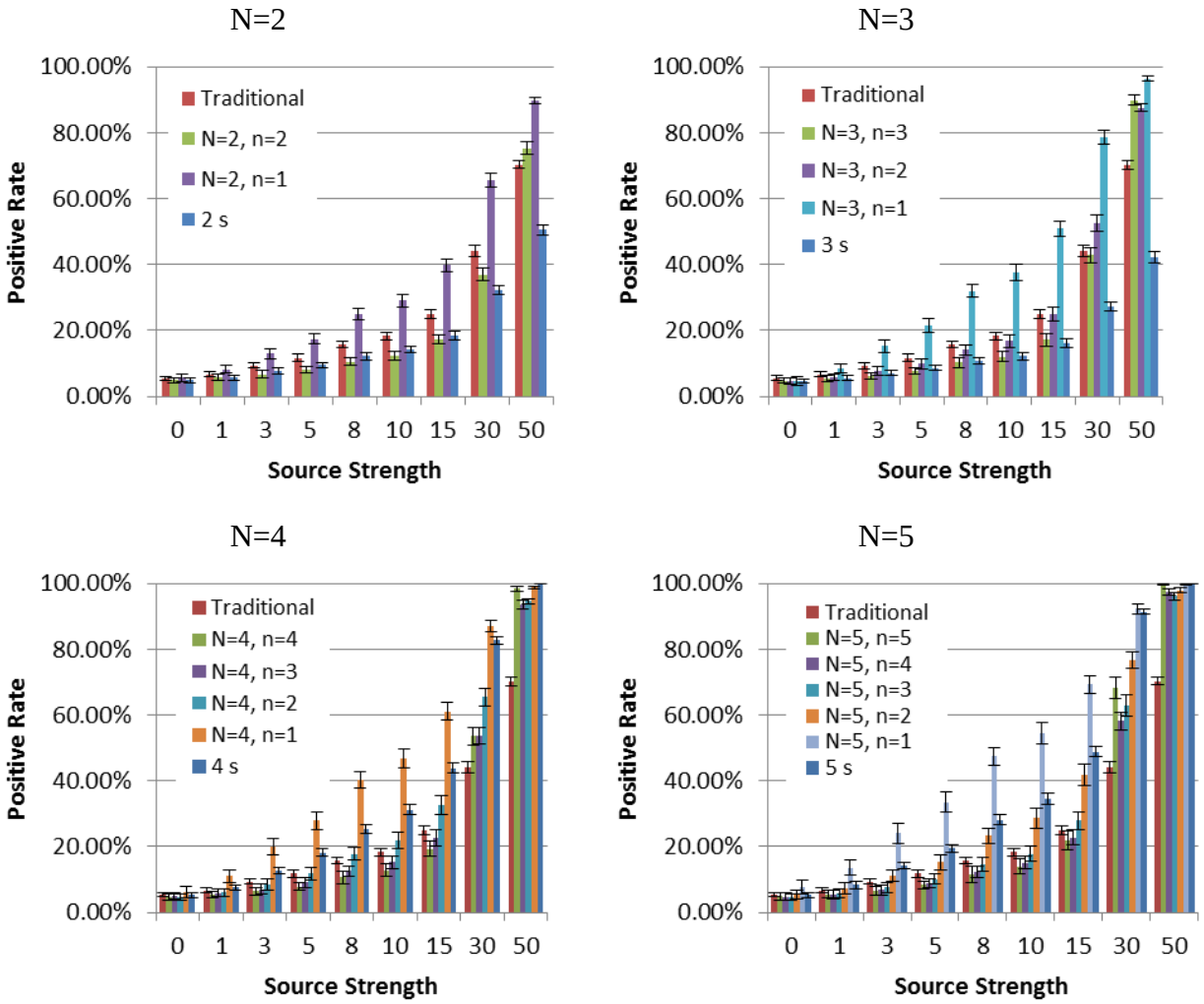

Figure 166 Positive Rate with Source Strength for Different n and N Values (Rectangular, b=500, Stochastic)

Time at First Detection

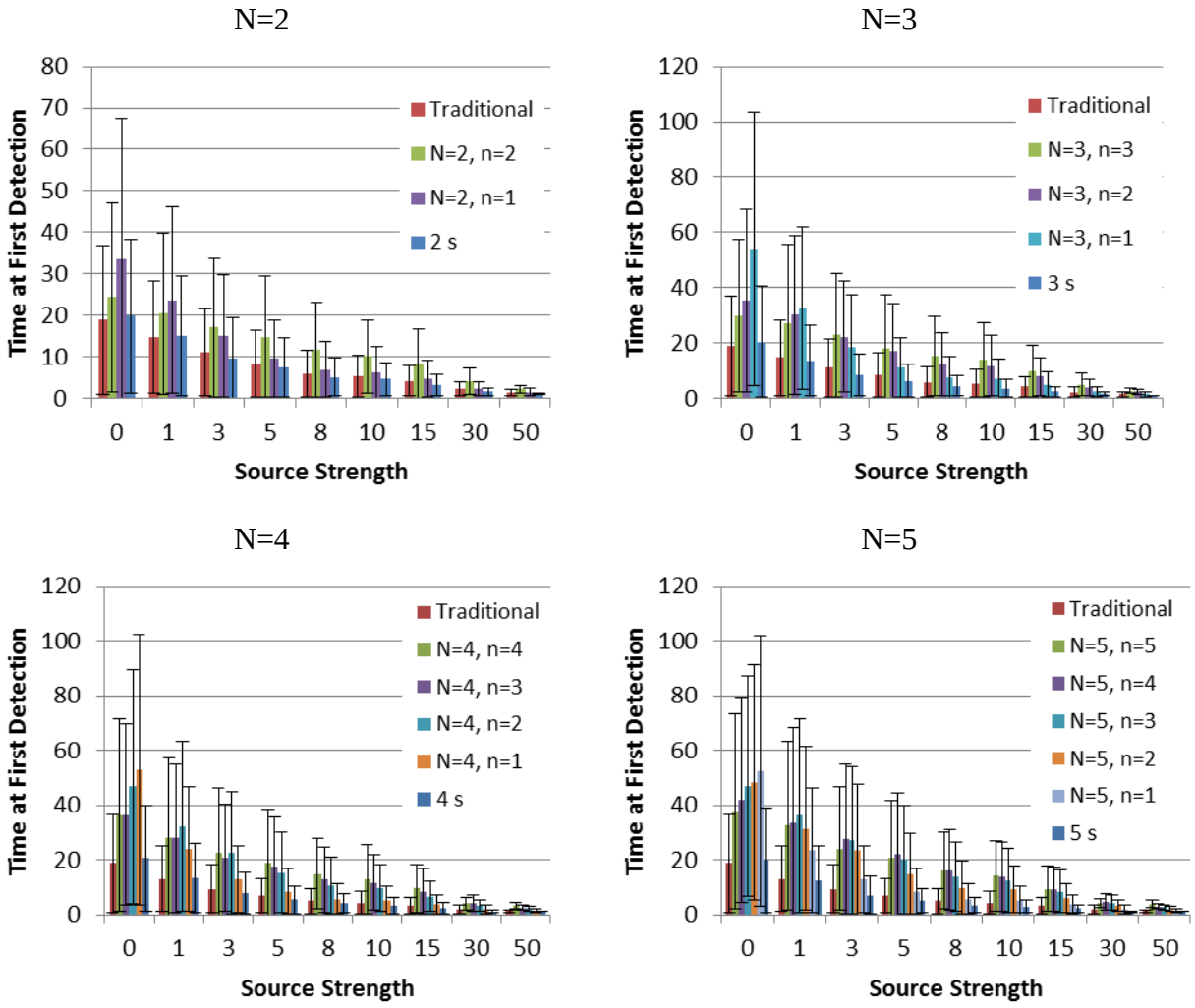

Figure 167 Time at First Detection with Source Strength for Different n and N Values (Rectangular, b=500, Stochastic)

Triangular

Comparison of Measurement Simulation Techniques

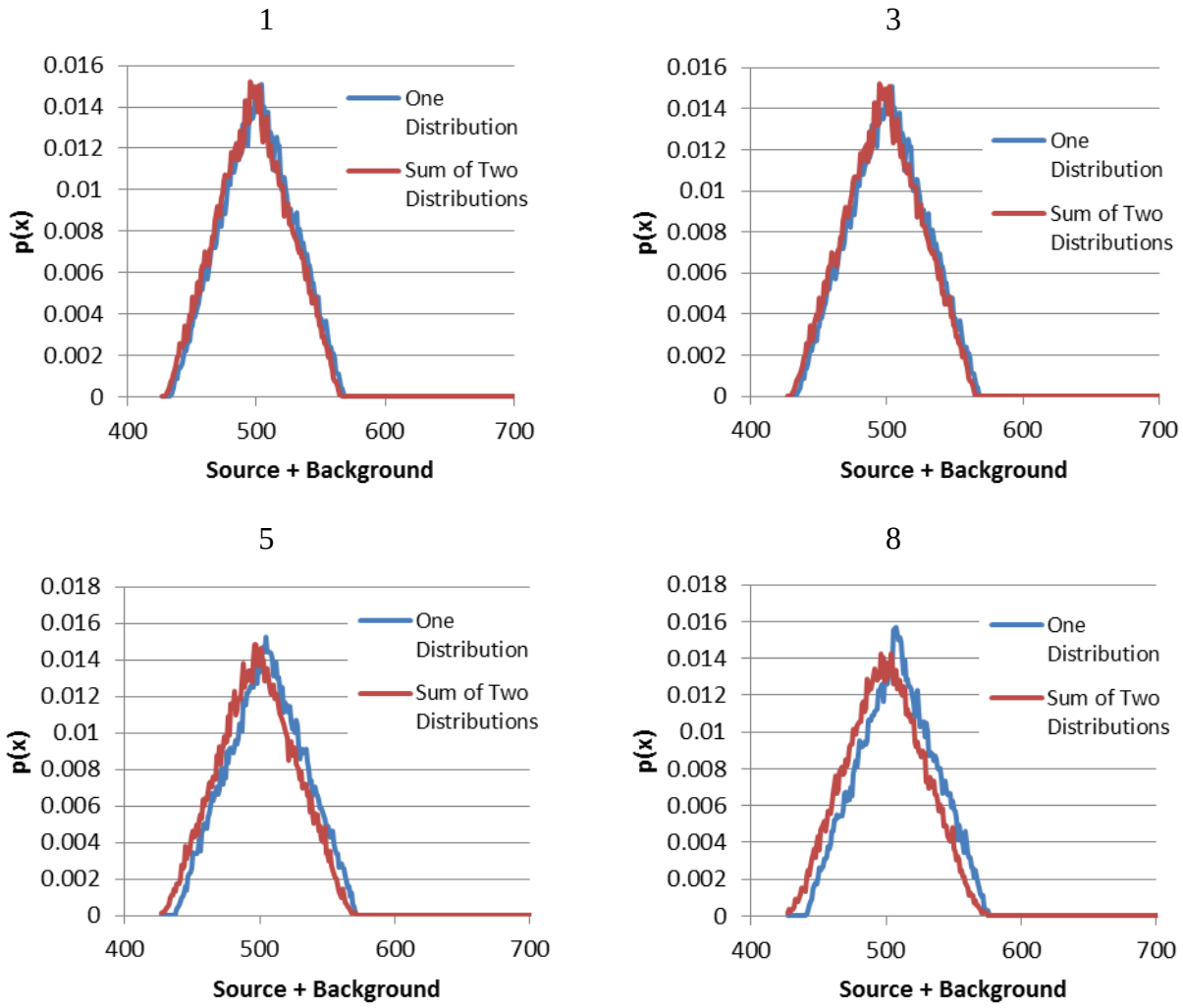

Figure 168 Probability Density Function Comparison for Two Measurement Simulation Techniques for Different Source Strengths (Triangular, b=500, s=1, 3, 5, 8, Stochastic)

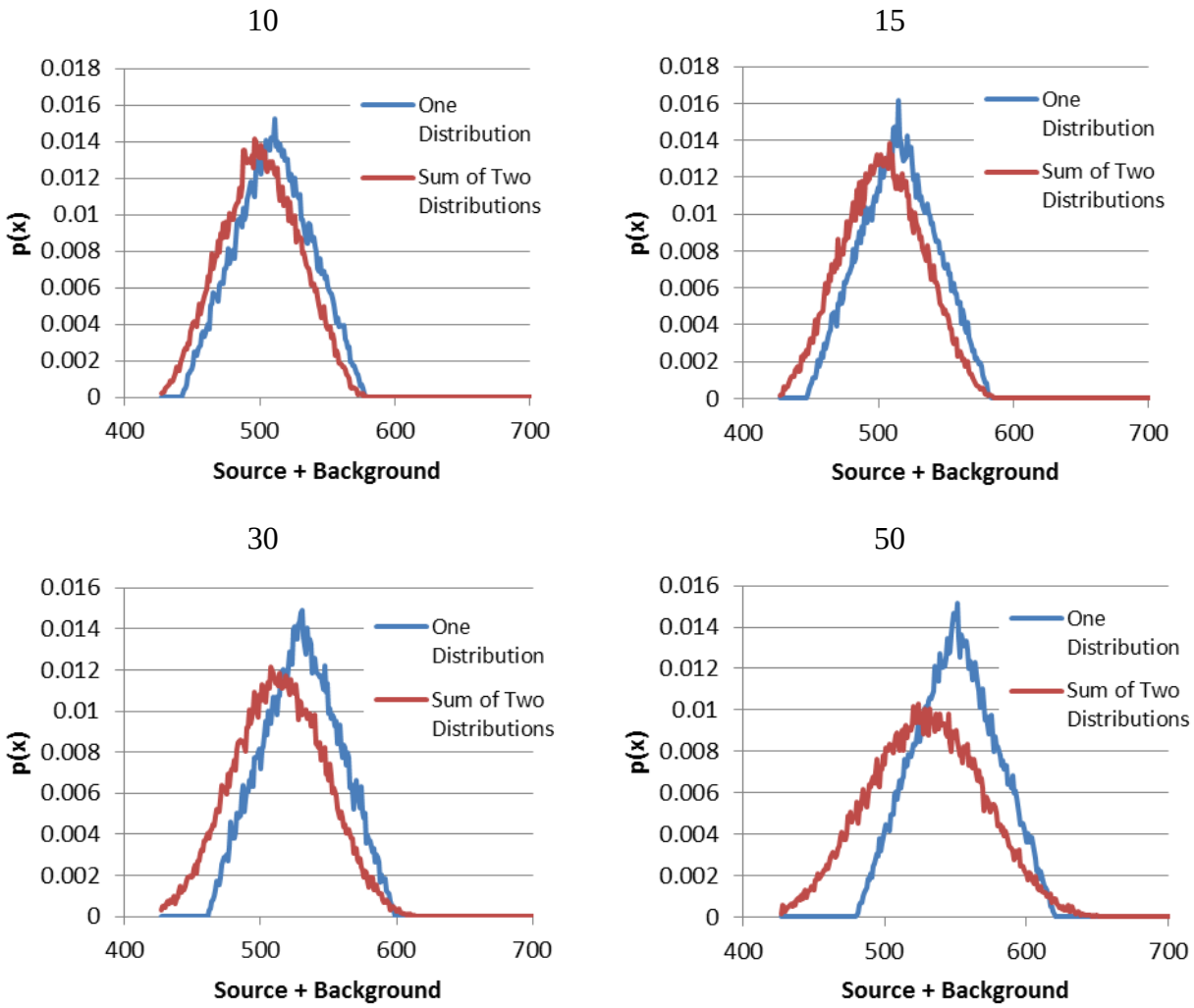

Figure 169 Probability Density Function Comparison for Two Measurement Simulation Techniques for Different Source Strengths (Triangular, b=500, s=10, 15, 30, 50, Stochastic)

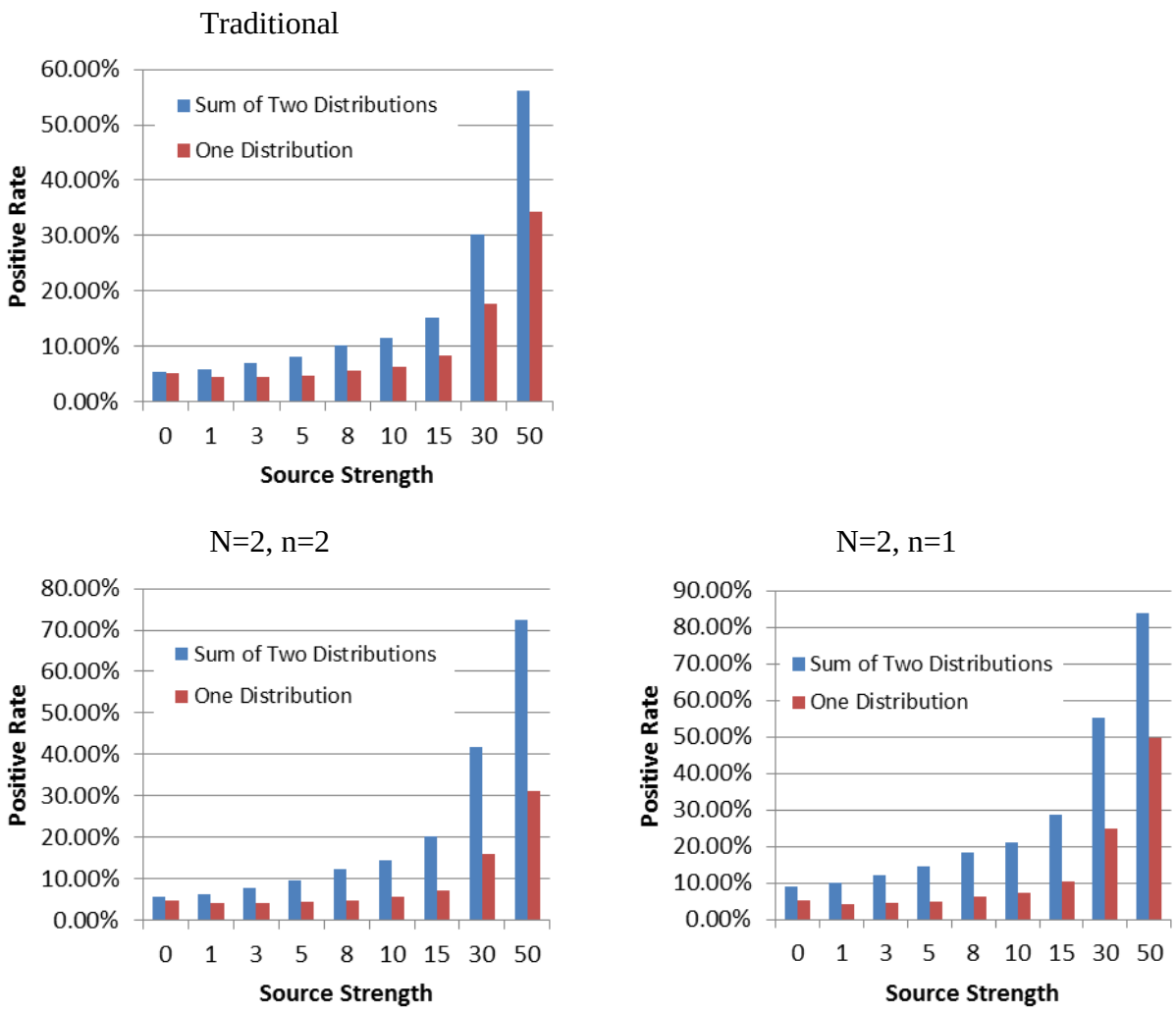

Figure 170 Positive Rate with Source Strength Comparison for Two Measurement Simulation Techniques (Triangular, b=500, Stochastic)

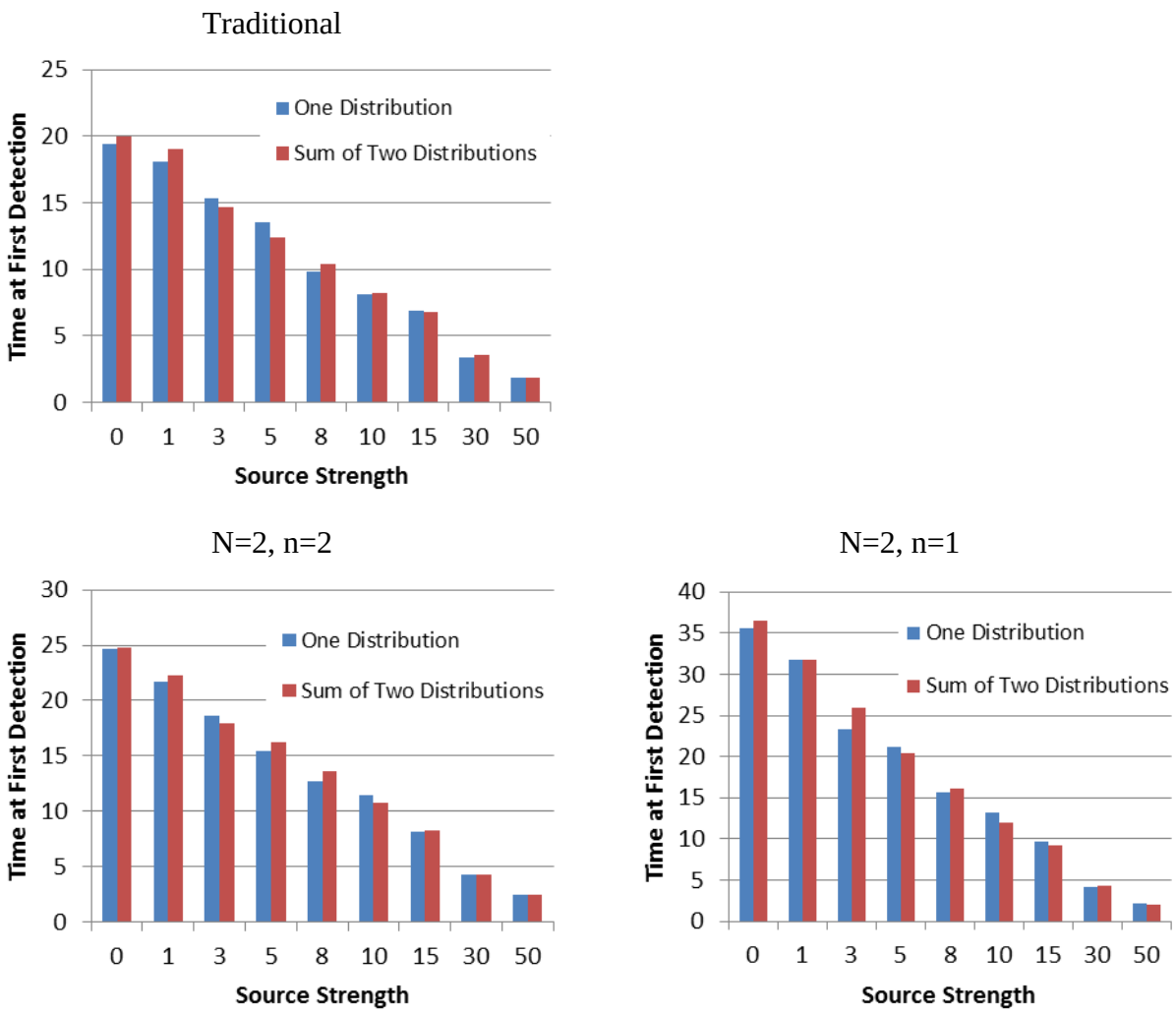

Figure 171 Time at First Detection with Source Strength Comparison for Two Measurement Simulation Techniques (Triangular, b=500, Stochastic)

Positive Rate

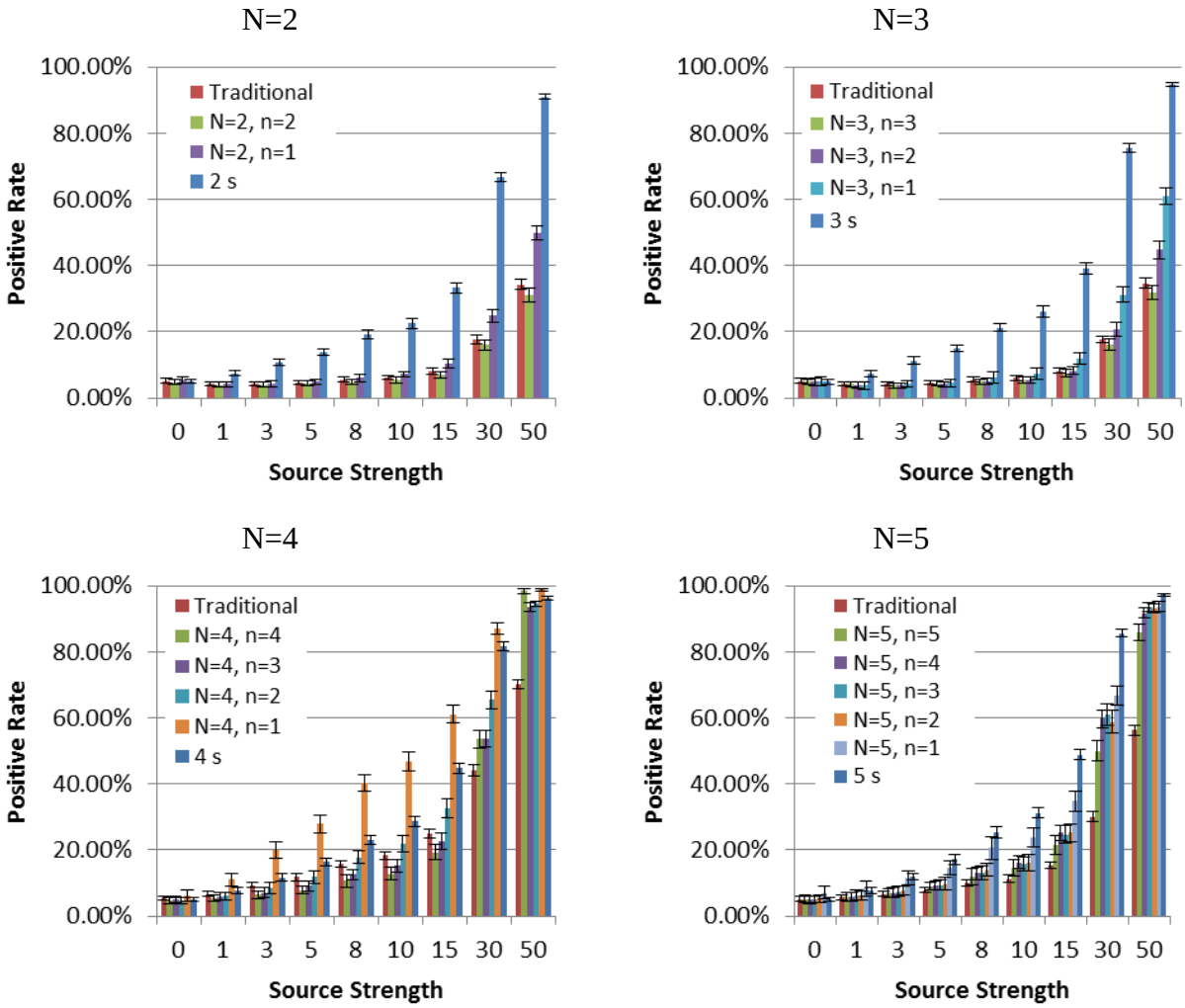

Figure 172 Positive Rate for Different n and N Values (Triangular, b=500)

Time at First Detection

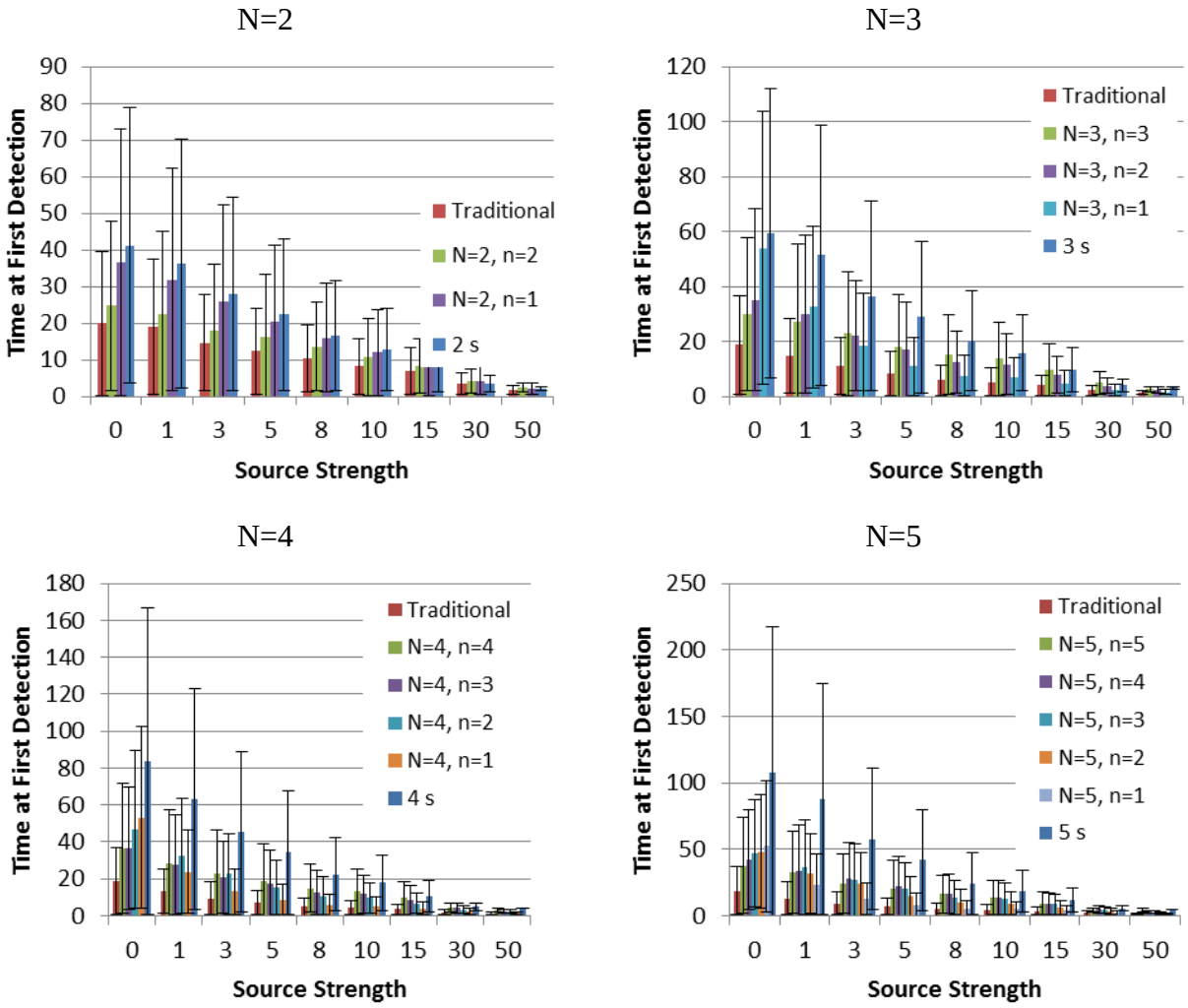

Figure 173 Time at First Detection for Different n and N Values (Triangular, b=500)

Sinusoidal

Comparison of Measurement Simulation Techniques

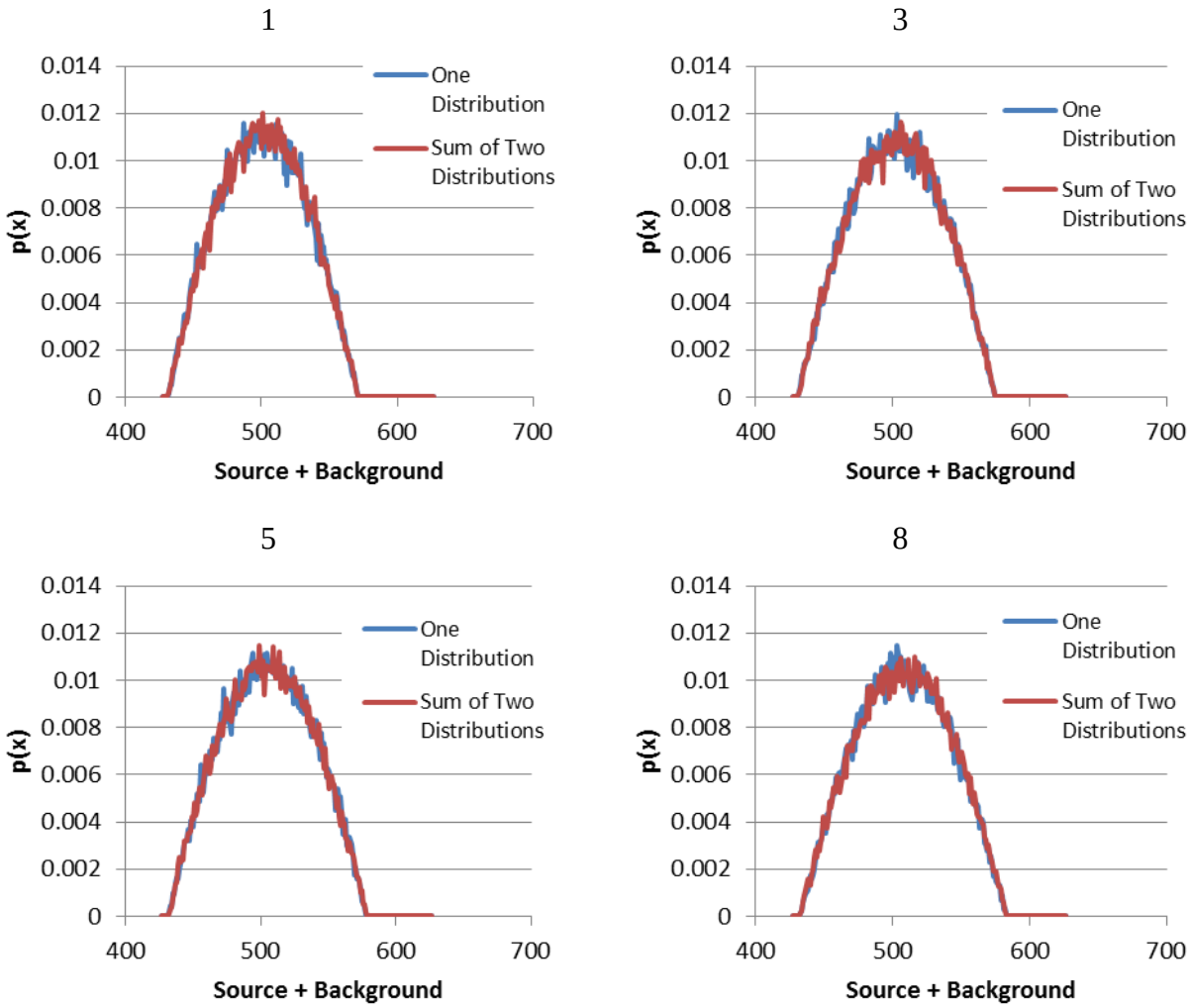

Figure 174 Probability Density Function for Two Measurement Simulation Techniques for Different Source Strengths (Sinusoidal, b=500, s=1, 3, 5, 8, Stochastic)

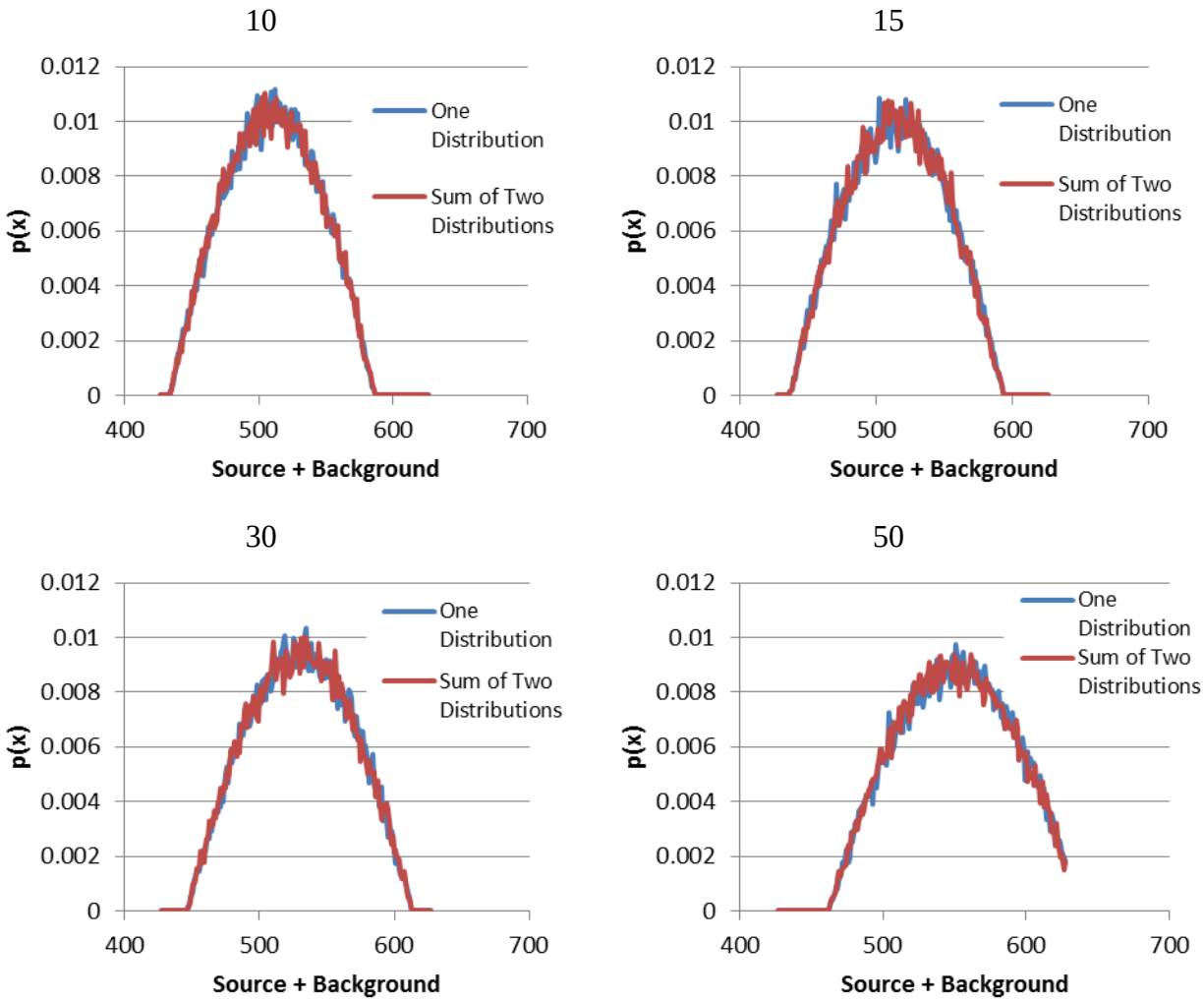

Figure 175 Probability Density Function for Two Measurement Simulation Techniques for Different Source Strengths (Sinusoidal, b=500, s=10, 15, 30, 50, Stochastic)

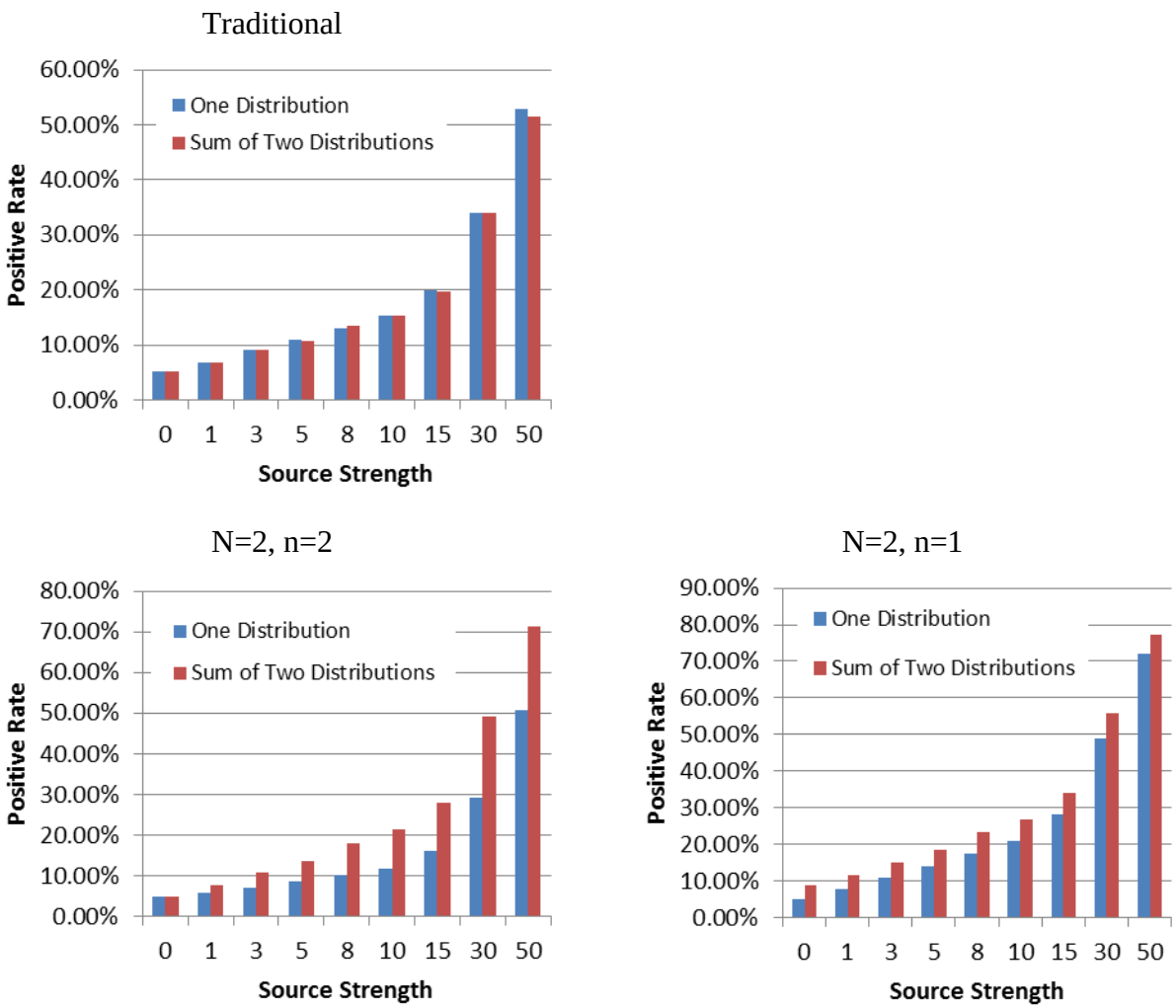

Figure 176 Positive Rate with Source Strength for Different n and N Values Comparison for Two Measurement Simulation Techniques (Sinusoidal, b=500, Stochastic)

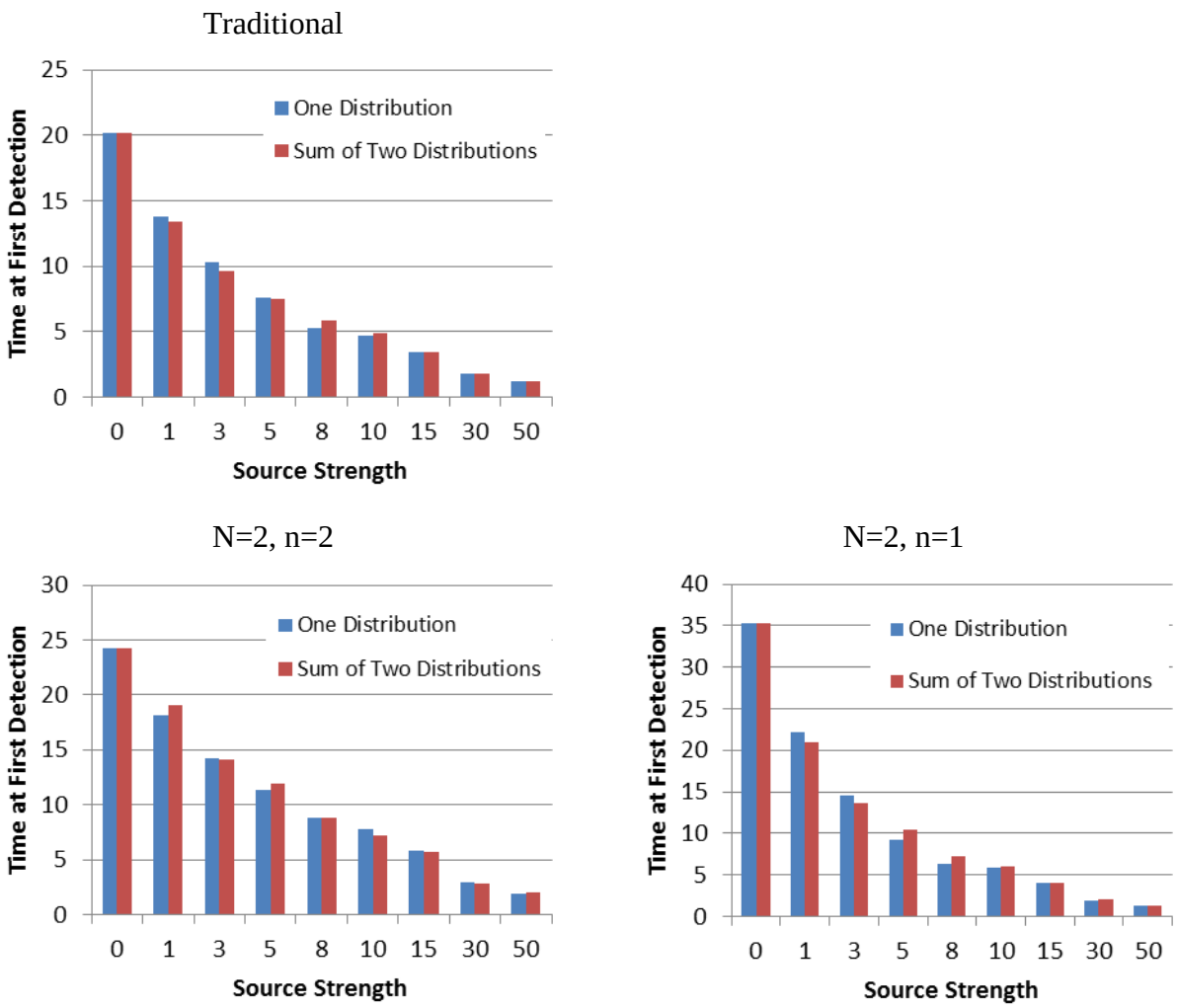

Figure 177 Positive Rate with Source Strength for Different n and N Values Comparison for Two Measurement Simulation Techniques (Sinusoidal, b=500, Stochastic)

Positive Rate

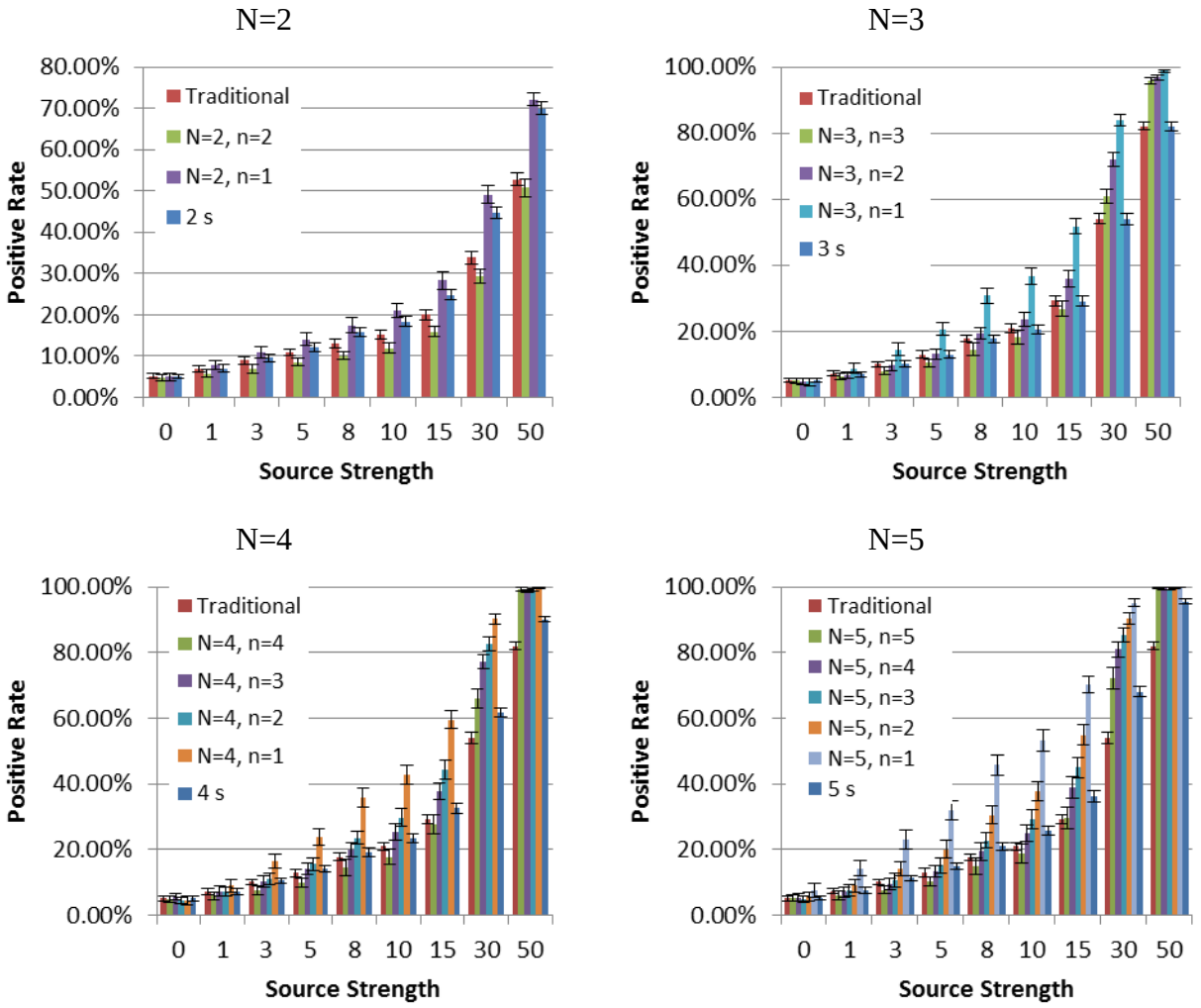

Figure 178 Positive Rate with Source Strength for Different n and N Values (Sinusoidal, b=500, Stochastic)

Time at First Detection

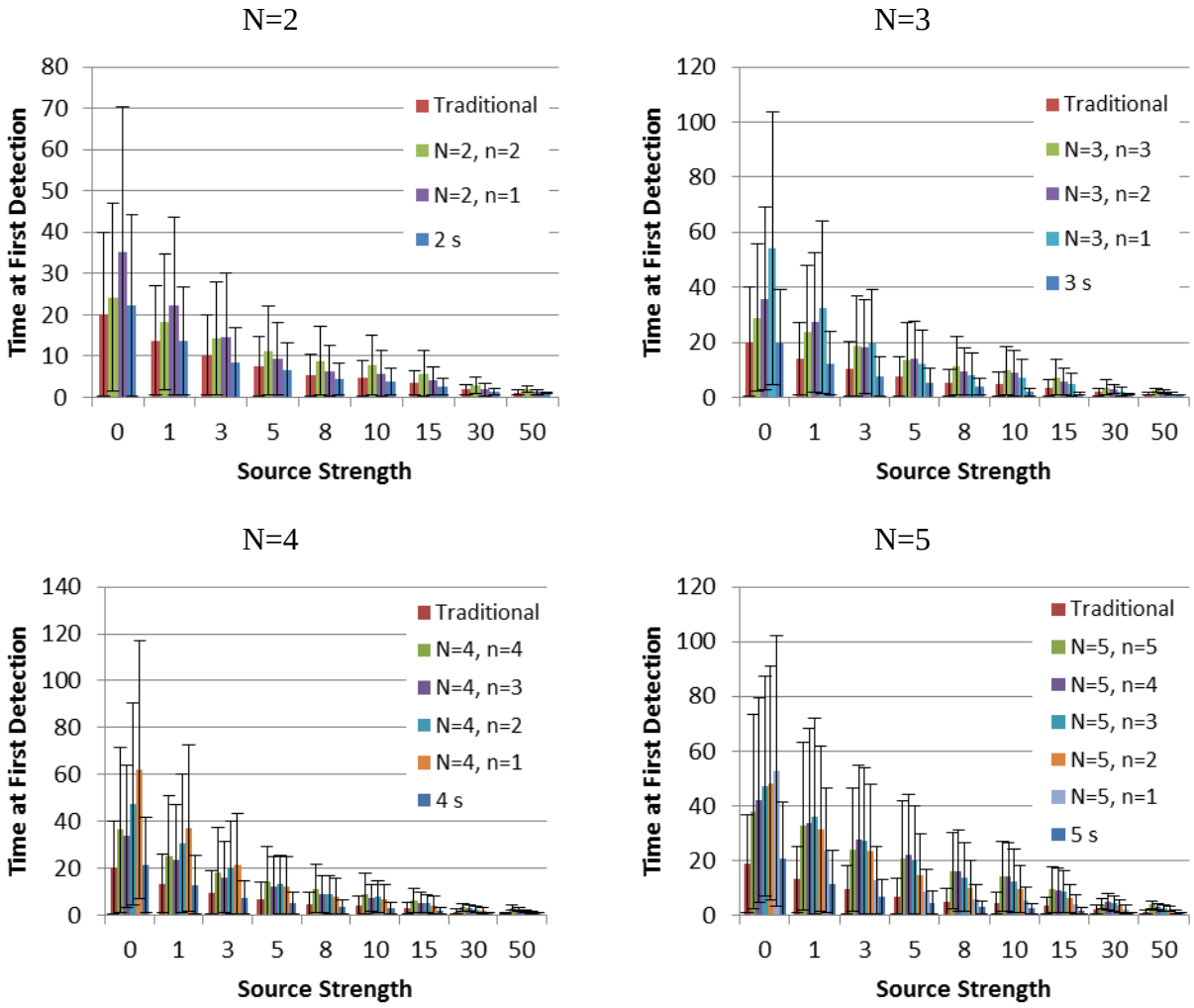

Figure 179 Time at First Detection with Source Strength for Different n and N Values (Sinusoidal, b=500, Stochastic)

Poisson

Comparison of Measurement Simulation Techniques

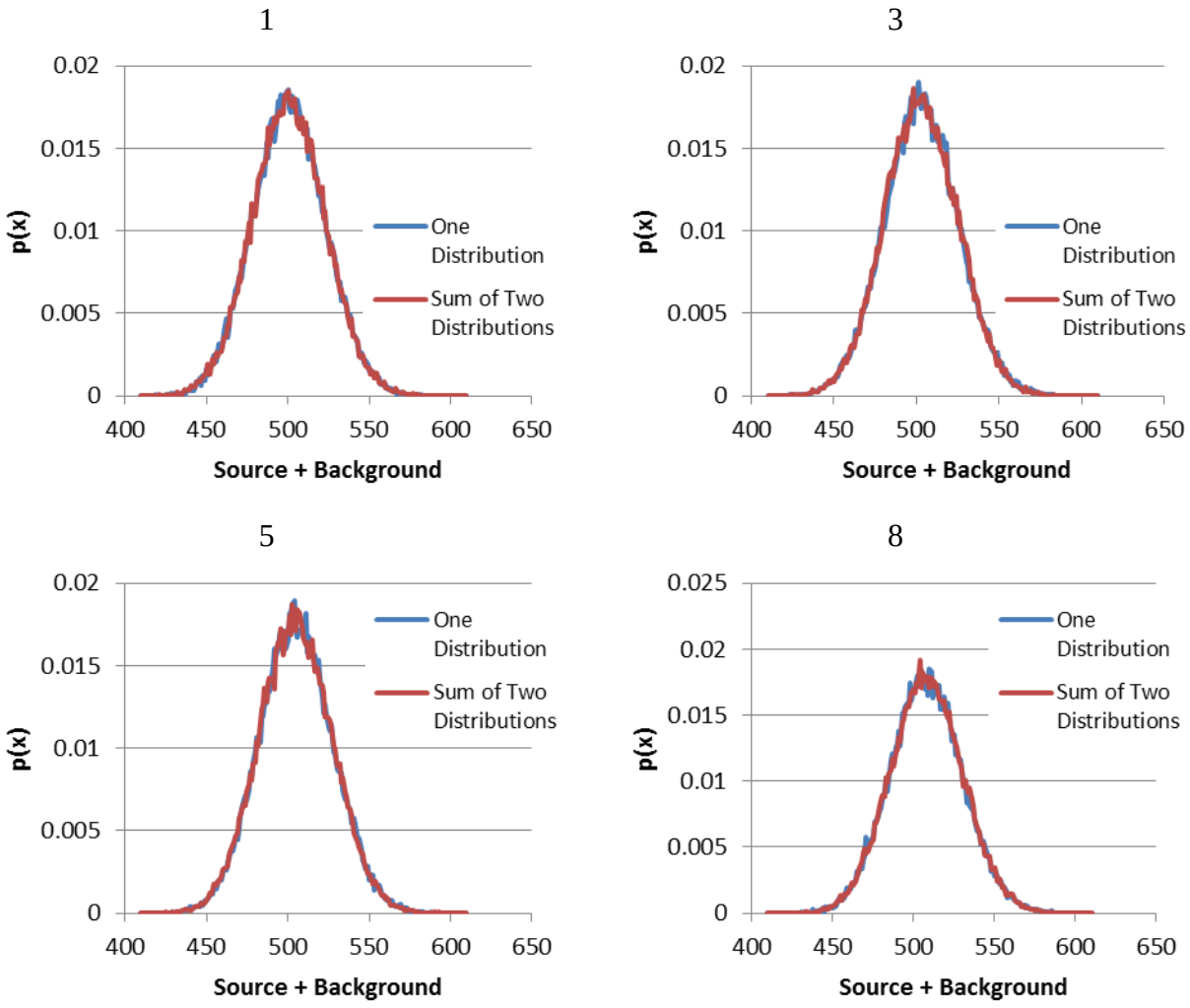

Figure 180 Probability Density Function Comparison for Two Measurement Simulation Techniques for Different Source Strengths (Poisson, b=500, s=1, 3, 5, 8, Stochastic)

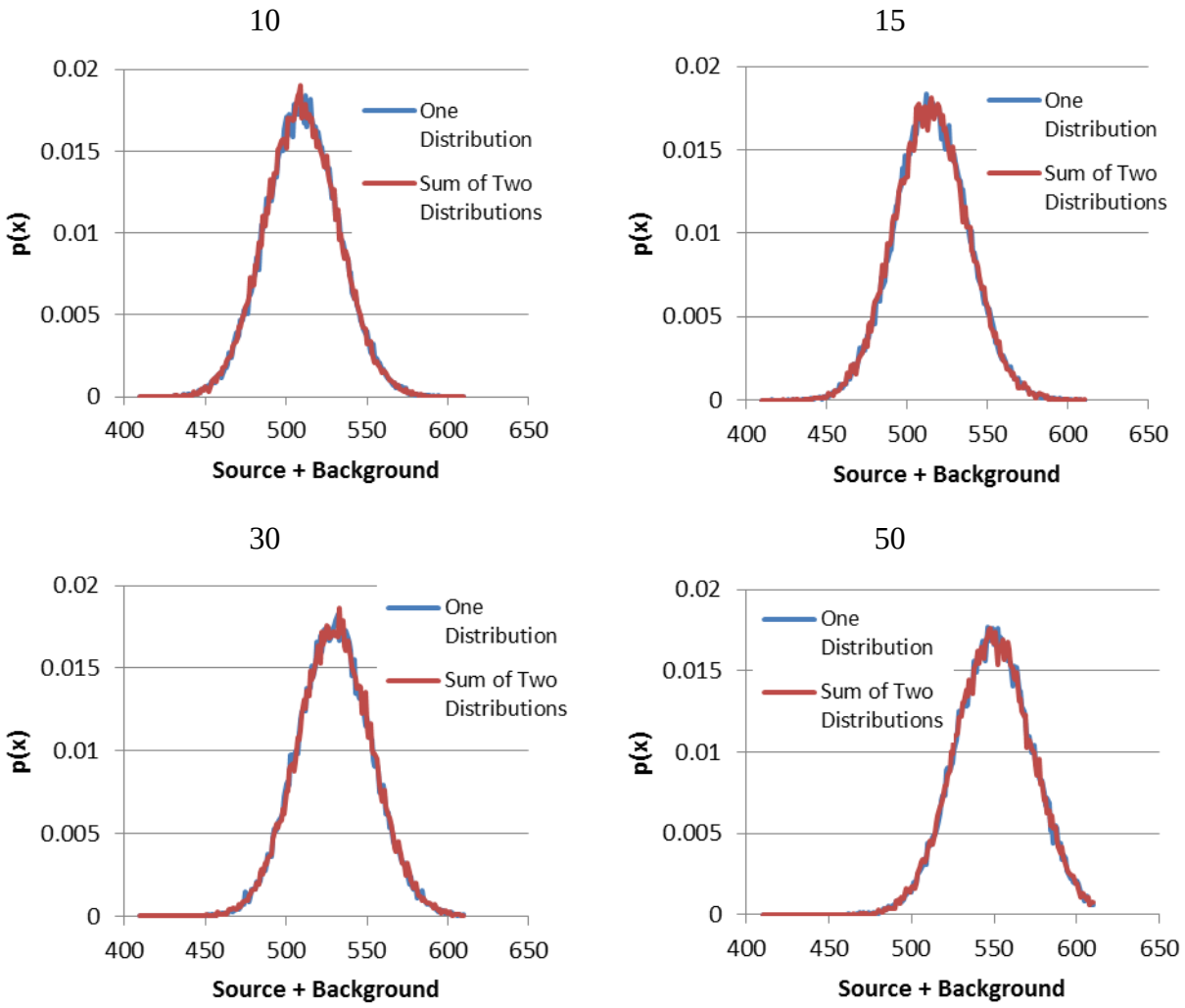

Figure 181 Probability Density Function Comparison for Two Measurement Simulation Techniques for Different Source Strengths (Poisson, b=500, s=10, 15, 30, 50, Stochastic)

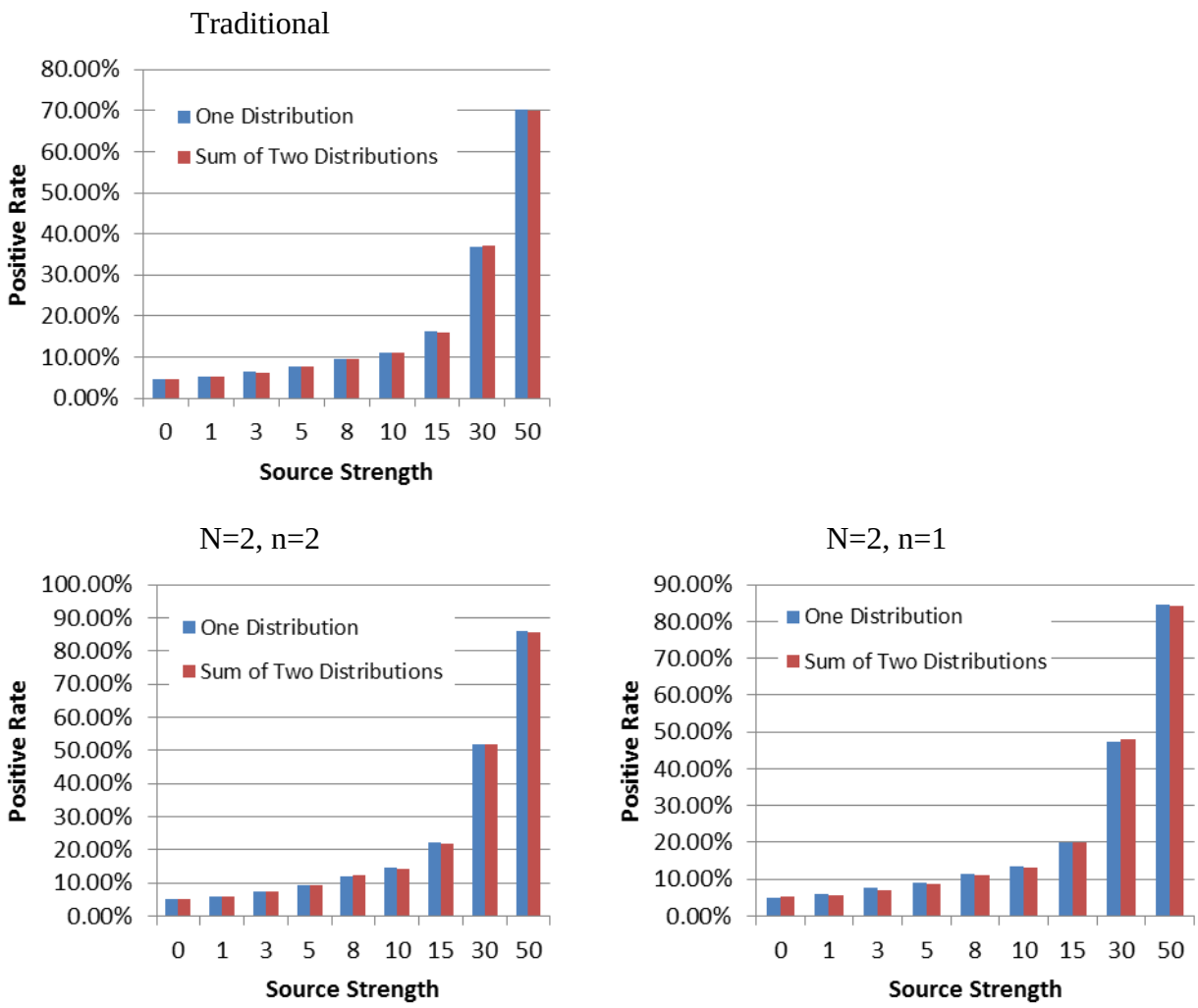

Figure 182 Positive Rate with Source Strength Comparison for Two Measurement Simulation Techniques (Poisson, b=500, Stochastic)

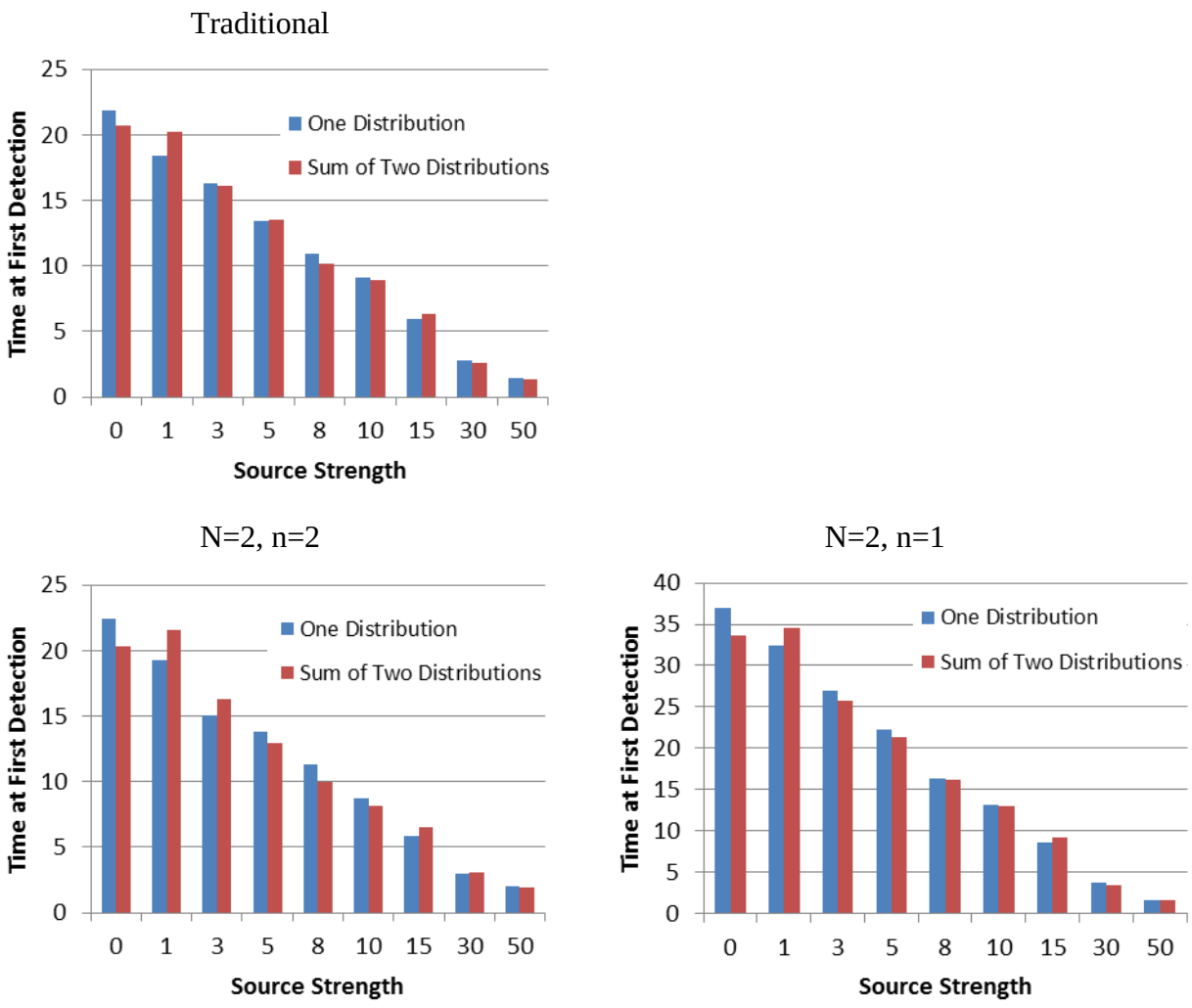

Figure 183 Time at First Detection with Source Strength Comparison for Two Measurement Simulation Techniques (Poisson, b=500, Stochastic)

Positive Rate

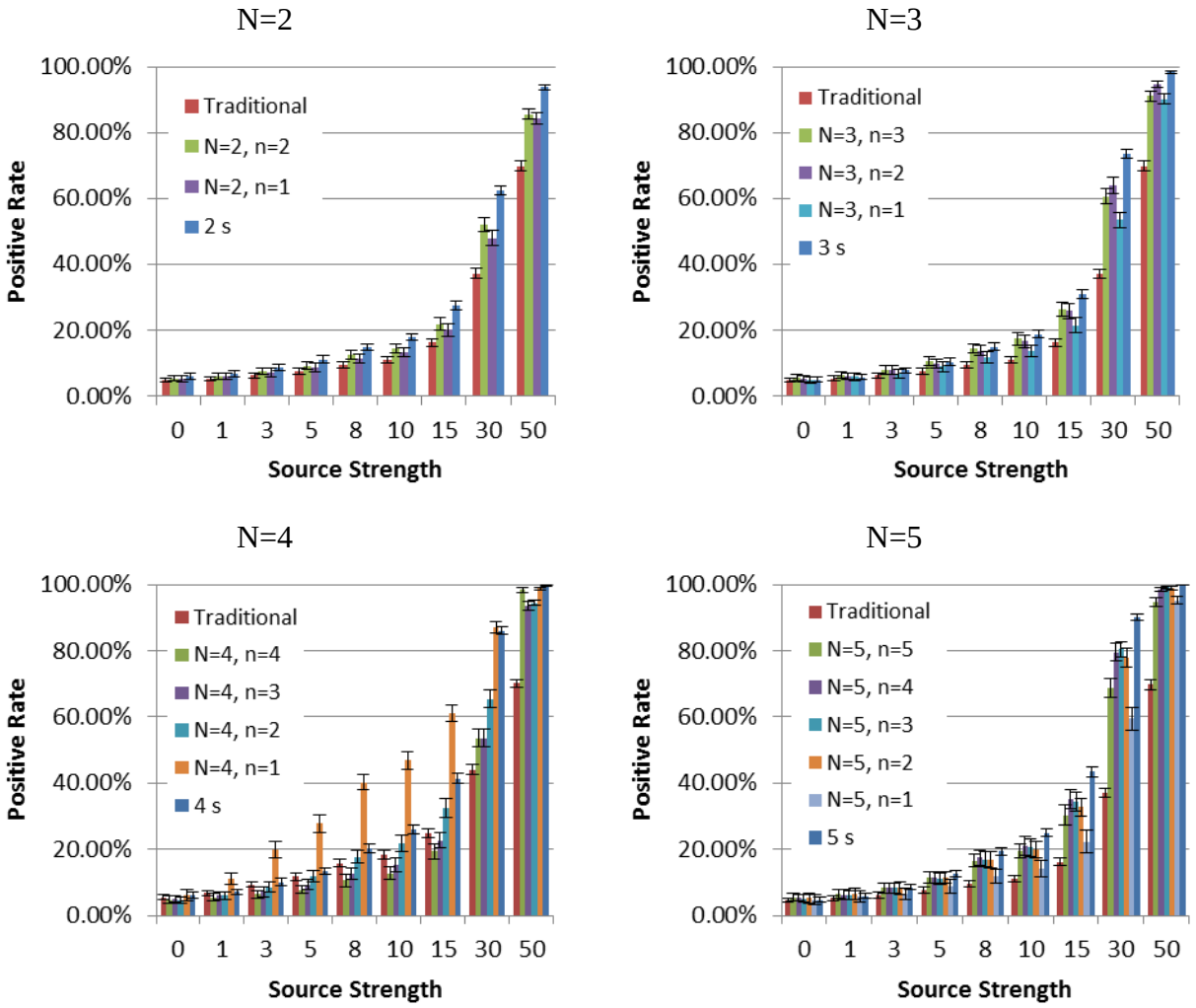

Figure 184 Positive Rate with Source Strength for Different n and N Values (Poisson, b=500, Stochastic)

Time at First Detection

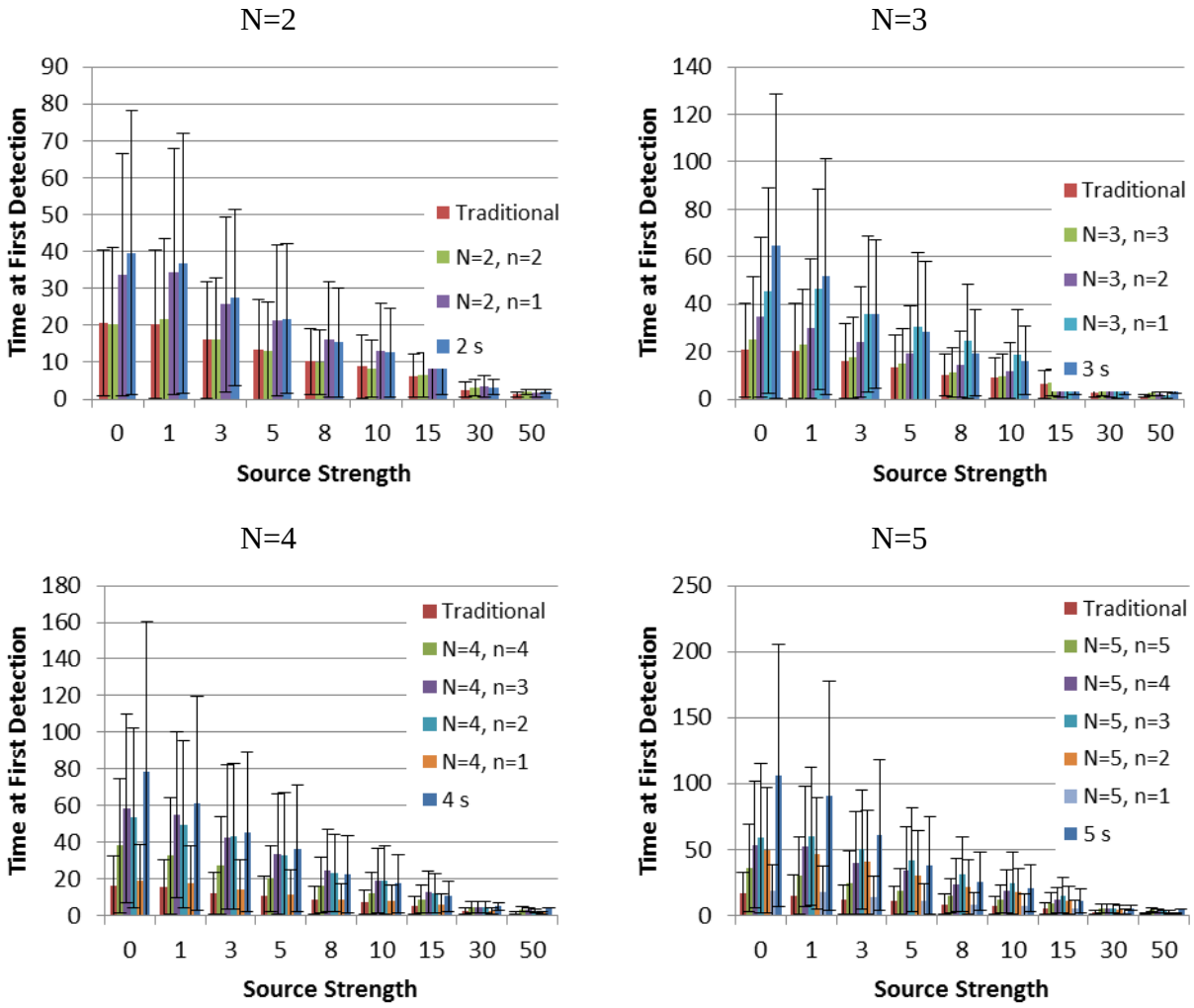

Figure 185 Time at First Detection with Source Strength for Different n and N Values (Poisson, b=500, Stochastic)

Gaussian

Comparison of Measurement Simulation Techniques

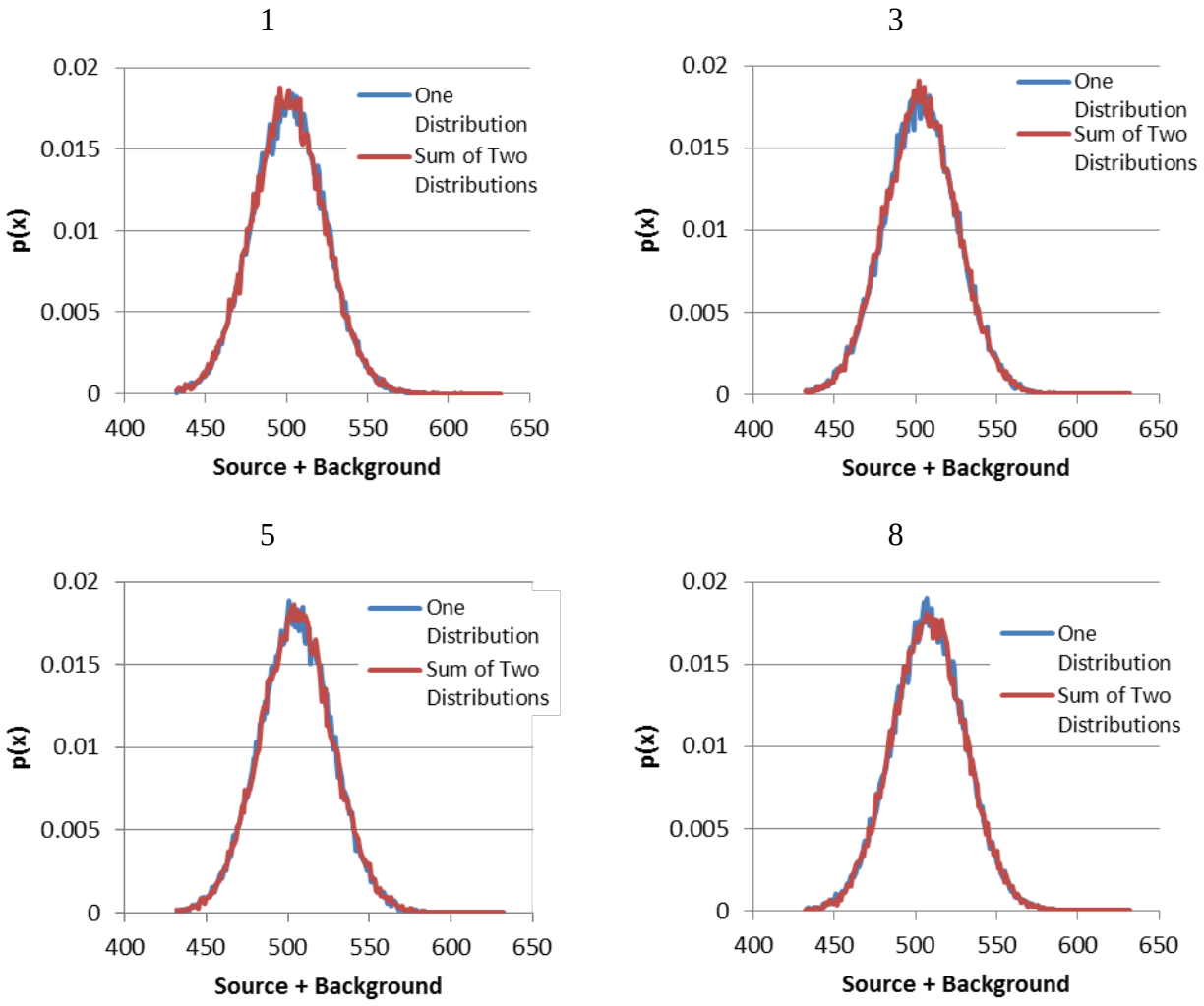

Figure 186 Probability Density Function Comparison for Two Measurement Simulation Techniques for Different Source Strengths (Gaussian, b=500, s=1, 3, 5, 8, Stochastic)

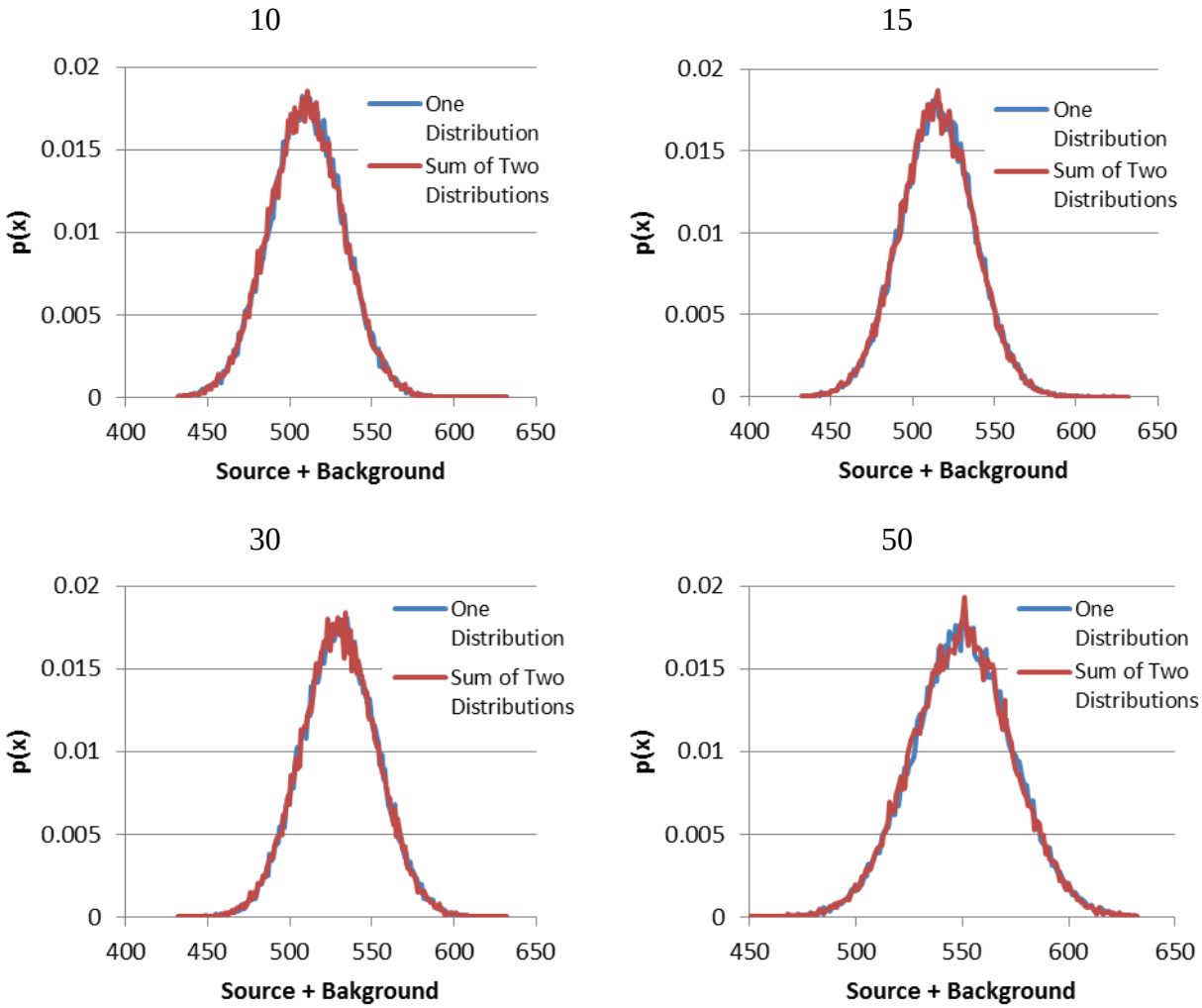

Figure 187 Probability Density Function Comparison for Two Measurement Simulation Techniques for Different Source Strengths (Gaussian, b=500, s=10, 15, 30, 50, Stochastic)

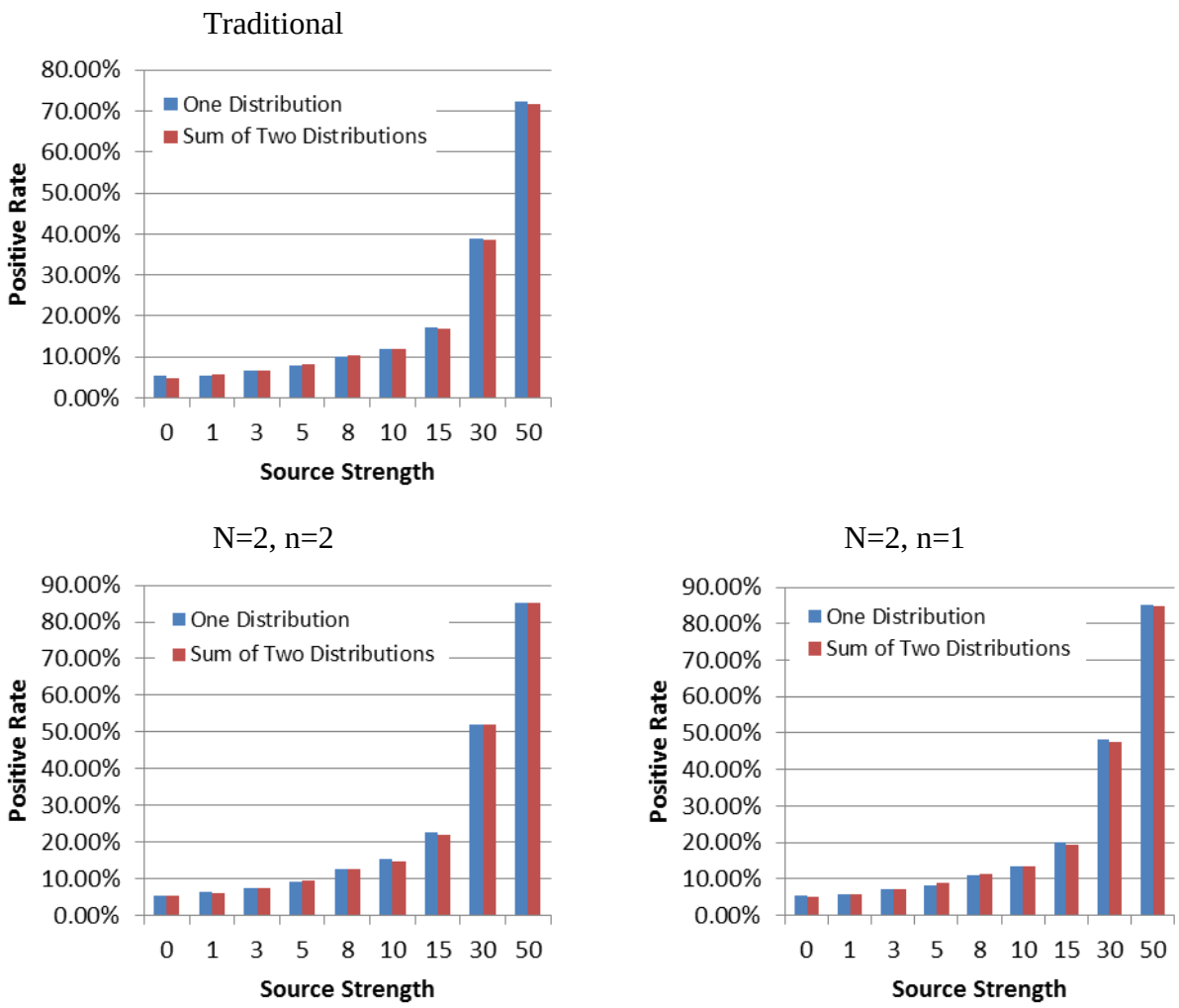

Figure 188 Positive Rate with Source Strength Comparison for Two Measurement Simulation Techniques (Gaussian, b=500, Stochastic)

Positive Rate

b=50

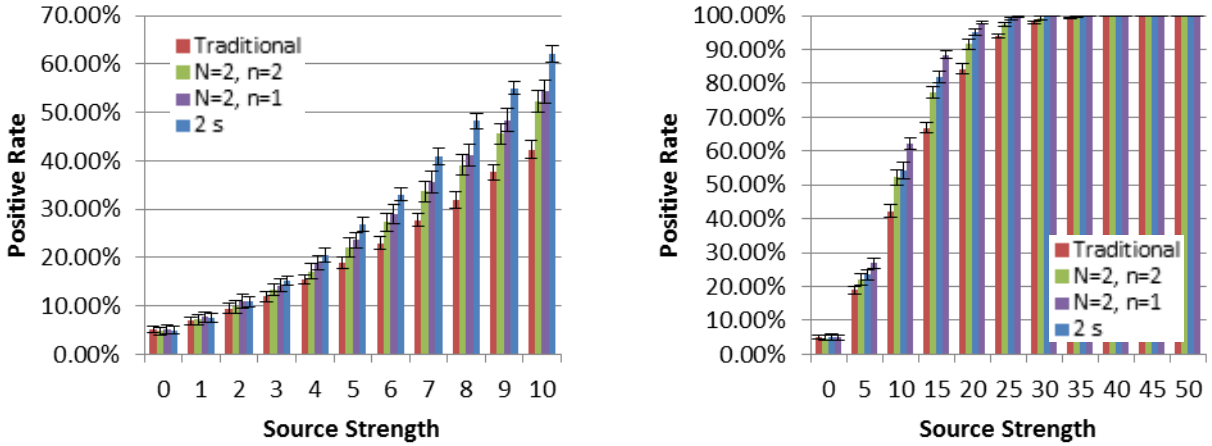

b=500

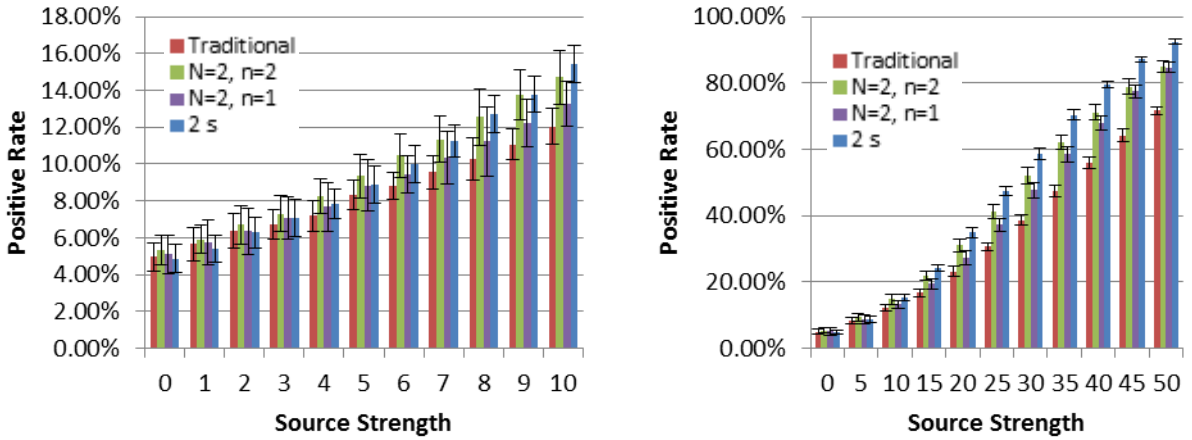

b=5000

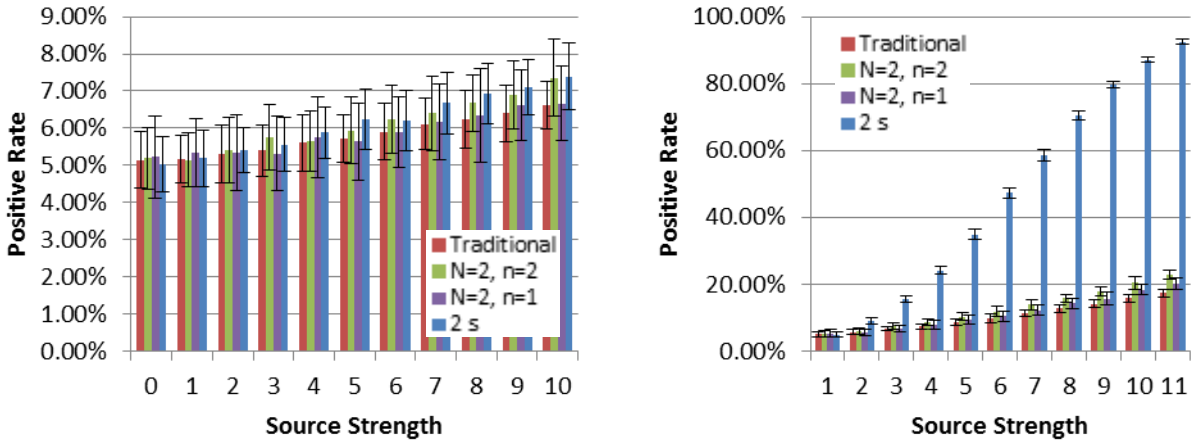

Figure 189 Positive Rate with Source Strength Comparison for Two Measurement Simulation Techniques for Different Background (Gaussian, N=2, b=50, b=500, b=5000, Stochastic)

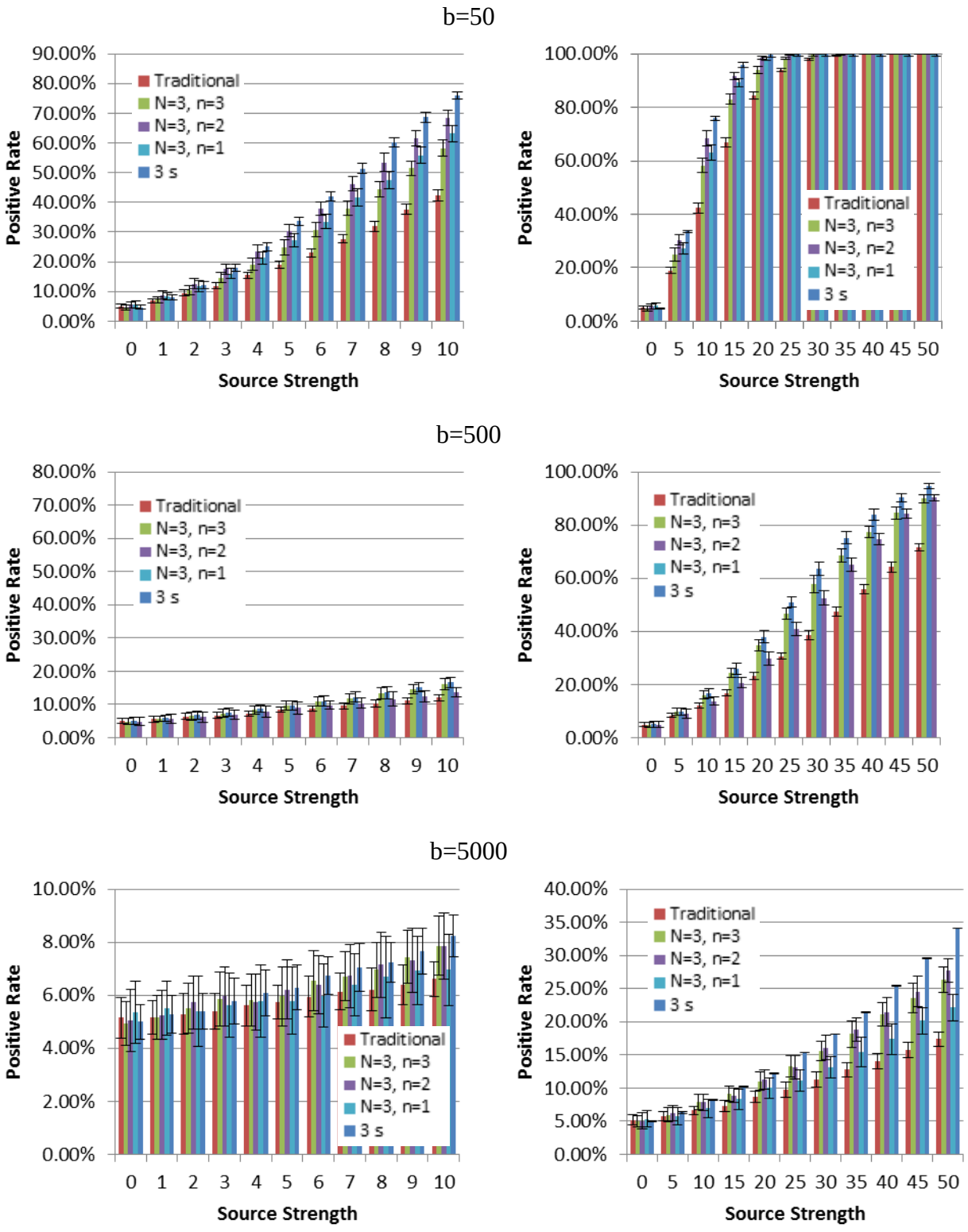

Figure 190 Positive Rate with Source Strength Comparison for Two Measurement Simulation Techniques for Different Background (Gaussian, N=3, b=50, b=500, b=5000, Stochastic)

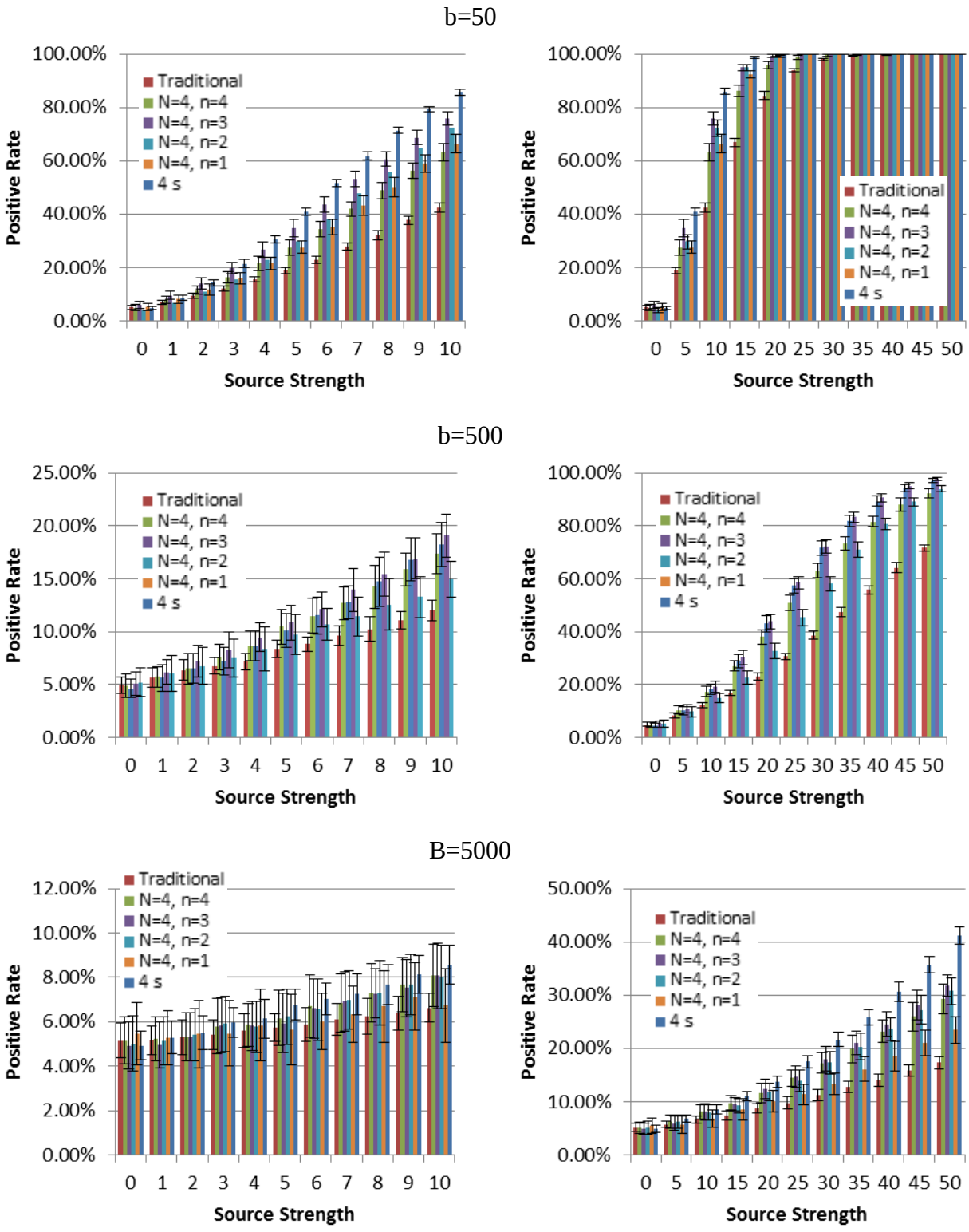

Figure 191 Positive Rate with Source Strength Comparison for Two Measurement Simulation Techniques for Different Background (Gaussian, N=4, b=50, b=500, b=5000, Stochastic)

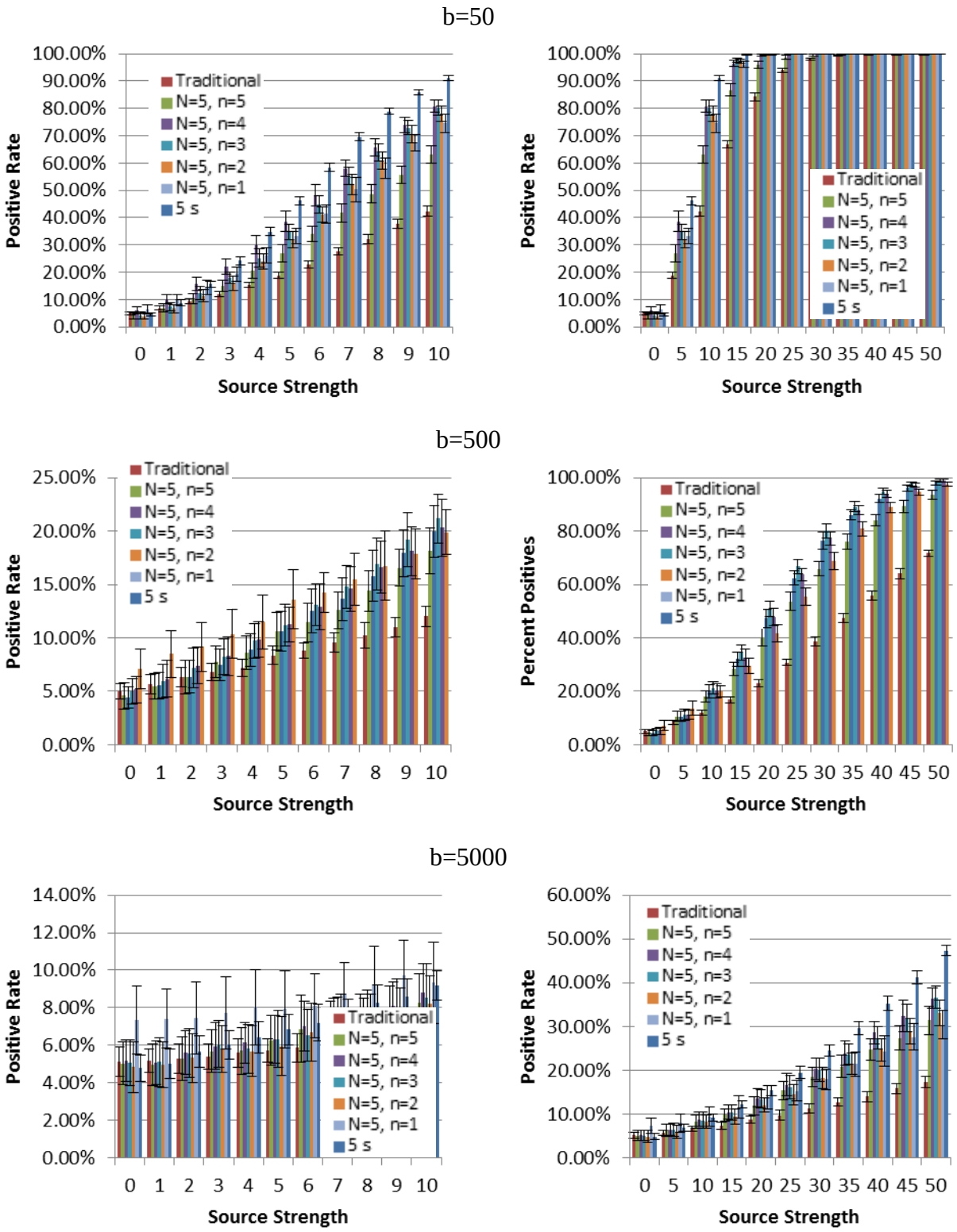

Figure 192 Positive Rate with Source Strength Comparison for Two Measurement Simulation Techniques for Different Background (Gaussian, N=5, b=50, b=500, b=5000, Stochastic)

Time at First Detection

b=50

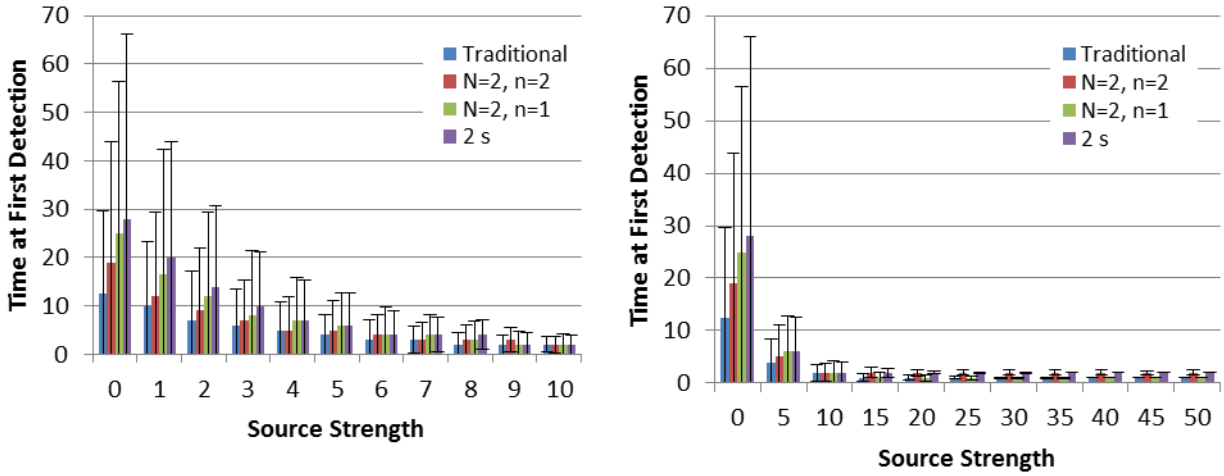

b=500

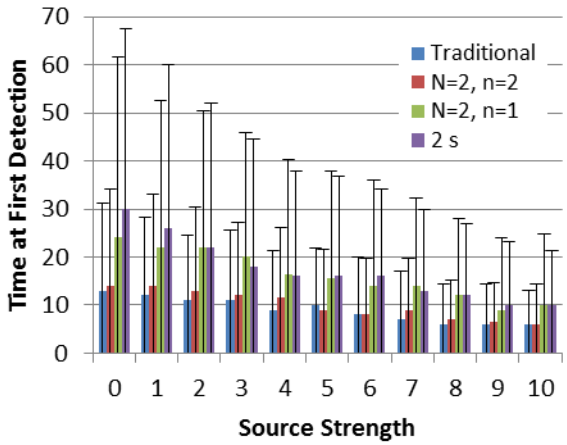

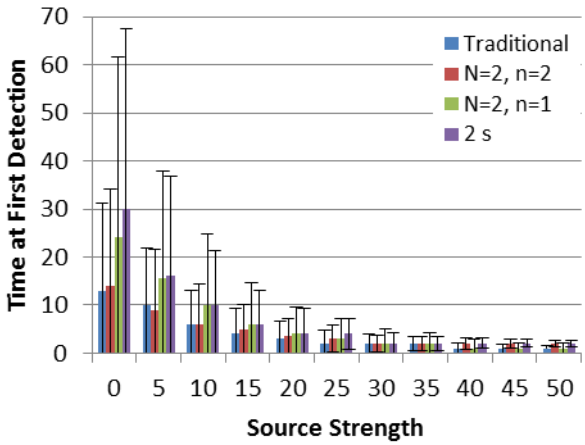

b=5000

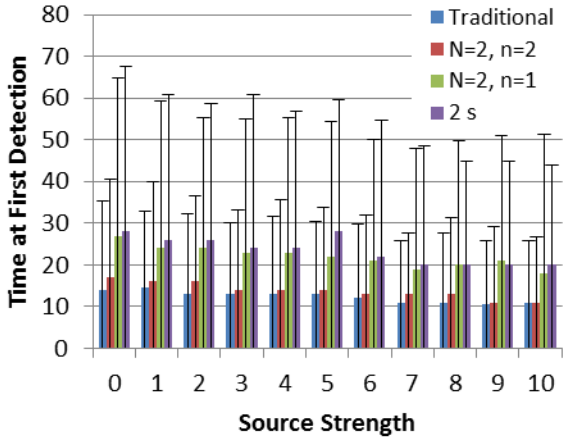

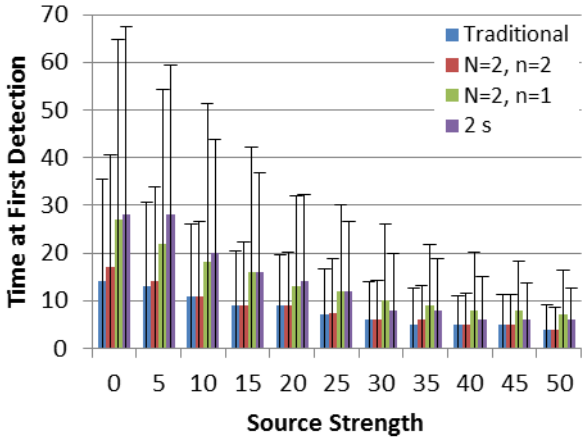

Figure 193 Time at First Detection with Source Strength Comparison for Two Measurement Simulation Techniques for Different Background (Gaussian, N=2, b=50, b=500, b=5000, Stochastic)

b=50

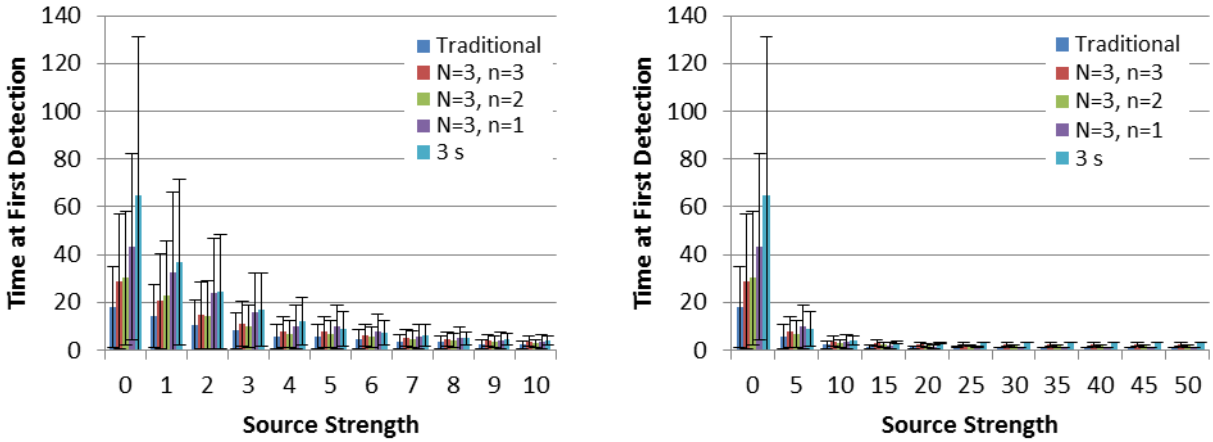

b=500

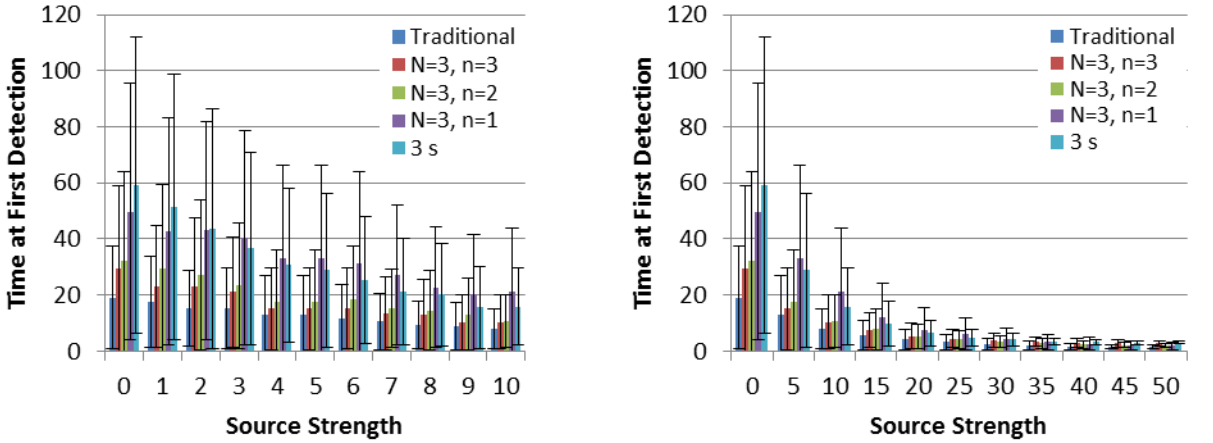

b=5000

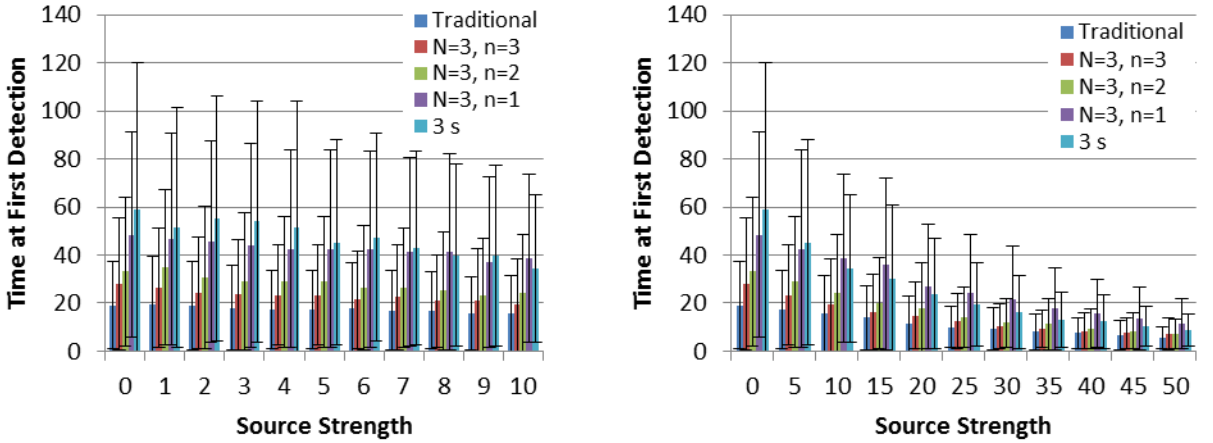

Figure 194 Time at First Detection with Source Strength Comparison for Two Measurement Simulation Techniques for Different Background (Gaussian, N=3, b=50, b=500, b=5000, Stochastic)

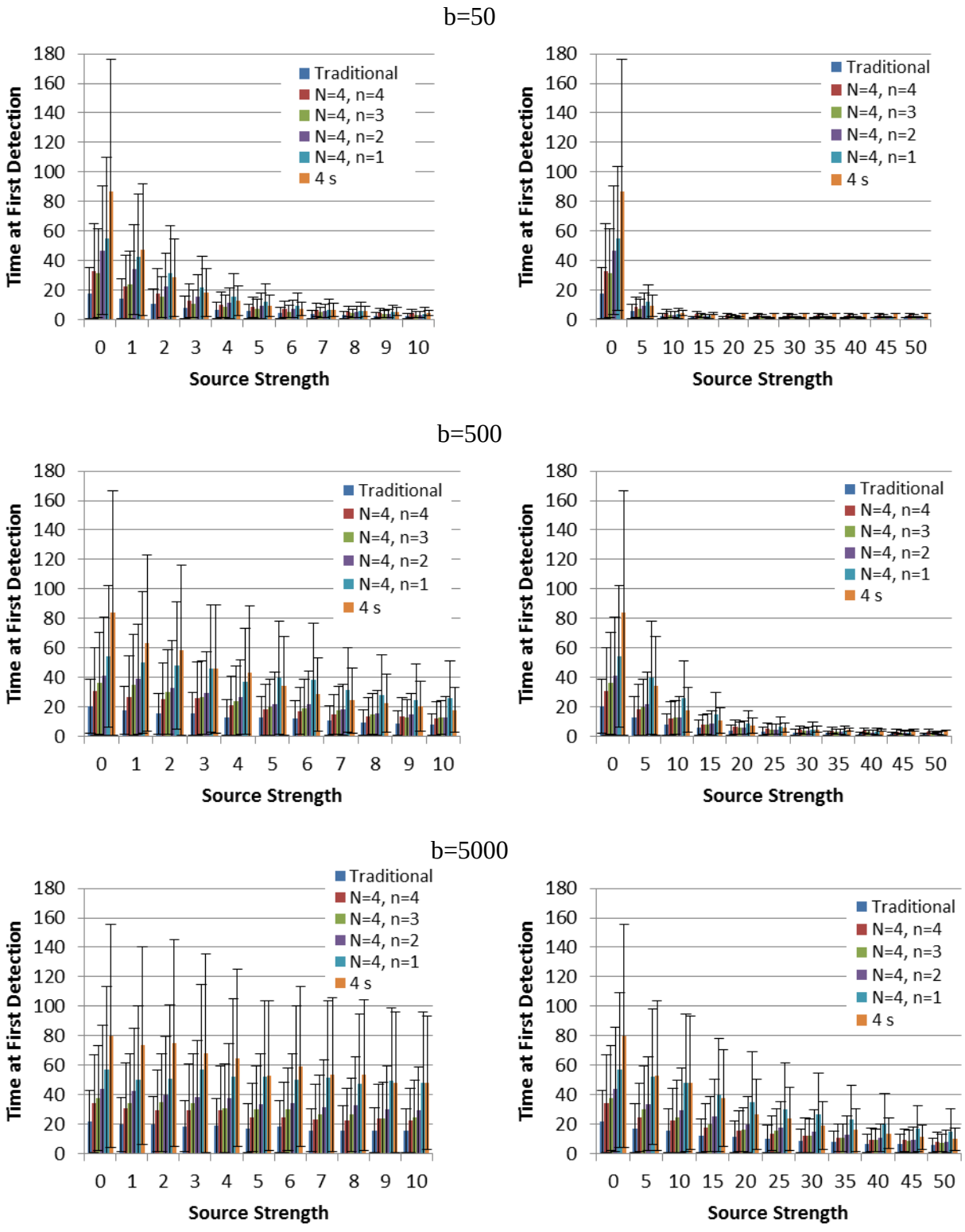

Figure 195 Time at First Detection with Source Strength Comparison for Two Measurement Simulation Techniques for Different Background (Gaussian, N=4, b=50, b=500, b=5000, Stochastic)

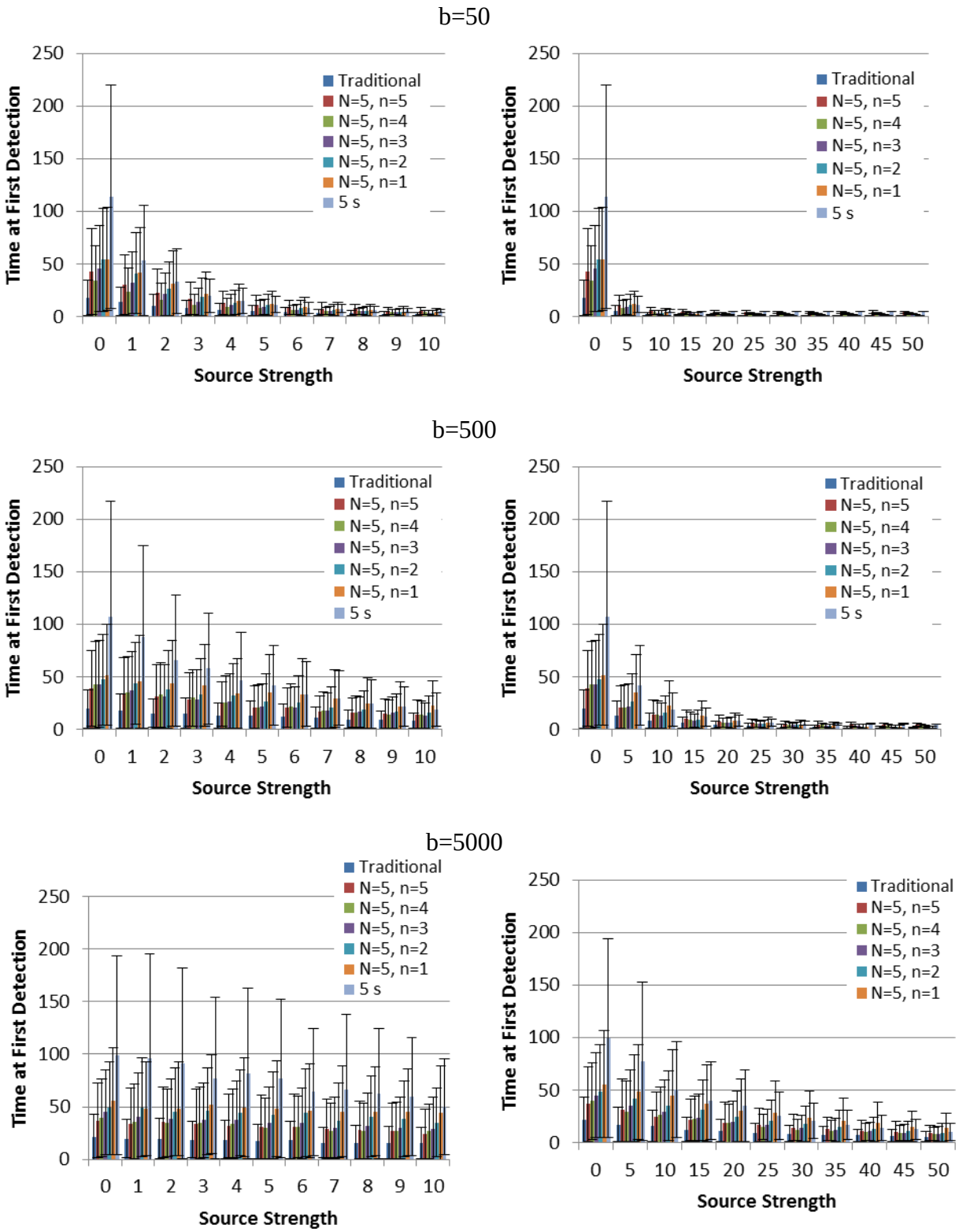

Figure 196 Time at First Detection with Source Strength Comparison for Two Measurement Simulation Techniques for Different Background (Gaussian, N=5, b=50, b=500, b=5000, Stochastic)

Comparison

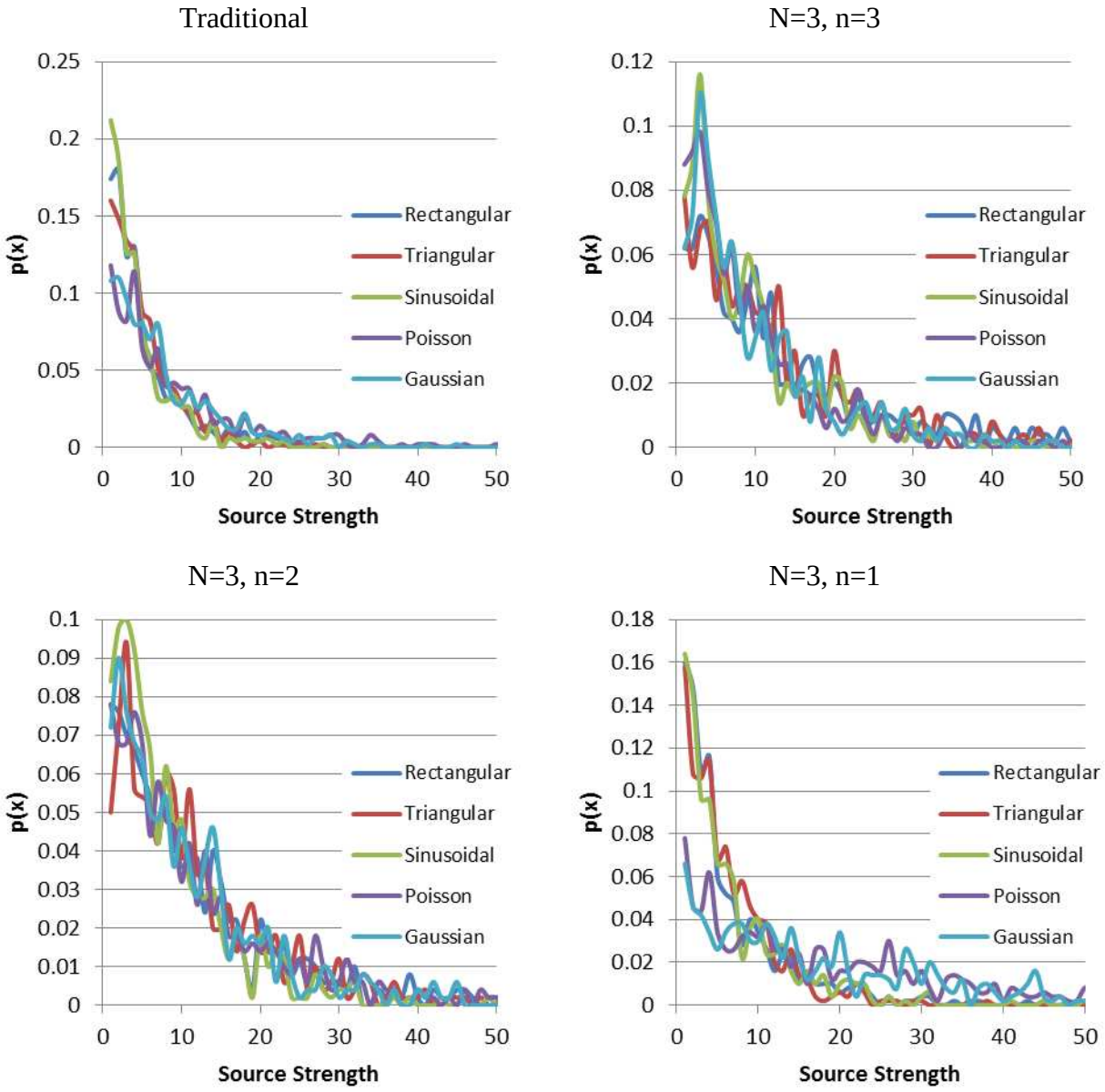

Figure 197 Time at First Detection Probability Density Function with Source Strength for Different Distributions (N=3, b=500, Stochastic)

APPENDIX C

Measurements & Simulation

Positive Rate

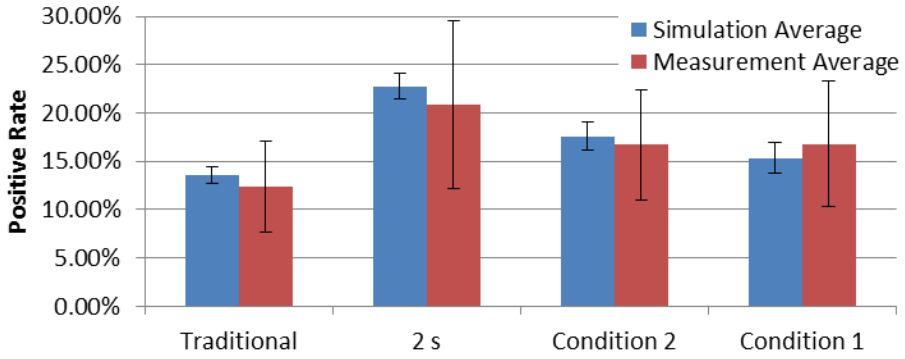

Figure 198 Positive Rate for Different n Values Comparison for Simulation and Measurement (Gaussian, b=669.24 C/s, N=2, Stochastic)

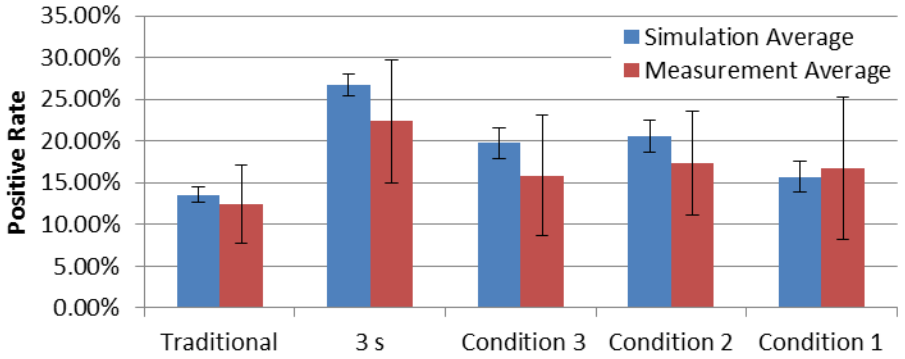

Figure 199 Positive Rate for Different n Values Comparison for Simulation and Measurement (Gaussian, b=669.24 C/s, N=3, Stochastic)

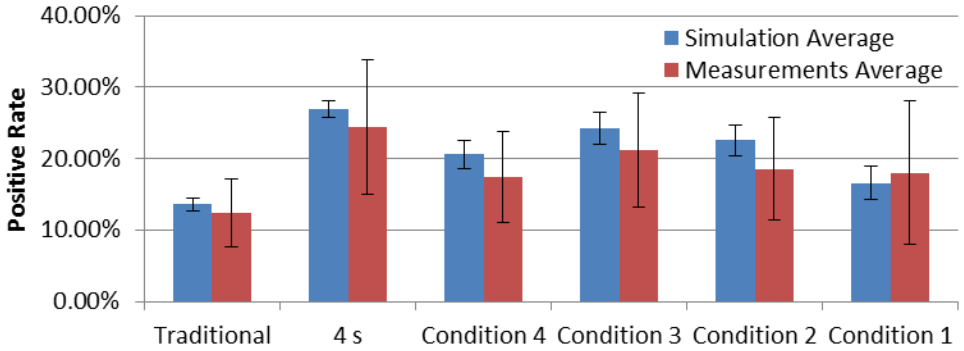

Figure 200 Positive Rate for Different n Values Comparison for Simulation and Measurement (Gaussian, b=669.24 C/s, N=4, Stochastic)

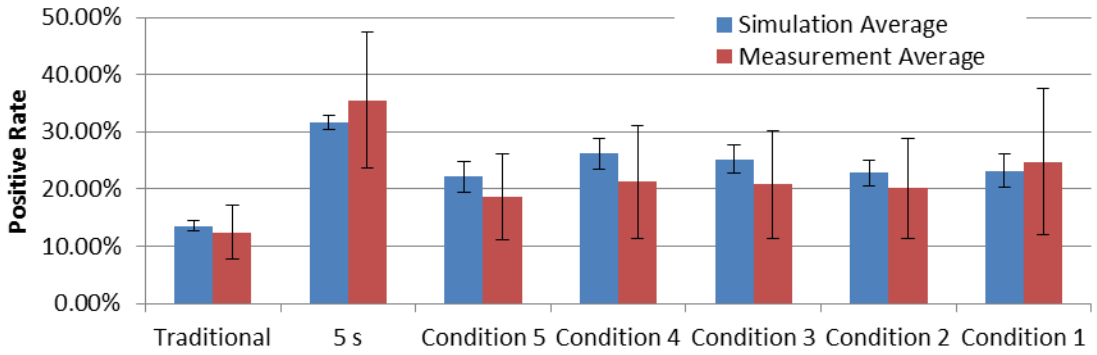

Figure 201 Positive Rate for Different n Values Comparison for Simulation and Measurement (Gaussian, b=669.24 C/s, N=5, Stochastic)

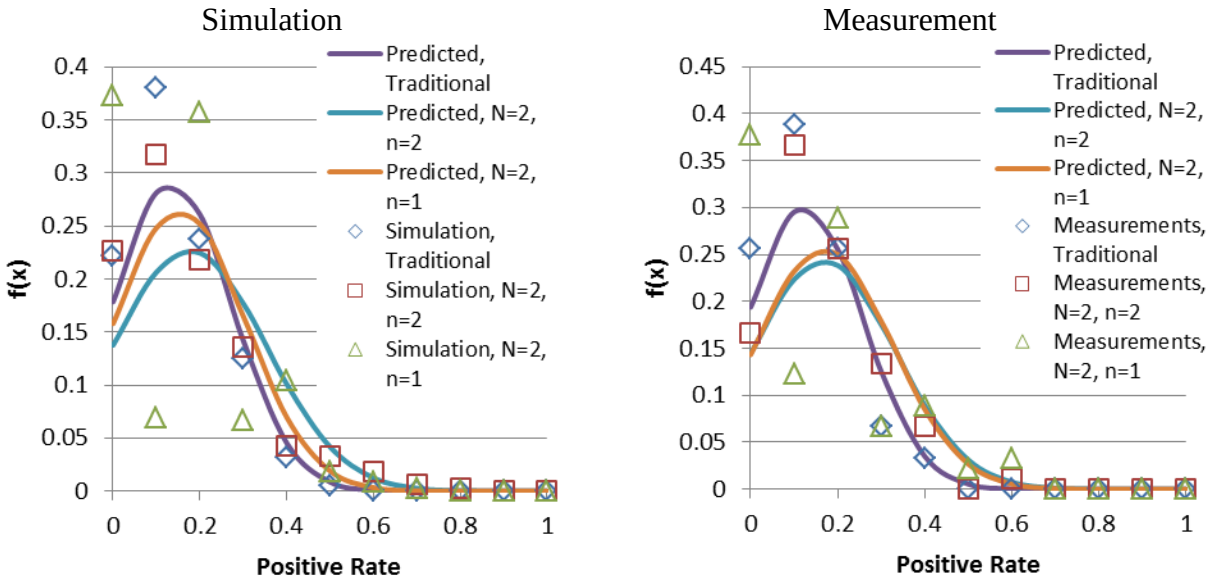

Figure 202 Positive Rate Probability Density Function Comparison for Simulation and Measurement for Different n Values (Gaussian, N=2, Stochastic)

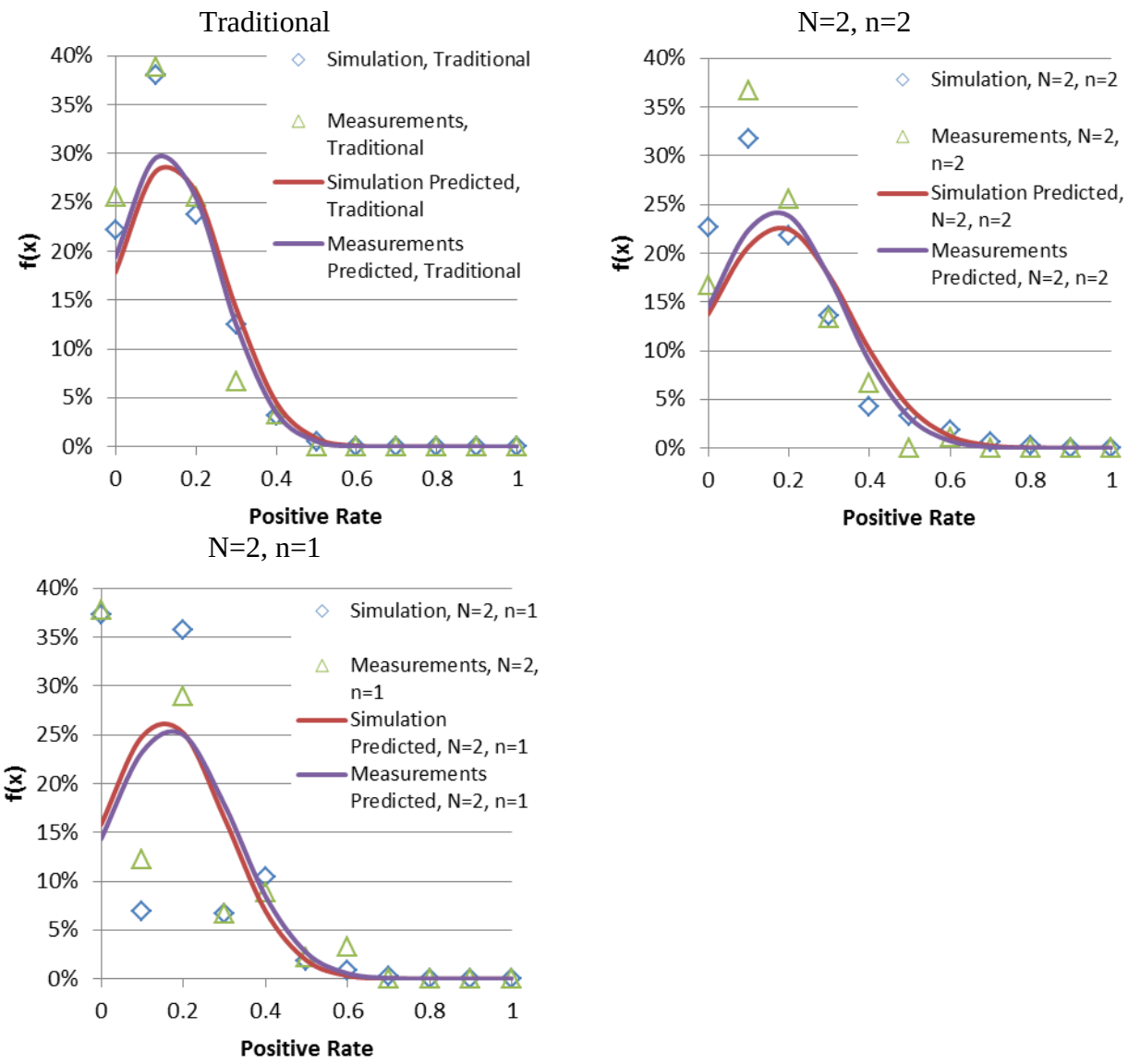

Figure 203 Positive Rate Probability Density Function Comparison for Simulation and Measurement for Different n Values (Gaussian, N=2, Stochastic)

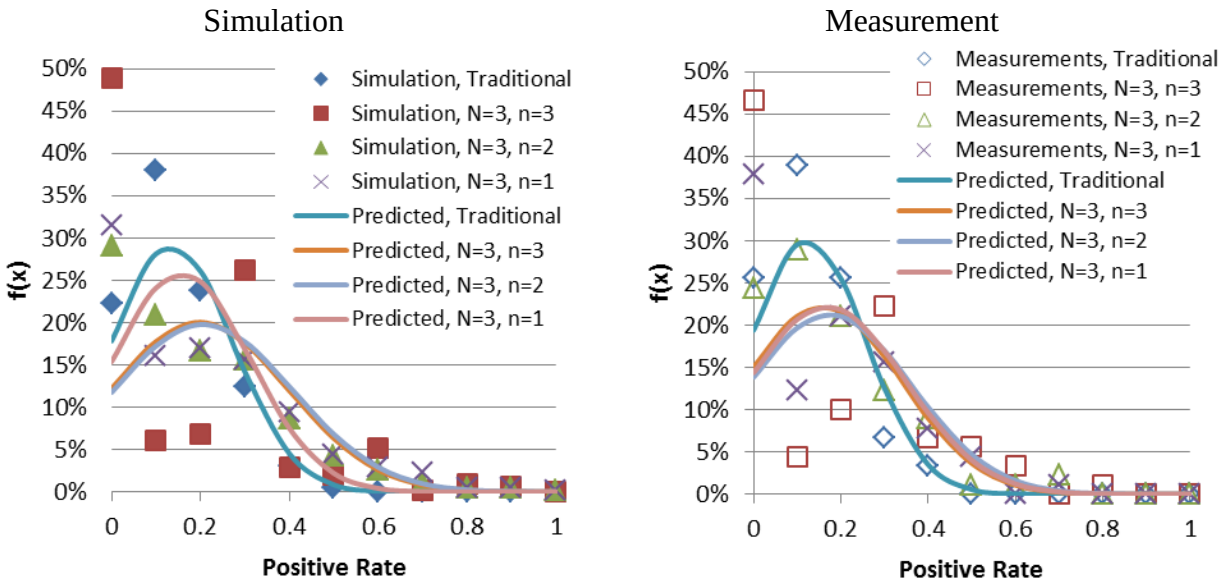

Figure 204 Positive Rate Probability Density Function Comparison for Simulation and Measurement for Different n Values (Gaussian, N=3, Stochastic)

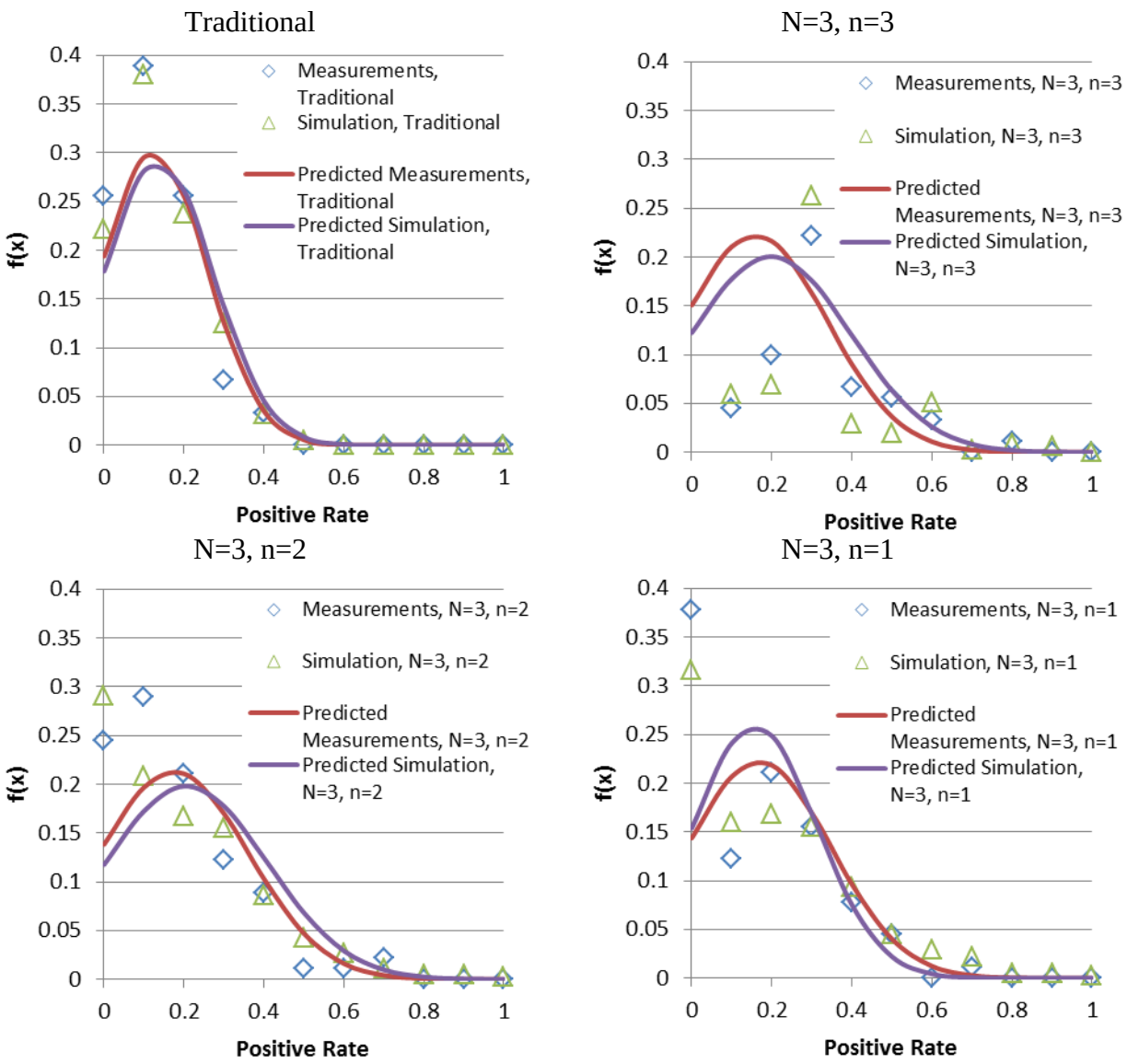

Figure 205 Positive Rate Probability Density Function Comparison for Simulation and Measurement for Different n Values (Gaussian, N=3, Stochastic)

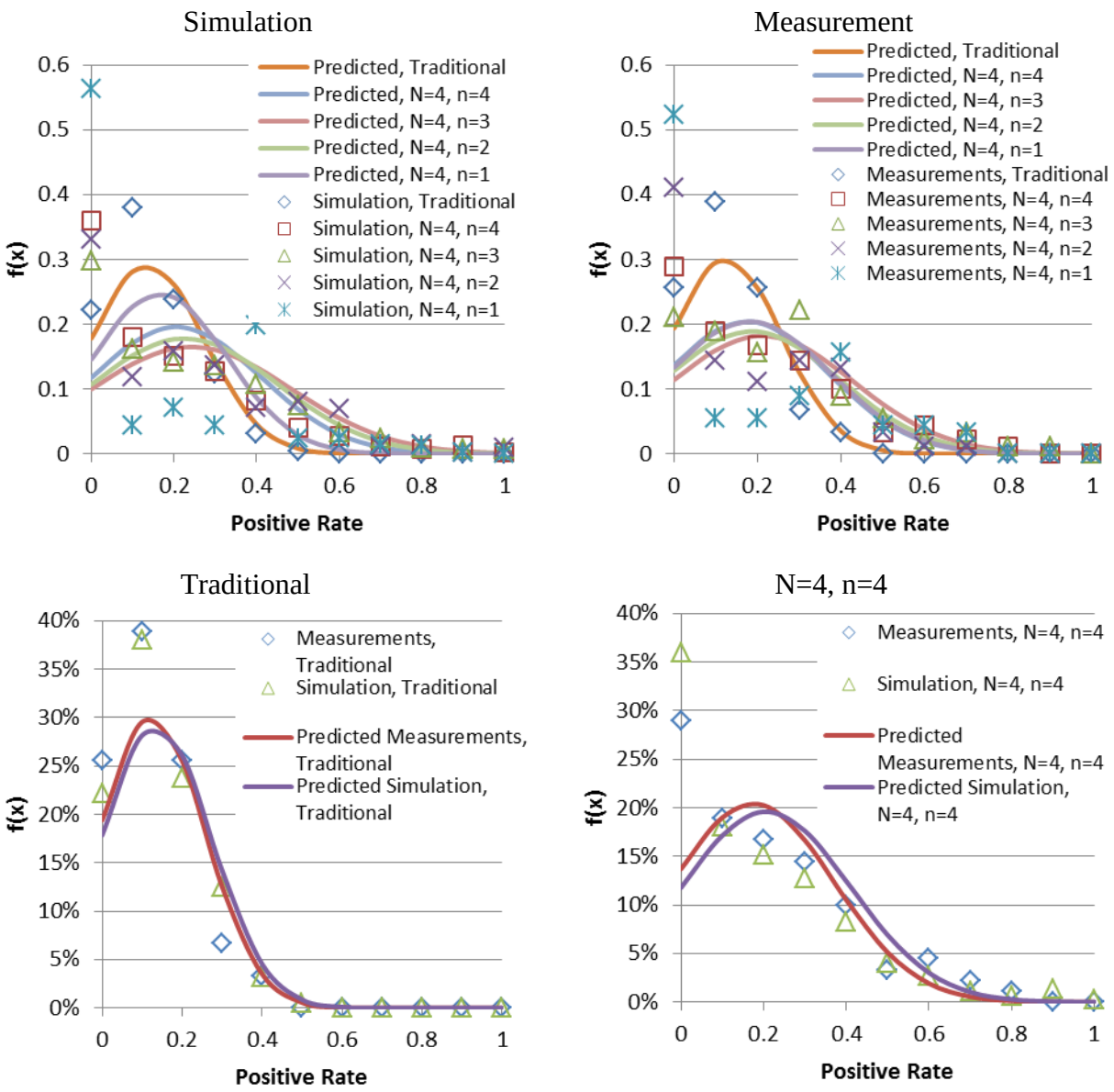

Figure 206 Positive Rate Probability Density Function Comparison for Simulation and Measurement for Different n Values (Gaussian, N=4, Stochastic)

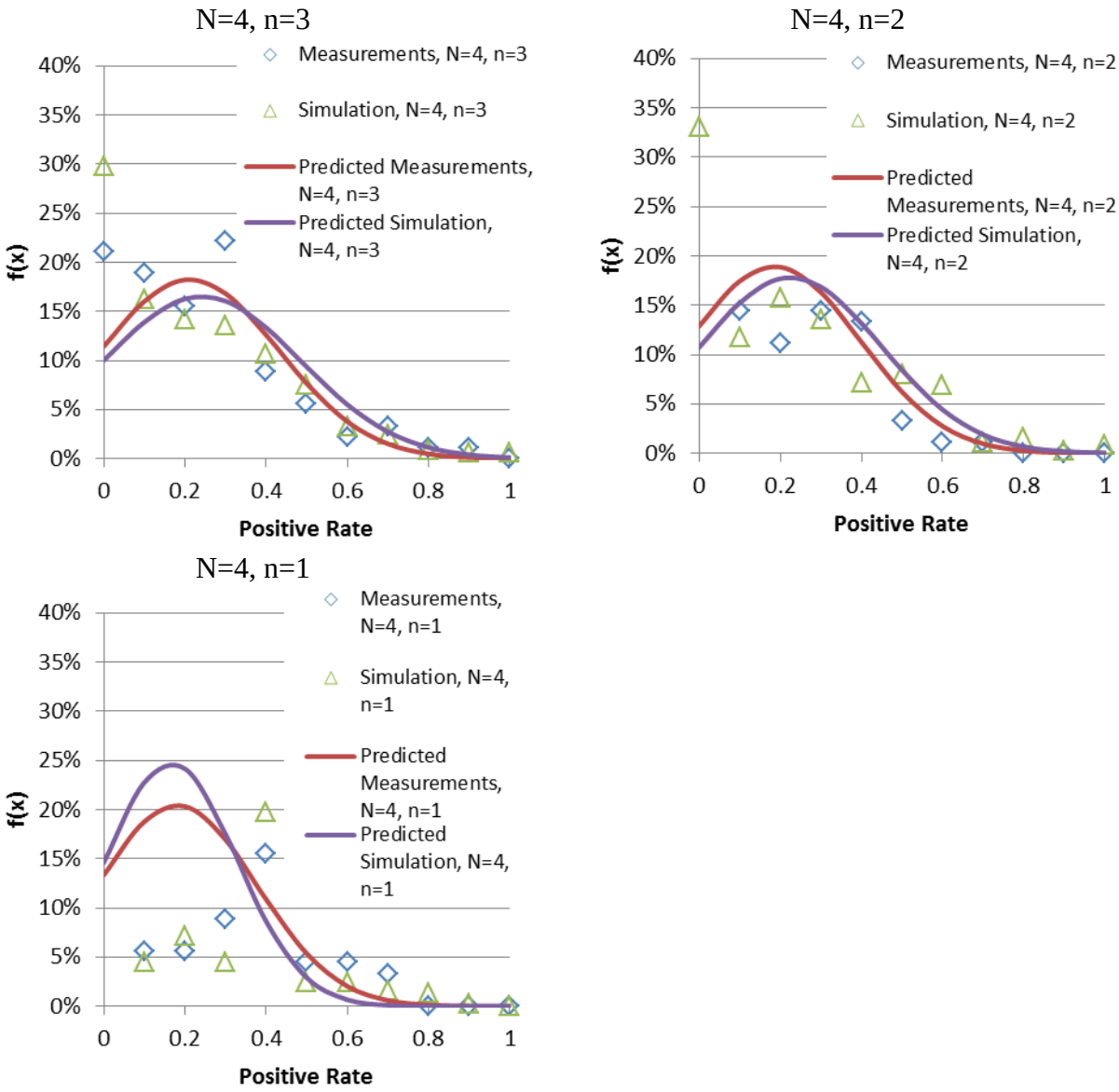

Figure 207 Positive Rate Probability Density Function Comparison for Simulation and Measurement for Different n Values (Gaussian, N=4, Stochastic)

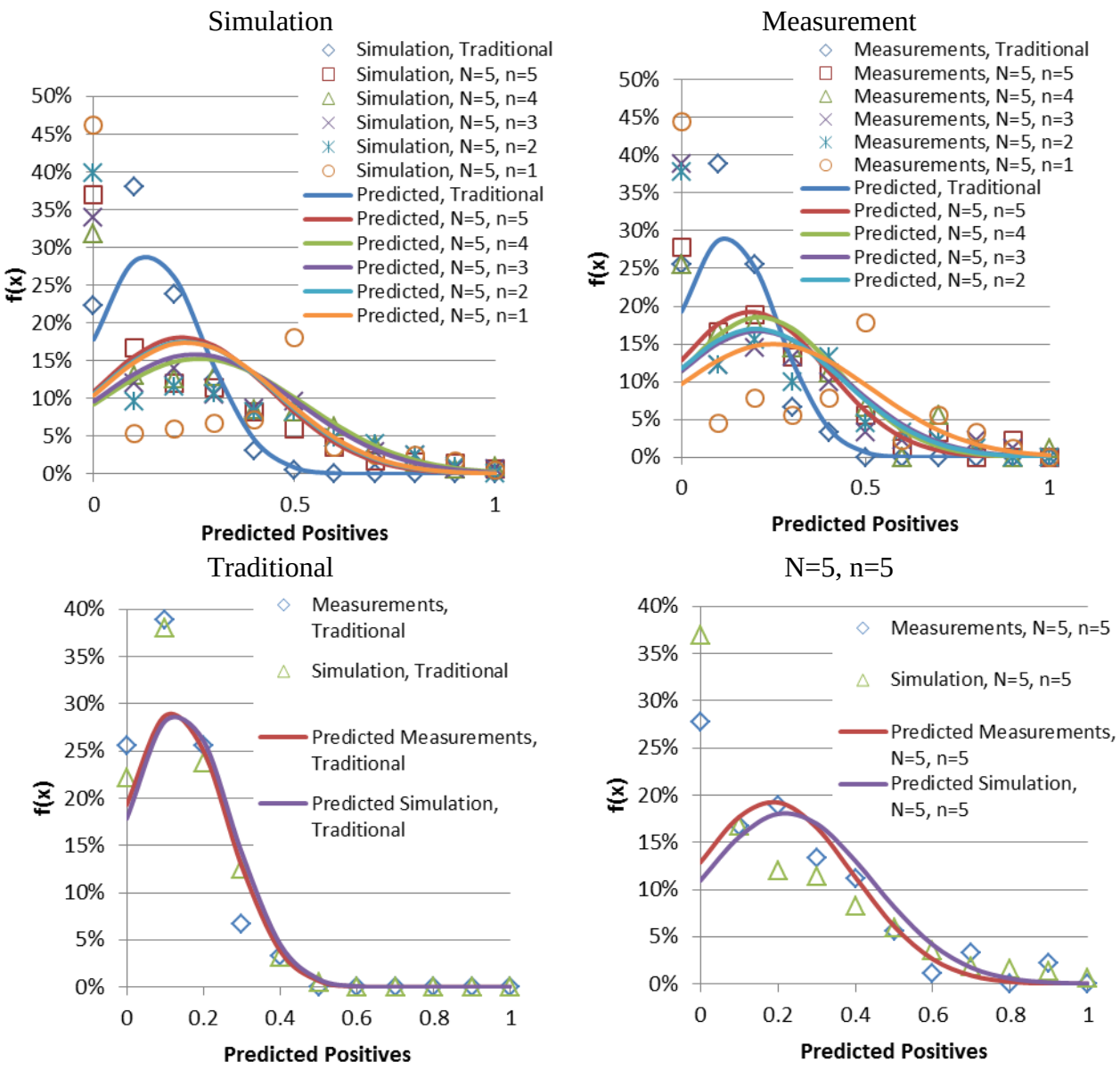

Figure 208 Positive Rate Probability Density Function Comparison for Simulation and Measurement for Different n Values (Gaussian, N=5, Stochastic)

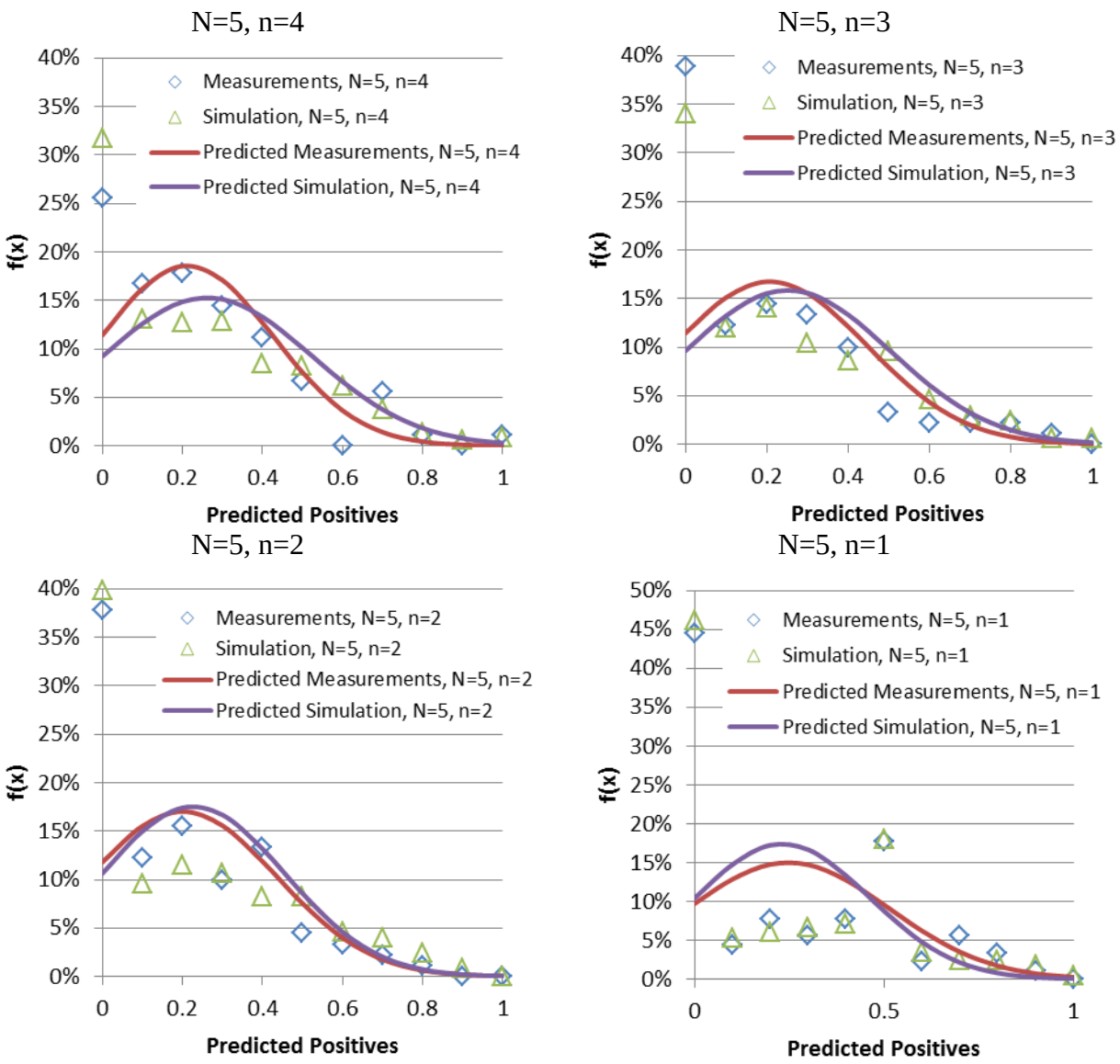

Figure 209 Positive Rate Probability Density Function Comparison for Simulation and Measurement for Different n Values (Gaussian, N=5, Stochastic)

Time at First Detection

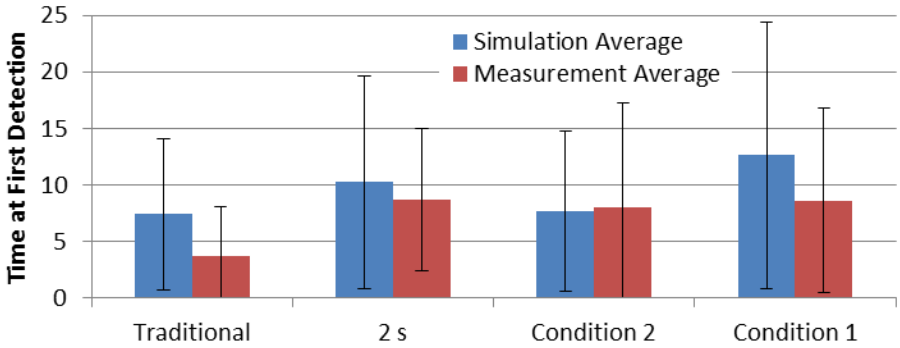

Figure 210 Time at First Detection for Different n Values Comparison for Simulation and Measurement (Gaussian, b=669.24 C/s, N=2, Stochastic)

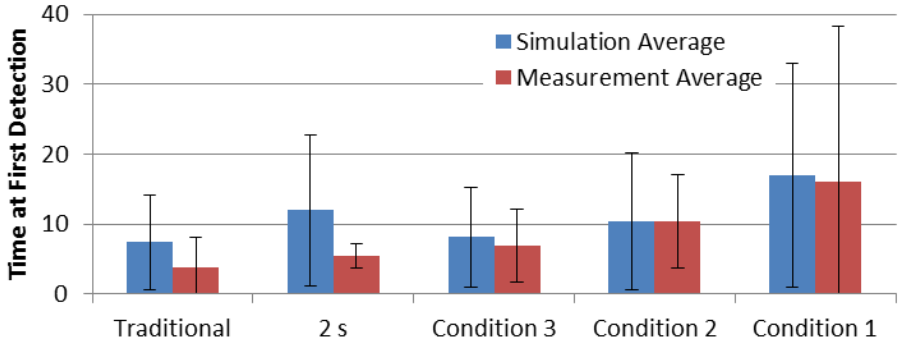

Figure 211 Time at First Detection for Different n Values Comparison for Simulation and Measurement (Gaussian, b=669.24 C/s, N=3, Stochastic)

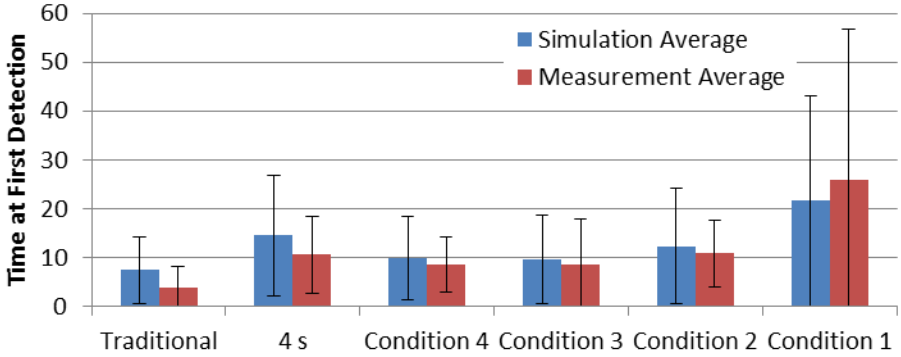

Figure 212 Time at First Detection for Different n Values Comparison for Simulation and Measurement (Gaussian, b=669.24 C/s, N=4, Stochastic)

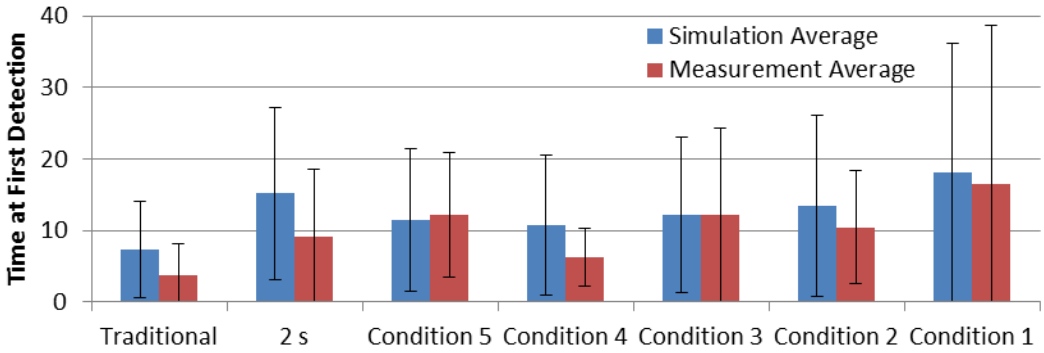

Figure 213 Time at First Detection for Different n Values Comparison for Simulation and Measurement (Gaussian, b=669.24 C/s, N=5, Stochastic)

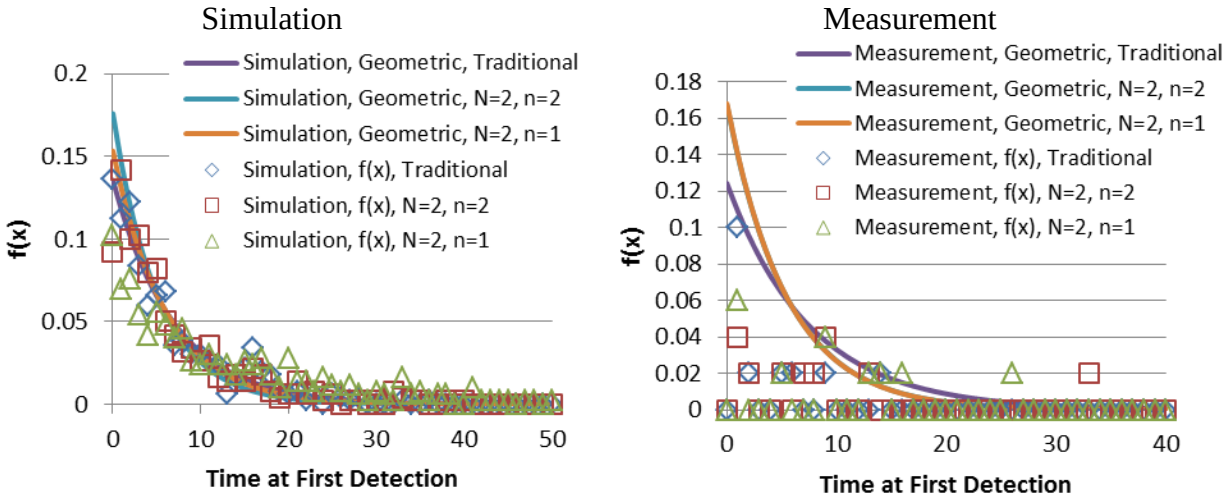

Figure 214 Time at First Detection Probability Density Function Comparison for Simulation and Measurement for Different n Values (Gaussian, N=2, Stochastic)

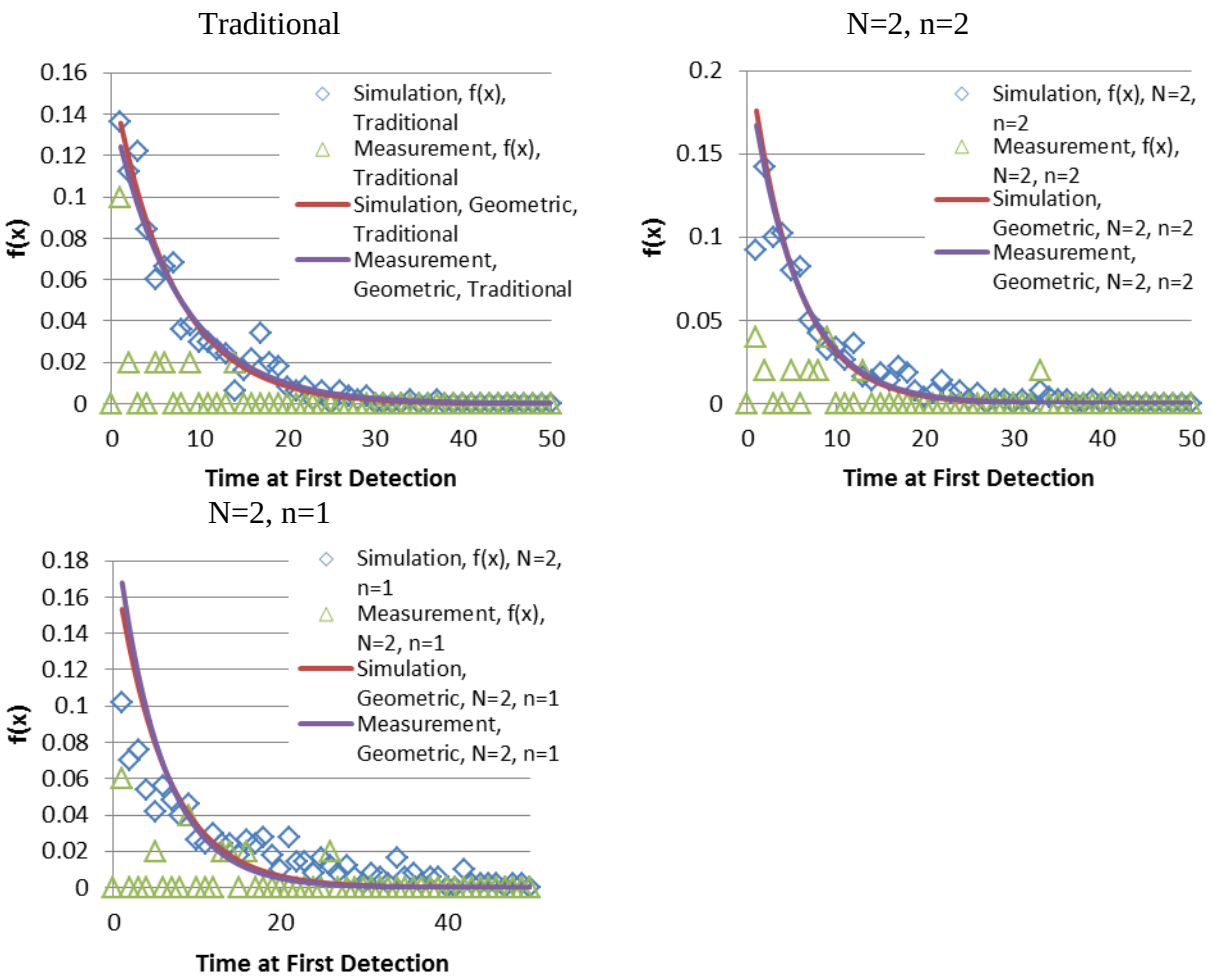

Figure 215 Time at First Detection Probability Density Function Comparison for Simulation and Measurement for Different n Values (Gaussian, N=2, Stochastic)

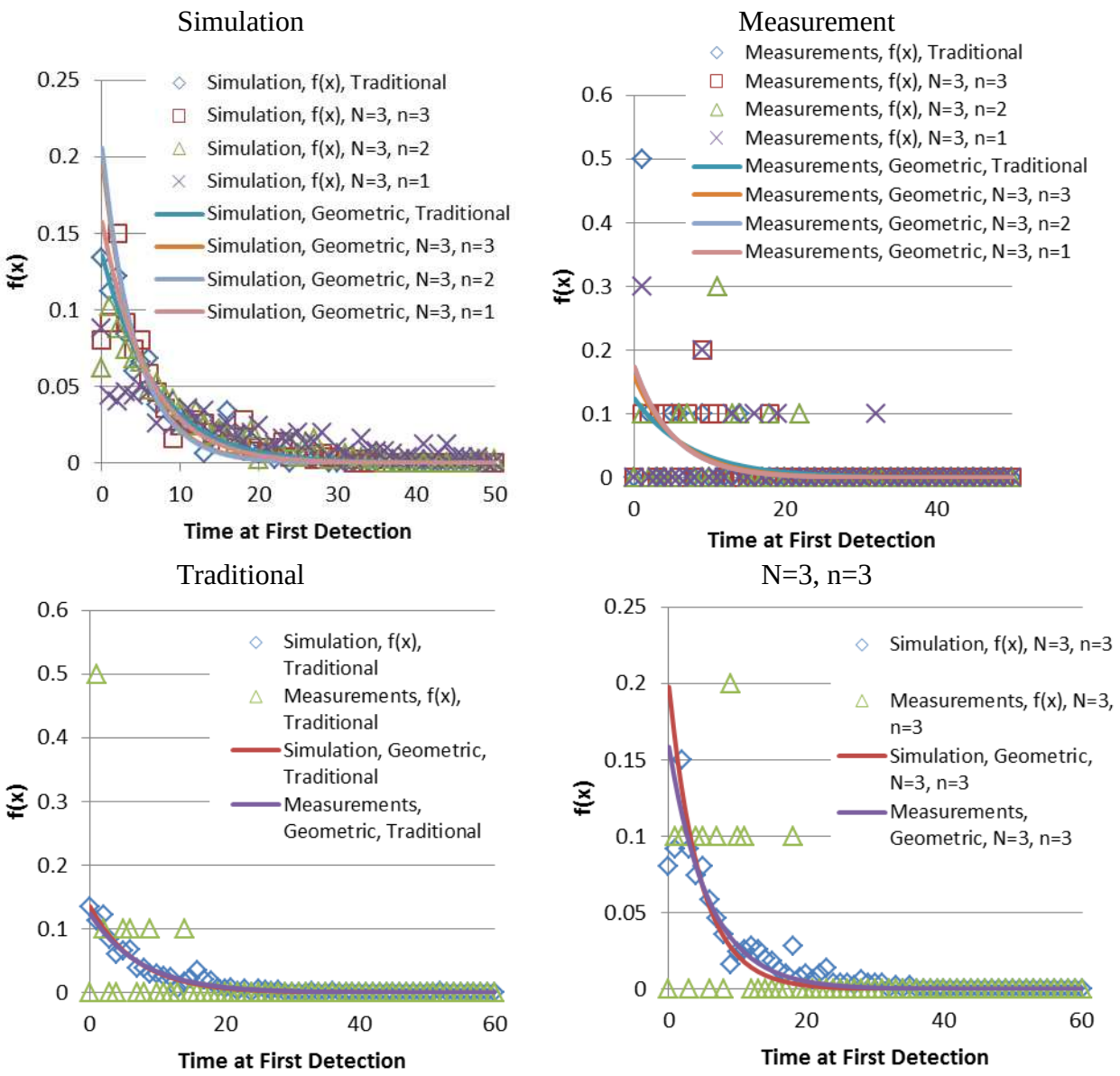

Figure 216 Time at First Detection Probability Density Function Comparison for Simulation and Measurement for Different n Values (Gaussian, N=3, Stochastic)

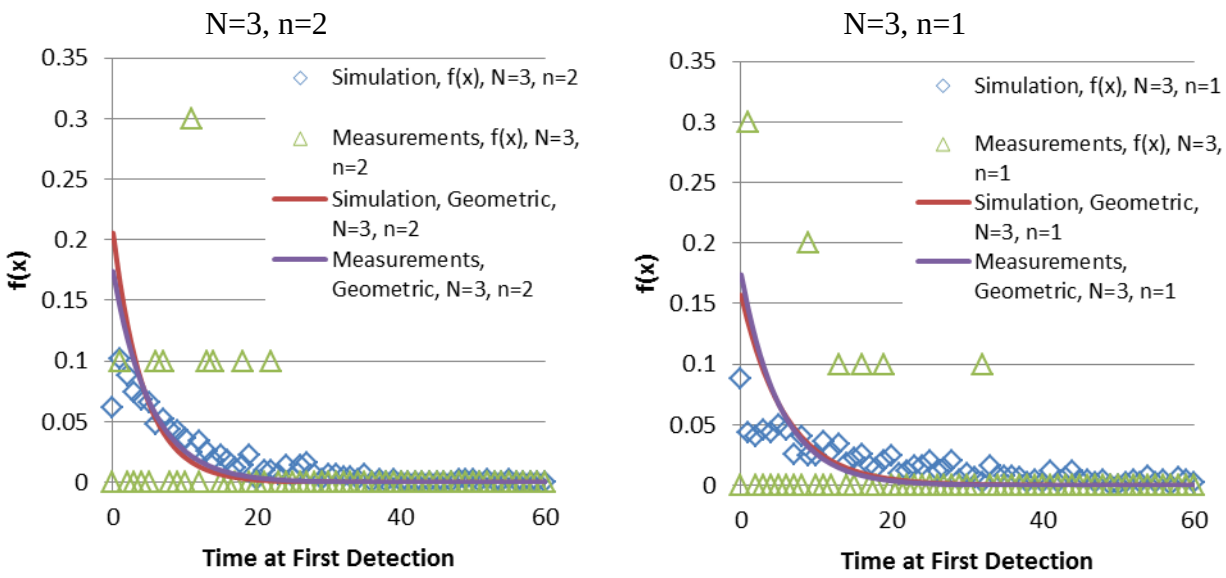

Figure 217 Time at First Detection Probability Density Function Comparison for Simulation and Measurement for Different n Values (Gaussian, N=3, Stochastic)

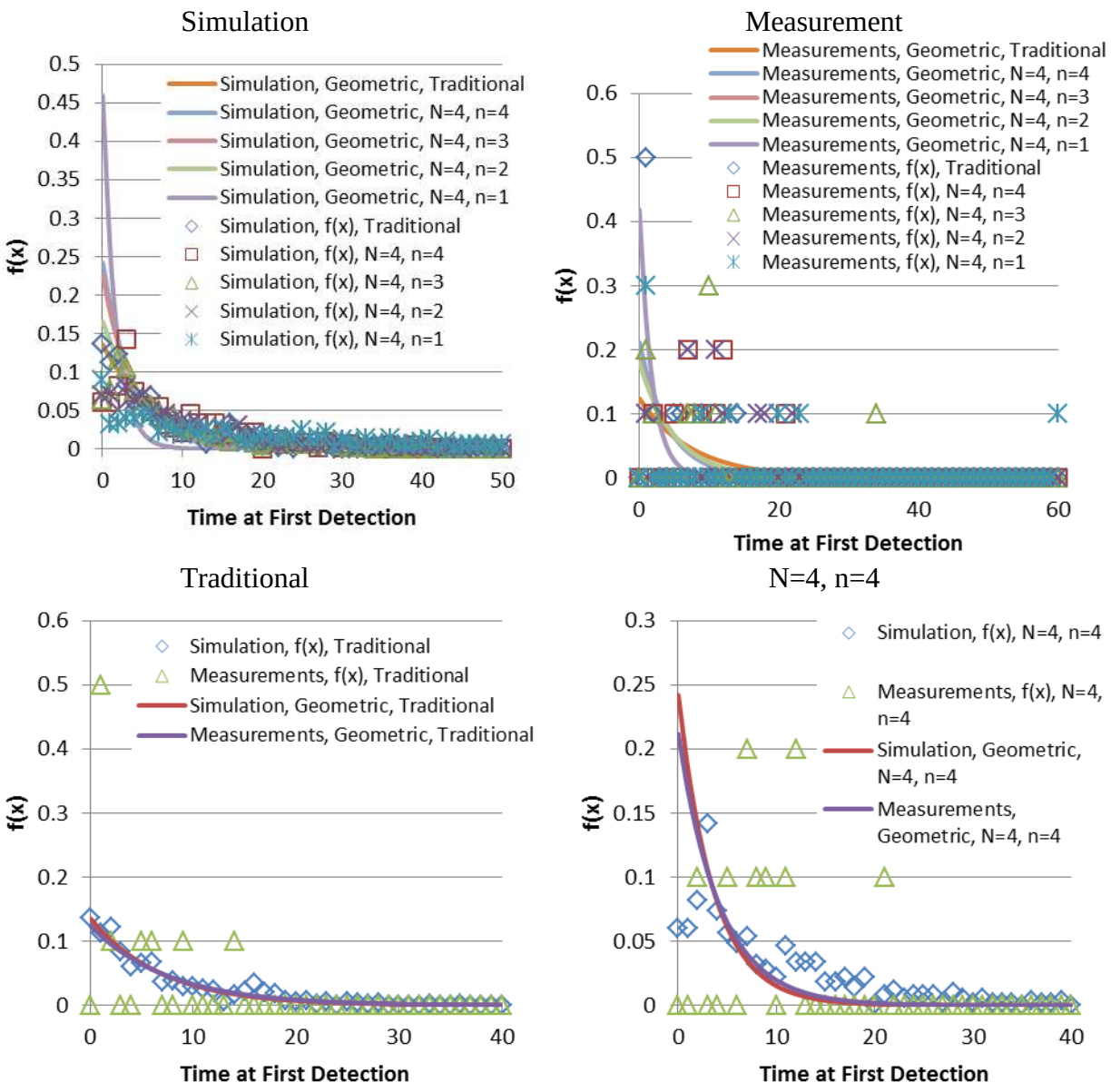

Figure 218 Time at First Detection Probability Density Function Comparison for Simulation and Measurement for Different n Values (Gaussian, N=4, Stochastic)

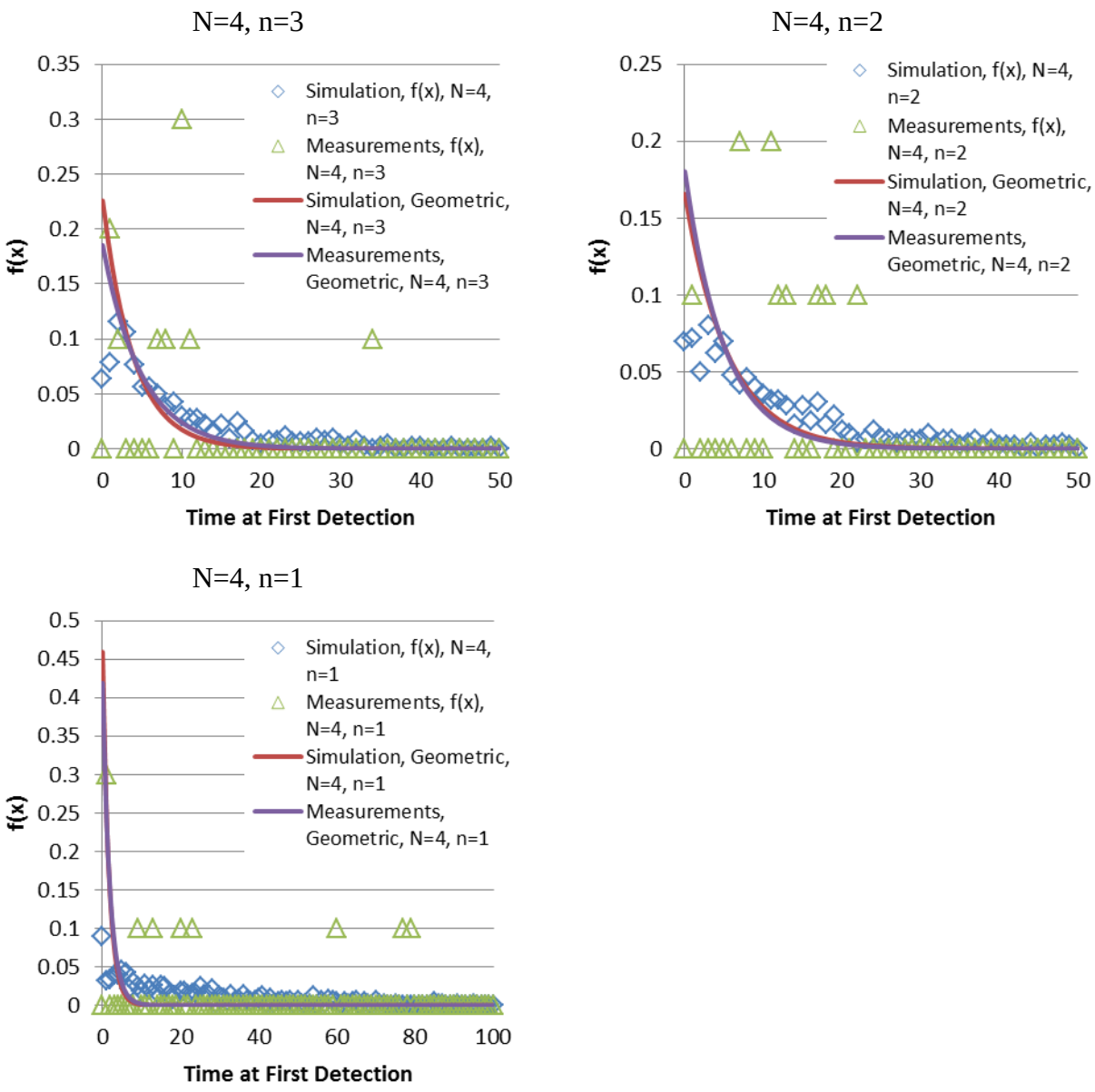

Figure 219 Time at First Detection Probability Density Function Comparison for Simulation and Measurement for Different n Values (Gaussian, N=4, Stochastic)

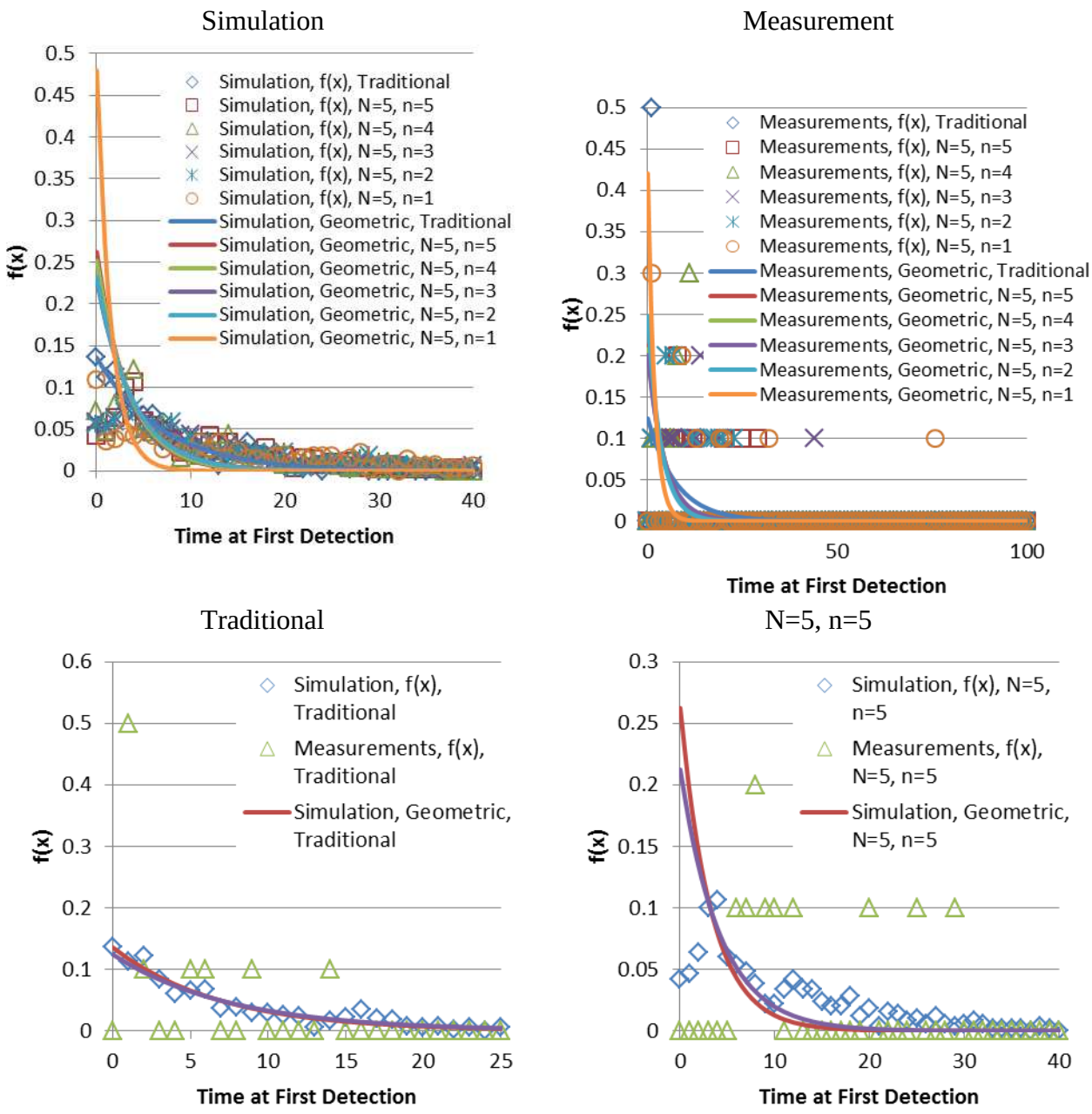

Figure 220 Time at First Detection Probability Density Function Comparison for Simulation and Measurement for Different n Values (Gaussian, N=5, Stochastic)

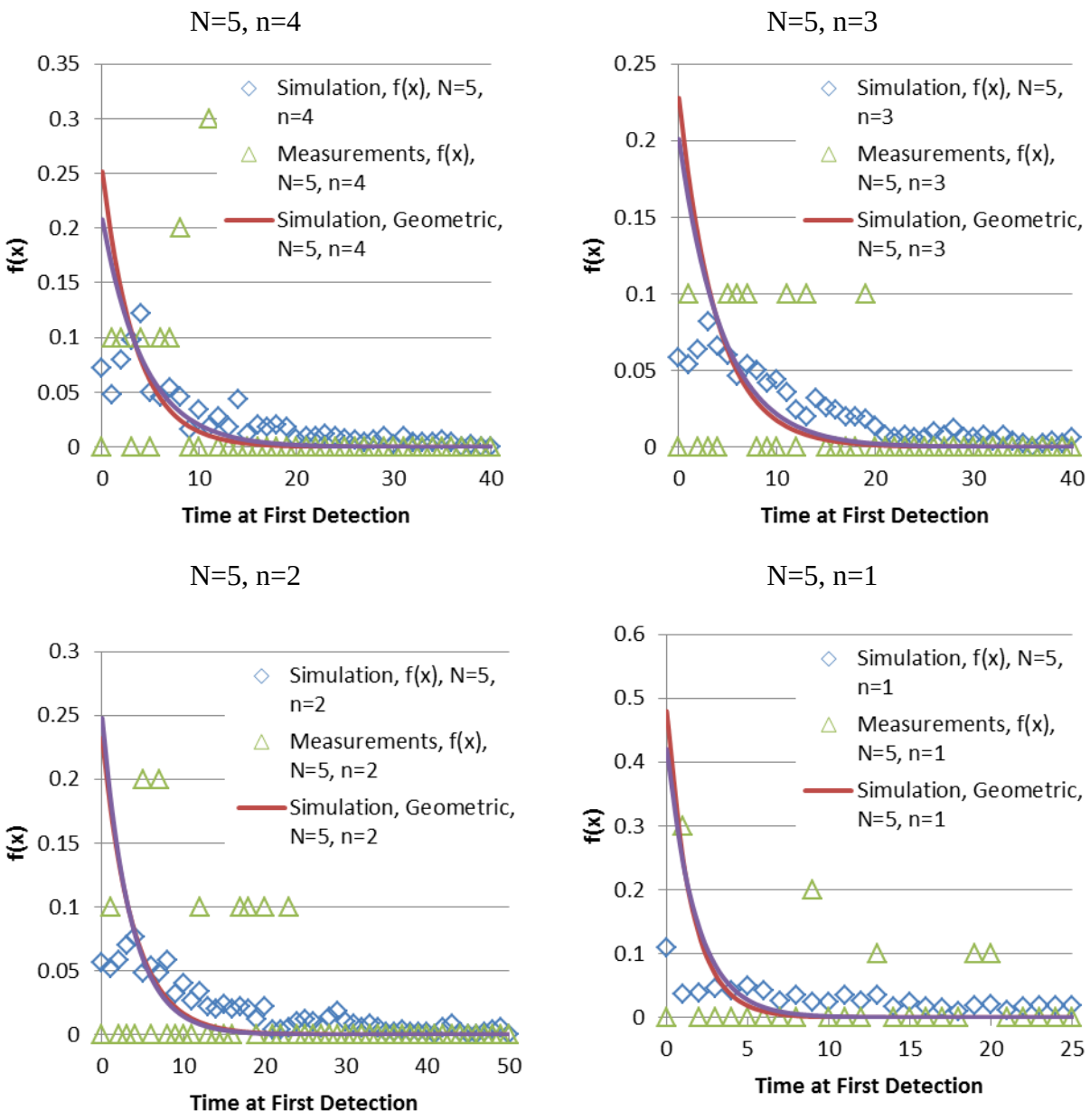

Figure 221 Time at First Detection Probability Density Function Comparison for Simulation and Measurement for Different n Values (Gaussian, N=5, Stochastic)